Ivan Makaris

Bitemporal Electromagnetism and the Antiphoton

Master's thesis in Applied Physics and Mathematics
Supervisor: Ingve Simonsen
Co-supervisor: Dag Wessel-Berg and John Ove Fjærestad
June 2022

Master's thesis

NTNU
Norwegian University of
Science and Technology

Ivan Makaris

Bitemporal Electromagnetism and the Antiphoton

Master's thesis in Applied Physics and Mathematics
Supervisor: Ingve Simonsen
Co-supervisor: Dag Wessel-Berg and John Ove Fjærestad
June 2022

Norwegian University of Science and Technology
Faculty of Natural Sciences
Department of Physics

NTNU
Norwegian University of
Science and Technology

Preface

Embarking on this Master's thesis at the esteemed Norwegian University of Science and Technology (NTNU) marked the start of an unexpected journey, one that transformed an initial free-time exploration into the very cornerstone of my thesis.

The genesis of this adventure began innocently enough. One day, seeking guidance on a complex math problem, I found myself in the office of Dag Wessel-Berg, son of Tore Wessel-Berg and who also later came to be one of the supervisors of this thesis, our conversation veered from the original topic to a discussion about quantum mechanics. Dag introduced me to his father's book, a pioneering work on bitemporal electromagnetism. Published in 2001, this underappreciated volume presents a seemingly classical theory that, intriguingly, predicts quantum phenomena illustrated through numerous simulations.

Interestingly, despite its astonishing simulations, this book was conspicuously absent from independent scientific citations. Borrowing a copy, I found myself enthralled but also daunted by the complexity of its contents. Undeterred, I delved deeper into the text and was particularly drawn to a chapter on the Stern-Gerlach experiment. Wessel-Berg had proposed potential weaknesses in the standard approach due to the overlooked divergence-free property of the magnetic field. Intrigued, I attempted my own simulations using more realistic parameters, and the results were nothing short of remarkable. These successful simulations made me realize Wessel-Berg's profound intuition for electromagnetism from his experience spanning over half a century. Yet, I observed that the early chapters of his book fell short in adequately elucidating the underpinnings of his theory. Despite this, the results undeniably spoke volumes about the theory's potential.

Determined to illuminate the obscured, I embarked on an mission to reverse-engineer the theoretical foundation from the book's simulations. This journey led me to apply and expand Wessel-Berg's theory to explain other physical phenomena, such as the Casimir effect, Unruh radiation, and simulating electron orbitals of atoms just to mention a few things. This exploration, while fruitful, exceeded the scope of this thesis, which had already become much longer that I had initially anticipated. Hence, I made the conscious decision to prioritize establishing a strong foundation for Wessel-Berg's theory, hoping to make it more accessible to others and, in doing so, avoid repeating the initial mistake of Wessel-Berg of under-prioritizing the theoretical groundwork in favor of the theory's fascinating results.

At the onset of the autumn term, I had planned to delve into Wessel-Berg's theory for my project assignment. It was an opportunity to navigate uncharted waters. Yet, for reasons I can no longer remember, I decided not to pursue it — a decision I soon came to regard with regret. As the term progressed, however, an unexpected door opened. I found myself guided by three dedicated supervisors - Dag Wessel-Berg, Ingve Simonsen, and John Ove Fjærestad, who shared my enthusiasm for the project. The moment I first presented the theory to them was a turning point. Their interest was piqued, and their curiosity sparked animated discussions. Their probing questions and constructive feedback transformed these dialogues into a crucible where my ideas could be shaped and refined. Much of what I presented to them was new territory. The theory of Wessel-Berg is not mainstream, and many of its concepts were novel to my supervisors. Yet, they dove into it with eagerness, investing their time and energy to grapple with its intricacies. This level of engagement was instrumental in shaping my thesis.

I want to express my profound gratitude for their involvement. They made my journey less solitary and more enriching. Their guidance, feedback, and unwavering support were pillars upon which this thesis was constructed. To my supervisors, I say, thank you. Your commitment to understanding my work made this thesis what it is today.

This thesis, therefore, is not just an academic milestone; it also represents a journey to elucidate the underrated brilliance of Wessel-Berg's theory. I hope it serves as a stepping stone, providing a clear foundation for his work and inspiring further explorations in this fascinating realm of physics.

<div align="right">

Ivan Makaris
Trondheim, April 2022

</div>

Abstract

Despite its tentative inaccuracies and somewhat unclear theoretical grounding, Tore Wessel-Berg's theory of *bitemporal electromagnetism*, a supposedly classical theory, showcases a surprising proficiency in simulating and predicting quantum phenomena [91]. This unexpected efficacy sparks a rigorous exploration into the theory's underlying mechanisms. The primary objectives of this thesis are to shed light on Wessel-Berg's theory's capacity to predict quantum phenomena, anchor the theory within the frameworks of contemporary physics, and construct a consistent theoretical foundation that fosters the derivation of Wessel-Berg's equations utilized in his simulations.

This thesis commences with an in-depth examination of entropy in physics, redefining it as the empirically accessible information of a physical state. Our work identifies an entropy problem in classical physics due to the requirement of a non-zero 'pixel size' for the delineation of entropy for continuous state spaces. A solution is proposed, based on the assumption of a theoretical minimum pixel size, which consequently leads to the emergence of the Wigner-Moyal formalism of quantum mechanics in phase space and standard quantum mechanics in Hilbert space. This examination essentially exposes the entropy problem as a defining characteristic of classical theories and thus identifies quantum theories as attempts at solving these problems, thereby offering a criterion to differentiate between quantum and classical models. This criterion is later used to demonstrate that classical electromagnetism exhibits an entropy problem akin to classical physics. The thesis then introduces bitemporal electromagnetism as a resolution to this problem and delves into the role of the antiphoton inherent in this theory.

A subsequent in-depth study of microscopic systems uncovers their deterministic and reversible nature, whilst the importance of conservation of energy and entropy in these systems is highlighted. An argument for retrocausality is presented, in which it is emphasized that a phase space trajectory's cause can be equally attributed to its future states as to its past states. This raises questions about traditional notions of causality in these systems.

Furthermore, an exploration of wave equations in Hilbert space is undertaken, comparing non-relativistic and relativistic formulations through energy relations. It is shown that relativistic systems expand their Hilbert spaces, accommodating both positive and negative energy solutions compared to their nonrelativistic counterparts. This groundwork then facilitates a deep dive into the antiphoton, focusing on its potential within the context of negative energy solutions inherent in relativistic formulations in circumventing the Hegerfeldt's theorem and accounting for the enigmatic $1/f$ noise in electrical circuits. A particular focus is placed on the challenges posed by negative energy solutions and their interpretation for charged particles and uncharged particles like the photon. The repercussions of excluding negative energy solutions are then highlighted with several examples. Although the negative energy solutions have historically been disregarded, the analysis shows that this disregard leads to particular consequences. One of these consequences results in inducing an entropy problem in which the mathematical framework in the theory is disconnected from actual empirical measurements, which are represented as Hermitian operators.

The final part of the thesis posits that contemporary electromagnetism is essentially a macroscopic theory, and thus a new microscopic theory of electromagnetism is proposed. Abiding by the microscopic properties of determinism, reversibility, and conservation of energy and entropy, this microscopic theory is constructed by leveraging time-advanced and time-retarded solutions of Maxwell's equations before extending into the bitemporal domain. This extension incorporates the antiphoton and thereby addresses the entropy problem of electromagnetism. The newly developed theory not only provides substantial support to Wessel-Berg's equations, but also rectifies missing links in his original work. Wessel-Berg's theory can therefore be viewed as a first-quantized theory of electromagnetism, where the antiphoton aids in solving the entropy problem in classical electromagnetism.

The thesis situates Wessel-Berg's theory within the broader spectrum of modern physics. The emphasis is placed on how the theory solves the entropy problem and circumvents Hegerfeldt's theorem, while considering existing literature where negative energy solutions have been beneficially utilized. The theory's resemblence to Feynman's path integral formulation is also discussed, enriching its comparison with established physical theories.

By revisiting and challenging the current understanding of entropy and its role in physical theories, this work sheds light on the intricacies of physical systems at various scales and bridges the gap between theoretical predictions of a theory and actual empirical measurements at finer scales. Fundamentally, this thesis elucidates Wessel-Berg's theory, solidifying its theoretical foundation.

Sammendrag

Til tross for dens tentative unøyaktigheter og noe uklare teoretiske grunnlag, viser Tore Wessel-Bergs teori om *bitemporal elektromagnetisme*, en tilsynelatende klassisk teori, en overraskende evne til å predikere kvantefenomener i sine simuleringer [91]. Disse gode resultatene motiverer en rigorøs utforskning av teoriens underliggende mekanismer. Hovedmålene for denne avhandlingen er å belyse Wessel-Bergs teori sin evne til å forutsi kvantefenomener, forankre teorien innenfor den moderne fysikkens rammer, og konstruere et konsistent teoretisk grunnlag som fremmer utledningen av Wessel-Bergs ligninger som brukes i hans simuleringer.

Denne avhandlingen begynner med en inngående undersøkelse av entropi i klassisk fysikk, der det redefineres som den empirisk tilgjengelige informasjonen for en fysisk tilstand. Arbeidet vårt identifiserer et entropiproblem i klassisk fysikk på grunn av kravet om en 'pikselstørrelse' ulik null for å spesifisere entropi for kontinuerlige tilstandsrom. En løsning blir foreslått basert på antagelsen om en teoretisk minste pikselstørrelse, noe som gir opphav til Wigner-Moyal formalismen for kvantemekanikk i faserom og standard kvantemekanikk i Hilbert-rom. Denne undersøkelsen avdekker entropiproblemet som en definisjonsmessig karakteristikk ved klassiske teorier, og identifiserer dermed kvanteteorier som forsøk på å løse disse problemene. Dette gir dermed et kriterium for å skille mellom kvantemodeller og klassiske modeller. Kriteriet brukes senere til å vise at klassisk elektromagnetisme også har et entropiproblem på lik linje med klassisk fysikk. Avhandlingen introduserer deretter bitemporal elektromagnetisme som en løsning på dette problemet og går dypere inn i rollen antifotonet spiller i denne teorien.

En påfølgende analyse av mikroskopiske systemer avdekker deres deterministiske og reversible natur, og legger vekt på viktigheten av bevaring av energi og entropi i disse systemene. Et argument for retrokausalitet blir presentert, der det påpekes at årsaken til en faserom-bane kan tilskrives like mye dens fremtidige tilstander som dens tidligere tilstander. Dette utfordrer tradisjonelle oppfatninger om årsakssammenhenger i disse systemene.

Videre utforskes bølgeligninger i Hilbert-rom, der ikke-relativistiske og relativistiske formuleringer sammenlignes gjennom energirelasjoner. Det vises at relativistiske systemer utvider sitt Hilbert-rom og inkluderer både positive og negative energiløsninger i forhold til deres ikke-relativistiske motparter. Dette grunnarbeidet muliggjør deretter en grundig utforskning av det mystiske antifotonet, med fokus på dets potensial i konteksten av negative energiløsninger som følger med relativistiske formuleringer i Hilbert-rom. Det legges spesielt vekt på utfordringene som følger med negative energiløsninger og deres tolkning for ladde partikler og nøytrale partikler som fotonet. Konsekvensene av å utelate negative energiløsninger blir deretter fremhevet gjennom flere eksempler. Selv om de negative energiløsningene historisk sett har blitt neglisjert på grunn av deres ikke-intuitive implikasjoner, viser analysen at dette fører til visse konsekvenser. En av konsekvensene resulterer i et entropiproblem der det matematiske rammeverket i teorien blir frakoblet faktiske empiriske målinger, representert av Hermitiske operatorer.

I den siste delen av avhandlingen argumenteres det for at moderne elektromagnetisme i bunn og grunn er en makroskopisk teori, og dermed foreslås en ny mikroskopisk teori for elektromagnetisme. Ved at determinisme, reversibilitet, og bevaring av energi og entropi overholdes som egenskaper for mikroskopiske systemer, blir denne teorien konstruert ved å benytte tidsavanserte og tidsforsinkede løsninger for Maxwells ligninger før teorien utvides til det bitemporale domenet. Denne utvidelsen inkorporerer antifotonet og løser dermed entropiproblemet i elektromagnetisme. Den nylig utviklede teorien gir ikke bare betydelig støtte til Wessel-Bergs ligninger, men retter også opp mange av svakhetene i hans originale arbeid. Wessel-Bergs teori kan derfor betraktes som en førstekvantisert teori for elektromagnetisme, der antifotonet bidrar til å løse entropiproblemet i klassisk elektromagnetisme.

Avhandlingen plasserer Wessel-Bergs teori innenfor det bredere spekteret av moderne fysikk. Det legges vekt på hvordan teorien løser entropiproblemet og omgår Hegerfeldts teorem, samtidig som eksisterende litteratur hvor negative energiløsninger har blitt brukt på en fordelaktig måte tas i betraktning. Teoriens likhet med Feynmans baneintegrasjonsformulering diskuteres også, noe som beriker sammenligningen med etablerte fysiske teorier.

Ved å gjennomgå og utfordre dagens forståelse av entropi og dens rolle i fysiske teorier, kaster dette arbeidet lys over de intrikate detaljene i fysiske systemer på ulike skalaer og bygger bro mellom teoretiske prediksjoner og faktiske empiriske målinger på mindre skalaer. Denne avhandlingen belyser Wessel-Bergs teori på en grunnleggende måte og styrker dens teoretiske fundament.

Table of Contents

List of Figures

List of Tables

1 Introduction

In 2001, Tore Wessel-Berg, a former professor at the Norwegian University of Science and Technology (NTNU), published the book *Electromagnetic and Quantum Measurements: A Bitemporal Neoclassical theory* [91]. This book lays the groundwork for a supposedly classical theory (which he refers to as 'neoclassical') that remarkably appears to predict a plethora of quantum mechanical phenomena, a feat demonstrated through numerous simulations contained within his book. Curiously enough, this potentially groundbreaking book has barely been cited within scientific literature, seemingly relegated to the corners of obscurity.

This apparent disregard might be attributed to Wessel-Berg's rather impenetrable writing style in the first chapters of his book, riddled with mathematical inaccuracies whilst lacking a coherent theoretical foundation for his equations later used in his simulations, which has deterred many from unraveling its potential. Some of these pitfalls may be attributed to the fact that Wessel-Berg was becoming old when writing his book. Additionally, his book was not proofread by anyone prior to publishing. Although numerous individuals have tried, the issues of Wessel-Berg's book have made his theory difficult to understand.

However, these shortcomings do not entirely eclipse the spark of brilliance that radiates from his book. There is an important aspect of the book that simply cannot be ignored: his mysterious, unexplained equations, while sprung from a precarious theoretical foundation, astonishingly succeed in their predictions regarding quantum phenomenon as evidenced by the simulations presented in the book. This peculiar observation, in itself, is a compelling enigma that warrants further investigation as it can have a potentially pivotal role in shedding light on the elusive bridge between classical and quantum mechanics, an endeavor that has challenged physicists for more than a century.

The dawn of the 20th century saw a revolution within the realm of physics. The emergence of certain inexplicable experiments led numerous physicists to conclude that conventional wisdom had to be abandoned to explain these observations, paving the way for quantum theory. It was thought that the world could have been governed by classical physics, but unfortunately, it was not. This line of reasoning was due to the fact that numerous physicists argued that everything else has been attempted to account for the discrepancy between theory and observation, which forced us to adopt quantum theory.

Fast forward to the present day, and we find Wessel-Berg's 'neoclassical' theory successfully explaining quantum phenomena in a novel way. The question that we must ask then, is how this seemingly classical theory achieves such quantum accuracy, especially in light of the 20th century understanding that every possible classical explanation had been exhausted.

In an attempt to answer this question, the author of this thesis has meticulously performed all of the simulations presented in Wessel-Berg's book and made them accessible via GitHub. Yet, these simulations alone do not explain the enigmatic nature of Wessel-Berg's theory. The ultimate goal of this thesis, therefore, is to delve deeper into the intricate fabric of his theory, exploring how it manages to mimic quantum phenomena, and how it compares to other well established theories of modern physics. This endeavour will hopefully make Wessel-Berg's theory more accessible to the scientific community.

1.1 Objectives and Approach

The aim of this thesis is to unravel the mystery shrouding Wessel-Berg's theory by accomplishing three primary objectives:

1. Determine why Wessel-Berg's Bitemporal Electromagnetism can predict quantum phenomena.

2. Situate this theory within the contemporary frameworks of modern physics.

3. Construct a theoretical basis which gives rise to the equations Wessel-Berg uses for his simulations.

Our journey will employ a meticulous approach, dissecting the theory's components in a gradual progression from basic concepts to complex paradigms. Subsequently, the theoretical aspects of the book will be critically examined, identifying potential gaps and ambiguities. The final step involves developing a robust theoretical groundwork that logically leads to Wessel-Berg's equations. The ultimate aim is to demystify the inner workings of the theory, and in doing so, unlock the reasons behind its success in replicating quantum behaviors.

1.2 Thesis Structure

The thesis unfolds across four distinct parts, each playing a crucial role in the collective endeavor to understand Wessel-Berg's theory:

Part I - A Reconsideration of Entropy: The exploration starts by redefining entropy in terms of empirical measurements, delving into classical theories' inherent entropy problems.

Part II - Bitemporal Causality and The Microcosm: Attention is then turned towards understanding microscopic systems within the realm of Hamiltonian mechanics, and its quantum analogue, the Wigner-Moyal formalism in phase space. The role of bitemporal causality is emphasized in these systems.

Part III - Understanding the Antiphoton: The third part dives deeper into the concept of antiphotons, engaging in a comparative analysis of relativistic and non-relativistic Hilbert space representations whilst examining the consequences of negative energy solutions.

Part IV - Bitemporal Electromagnetism: The final part culminates in a robust development of a microscopic theory of electromagnetism, addressing gaps in Wessel-Berg's original theory and showcasing an example to solidify the central tenets of this study.

The reason behind the form of the above structure can be understood by the following discussion:

In the early 1900s, the call for a departure from conventional wisdom was grounded in the emergence of novel experiments that challenged existing theories. This thesis contends that this line of reasoning regarding the rejection of conventional wisdom is not only flawed at its core but also demonstrates that classical physics could never have provided an accurate description of the natural world due to its inherent shortcomings in describing a fundamental and essential concept like entropy adequately. Moreover, it is argued that quantum theory arises quite naturally as a resolution to these fundamental issues within classical physics.

In the expansive realm of physics, most minds labor tirelessly to the challenge of molding mathematical models to fit empirical 'measurements'. Yet, in this fervent pursuit, it seems only a scant few pause to contemplate the very nature of the notion of 'measurement' itself – an underlying cornerstone that too often goes unexamined. And fewer still ponder how such a concept might even be quantified, a process intimately tied to the fundamental concept of entropy. For it is in this precise nuanced exploration that the foundations of quantum theory emerge, illustrating the subtle and profound interplay between observation and physical reality.

So, this is where our journey commences – at the crossroads of measurement, entropy, and the fundamental understanding of the world around us. Through a thoughtful dissection of Wessel-Berg's theory, we seek to challenge conventional wisdom regarding the misleading discussion regarding the distinction between quantum and classical theories in physics.

Part I

A Reconsideration of Entropy

It is essential to acknowledge from the outset that the primary objective of scientific inquiry is *not* to uncover absolute truths, which for the purposes of this particular argument, can be defined as absolutely accurate information. Rather, science aims at developing models that have predictive capabilities regarding the physical world. As far as the world that we perceive around us is concerned, we do not know, and moreover, we cannot know for absolute certainty whether a reality external to ourselves truly exists. What we do know is that we experience sensory stimuli and it would thus far appear that manipulating the external observable world around us results in consistent sensory inputs.

Distinct methods of environmental manipulation appear to result in different perceived sensory inputs. For instance, applying an ice pack to the skin creates a sensation of cold, whereas pinching the skin too hard results in pain. This simple yet fundamental principle underpins the scientific method: through the manipulation of some external environmental variables A, B, and C results in the perception of sensory stimuli X, Y, and Z. That is, through observation and experimentation, patterns in the world can be discovered, which can be leveraged to make predictions about future empirical observations.

Despite the scientific method, there still exists, and will always exist, an insurmountable epistemic barrier between what we perceive and what is truly physically 'real'. This accounts for the fact that nothing in science can ever be proven, as nothing regarding the physical realm can be established with unassailable certainty. This is because science operates inductively via description rather than definition. As a result, the scientific method abstains from pursuing proofs, for which there is an absence of an established scientific standard. Instead, the method concentrates exclusively on devising predictive models founded on empirical patterns discerned in nature.

In stark contrast, mathematics is preoccupied with proofs due to its inherent deductive nature, which is rooted in definitions. Mathematics commences with a set of axioms governing the behavior of a set of elements. As these axioms are examined, combined, and formalized in proofs, novel theorems emerge and can be further amalgamated in various ways, ultimately resulting in an interconnected network of theorems, with the first principles forming the foundation of this metaphorical pyramid.

How can we verify the validity of these first principles? To put it differently, how can we ensure that the assertion that two plus two truly equals four or that a triangle always possesses three sides? The answer lies in the fact that these first principles are purely definitional in character. Just as the impossibility of having a meat eating vegetarian or an empty cup that is filled with water, the definitions inherent to these statements can therefore not be challenged nor contradicted. Although the rules governing mathematics may appear as arbitrary as those of poker or chess, mathematics appears to be more effective in describing observable reality than alternative deductive systems, such as the rules of chess. Physics, therefore, is the attempt in applying mathematical frameworks to describe reality, which is not as straight forward as one might first presume. This is because the physical states of reality are no longer definitional and are instead rooted in empiricism through observations.

In employing mathematics to describe the real world, it is imperative to establish a connection between a specific abstract mathematical framework to the corresponding physical states in reality that one is attempting to describe. To accomplish this, the information one possesses regarding these physical states must be identified, properly defined and quantified. This necessitates the formulation of an appropriate and self-consistent definition of entropy, which functions as a bridge between abstract mathematical models and the information one possesses of the actual, physical and empirical states of reality. Consequently, it is posited in this thesis that information theoretic entropy is among the most fundamental quantities that must be accurately defined in order to ensure a coherent depiction of the world. The widely-used Gibbs and Boltzmann equilibrium entropies in thermodynamics have their limitations, necessitating a more general and consistent

definition of entropy for the microscopic realm that will be shown to be critical in our future discussions.

In this part, we consider a modified definition of entropy which will form the foundation for describing our microscopic systems throughout the remainder of this thesis. While our definition is based on Shannon's information theory, it differs slightly from both that definition and the definition of entropy in thermodynamics. Our definition is instead intended to quantify the knowledge that can be gained about the state of a physical system under study through empirical measurements. Perfect knowledge of the state corresponds to an entropy of zero, while an entropy greater than zero indicates uncertainty about the state of the system. Importantly, our definition of entropy is based solely on knowledge obtained through empirical measurements, which necessarily involve interacting with the system being studied.

To illustrate these ideas, we first consider the entropy within *discrete* state spaces using coins and cards. We then extend our discussion to *continuous* state spaces, where the concept of a 'pixel' is inevitably forced upon us. This is not a mere optional feature, but rather a fundamental requirement for the delineation of entropy within these continuous realms.

2 Modified Definition of Entropy for Discrete States

Entropy, within the context of a discrete state space, is a quantification of the physical resources required to fully document the actual state of a system. Performing a measurement on the system can diminish the entropy, thereby enhancing our understanding of the system's state. The definition of entropy is such that when it is minimized to 0, it signifies complete knowledge of the state.

2.1 Entropy in Discrete State Spaces

To quantify the entropy of a discrete state space system, we employ Shannon entropy, a measure predicated on the pre-existing knowledge about the examined system [81]. This particular definition of entropy springs from two foundational prerequisites, dictating its unique mathematical form. Consequently, our discourse commences with an exploration of the Shannon entropy formulation's underpinnings, guided by these prerequisites.

Consider a measurement of some system, where the possible outcomes of the measurement have probabilities $\mathcal{P}_1, \ldots, \mathcal{P}_N$. If the measurement gives a low probable realisation, we regard the information content of the realisation as high, and vice versa. Furthermore, if we perform two *independent* measurements on our system, the information gained should be additive. Let $U(\mathcal{P})$ denote the information content obtained by measuring a realisation with probability $\mathcal{P}$. We wish to quantify the information, or variability, of $\mathcal{P}$ using a definition of entropy that has the aforementioned properties. Thus, our first task is to find a function $U(\cdot)$ that satisfies the following two requirements:

1. **Requirement 1:** *Additivity of independent systems*

   If we have two independent systems with corresponding probabilities $\mathcal{P}$ and $\mathcal{Q}$, then the total entropy of the combined system should be the sum of their individual entropies

   $$U(\mathcal{P} \cdot \mathcal{Q}) = U(\mathcal{P}) + U(\mathcal{Q}). \tag{2.1}$$

2. **Requirement 2:** *Surprise factor*

   The function should be a continuous, decreasing function of the probability of an event. If the probability of an event is lower, the surprise (or information content) should be higher. Conversely, if the probability of an event is higher, the surprise should be lower.

The only function that satisfies these two requirements is the logarithmic function

$$U(\mathcal{P}) = -c \log(\mathcal{P}), \tag{2.2}$$

where c is a freely chosen positive constant as it can always be eliminated through a change of base of the logarithm.

Proof. Our function $U(\cdot)$ should satisfy the functional equation $U(xy) = U(x) + U(y)$ and be differentiable at 1. Based on the first property, it can be deduced that $U(x \cdot 1) = U(x) + U(1)$, leading to the conclusion that $U(1) = 0$.

For $x \neq 0$, the derivative of the function U at x is calculated as follows

$$\begin{aligned} U'(x) &= \lim_{h \to 0} \frac{U(x+h) - U(x)}{h} = \lim_{h \to 0} \frac{U(x(1 + \frac{h}{x})) - U(x)}{h} \\ &= \lim_{h \to 0} \frac{U(x) + U(1 + \frac{h}{x}) - U(x)}{h} = \frac{1}{x} \lim_{h \to 0} \frac{U(1 + \frac{h}{x})}{\frac{h}{x}}. \end{aligned} \tag{2.3}$$

Given that $U(1) = 0$, this results in

$$U'(x) = \frac{1}{x} \lim_{h \to 0} \frac{U(1 + \frac{h}{x}) - U(1)}{\frac{h}{x}} = \frac{U'(1)}{x},$$

as $U'(1)$ was assumed to exists. Therefore, we can conclude that $U'(x)$ exists for all $x \neq 0$ and $U'(x) = \frac{U'(1)}{x} = -\frac{c}{x}$, where $c \geq 0$ is a constant, and the negative sign is due to Requirement 2.

In the case where $c = 0$, the function U would equal a constant a. However, as $U(1) = 0$, this constant must equal zero, resulting in $U(x) = 0$. On the other hand, if $c > 0$, the function U can be expressed as $U(x) = -c \ln |x| + a$. Given that $U(1) = 0$, it follows that $a = 0$, leading to the final conclusion $U(x) = -c \ln |x|$ for any $c \in \mathbb{R}^+$. The constant c can always be discarded by utilizing the change of base formula for logarithms

$$\log_b x = \frac{1}{\ln b} \ln x, \tag{2.4}$$

where c can be set to $c = \frac{1}{\ln b}$. $\qquad \square$

Let's denote the entropy of a system as $S = S(\mathcal{P})$, where $\mathcal{P}$ is a probability distribution. In our case, $\mathcal{P} = \{\mathcal{P}_1, \mathcal{P}_2, \ldots, \mathcal{P}_N\}$ represents the probabilities of N different outcomes in a discrete system. Thus, given that we wish to quantify the amount of information in any discrete system, the *Shannon entropy* $S(\mathcal{P})$ is simply the expectation value of $U(\mathcal{P})$, i.e. $S = S(\mathcal{P}) = \langle U(\mathcal{P}) \rangle$. Specifically, Shannon entropy is computed as a sum over all possible states of the system given our prior knowledge, and is given by

$$S = S(\mathcal{P}) = -\sum_{i=1}^{N} \mathcal{P}_i \ln(\mathcal{P}_i), \tag{2.5}$$

where we will use the natural logarithm throughout the thesis. Each value $\mathcal{P}_i$ can be interpreted as the probability of the system being in the ith state where N is the total number of possible states that can exist based on our current knowledge of the system. Thus, the Shannon entropy can be viewed as the knowledge the physicist possesses about the state of the system.

Importantly, $S(\mathcal{P})$ can be viewed as the physical resource required to encode the information that can be gathered from a particular measurement. For instance, if we set $c = \frac{1}{\ln(2)}$, then $S(\mathcal{P})$ would represent the number of binary digits (or bits) necessary to record the measurement's outcome. Given that the universe's resources are finite, it follows that the entropy of any measurement must likewise be finite.

2.1.1 Entropy and Measurement: An Illustration with a Deck of Playing Cards

To illustrate the connection between entropy, measurement, and knowledge of a state, let's consider a simple example involving a standard deck of 52 playing cards. In this case, we can define a

stochastic variable $X = \{X_s, X_n\}$, where X represents the state of the card, X_s represents the suit of a card (hearts, diamonds, clubs, or spades), and X_n represents the number of the card (1 through 10, Jack, Queen, King). Both X_s and X_n represent independent measurements that can be made on the state X.

Before any measurement is made, our knowledge about the state of the card is completely uncertain. The card could be any one of the 52 possibilities with equal probability. Therefore, the Shannon entropy of the system is given by

$$S(\mathcal{P}(X)) = -\sum_{i=1}^{52} \frac{1}{52} \ln\left(\frac{1}{52}\right) = \ln(52). \tag{2.6}$$

This represents the maximum entropy, corresponding to the maximum uncertainty about the state of the card known to us.

Now, suppose we perform a measurement of the suit of the card, X_s. This measurement reduces our uncertainty about the state of the card. Regardless of the outcome, we now know that the card is one of 13 possibilities (the number of cards in each suit). Therefore, the entropy of the system after this measurement is

$$S(\mathcal{P}(X|X_s)) = S(\mathcal{P}(X)) - S(\mathcal{P}(X)_s) = \ln(52) - \ln(4) = \ln(13). \tag{2.7}$$

The term $S(\mathcal{P}(X_s)) = \ln(4)$ represents the entropy of the suit measurement, which has four equally likely outcomes. The subtraction of $S(\mathcal{P}(X_s))$ from $S(\mathcal{P}(X))$ reflects the reduction in uncertainty about the state of the card due to the suit measurement.

Finally, suppose we perform a second measurement of the number X_n. This measurement further reduces our uncertainty about the state of the card. Regardless of the outcome, we now know the exact state of the card. Therefore, the entropy of the system after this measurement is

$$S(\mathcal{P}(X|X_s, X_n)) = S(\mathcal{P}(X|X_s)) - S(\mathcal{P}(X_n)) = \ln(13) - \ln(13) = 0. \tag{2.8}$$

The term $S(\mathcal{P}(X_n)) = \ln(13)$ represents the entropy of the number measurement, which has 13 equally likely outcomes. The subtraction of $S(\mathcal{P}(X_n))$ from $S(\mathcal{P}(X|X_s))$ reflects the further reduction in uncertainty about the state of the card due to the number measurement.

This example illustrates how entropy is tied to our knowledge of a system and how measurements can reduce entropy by increasing our knowledge. It also shows how the Shannon entropy formula can be used to quantify this knowledge in a discrete system.

2.1.2 Coin State Spaces

Building on the previous example with the deck of cards, let's consider another system that can illustrate the use of Shannon entropy in describing the knowledge we possess regarding physical states. This time, we will consider a system consisting of a strip of 100 coins, each of which can be in one of two states: heads or tails.

Suppose we have perfect knowledge of the system, knowing that the strip contains 100 heads and 0 tails. In this case, there is no uncertainty about the state of the system, and the entropy is zero. This is analogous to knowing both the suit and the number of a card in the deck.

However, suppose we know that the strip contains 99 heads and 1 tail, but we do not know the location of the tail along the coin strip. Given this information, there are 100 possible states for the system, and the entropy can be computed as

$$S = -\sum_{i=1}^{100} \mathcal{P}_i \ln(\mathcal{P}_i) = -\sum_{i=1}^{100} \frac{1}{100} \ln\left(\frac{1}{100}\right) = \ln(100), \tag{2.9}$$

assuming all configurations are equally likely. If we were to gain additional knowledge about the location of the tail, the entropy would reduce to 0, indicating perfect knowledge of the system. This highlights that the entropy of a system depends solely on the prior knowledge we have about it, and not on its actual state. The coins could be in the same configuration, but our entropy, i.e. our uncertainty, changes with our knowledge of the system.

If we have no prior knowledge about the system other than the fact that it consists of a strip of 100 coins, each with two possible outcomes, then there are 2^{100} possible states for the system, and the entropy can be computed as $S = \ln\left(2^{100}\right)$.

It is important to emphasize that knowledge of the state of any system can only be attained through empirical measurements. In this coin example, the state of the system is easily observable if one is allowed to look at the coins. However, other types of systems may be more difficult to measure, or may have several sources of uncertainty affecting the knowledge that one can possibly acquire about its state. Hypothetical knowledge, i.e., knowledge that is not based on something that is empirically possible to measure in principle, is strictly forbidden as it can lead to inconsistencies, as we shall see later.

2.1.3   Macroscopic Vs. Microscopic

Loosely speaking, macroscopic states pertain to the observable and measurable characteristics of a system on a large scale. These states can be directly perceived and quantified using conventional instruments and techniques. On the other hand, microscopic states refer to the states and configurations of individual constituents or smaller components that give rise the larger macroscopic system. In essence, macroscopic states represent the collective behavior and emergent properties of the system as a whole, while microscopic states delve into the detailed characteristics of its individual constituents. In this section, we illustrate the difference between macroscopic and microscopic states with a toy example. Again, we use the example of a strip of coins, but extend the strip to consist of M coins. Furthermore, we assume that the coins are independent and that there is a 50% chance of each coin being a tail, and denote the probability of a coin landing on tails as $P_t = 0.5$. Consider a macroscopic variable, T, representing the percentage of tails in a configuration of $M = 100$ coins. The variable T is macroscopic because for a particular value of T, say $T = 1\%$, there are $N = 100$ distinct microscopic states associated with it.

In general, the number of microscopic states of M coins corresponding to each macroscopic observed value of T is given by the function

$$N(T, M) = \binom{M}{T/100 \cdot M}.$$

The probability of T given M and P_t is thus binomially distributed, which can be approximated by a normal distribution as M becomes large and P_t is close to 0.5. The density curve is shown to the left in Figure 1 for $M = 100$, $M = 1,000$ and $M = 1,000,000$. We observe that the peaks are at $T = 50\%$, which means that the macrostate associated with $T = 50\%$ corresponds to the highest microstate count. It is evident that the tendency of the narrowing of the density curves increases with increasing number of coins M in the system, since the corresponding density curves become more narrow. In this example, what can be referred to as the equilibrium macrostate, is set to $T = 50\%$, since it is associated with the highest microstate count. This is also apparent in the right panel of Figure 1, where the probability of the equilibrium state in a small interval $\mathrm{d}T$ around $T = 50\%$ is plotted against the total number of coins, M, in the system. The graph shows that the probability of the equilibrium state approaches 1 for larger M.

This coin example shows that, for a system with a large number of coins, e.g. $M = 10^{23}$, assuming the equilibrium state $T = 50\%$, by neglecting all non-equilibrium states, is a good assumption without any other prior knowledge since most of the microstates correspond to this equilibrium macrostate. This is the principle on which the thermodynamic entropy definition relies, which is different to the definition of entropy considered in this thesis.
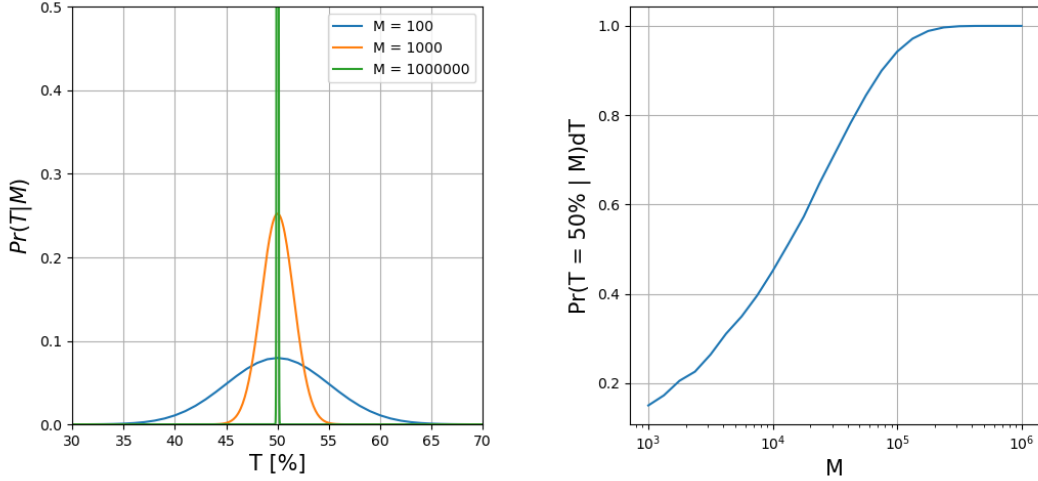
Figure 1: LEFT: Probability density function of the percentage of M independent coins that are tails, given by the variable T, when the probability of each coin being tail is 0.5. Note that the peaks are at $T = 50\%$ (the equilibrium state) and the density curves become more narrow as M increases. **RIGHT**: Probability of equilibrium state $T = 50\%$ for number of coins M in the system. The probability has been calculated from a small interval $\mathrm{d}T$ around $T = 50\%$, that has been kept constant for all M.

2.1.4 Connection to Thermodynamic Entropies

With the definition of Shannon entropy in (2.5), the entropy in thermodynamics is merely the entropy of the equilibrium macrostate, making it a special case of the Shannon entropy.

That is, the thermodynamic entropy measures the level of uncertainty associated with a system in equilibrium.

Consider a gas consisting of a given number of particles in a container, which we assume to be in an equilibrium state with a specified volume, temperature and pressure. Since thermodynamic quantities, such as temperature and pressure, are only defined for systems in equilibrium, the system must be in equilibrium for us to calculate its thermodynamic entropy accurately. The thermodynamic entropy then corresponds to the uncertainty linked with all possible microstates of the gas in equilibrium. That is, all other non-equilibrium states are excluded, similar to excluding states for which $T \neq 50\%$ in the coin example when the system consists of a large number of coins.

The connection between thermodynamic Gibbs entropy S_{TG} and Shannon entropy S can be elucidated by examining the definition of temperature. The temperature is defined as

$$\frac{1}{T} = \frac{\partial S_{TG}}{\partial E}, \tag{2.10}$$

where E represents the energy of the system and T denotes the temperature. It is crucial to stress that the thermodynamic Gibbs entropy (S_{TG}) must be considered as the entropy at thermodynamic equilibrium, as temperature is not well-defined for non-equilibrium systems. Furthermore, it is important to note that S_{TG} is an *intensive* quantity, expressed in units of Joules per Kelvin, whereas entropy as defined in this thesis is also an intensive quantity, but is dimensionless. Given that the units of Kelvin are derived from Celsius, which is based on the arbitrary standards set by humans (i.e., the boiling and freezing points of water at atmospheric pressure), the Boltzmann constant k_B serves as a bridge between the arbitrary unit of Kelvin and energy, which is based on the meter, second, and kilogram. Thus, the thermodynamic entropy acquires its meaning from Equation (2.10) through the very definition of temperature. Nonetheless, if one applies Shannon entropy S to Equation (2.10), temperature derives its meaning from more fundamental concepts, such as energy and entropy, according to the following relation

$$\beta = \frac{1}{k_B T} = \frac{\partial S}{\partial E}. \tag{2.11}$$

Here, β possesses units of inverse energy, signifying that entropy S is dimensionless and independent of the choice of units. The connection between the thermodynamic Gibbs entropy and Shannon entropy is that the former is only valid for equilibrium states, where $k_B S = S_{TG}$, whereas the latter is more comprehensive as it can be utilized in non-equilibrium states. There are additional differences between thermodynamic entropies and our modified definition using Shannon entropy that we will discuss in the subsequent sections. These differences are inherent to the empirical nature of measurement in our the entropy definition.

Lastly, we briefly compare the two forms of entropy utilized in thermodynamics: Boltzmann's entropy S_{TB} and Gibbs entropy S_{TG}, which are defined as

$$S_{TB} = k_B \ln(W) = k_B \ln \left(\frac{M!}{\prod_{i=1}^{N} m_i!} \right), \qquad S_{TG} = -k_B \sum_i \mathcal{P}_i \ln \mathcal{P}_i, \tag{2.12}$$

respectively. Boltzmann's entropy S_{TB} is an *extensive* measure that represents the variability of the state of particles of a single microstate in equilibrium, while Gibbs entropy describes the variability of microstates within a macrostate in an ensemble [37]. Here, W represents total number of possible permutations in which a total of $M = \sum_{i=1}^{N} m_i$ particles can occupy N distinct states within a microstate, where the ith state contains m_i particles. As a consequence, the probability of a randomly chosen particle in the microstate to occupy the ith state is denoted as $\mathcal{P}_i^* = \frac{m_i}{M}$.

Additionally, the Gibbs entropy is more general than the Boltzmann entropy, with the latter being a special case for situations where the number of states in an ensemble is large, and the individual states are independent and identically distributed. This kind of scenario allows us to express the probability of the ensemble microstate from the probabilities of its constituents as

$$\mathcal{P} = \prod_{i=1}^{M} \mathcal{P}_i^* = (\hat{\mathcal{P}}^*)^M, \tag{2.13}$$

where the product sum results from our independence assumption and $\hat{\mathcal{P}}^* = \mathcal{P}_i^*$ is a consequence of the identically distributed nature of the system. In such cases, the two entropies can be related by employing Stirling's approximation $\ln(M!) \approx M \ln(M) - M$ when $M \gg 1$, so that

$$S_{TB} = k_B \ln(W) \approx M S_{TG} = M k_B S. \tag{2.14}$$

Under Shannon's definition of entropy, where non-equilibrium states are can also be considered, zero entropy corresponds to the perfect specification of a state. This means perfect knowledge of the state of the system with the absence of uncertainties. Suppose we somehow *hypothetically* possessed the information regarding the positions and momenta of all particles in the aforementioned gas container at an arbitrary instant of time. In this case the entropy would correspond to zero. However, it should be emphasized that obtaining such information empirically is a completely different matter and will be discussed later.

2.1.5 Unit and Coordinate Independence

It is essential to note that the numerical value of the discrete Shannon entropy, defined in (2.5), is not influenced by the choice of units used to describe the system of interest. If we were to employ the standard deviation σ as a measure of variability instead of calculating the Shannon entropy, the numerical value of σ would be dependent on the arbitrary choice of units.

For instance, consider a 1D system with N possible distinct states, denoted by x_i, and corresponding probabilities $\mathcal{P}_i$ obtained based on system measurements. The calculation of the standard deviation yields

$$\sigma = \left(\sum_{i=1}^{N} \mathcal{P}_i (x_i - \mu)^2 \right)^{\frac{1}{2}}, \qquad \mu = \sum_{i=1}^{N} \mathcal{P}_i x_i.$$

The precise numerical value of the standard deviation depends on the units in which x_i is measured. If we perform a random variable substitution to introduce new units, such that the new variable $x_i' = Cx_i$, where C is an arbitrary scaling constant. The standard deviation in the new units, denoted by σ', is expressed in terms of the old units as $\sigma' = C\sigma$. Although a coordinate transformation changes the value of the standard deviation due to the altered units, its physical significance remains constant. This is because the variability is simply expressed in different units that represents the same physical quantity. However, this means that using standard deviation to compute the variability of a system necessitates the specification of a unit to convey its physical significance.

Entropy, on the other hand, is argued to be a much more fundamental quantity that is independent of the choice of units and is therefore dimensionless. As a result, the Shannon entropy given by (2.5) is unit-independent. This property arises from the fact that the exact values x_i are not used in the calculation of entropy. Instead, entropy depends solely on the probability distribution of the system and is expressed by the values $\mathcal{P}_i$ in formula (2.5). Because the natural logarithm is used, the resulting quantity is dimensionless. This property is crucial in physics. We will see that extending the discrete Shannon entropy to describe continuous state spaces indirectly introduces coordinate dependence, necessitating a specification of unit binning.

2.2 Hamiltonian Mechanics and Phase Space

In order to utilize our definition of entropy for physical systems, we introduce phase space within the framework of Hamiltonian mechanics, that provides a means to visualize and describe physical states in further discussions on entropy.

2.2.1 Phase Space Trajectories and Conservation of Energy

We will begin our discussion on Hamiltonian Mechanics by considering a single particle in 1D. The particle's motion is governed by a time-independent Hamiltonian $H(x, p)$, where x is the position and p is the canonical momentum. The equations of motion for this particle can be obtained by solving Hamilton's equations, which are given by

$$\frac{\mathrm{d}x}{\mathrm{d}t} = \frac{\partial H}{\partial p}, \qquad \frac{\mathrm{d}p}{\mathrm{d}t} = -\frac{\partial H}{\partial x}, \tag{2.15}$$

when provided with initial conditions $x(t_0)$ and $p(t_0)$ at a specific time t_0. The possible initial conditions corresponding to various combinations of $x(t_0)$ and $p(t_0)$ can be represented by points in phase space. We define an arbitrary vector $\boldsymbol{r}(t_0) = [x(t_0), p(t_0)]^\intercal$ that represents the initial conditions as a single point in phase space at a time t_0. The instantaneous temporal evolution of this phase space vector can be expressed as a vector field $\boldsymbol{S}(x, p) = \boldsymbol{S}(\boldsymbol{r})$ evaluated at any point in phase space. This vector field is given by

$$\boldsymbol{S}(x, p) = \frac{\mathrm{d}\boldsymbol{r}(t)}{\mathrm{d}t} = \begin{bmatrix} \frac{\mathrm{d}x}{\mathrm{d}t} \\ \frac{\mathrm{d}p}{\mathrm{d}t} \end{bmatrix} = \begin{bmatrix} \frac{\partial H}{\partial p} \\ -\frac{\partial H}{\partial x} \end{bmatrix},$$

which is obtained by direct substitution from Hamilton's equations.

Figure 2a shows a vector field $\boldsymbol{S}(\boldsymbol{r})$ as the green arrows, together with one specific integral curve (blue line) that follows the vector field, representing the trajectory of a particle starting with position $\boldsymbol{r}(t_0)$ in/at the upmost point on the blue line. The integral curve can be determined by following the vector field in discrete time steps of $\mathrm{d}t$. The position and momentum of the particle at a specific time t can be obtained by recursively applying

$$\boldsymbol{r}(t + \mathrm{d}t) = \boldsymbol{r}(t) + \boldsymbol{S}(\boldsymbol{r}(t))\,\mathrm{d}t,$$

at incremental points along the trajectory.
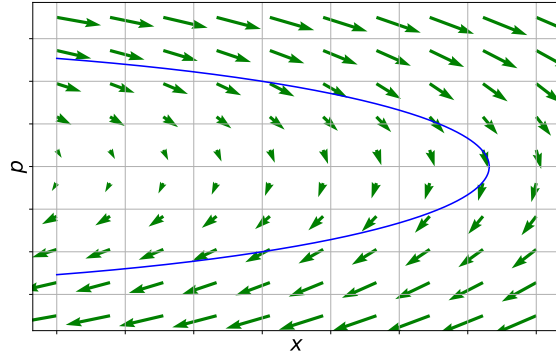
(a)
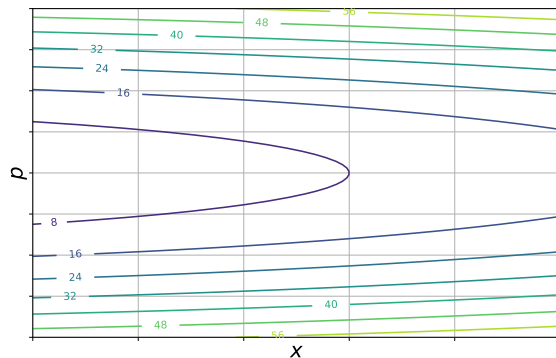
(b)

Figure 2: (a) A vector field $\boldsymbol{S}(\boldsymbol{r})$ in phase space, given by the green arrows, which corresponds to a time-independent Hamiltonian and is divergence free. One particular integral curve (blue line) is shown, representing the trajectory of a particle starting with position $\boldsymbol{r}(t_0)$ in/at the upmost point on the blue line. **(b)** Phase space trajectories for the same vector field corresponding to different values of the Hamiltonian. These curves thus form contours of the Hamiltonian.

In general, if the Hamiltonian is a function of position and momentum, $H(x, p)$, then the time derivative of the Hamiltonian along the phase space trajectory is given by

$$\frac{\mathrm{d}H}{\mathrm{d}t} = \frac{\partial H}{\partial x}\frac{dx}{dt} + \frac{\partial H}{\partial p}\frac{dp}{dt} = 0, \tag{2.16}$$

which shows that the value of the Hamiltonian is constant along any phase space trajectory in Hamiltonian mechanics. This is known as Hamilton's principle of conservation of energy. This leads to a set of trajectories that form contours of the Hamiltonian, as illustrated in Figure 2b, where the Hamiltonian values are drawn along each contour. It is worth noting that these trajectories never cross each other, which is a general condition resulting from the fact that the divergence of the vector field corresponding to the equations of motion is zero, i.e.

$$\boldsymbol{\nabla} \cdot \boldsymbol{S}(x, p) = \frac{\partial}{\partial x}\left(\frac{\partial H}{\partial p}\right) + \frac{\partial}{\partial p}\left(-\frac{\partial H}{\partial x}\right) = 0.$$

If this was not the case and trajectories were to cross, the resulting phase space trajectory associated with the equations of motion would not have a unique solution since one would not know which trajectory the particle would take.

To elaborate, suppose there were two trajectories crossing each other at a point $\boldsymbol{r_0} = [x_0, p_0]^{\intercal}$ in phase space, as shown in the right panel of Figure 3. If we were to solve for the phase space trajectory associated with the equations of motion using (2.15) and initial conditions corresponding

to the point of intersection $\boldsymbol{r_0}$, we would not have a unique solution since we would not know which of the two trajectories the particle would follow. In contrast, the left panel of Figure 3 illustrates trajectories that do not cross. In this case, the trajectory, given the point $\boldsymbol{r_0}$, is uniquely decided.
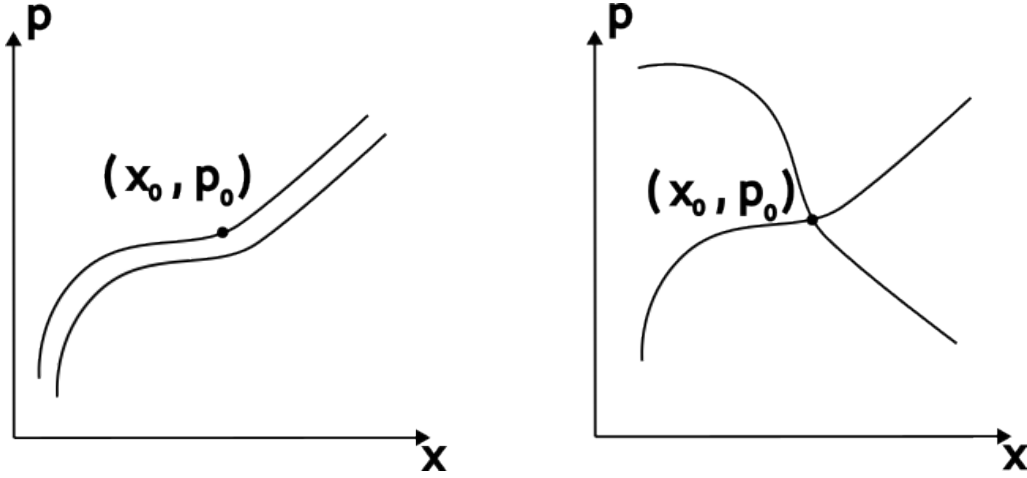
Figure 3: LEFT: Trajectories in phase space that do not cross, due to a divergence-free vector field. Note that the path from the point $\boldsymbol{r_0} = [x_0, p_0]^\intercal$ therefore is uniquely decided. **RIGHT:** Trajectories that cross, resulting from a vector field with non-zero divergence. Thus, the trajectory from the point $\boldsymbol{r_0} = [x_0, p_0]^\intercal$ does not have a unique solution.

Example

Consider a system comprising M particles moving in 3D. Here, the term 'phase space diagram' refers to a graphical representation of the system in a $6M$-dimensional space. Each dimension corresponds to a particular attribute of the particles, specifically, their position and momentum, contributing three dimensions each.
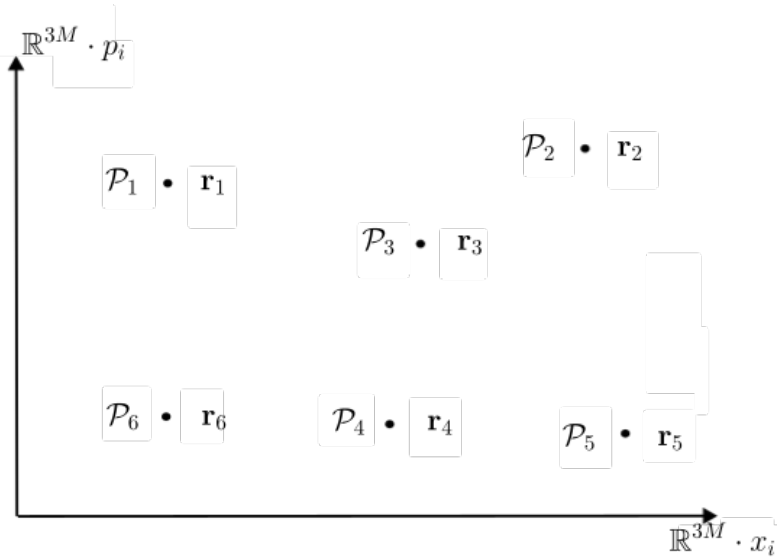
Figure 4: Illustration of $N = 6$ hypothetically possible states for a system of M particles in 3D. The possible states are represented by vectors $\boldsymbol{r}_i$ in a $6M$-dimensional phase space with corresponding probabilities $\mathcal{P}_i$ for $i = 1, \ldots, N$.

Consequently, a particular state i of all M particles at time t_0 corresponds to a single point in phase space and is represented by a $6M$-dimensional phase space vector $\boldsymbol{r}_i(t_0) = [\boldsymbol{x}_i^{(3M)}, \boldsymbol{p}_i^{(3M)}]^\intercal$. Here,

$\boldsymbol{x}_i^{(3M)}$ represents the vector of all position components for all M particles in state i and $\boldsymbol{p}_i^{(3M)}$ is the vector of all momentum components for all M particles in state i. Suppose we hypothetically measure the system and ascertain the presence of N possible states (points in phase space) at t_0, represented by $\boldsymbol{r}_i(t_0)$ for $i = 1, 2, \ldots, N$, with corresponding probability $\mathcal{P}_i$ of the system occupying the ith state. An example of some hypothetically possible states, given by points in phase space with associated probabilities, is illustrated in Figure 4 for $N = 6$. For a general system of particles in 3D as described here, the entropy of the system can then be written in the form of (2.5), i.e. $S = -\sum_{i=1}^{N} \mathcal{P}_i \ln(\mathcal{P}_i)$. The entropy of the system, in this discrete case, is independent of specific initial coordinates $\boldsymbol{r}_i(t_0)$ in phase space and thus would not change under a coordinate transformation.

3 Entropy for Continuous State Spaces

The Shannon entropy in (2.5) is a measure for the entropy of a discrete system. The process of extending the discrete Shannon entropy formula to continuous probability distributions is not straightforward. One reason for this complexity stems from the physical nature of information – that is, we have finite resources for recording the information about a physical state. This constraint is pivotal when considering the extension of Shannon entropy to continuous distributions. As we shall see, to maintain dimensional consistency within the continuous state space, it becomes necessary to introduce a smallest scale, or pixel size, in the state space.

To understand why, consider a probability density function $\rho(x)$ where the corresponding continuous random variable X has values in some interval A. Consequently, the probability density function has unit $[\rho] = [X]^{-1}$. Let Δ be a given quantity with the same dimension as $[X]$ (in case of a finite interval A, $|\Delta|M = |A|$ for some integer M). Let N be a positive integer, and define $\Delta x = \frac{\Delta}{N}$, as shown in Figure 5. We discretize the continuous probability distribution by defining

$$\mathcal{P}_i = \int_{i\Delta x}^{(i+1)\Delta x} \rho(x)\,\mathrm{d}x, \tag{3.1}$$

where $i \in Q$ for some index set Q. Here, the union of all intervals $\cup_{i \in Q}[i\Delta x, (i+1)\Delta x] = A$. Obviously, the set $\{\mathcal{P}_i\}$ defines a discrete probability distribution. As a consequence, both the sum of $\mathcal{P}_i$ and the integral of $\rho(x)$ can be written as

$$\sum_{i \in Q} \mathcal{P}_i = 1, \qquad \int_{-\infty}^{\infty} \rho(x)\,\mathrm{d}x = 1.$$

We adopt the convention that $\rho(x) = 0$ for all $x \notin A$. This allows us to use the discrete formula given by (2.5).
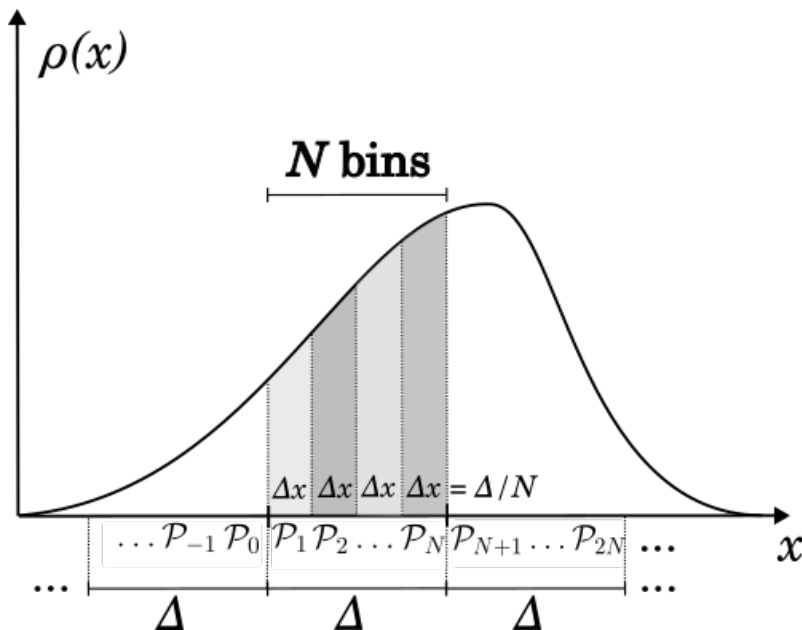
Figure 5: Illustration of set-up for the process of extending the discrete Shannon entropy to continuous state spaces. The graph shows the probability density function $\rho(x)$ for a continuous random variable X. Each unit of x, denoted by Δ, is divided into N smaller intervals (bins), each with length $\Delta x = \Delta/N$. The quantity $\mathcal{P}_i$ is the probability of obtaining x in the ith interval.

The Shannon entropy formula for continuous distributions, denoted as $S(\rho(x))$, is obtained from the discrete counterpart by defining the average probability density for each interval i as $\hat{\rho}_i = \frac{\mathcal{P}_i}{\Delta x}$

by applying the mean value theorem. Then, (2.5) becomes

$$-\sum_i \mathcal{P}_i \ln\left(\mathcal{P}_i\right) = -\sum_i \hat{\rho}_i \Delta x \ln\left(\hat{\rho}_i \frac{\Delta}{N}\right) = -\ln\left(\frac{1}{N}\right) - \sum_i \hat{\rho}_i \ln\left(\hat{\rho}_i \Delta\right) \Delta x. \qquad (3.2)$$

Here, we can see that $\Delta = 1[x]$ fixes the dimensional inconsistencies in Equation (3.2) that would arise from taking the natural logarithm of the probability density, which has units of the inverse of the random variable. Noticeably, the second term on the right-hand side of Equation (3.2) represents a Riemann sum, an integral approximation that sums products of function evaluations with interval lengths.

Taking the limit of Equation (3.2) as the number of discrete intervals N per unit of x goes to infinity results in

$$S(\rho(x)) = \lim_{N\to\infty}\left(-\sum_i \mathcal{P}_i \ln\left(\mathcal{P}_i\right)\right) = -\int_{-\infty}^{\infty} \rho(x) \ln\left(\rho(x)\Delta\right) \mathrm{d}x + \lim_{N\to\infty} \ln\left(N\right) = \infty.$$

This makes intuitive sense because as $N \to \infty$, the number of possible states becomes infinite since there are infinitely many numbers between 0 and 1 on the real number line. Consequently, infinite precision would be required to specify the entropy. To overcome this problem and therefore avoid the dire consequences of continuously performing Riemann sums, we introduce a 'pixel-based' definition of the continuous Shannon entropy, denoted by $S_I(\rho(x))$. This 'pixel-based' approach is defined as the entropy difference between the distribution of interest, $\rho(x)$, and a uniform distribution $\widetilde{\rho}_I(x) = (b-a)^{-1}$ over the interval $a \leq x \leq b$, where $I = b - a$ will later be identified as the pixel size, which will denote the length of the interval used to discretize the continuous distribution. Throughout the section, we will refer to $\widetilde{\rho}_I(x) = (b-a)^{-1}$ as the uniform reference distribution with a width corresponding to the pixel size I. The resulting pixel based continuous Shannon entropy is

$$S_I(\rho(x)) = S(\rho(x)) - S(\widetilde{\rho}_I(x))$$
$$= -\int_{-\infty}^{\infty} \rho(x) \ln\left(\rho(x)\Delta\right) \mathrm{d}x + \lim_{N\to\infty} \cancel{\ln(N)} + \int_a^b \frac{1}{I} \ln\left(\frac{\Delta}{I}\right) \mathrm{d}x - \lim_{N\to\infty} \cancel{\ln(N)},$$

where the terms containing the limits cancel each other. By noting that the term $\int_a^b \frac{1}{I} \ln\left(\Delta/I\right) \mathrm{d}x = \ln\left(\Delta/I\right) = -\ln\left(I/\Delta\right) \int_{-\infty}^{\infty} \rho(x)\,\mathrm{d}x$, this equation can be rewritten as

$$S_I(\rho(x)) = -\int_{-\infty}^{\infty} \rho(x) \ln\left(\rho(x)\Delta\right) \mathrm{d}x - \int_{-\infty}^{\infty} \rho(x) \ln\left(\frac{I}{\Delta}\right) \mathrm{d}x$$
$$= -\int_{-\infty}^{\infty} \rho(x) \ln\left(\rho(x)I\right) \mathrm{d}x. \qquad (3.3)$$

With the pixel size I, the continuous pixified Shannon entropy $S_I(\rho(x))$ of a probability density function $\rho(x)$ is the difference between the entropy of the distribution itself and the entropy of a uniform distribution on an interval of length I.

Hence, the integral in Equation (3.3) with pixel size I does not represent the uncertainty of a system with the probability distribution of $\rho(x)$, but rather the uncertainty of the system within the precision of a pixel size I, that is, the uncertainty compared to a uniform distribution of one pixel length. Thus, in our endeavor to extend the discrete definition of entropy to continuous state spaces, the pixel was forced upon us. In other words, to entertain the concept of continuous entropy, the presence of a pixel is indispensable.

We illustrate these ideas with an example. Suppose the random variable X has a normal distribution with mean $\mu = 3$ and variance $\sigma^2 = 4$, which has support on the interval $(-\infty, \infty)$. However, imagine that it is possible to measure the outcome so that we can narrow the outcome down to

an arbitrary interval of length 1 (corresponding to pixel size or precision $I = 1[x]$) with uniform distribution, e.g. on the interval $[1, 2]$. This is illustrated in Figure 6, where the normal distribution $\mathcal{N}(3, 4)$ and the uniform distribution on $[1, 2]$ are shown by the red and blue curves, respectively. From the figure, it makes intuitive sense that the information that the outcome is some place at the smaller interval $[1, 2]$ represents even more information (less uncertainty) than the broader normal distribution, since the uniform probability density function gives higher values, i.e. is more peaked. Thus, if I is the smallest possible interval for which it is possible to measure the outcome with the available equipment, this represents 'perfect' (as perfect as it can get) knowledge. The entropy $S_I(\rho(x))$ is then a measure of how large the 'extra' uncertainty, of the normal distribution in this case, is compared to the least uncertainty that is possible to achieve, which we assume to be given by a uniform reference distribution on an arbitrary interval of length I.
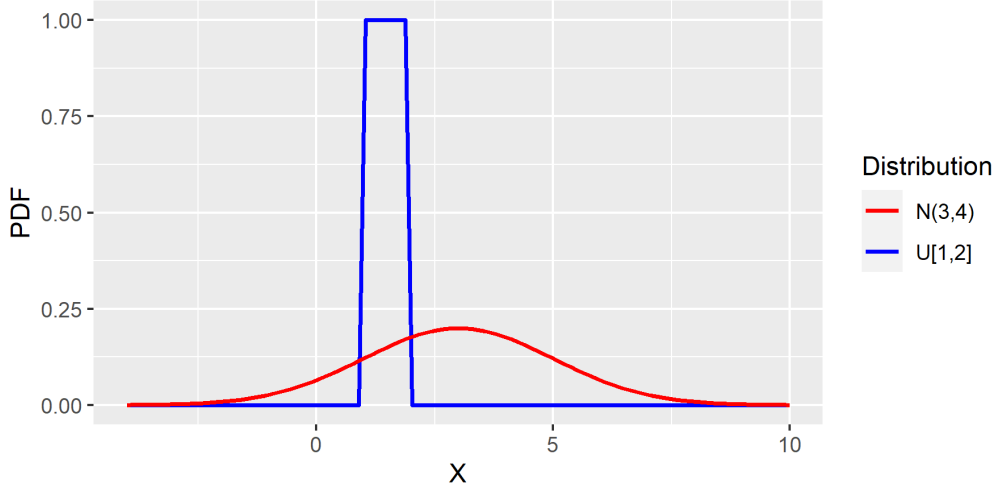
Figure 6: Illustrative example of interpretation of the pixified Shannon entropy for continuous state spaces, $S_I(\rho(x))$. A random variable X whose distribution is $\mathcal{N}(3, 4)$ (red curve) on $(-\infty, \infty)$, but can be measured to be on a smaller interval of length I, and is then assumed to be uniform on the interval. Here, the uniform distribution on $[1, 2]$ is shown by the blue curve. In this case, the entropy $S_I(\rho(x))$ represents the 'extra' uncertainty of the normal distribution compared to the more informative uniform distribution.

3.1   The Challenges of Continuous Entropy

As opposed to the discrete entropy, the continuous definition of entropy given in equation (3.3) entails two issues that need to be addressed:

1. The entropy value depends on the choice of coordinates

2. The entropy can have negative values.

These issues are illustrated in the subsequent sections.

3.1.1   Negative Entropy

To demonstrate the fact that the continuous entropy can obtain negative values, consider the distribution of interest of a continuous random variable X to be a uniform distribution $\rho(x) = \frac{1}{d-c}$ over the interval $c \leq x \leq d$. As before, let I be the pixel size of the uniform reference distribution. Using Equation (3.3), the pixified continuous entropy can be computed as follows:

$$S_I(\rho(x)) = -\int_{-\infty}^{\infty} \rho(x) \ln\left(\rho(x)I\right) \mathrm{d}x = -\int_{c}^{d} \frac{1}{d-c} \ln\left(\frac{I}{d-c}\right) \mathrm{d}x = \ln\left(\frac{d-c}{I}\right).$$

If $d - c = I$, then the uncertainty of the system is entirely contained within the pixel interval I, as illustrated in Figure 7a, resulting in $S_I = \ln 1 = 0$ as mentioned earlier. For interval lengths $d - c > I$, the entropy is positive, since the distribution of interest involves more uncertainty than the maximal information it is possible to obtain with a smaller interval I (Figure 7b). However, for $0 < d - c < I$, the entropy is negative, since, by definition, the pixel size I represents the uniform reference distribution against which we measure the 'extra' uncertainty of the distribution of interest. Thus, by hypothetically saying that one can measure x even more precisely than within an interval of size I, as illustrated in Figure 7c, this results in negative values for $S_I(\rho(x))$. The concept of negative entropy poses its own set of problems, which will be addressed in Section 3.4.

(a)

(b)

(c)
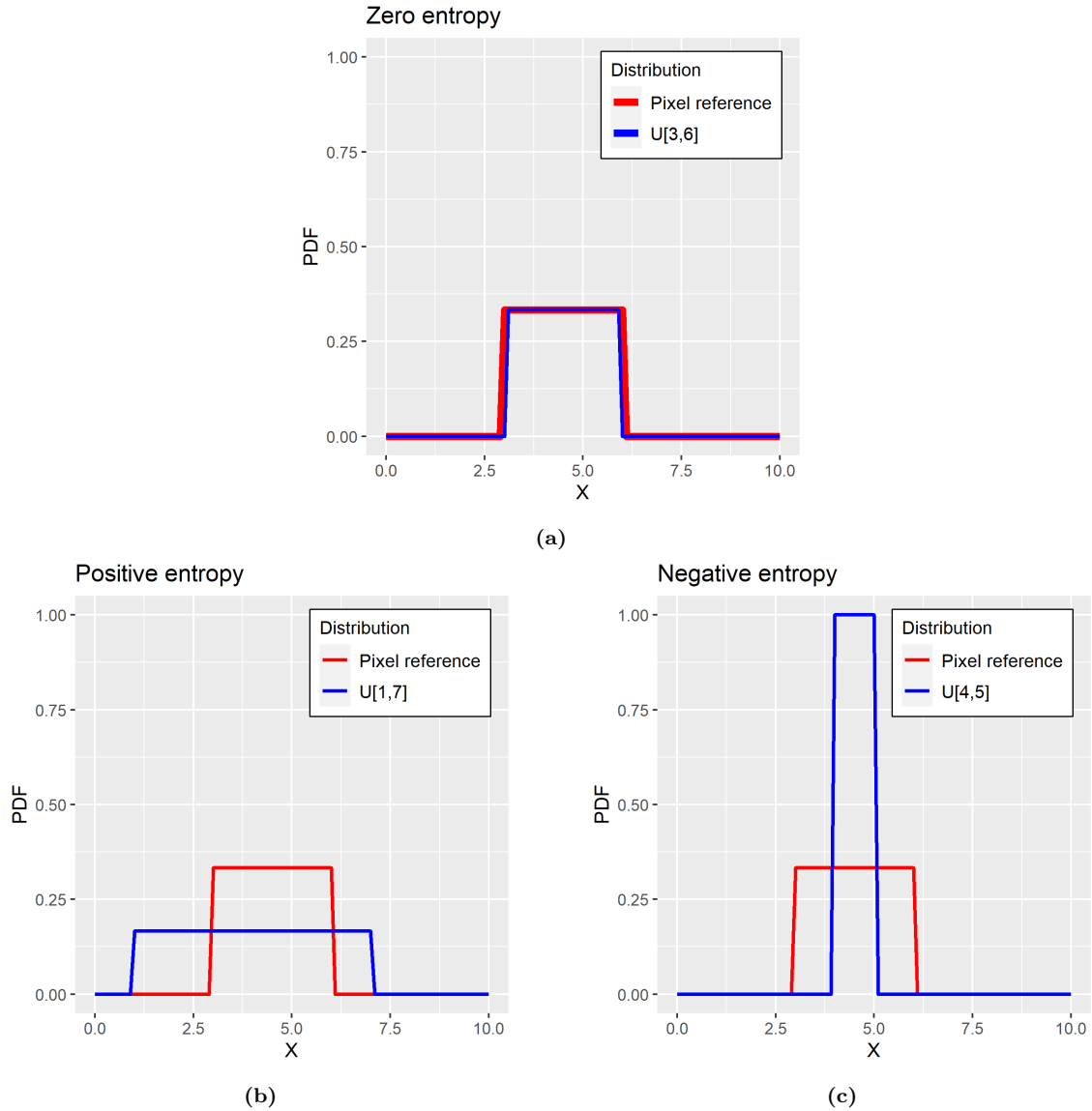
Figure 7: Illustration of zero, positive and negative entropy for continuous variables. The red curve shows a uniform reference distribution for a pixel size I, which is set to 3 here. The blue lines represent other uniform distributions on intervals that are **(a)** equal to, **(b)** larger or **(c)** smaller than the pixel reference I.

3.1.2 Coordinate Dependence Problem

Consider a continuous random variable X with density function $\rho_x(x)$, and let Y be a new random variable obtained from X via a variable substitution $Y = f(X)$. The probability density function

of Y, denoted by $\rho_y(y)$, is related to that of X via the Jacobian determinant as

$$\rho_x(x) = \rho_y(y) \left| \frac{\partial y}{\partial x} \right|, \tag{3.4}$$

which ensures that the integral of the probability density function over the support of the variable is equal to unity for both distributions, i.e.

$$1 = \int \rho_y(y)\, \mathrm{d}y = \int \rho_y(y) \left| \frac{\partial y}{\partial x} \right| \mathrm{d}x = \int \rho_x(x)\, \mathrm{d}x = 1.$$

Thus, the pixified Shannon entropy of the density function of x, $S_I(\rho_x(x))$, is equal to that of y, $S_I(\rho_y(y))$, up to a logarithmic term involving the Jacobian determinant. Specifically, a change of variable substitution given by (3.4) for a given pixel I, we have

$$
\begin{aligned}
-\int \rho_x(x) \ln\left(\rho_x(x) I\right) \mathrm{d}x &= -\int \rho_y(y) \left| \frac{\partial y}{\partial x} \right| \ln\left(\rho_y(y) \left| \frac{\partial y}{\partial x} \right| I \right) \mathrm{d}x \\
&= -\int \rho_y(y) \ln\left(\rho_y(y) I\right) \mathrm{d}y - \int \rho_y(y) \ln\left(\left| \frac{\partial y}{\partial x} \right|\right) \mathrm{d}y,
\end{aligned}
\tag{3.5}
$$

which shows that the continuous entropy is coordinate dependent.

It could be argued that the pixel size, I, can be interpreted as a uniform distribution of length I. This would result in a logarithm in Equation (3.5) of $\ln\left(\frac{\rho_x(x)}{\widetilde{\rho}I(x)}\right)$, and a change of variable would result in the Jacobian determinants of both distributions canceling each other out. This means that $\ln\left(\frac{\rho_y(y)\left|\frac{\partial y}{\partial x}\right|}{\widetilde{\rho}_I(y)\left|\frac{\partial y}{\partial x}\right|}\right) = \ln\left(\frac{\rho_y(y)}{\widetilde{\rho}_I(y)}\right)$, creating the illusion of coordinate invariance. In reality, this appearance of coordinate invariance is simply the result of adjusting the pixel size, or binning, appropriately to ensure that the entropy remains invariant. Re-expressing the pixel I as a uniform distribution results in the Kullback-Leibler divergence formula [21]. The Kullback-Leibler divergence also known as relative entropy, is a measure of the difference between two probability distributions. It is widely used in information theory and machine learning as a measure of the dissimilarity between two probability distributions.

The Kullback-Leibler divergence does not fully solve the problem of coordinate invariance since it is simply hiding the problem by making it explicit. In physics, the concept of coordinate independence is crucial. It stipulates that physical quantities and their laws should not depend on the chosen method of description. Simply put, all physical quantities must maintain their values, irrespective of how they are described. When the Kullback-Leibler divergence is employed, the entropy becomes dependent on the probability density $\widetilde{\rho}_I(x)$, which represents the bin density. This dependence on the bin density is not a problem from an information theoretic standpoint, but certainly is a problem in physics due to the argument of invariance of physical quantities, that demand generality as opposed to having the status of being a special case. This is because in the field of information theory, the continuous form of Shannon entropy is utilized to quantify the variability of elements within a distribution. As we have already witnessed, the entropy value may be negative if the variability is lower than the pixel size. Consequently, the entropy value is dependent on the unit of measurement and is not coordinate independent. To mitigate this issue, the choice of bin density can be made explicit through the use of Kullback-Leibler divergence, thereby seemingly giving the appearance of rendering the entropy value coordinate invariant. Despite this, it must be emphasized that the explicit choice of binning remains an arbitrary decision that ultimately corresponds to a choice of unit, and therefore, the entropy value is not truly coordinate independent. This concept holds significant importance in the realm of physics, where we shall come to see in Section 3.2.2 that in phase space, areas are preserved under canonical transformations, which means that it provides a manifold over which physical states exhibit true coordinate invariance, where the the pixel size is preserved during these transformations.

3.2 Entropy in Phase Space

We begin this section with an example of how entropy is conventionally regarded in phase space before we show that entropy is coordinate invariant under canonical transformation.

3.2.1 Example of Entropy in Phase Space

In physics, the specification of energy and entropy enables the solution of any system. In this example, we illustrate how entropy is usually regarded in phase space in classical physics in order to later understand the limitations of this approach.

Consider the setup depicted in Figure 8, where the upper part depicts a cannon tilted at an angle θ_0 relative to the ground and firing a cannon ball with magnitude of momentum p_0. We emphasize that these quantities are assumed to be the exact initial values, and the initial state (θ_0, p_0) is illustrated as a point in phase space (θ, p). The entropy of the initial state (θ_0, p_0) is then $S = 0$, reflecting the fact that the system's state is precisely known and devoid of any uncertainties. Since the initial state of the system is exactly known, one can also know exactly where the cannon ball lands (assuming that the angle and momentum are the only factors affecting the cannon ball).

Conversely, the configuration in the lower part of the figure, while almost identical to the upper, differs in that the state variables θ and p now have uncertainties $\Delta\theta$ and Δp, respectively, such that the initial state $(\theta_0, p_0) \rightarrow (\theta_0 \pm \Delta\theta, p_0 \pm \Delta p)$. This scenario, which involves uncertainty, is depicted as an area of size $4\Delta\theta\Delta p$ in phase space. Given that all states within the uncertainty bounds have an equal likelihood of representing the actual state of the system, the entropy becomes $S > 0$. This occurs because the system's state is no longer exactly known. The final state, i.e. the landing position of the cannon ball, is then also expected to be uncertain with $S > 0$, corresponding to multiple possible states, as all possible states within the bounds of the uncertainty are followed from initial states using Hamilton's equations. It will be demonstrated that, in Hamiltonian mechanics, entropy is always conserved. This is known as *Liouville's theorem*.

In classical physics, the exact state of a system is typically represented as a single point in phase space. This approach, however, has its limitations, as we shall demonstrate in the sections that follow.
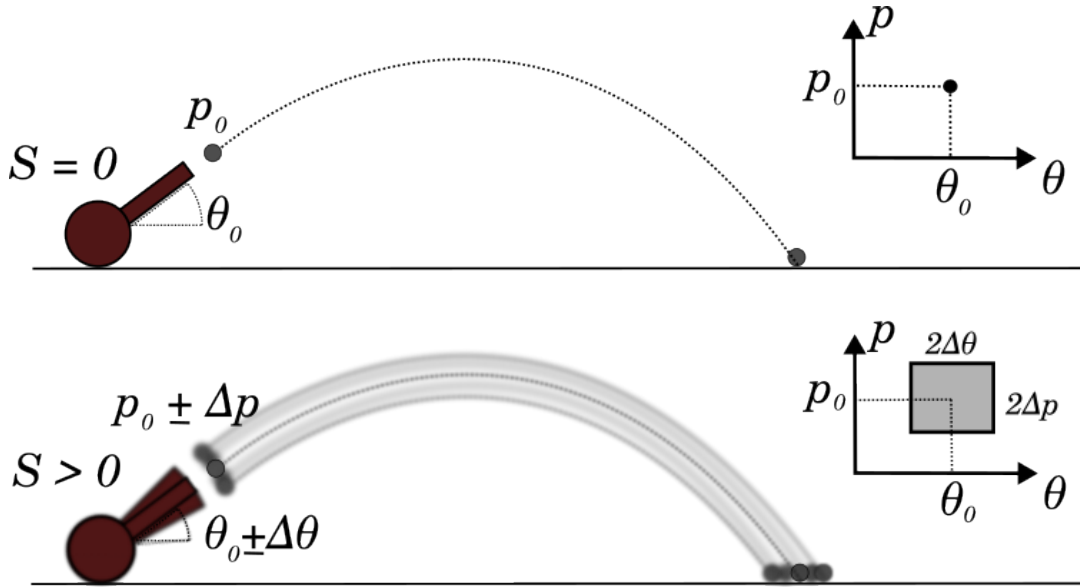
Figure 8: UPPER: A cannon tilted at an angle θ_0 relative to the ground, firing a cannon ball with magnitude of momentum p_0. The initial state, given by (θ_0, p_0), is considered to be exactly known, illustrated by a point in phase space. **LOWER:** The same setup, but with uncertainties $\Delta\theta$ and Δp associated with the initial state variables. The initial state is then $(\theta_0 \pm \Delta\theta, p_0 \pm \Delta p)$, illustrated as an area of size $4\Delta\theta\Delta p$ in phase space.

3.2.2 Entropy Coordinate Invariance in Phase Space

As discussed in Section 3.1.2, the coordinate dependence of entropy in continuous random variables poses a significant challenge. To address this issue, we introduce the concept of classical phase

space. This space, a symplectic manifold, offers a unique attribute - Shannon entropy quantities within it are invariant under coordinate transformations [37]. This section provides a mathematical demonstration of this property.

Consider an n-dimensional Hamiltonian system, given by the state variables $(\boldsymbol{x}, \boldsymbol{p})$, where $\boldsymbol{x} = (x_1, x_2, \ldots, x_n)^\intercal$ and $\boldsymbol{p} = (p_1, p_2, \ldots, p_n)^\intercal$. A change of canonical coordinates $(\boldsymbol{x}, \boldsymbol{p}) \rightarrow (\boldsymbol{X}, \boldsymbol{P})$, where $\boldsymbol{X} = (X_1, X_2, \ldots, X_n)^\intercal$ and $\boldsymbol{P} = (P_1, P_2, \ldots, P_n)^\intercal$, can be obtained through a canonical transformation. A purely positional coordinate transformation $\boldsymbol{X} = \boldsymbol{f}(\boldsymbol{x})$ through a function $\boldsymbol{f} = (f_1, f_2, \ldots, f_n)^\intercal$, that depends solely on position variables $\boldsymbol{x}$, implies that the conjugate momentum also transforms in a way that preserves the form of Hamilton's equations. Specifically, the ith component of $\boldsymbol{X}$ and $\boldsymbol{P}$ are then given by

$$X_i = f_i(x_1, x_2, \ldots, x_n) \implies P_i = \sum_j \frac{\partial x_j}{\partial X_i} p_j.$$

To show how the entropy in the new coordinates relates to the old, as in Equation (3.5), the determinant of the Jacobian is computed. The Jacobian matrix of the transformation is now a $2n \times 2n$ matrix, and its determinant is

$$|\boldsymbol{J}| = \left| \frac{\partial(\boldsymbol{X}, \boldsymbol{P})}{\partial(\boldsymbol{x}, \boldsymbol{p})} \right| = \begin{vmatrix} \frac{\partial \boldsymbol{X}}{\partial \boldsymbol{x}} & \frac{\partial \boldsymbol{X}}{\partial \boldsymbol{p}} \\ \frac{\partial \boldsymbol{P}}{\partial \boldsymbol{x}} & \frac{\partial \boldsymbol{P}}{\partial \boldsymbol{p}} \end{vmatrix} = \left| \frac{\partial \boldsymbol{X}}{\partial \boldsymbol{x}} \right| \left| \frac{\partial \boldsymbol{P}}{\partial \boldsymbol{p}} \right| - \left| \frac{\partial \boldsymbol{X}}{\partial \boldsymbol{p}} \right| \left| \frac{\partial \boldsymbol{P}}{\partial \boldsymbol{x}} \right| = \left| \frac{\partial \boldsymbol{X}}{\partial \boldsymbol{x}} \right| \left| \frac{\partial \boldsymbol{P}}{\partial \boldsymbol{p}} \right|,$$

where we have used that $\frac{\partial \boldsymbol{X}}{\partial \boldsymbol{p}} = \boldsymbol{0}$ in the last step, since $\boldsymbol{X} = \boldsymbol{f}(\boldsymbol{x})$ depends on the old positional coordinates only. Moreover, calculating the ij^{th} element of $\frac{\partial \boldsymbol{P}}{\partial \boldsymbol{p}}$ gives

$$\frac{\partial P_i}{\partial p_j} = \frac{\partial}{\partial p_j} \sum_k \frac{\partial x_k}{\partial X_i} p_k = \sum_k \frac{\partial x_k}{\partial X_i} \delta_{jk} = \frac{\partial x_j}{\partial X_i},$$

meaning that

$$\left(\frac{\partial \boldsymbol{P}}{\partial \boldsymbol{p}} \right) = \left(\frac{\partial \boldsymbol{x}}{\partial \boldsymbol{X}} \right)^\intercal.$$

Since the determinant is invariant to the transpose and by using the relation between the determinant of inverse matrices, we obtain

$$\left| \frac{\partial \boldsymbol{P}}{\partial \boldsymbol{p}} \right| = \left| \frac{\partial \boldsymbol{x}}{\partial \boldsymbol{X}} \right| = \frac{1}{\left| \frac{\partial \boldsymbol{X}}{\partial \boldsymbol{x}} \right|}.$$

Substituting this into the expression for the Jacobian determinant above yields

$$|\boldsymbol{J}| = \left| \frac{\partial \boldsymbol{X}}{\partial \boldsymbol{x}} \right| \frac{1}{\left| \frac{\partial \boldsymbol{X}}{\partial \boldsymbol{x}} \right|} = 1.$$

This ensures that $\rho_{xp}(\boldsymbol{x}, \boldsymbol{p}) = \rho_{XP}(\boldsymbol{X}, \boldsymbol{P})$, analogous to Equation (3.4). In other words, the probability densities are invariant under canonical transformations. Consequently, the entropy for the system given by $(\boldsymbol{x}, \boldsymbol{p})$ is related to the system given by the transformed variables $(\boldsymbol{X}, \boldsymbol{P})$ through

$$S_I(\rho_{xp}(\boldsymbol{x}, \boldsymbol{p})) = - \int \rho_{xp}(\boldsymbol{x}, \boldsymbol{p}) \ln \left(\rho_{xp}(\boldsymbol{x}, \boldsymbol{p}) I \right) \mathrm{d}\boldsymbol{x} \, \mathrm{d}\boldsymbol{p}$$

$$= - \int \rho_{XP}(\boldsymbol{X}, \boldsymbol{P}) \ln \left(\rho_{XP}(\boldsymbol{X}, \boldsymbol{P}) I \right) \mathrm{d}\boldsymbol{X} \, \mathrm{d}\boldsymbol{P} = S_I(\rho_{XP} \rho_{XP}(\boldsymbol{X}, \boldsymbol{P})),$$

where the symbol $I = \prod_i I_{x_i} I_{p_i}$ denotes the volume of the resolution pixel in $2n$-dimensional phase space. That is, the pixified continuous Shannon entropy is also invariant under canonical transformations. This is in contrast to the result in Equation (3.5), where the continuous entropy in general was shown to be coordinate dependent. Hence, the introduction of classical phase space with its inherent use of canonical transformations effectively resolves the issue of coordinate dependence. This significant finding establishes a solid basis for a more comprehensive understanding of entropy in phase space, paving the way for the next stage of our discussion.

3.3 Hirschman's Uncertainty Principle

The Hirschman uncertainty relation establishes a lower bound on the sum of temporal and spectral Shannon entropies for a function and its corresponding Fourier transform [60]. The introduction of this general result will prove to be valuable in our future discussions as we attempt to resolve the issue of negative entropy. Consider $\psi(x)$ as a function, and its Fourier transform, $\phi(k)$, which are interconnected via the following relations

$$\psi(x) = \frac{1}{\sqrt{2\pi}} \int_{-\infty}^{\infty} \phi(k) e^{ikx} dk, \tag{3.6}$$

and

$$\phi(k) = \frac{1}{\sqrt{2\pi}} \int_{-\infty}^{\infty} \psi(x) e^{-ikx} dx. \tag{3.7}$$

The function $\psi(x)$ is normalized, and due to Plancherel's theorem [74], its Fourier transform $\phi(k)$ is also normalized, i.e.

$$\int_{-\infty}^{\infty} |\phi(k)|^2 dk = \int_{-\infty}^{\infty} |\psi(x)|^2 dx = 1. \tag{3.8}$$

Consequently, $\rho_k(k) = |\phi(k)|^2$ and $\rho_x(x) = |\psi(x)|^2$ can be treated as probability densities. The lower bound for the sum of their continuous Shannon entropies with pixels of unit length is

$$S_I(|\phi|^2) + S_I(|\psi|^2) \equiv -\int_{-\infty}^{\infty} |\phi(k)|^2 \ln |\phi(k)|^2 dk - \int_{-\infty}^{\infty} |\psi(x)|^2 \ln |\psi(x)|^2 dx \geq \ln \pi e, \tag{3.9}$$

referred to as the Hirschman uncertainty principle. Initially conjectured by Hirschman [60], this principle was later substantiated by Beckner in 1975 [8].

In the context of the Hirschman uncertainty principle, the pixel size is not explicitly used in the entropy calculations. This is a consequence of the Fourier transform that relates the position and wavenumber distributions. The Fourier transform inherently carries a change of units, where the pixel size in the wavenumber space is the inverse of the pixel size in the position space. Therefore, the product of the pixel sizes in both spaces is dimensionless, which allows us to omit explicit mention of the pixel size in the entropy calculations. This is in contrast to other parts of this thesis where the pixel size is explicitly included in the entropy calculations. Furthermore, we can choose a normalization condition such that the pixel size is dimensionless and set to unity. This simplifies the entropy calculations without affecting the fundamental nature of the uncertainty relation.

We can reformulate the sum of the entropies presented in Equation 3.9 as follows

$$S_I(|\phi|^2) + S_I(|\psi|^2) = -\int_{-\infty}^{\infty} \int_{-\infty}^{\infty} \rho_k(k)\rho_x(x) \ln \left(\rho_k(k)\rho_x(x) \right) dk\, dx \geq \ln \pi e, \tag{3.10}$$

by regarding the square magnitudes of both functions as probability densities. The inequality becomes an equality, reaching saturation, when the function $\rho_x(x) = |\psi(x)|^2$ follows a Gaussian distribution. Given the characteristics of Equation (3.7), this suggests that $\rho_k(k) = |\phi(k)|^2$ is also Gaussian. Consequently, we obtain

$$-\int_{-\infty}^{\infty} \int_{-\infty}^{\infty} \rho_k(k)\rho_x(x) \ln \left(\rho_k(k)\rho_x(x) \right) dk\, dx = \ln \pi e. \tag{3.11}$$

3.4 Addressing Negative Entropy

In this section, we will establish why negative entropy is non-physical, and then present a potential solution to this issue. To overcome the issue of negative entropy, we redefine entropy as the empirical information about the state of a system, rather than hypothetical information. Recognizing that all empirical measurements inherently possess uncertainties, we propose the existence of a theoretical limit on the precision attainable in measuring the state of a system. This limit

has consequences for the calculation of entropy, particularly with respect to the pixel sizes in the continuous entropy definition. As such, only empirical observations can be incorporated into the entropy calculation, rather than hypothetical or theoretical considerations. This is attributed to the fact that hypothetical considerations of physical states can give rise to paradoxical phenomena, such as Maxwell's Demon.

3.4.1 Problem Associated With Negative Entropy

In this section, we argue why negative entropy is non-physical. Consider two independent systems, A and B, represented by density functions $\rho_A(x)$ and $\rho_B(y)$, respectively. Since the systems are independent, their joint distribution is $\rho_{AB}(x, y) = \rho_A(x)\rho_B(y)$. We set the pixel size for system A and B to be I_x and I_y, respectively, so that the two-dimensional pixel size is $I = I_{AB} = I_x I_y$. The entropy $S_{I,AB} = S_I(\rho_{AB}(x, y))$ of the joint systems can then be calculated as the sum of their individual entropies, which is shown by the following calculation

$$
\begin{aligned}
S_{I,AB} &= -\iint \rho_A(x)\rho_B(y) \ln\left(\rho_A(x)\rho_B(y)I_x I_y\right) \mathrm{d}x\,\mathrm{d}y \\
&= -\int \rho_A(x) \ln\left(\rho_A(x)I_x\right) \mathrm{d}x \int \rho_B(y)\,\mathrm{d}y - \int \rho_B(y)\ln\left(\rho_B(y)I_y\right)\mathrm{d}y \int \rho_A(x)\,\mathrm{d}x \\
&= S_{I_x,A} + S_{I_y,B}.
\end{aligned}
$$

The additivity property of entropy for independent systems is important for physical interpretation. This is not a inherent feature, but rather a necessity for any entropy formula. In the general case of an empty system, $\varnothing$, which contains nothing, the entropy is defined as zero, i.e. $S_\varnothing = 0$, as the state of the system is known exactly because there is nothing to specify. For any system D with corresponding entropy $S_D \geq 0$, the entropy of the combined system $D \cap \varnothing$ should be equal to the entropy of system D alone

$$
S_{D\varnothing} = S_D + S_\varnothing = S_D,
$$

in order for the concept of entropy to maintain a consistent physical interpretation.

However, when dealing with continuous state spaces, classical physics represents a perfectly specified state of a system as a single point $\boldsymbol{r}_0 = (x_0, p_0)_\mathsf{T}$ in phase space, depicted by a Dirac-delta function, $\delta(\boldsymbol{r} - \boldsymbol{r}_0)$. We denote this system by C, whose entropy can be given *informally* as

$$
S_{I,C} = -\int \delta(\boldsymbol{r} - \boldsymbol{r}_0) \ln\left(\delta(\boldsymbol{r} - \boldsymbol{r}_0)I\right) \mathrm{d}\boldsymbol{r} = -\infty. \tag{3.12}
$$

More formally, one would have to express the Dirac delta function as a limit of the Gaussian distribution

$$
\delta(\boldsymbol{r} - \boldsymbol{r}_0) = \delta(x - x_0)\delta(p - p_0) = \lim_{\epsilon \to 0^+}\left(\frac{1}{\epsilon\sqrt{2\pi}}e^{-\frac{(x-x_0)^2}{2\epsilon^2}}\right)\left(\frac{1}{\epsilon\sqrt{2\pi}}e^{-\frac{(p-p_0)^2}{2\epsilon^2}}\right), \tag{3.13}
$$

in the integral (3.12) by utilizing the limit in which the standard deviation $\epsilon \to 0^+$ from the positive side. Upon examining (3.12), it becomes apparent that the entropy diverges towards negative infinity. This implies a paradoxical situation where one has infinitely more knowledge about the state of the system compared to a system with a complete state description, which has zero entropy. In general, since entropy is characterized by being additive, negative values would not make physical sense, because the least one can add to an existing system, e.g. D, is no system at all, i.e. the empty system $\varnothing$ with $S_\varnothing = 0$. Thus, the contribution $S_{I,C} = -\infty$ to the total entropy of the joint system $D \cap C$ does not make physical sense. This is what we will refer to as the classical entropy problem.

3.4.2 Interplay Between Entropy and Standard Deviations in Phase Space

Given some constant value of entropy S_{I0}, we wish to find the probability density function $\rho = \rho(x, p)$ for which the product of the standard deviations of position and momentum, $\sigma_x \sigma_p$

is minimal. This can be accomplished by the method of Lagrange multipliers. We set up the Lagrangian function

$$L(x, p, \lambda_1, \lambda_2) = \sigma_x^2 \sigma_p^2 - \lambda_1 \left(\iint \rho \mathrm{d}x \mathrm{d}p - 1 \right) - \lambda_2 \left(- \iint \rho \ln \left(\rho I_x I_p \right) \mathrm{d}x \mathrm{d}p - S_{I0} \right), \qquad (3.14)$$

where $\sigma_w^2 = \iint \rho \cdot (w - \mu_w)^2 \mathrm{d}x \mathrm{d}p$ and $\mu_w = \iint w \rho \mathrm{d}x \mathrm{d}p$ for $w \in \{x, p\}$. The first constraint ensures that the total probability is equal to one, while the second constraint relates to the entropy of the system. Minimizing $\sigma_x^2 \sigma_p^2$ subject to these constraints involves finding the functional derivative of L with respect to ρ. The functional derivative, denoted as $\delta L / \delta \rho$, measures the change in the functional L due to a small change in the function ρ. We seek a solution for ρ such that the functional derivative vanishes, i.e., $\delta L / \delta \rho = 0$. This results in a 2D Gaussian distribution

$$\rho(x, p) = \rho_G(x, p) = e^{\frac{\lambda_1 - \lambda_2}{\lambda_2}} e^{-\frac{(x - \mu_x)^2 \sigma_p^2}{\lambda_2}} e^{-\frac{(p - \mu_p)^2 \sigma_x^2}{\lambda_2}} = \left(\frac{1}{\sqrt{2\pi} \sigma_x} e^{-\frac{(x - \mu_x)^2}{2\sigma_x^2}} \right) \left(\frac{1}{\sqrt{2\pi} \sigma_p} e^{-\frac{(p - \mu_p)^2}{2\sigma_p^2}} \right),$$

where the Lagrange multipliers λ_1 and λ_2 are determined by satisfying the constraints in (3.14). Observe that this density function can be written as a product, i.e. $\rho_G(x, p) = \rho_x(x) \cdot \rho_p(p)$, of two Gaussian distributions $\rho_x(x)$ and $\rho_p(p)$. This also implies independence between x and p in this particular case. We primarily focus on this case in this section and will consider a more general case in Section 7. The entropy of this 2D Gaussian distribution, using an arbitrary pixel size $I = I_x I_p$, is given by

$$S_{I0,G} = - \iint \rho_G \ln \left(\rho_G I_x I_p \right) \mathrm{d}x \mathrm{d}p = \ln \left(\frac{2\pi e \sigma_x \sigma_p}{I_x I_p} \right). \qquad (3.15)$$

Rearranging this equation yields

$$\sigma_x \sigma_p = \frac{\left(\frac{I_x I_p}{\pi e} \right)}{2} e^{S_{I0,G}}. \qquad (3.16)$$

It is crucial to emphasize that this expression is anticipated to signify an inequality, i.e.

$$\sigma_x \sigma_p \geq \frac{\left(\frac{I_x I_p}{\pi e} \right)}{2} e^{S_{I0}}, \qquad (3.17)$$

for general non-Gaussian distributions $\rho(x, p)$ with entropy S_{I0} that do not minimize (3.14). Nevertheless, saturation of the inequality, as given in (3.16), occurs when the joint probability distribution adheres to a two-dimensional Gaussian distribution.

3.4.3 The Relationship Between Pixel Size and Entropy in Phase Space

If the entropy in (3.16) is set to its lowest possible value $S_{I0} = 0$, the expression becomes

$$\sigma_x \sigma_p = \frac{\left(\frac{I_x I_p}{\pi e} \right)}{2}. \qquad (3.18)$$

In this case, the relation expresses how the pixel size $I_x I_p$ must vary with the spread of $\rho_G(x, p)$, represented by the standard deviations σ_x and σ_p, in order to maintain 'perfect' information $S_{I0} = 0$. Hypothetically, $\sigma_x \sigma_p$ can be made arbitrarily small, in which case the pixel size $I_x I_p$ must also decrease accordingly towards zero in order to maintain $S_{I0} = 0$.

If $\sigma_x \sigma_p$ theoretically is even smaller relative to $I_x I_p$ according to this relation, the entropy does not remain constant, and the entropy attains negative values instead. Therefore, the pixified entropy (of a 2D Gaussian distribution)

$$S_{I,G} = - \iint \rho_G(x, p) \ln \left(\rho_G(x, p) I_x I_p \right) \mathrm{d}x \, \mathrm{d}p, \qquad (3.19)$$

may hypothetically become negative, as we have seen in previous examples. However, due to the fact that $\rho_G(x, p)$ is determined empirically from the measurement of the system state, and all measurements by nature have associated uncertainties, σ_x and σ_p cannot be made arbitrarily small in practice. As a result, the pixel size $I_x I_p$ has an important physical interpretation; it must correspond to the pixel size related to the most precise measurement (i.e. smallest $\sigma_x \sigma_p$) possible to achieve in practice.

3.4.4 Theoretical Limit on Measurement Precision in Physics

Inherent to all physical measurements are uncertainties, indicating the existence of a theoretical limit to the precision attainable when measuring a system's state, independent of external factors, including the system's environment. We revisit Equation (3.18), which gives a lower bound of the product of standard deviation of position and momentum for a probability density $\rho(x,p)$. Let us suppose that this theoretical precision limit corresponds to an unknown constant $\Gamma = \frac{I_x I_p}{\pi e}$, i.e.

$$\min\left(\frac{I_x I_p}{\pi e}\right) = \Gamma.$$

By employing $I_x I_p = \pi e \Gamma$ as a pixel size, the entropy of an arbitrary phase space distribution $\rho(x,p)$ can be written as

$$S_I = -\iint \rho(x,p)\ln\left(\rho(x,p)\Gamma \pi e\right)\mathrm{d}x\,\mathrm{d}p. \tag{3.20}$$

Given that Γ represents the minimum precision limit, and $\rho(x,p)$ cannot be measured with higher precision than this limit, it follows that $S_I \geq 0$ by definition. This leads to the inequality:

$$\ln\left(\pi e\right) \leq -\iint \rho(x,p)\ln\left(\rho(x,p)\Gamma\right)\mathrm{d}x\,\mathrm{d}p, \tag{3.21}$$

which bears a striking resemblance to *Hirschman's uncertainty relation* in (3.10). Later, in Section 7, we will identify $\rho(x,p)$ with the Wigner function, $W(x,p)$, which satisfies inequality (3.21) for non-negative $W(x,p)$, i.e. $W(x,p) \geq 0, \forall x,p$. Alternatively, we can guarantee that (3.21) is satisfied by transitioning to Hilbert space using Hirschman's uncertainty relation, introducing $\psi(x)$ and its Fourier transform $\phi(p)$ such that

$$|\psi(x)|^2 = \int_{-\infty}^{\infty} W(x,p)\,\mathrm{d}p, \qquad |\phi(p)|^2 = \int_{-\infty}^{\infty} W(x,p)\,\mathrm{d}x, \tag{3.22}$$

which satisfies (3.21) due to the nature of the Fourier transform. We will discuss this in more detail in Section 7, but for now, we will elaborate on the special case involving a 2D Gaussian distribution.

Gaussian Special Case

Assuming the probability density in (3.20) is Gaussian, $\rho_G(x,p) = \rho_x(x)\rho_p(p)$, with the product of standard deviations given by $\sigma_x\sigma_p = \frac{\Gamma'}{2}$ for some Γ', we can compute the entropy of $\rho_G(x,p)$ using (3.15), resulting in

$$S_{I,G} = -\iint \rho_x(x)\rho_p(p)\ln\left(\rho_x(x)\rho_p(p)\Gamma\pi e\right)\mathrm{d}x\,\mathrm{d}p = \ln\left(\frac{2\pi e\left(\frac{\Gamma'}{2}\right)}{\Gamma\pi e}\right) = \ln\left(\frac{\Gamma'}{\Gamma}\right). \tag{3.23}$$

Thus, $\Gamma' \geq \Gamma$ is required to ensure that the entropy $S_{I,G} \geq 0$. For zero entropy states $S_{I,G} = 0$, which implies $\Gamma' = \Gamma$, the expression in (3.23) can alternatively be written as

$$-\iint \rho_x(x)\rho_p(p)\ln\left(\rho_x(x)\rho_p(p)\Gamma\right)\mathrm{d}x\,\mathrm{d}p = \ln\left(\pi e\right). \tag{3.24}$$

Similar to before, this equation closely resembles Hirschman's uncertainty formula, given by (3.11) for the Gaussian special case. Upon comparison, we can observe that a variable substitution $p \to k$ such that $\rho_k(k) = \left|\frac{\mathrm{d}p}{\mathrm{d}k}\right|\rho_p(p)$, where we identify $\Gamma = \left|\frac{\mathrm{d}p}{\mathrm{d}k}\right| \implies \mathrm{d}p = \Gamma\,\mathrm{d}k$, results in (3.24) being on the same form as (3.11). Thus, introducing and working with $\psi(x)$ and its Fourier transform $\phi(k)$ signifies a transition to Hilbert space, and implies that (3.24) can be indirectly satisfied by the nature of the Fourier transform. In this Gaussian special case, the functions $\psi(x)$ and $\phi(k)$ are related to the 2D Gaussian distribution through $\rho_G(x,p) = \rho_x(x)\rho_p(p) = \rho_x(x)\rho_k(k)/\Gamma$, where $\rho_x(x) = |\psi(x)|^2$ and $\rho_k(k) = |\phi(k)|^2$, as discussed in Section 3.3.

Connection to Quantum Mechanics

It is noteworthy that the expression in (3.17) shares a strong resemblance with the quantum mechanical uncertainty relation. When $S_{I0} = 0$, the limit of precision is delineated by $\left(\frac{I_x I_y}{\pi e}\right) = \Gamma$. In quantum mechanics, the energy E and momentum p are related to the angular frequency ω and the wave number k by the following relations

$$E = \hbar\omega, \qquad p = \hbar k, \tag{3.25}$$

where $\hbar$ is Planck's constant serving as the constant of proportionality.

By identifying our limit of precision with Planck's constant, such that $\Gamma = \hbar$, we establish a link between momentum and wave number, given by $p = \hbar k$, analogous to $p = \Gamma k$ in the previous discussion. Consequently, this elucidates that the distribution of k in Hirschman's uncertainty is connected to that of momentum as follows

$$|\phi(k)|^2 = \rho_k(k) = \left|\frac{\mathrm{d}p}{\mathrm{d}k}\right| \rho_p(p) = \hbar\rho_p(p),$$

in a manner that is consistent with the earlier analysis.

3.5   Connection to Hilbert Space and Quantum Mechanics

In Section 3.4.4, the utilization of a function $\psi(x)$ and its Fourier transform $\phi(k)$, which adhere to Equations (3.6), (3.7) and (3.8), was discussed in relation to phase space when defining a theoretical limit of presicion. This not only guarantees non-negative entropy, but also facilitates the introduction of a Hilbert space formulation to describe physical states. A more comprehensive examination of this is presented in Section 7.

3.5.1   Entropy Maximization in Gaussian Distributions

In this section, we investigate the properties of continuous probability distributions of a random variable X with a finite mean μ and variance σ^2, defined over the entire real line $(-\infty, \infty)$. Our goal is to identify the distribution $\rho(x)$ that exhibits the highest entropy for given values of variance σ^2 and mean μ. To achieve this, we utilize the method of Lagrange multipliers, which leads to the following functional

$$L(x, \lambda_1, \lambda_2) = -\int_{-\infty}^{\infty} \rho \ln(\rho)\, \mathrm{d}x - \lambda_1 \left(\int_{-\infty}^{\infty} \rho\, \mathrm{d}x - 1\right) - \lambda_2 \left(\int_{-\infty}^{\infty} (x-\mu)^2 \rho\, \mathrm{d}x - \sigma^2\right). \tag{3.26}$$

Upon setting the functional derivative $\delta L = 0$, we deduce that the resulting distribution is a Gaussian distribution

$$\rho(x) = \frac{1}{\sqrt{2\pi}\sigma} e^{-\frac{(x-\mu)^2}{2\sigma^2}}. \tag{3.27}$$

This result implies that the Gaussian distribution, also known as the normal distribution, possesses the highest entropy among all distributions defined over $(-\infty, \infty)$ with finite first and second moments. Conversely, for any specified entropy value S_{I0}, the Gaussian distribution will possess the minimal standard deviation when compared to all other distributions with finite first and second moments, which is congruent with the results in Section 3.4.2.

3.5.2   Incorporating Hirschman's Functions

Next, we consider a quantum mechanical wave function $\psi(x)$ in Hilbert space (analogously to $\psi(x)$ regarding Hirschman's uncertainty) with a squared magnitude that follows a Gaussian distribution with mean zero and standard deviation σ_x. This is given by

$$\psi(x) = \frac{1}{(2\pi\sigma_x^2)^{1/4}} e^{-\frac{x^2}{4\sigma_x^2}}, \qquad |\psi(x)|^2 = \frac{1}{\sqrt{2\pi}\sigma_x} e^{-\frac{x^2}{2\sigma_x^2}}. \tag{3.28}$$

The Fourier transform of $\psi(x)$ is defined as

$$\phi(k) = \frac{1}{\sqrt{2\pi}} \int_{-\infty}^{\infty} \psi(x) e^{-ikx} \, \mathrm{d}x = \left(\frac{2\sigma_x^2}{\pi} \right)^{1/4} e^{-k^2 \sigma_x^2}. \tag{3.29}$$

The squared magnitude of $\phi(k)$ is also a Gaussian distribution

$$|\phi(k)|^2 = \frac{1}{\sqrt{2\pi} \left(\frac{1}{2\sigma_x} \right)} e^{-\frac{k^2}{2\left(\frac{1}{2\sigma_x} \right)^2}} = \frac{1}{\sqrt{2\pi}\sigma_k} e^{-\frac{k^2}{2\sigma_k^2}}, \tag{3.30}$$

with mean zero and standard deviation $\sigma_k = \frac{1}{2\sigma_x}$. This result is quite general which means that it can also be derived with a non-zero mean μ as well. The product of these standard deviations satisfies the uncertainty relation since

$$\sigma_x \sigma_k = \frac{1}{2}. \tag{3.31}$$

Assuming that the momentum p and the wave number k are proportional to each other with a proportionality constant $\hbar$, such that $p = \hbar k$, we can derive the uncertainty relation in the context of Gaussian wave functions for x and p instead. Since $k \sim \text{Gaussian}(0, \sigma_k^2)$, we have $p \sim \text{Gaussian}(0, \sigma_k^2 \hbar^2)$. Multiplying both sides of Equation (3.31) by $\hbar$, and using that $\sigma_k \hbar = \sigma_p$, results in

$$\sigma_x \sigma_p = \frac{\hbar}{2}. \tag{3.32}$$

This equation represents the uncertainty relation for Gaussian wave functions, which highlights the inherent trade-off between the precision of position and momentum measurements in quantum mechanics. This implies that relating position to momentum through the Fourier transform ensures the preservation of the minimal pixel constraint.
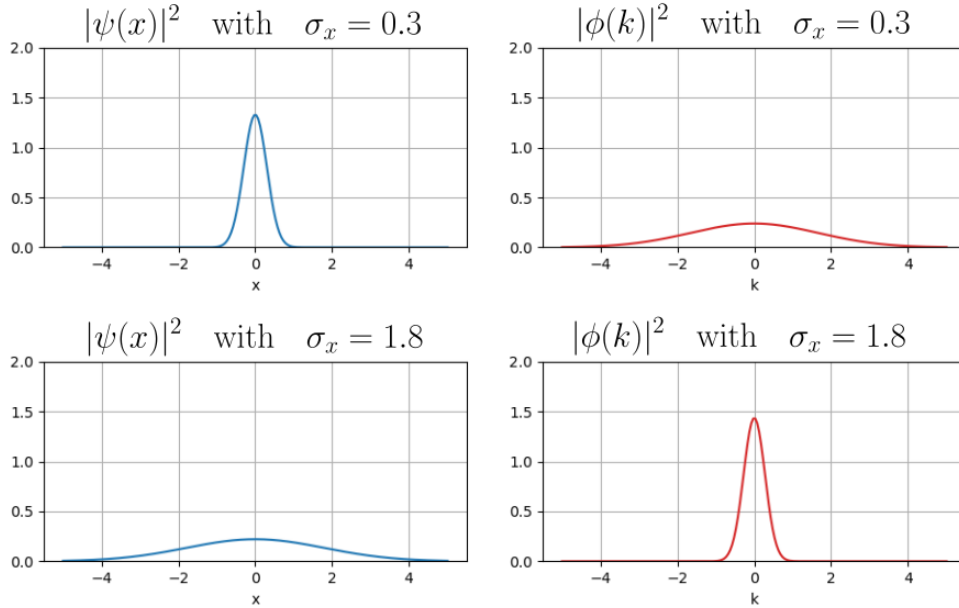
Figure 9: Trade-off between uncertainty of x and k. The density function of x is $|\psi(x)|^2 \sim \text{Gaussian}(0, \sigma_x^2)$, shown by the blue lines. The corresponding density function of k is $|\phi(k)|^2 \sim \text{Gaussian}(0, \sigma_k^2)$, shown by the red lines. **UPPER:** Density functions for x and k, where $\sigma_x = 0.3$, corresponding to $\sigma_k \approx 1.67$ through the uncertainty relation. **LOWER:** Density functions for x and k, where, $\sigma_x = 1.8$, corresponding to $\sigma_k \approx 0.28$.

Example: The relation (3.31) represents the joint uncertainty of x and k, as their standard deviations are multiplied. The trade-off between uncertainty of x and k is illustrated in Figure 9. In the upper part, the square magnitude of $\psi(x)$ is a Gaussian distribution with standard deviation $\sigma_x = 0.3$, which is shown by the blue line. With this standard deviation for x, and using (3.31), we

must have $\sigma_k = \frac{1}{2\sigma_x} = \frac{1}{2 \cdot 0.3} \approx 1.67$. In contrast to the more narrow distribution for x, this results in a broader distribution for k, shown by the red line. Similarly, setting $\sigma_x = 1.8$, corresponding to $\sigma_k \approx 0.28$, results in the distribution of x being broader (more uncertain) than the distribution of k, as shown in the lower part of the figure.

3.5.3 General Uncertainty Relation Through Fourier Analysis

The result in (3.31), derived for a Gaussian distribution $\rho_x(x) = |\psi(x)|^2$, shows that wave functions with this property saturate the general uncertainty relation

$$\sigma_x \sigma_k \geq \frac{1}{2}. \tag{3.33}$$

We emphasize that this inequality applies for any general probability distributions $\rho_x(x) = |\psi(x)|^2$ for the position x, but is saturated when ρ_x is Gaussian. In Sections 3.4.2 and 3.5.1, it was shown that the Gaussian distribution exhibits the smallest standard deviation for a given value of entropy, which provides an explanation for this.

Note that (3.33) is quite general and does not directly involve quantum mechanics. Applying the postulate $\hbar k = p$ from (3.25), we obtain in general that $\sigma_p^2 = \text{Var}(p) = \text{Var}(\hbar k) = \hbar^2 \text{Var}(k) = \hbar^2 \sigma_k^2$, or $\sigma_p = \hbar \sigma_k$. Multiplying both sides of (3.33) by $\hbar$ we obtain the uncertainty relation

$$\sigma_x \sigma_p \geq \frac{\hbar}{2},$$

for general probability distributions $\rho_x(x) = |\psi(x)|^2$. Similar to (3.33), this is saturated when ρ_x is Gaussian, as given by the result in (3.32), which sets the limit in (3.17) for $I_x I_p$ for which $S_{I0} = 0$. That is, the limit to how precisely one can measure a system is satisfied by the postulate that the momentum is proportional to the spatial Fourier wave number k, with constant of proportionality being $\hbar$.

3.5.4 Avoiding Negative Entropy Using Hilbert Space

By using the relation $p = \hbar k$, we use the following notation of the wave function of x and its Fourier transform throughout this section:

$$\psi(x) = \frac{1}{\sqrt{2\pi\hbar}} \int_{-\infty}^{\infty} \phi(p) e^{ipx/\hbar} dp, \qquad \phi(p) = \frac{1}{\sqrt{2\pi\hbar}} \int_{-\infty}^{\infty} \psi(x) e^{-ipx/\hbar} dx.$$

Employing the function $\psi(x)$ such that $\rho_x(x) = |\psi(x)|^2$ and relating it to $\phi(p)$ via the Fourier transform, where $\rho_p(p) = |\phi(p)|^2$, guarantees that the condition $S < 0$ cannot be achieved due to the inherent properties of the Fourier transform. This approach utilizes a Hilbert space representation of states, considering that $\psi(x)$ can be formulated as a linear combination of an infinite set of dimensionless orthogonal basis vectors $e^{ipx/\hbar}$, with $\phi(p)$ acting as the Fourier coefficients for the linear expansion.

To demonstrate that the set $e^{ipx/\hbar}$ constitutes orthogonal basis vectors, it is essential to establish that the inner product of any two distinct vectors within this set is zero. Let us consider two disparate wave vectors, p_1 and p_2, from the set, corresponding to the functions $e^{ip_1x/\hbar}$ and $e^{ip_2x/\hbar}$, respectively. Within square-integrable functions, the inner product of the functions f and g is defined as follows

$$\langle f, g \rangle = \int_{-\infty}^{\infty} f^*(x) g(x) \, dx. \tag{3.34}$$

Here, $f^*(x)$ denotes the complex conjugate of the function $f(x)$. To verify orthogonality, the inner product of the two aforementioned functions must be evaluated, so we calculate

$$\langle e^{ip_1x/\hbar}, e^{ip_2x/\hbar} \rangle = \int_{-\infty}^{\infty} e^{i(p_2-p_1)x/\hbar} \, dx = 2\pi\hbar\delta(p_2 - p_1). \tag{3.35}$$

Under this condition, the integral evaluates to a Dirac delta function which becomes zero when $p_1 \neq p_2$. This result confirms that the functions $e^{ipx/\hbar}$ are orthogonal in the Hilbert space of square-integrable functions for distinct values of p.

It is important to emphasize that the Hilbert space formulation provides a comprehensive framework for representing quantum states. This infinite-dimensional vector space is endowed with an inner product, facilitating the computation of probabilities and expectation values. The employment of orthogonal basis vectors ensures that the states preserve their orthogonality, offering a solid foundation for the representation and analysis of quantum systems.

In summary, the significance of the phase space pixel area in relation to a phase space distribution must be interpreted. One way to quantify the physical width of the distribution is through its standard deviation. The pixel size is associated with an area, which can be connected to probability distributions through the product of their standard deviations, given that these distributions have finite standard deviations. Each distribution has an associated entropy, particularly those with finite second moments. Among all distributions with a specified value of entropy, the Gaussian distribution exhibits the smallest possible standard deviation. As a result, the pixel area in phase space can be represented by $\hbar/2$, denoting the pixel as the smallest achievable product of standard deviations, i.e. $\sigma_x \sigma_p$, which ensures that the entropy is non-negative. Alternatively, the pixel may be represented by $I_x I_p = \hbar \pi e$, corresponding to the area of the narrowest uniform distribution attainable, which represents information corresponding to zero entropy.

The notion of the pixel bears a strong resemblance to the common understanding of a computer display. When enlarging an image on a display, more complexities are unveiled. Nevertheless, as the magnification process progresses, individual pixels become noticeable. Amplifying these pixels further does not reveal new information pertaining to the image, since each pixel consists merely of a single color. Consequently, the pixel denotes the constraints on the image's resolution.

In the context of phase space, the appearance of a pixel indicates that the resolution threshold of the physical states has been reached, suggesting that further subdivision into finer independent components is empirically unattainable. Each pixel represents the smallest unit that contains all the information that can be obtained empirically about the state. Thus, the pixel also represents a zero entropy state, where no further details can be extracted. This implies that subdividing the state into finer, independent parts would reveal new information, which is not possible because the state was assumed to possess zero entropy prior to its subdividing. In summary, the pixel encompasses the maximum amount of information that can be extracted through empirical means, highlighting the limitations of further subdivision.

4 Entropy and Epistemology in Science

The main topic of this section is to establish a proposition regarding the connection between entropy and empiricism for our entropy definition by arguing from an epistemological point of view. This proposition is then compared the description of physical states in quantum mechanics.

4.1 The Empirical Nature of Entropy

In science, the ultimate objective is to construct models with predictive capability. This is achieved through continuous refinement of existing models through empirical testing.

4.1.1 Objectivity of Science

In the realm of scientific inquiry, it is of paramount importance to maintain objectivity in all aspects, from observations to conclusions. This emphasis on objectivity is not simply derived from common sense but is instead rooted in philosophical foundations.

In the pursuit of accurate representations of reality within a chaotic environment characterized by diverse individual perspectives and belief systems, it is posited that scientific endeavors ought to prioritize objectivity. The attainment of objectivity plays a pivotal role in fostering a coherent comprehension of the world, with the present argument asserting that empiricism is the key to achieving objectivity.

The epistemological underpinnings of scientific investigation are grounded in empiricism, a philosophical perspective that posits that knowledge can only be acquired through measurable, observable, or independently verifiable phenomena. Within the context of empiricism, there is no allowance for subjective interpretation.

For instance, a question regarding the aesthetic appearance of a particular painting may elicit different opinions from different individuals, making the answer to such a question subjective, as it relies on whom is being consulted. Objectivity, on the other hand, is achieved through the use of empirical methods. Consider the assertion that "the average height of males exceeds that of females in Norway"—a statement deemed objective once particular concepts are delineated. These include defining height and its associated measurement protocol, providing a mathematical explication for the term 'average', and establishing the criteria for male and female classifications along with a method for differentiation. With these specifications, the aforementioned statement is considered objective, as it is universally agreed upon, independent of the individual being consulted. This is due to the fact that the natural world exists independently of how one chooses to perceive it. Consequently, the primary objective of scientific endeavors should be to concentrate on objective phenomena, which can be precisely delineated via empirical assessments which are inherently grounded in objectivity.

The challenge of eschewing subjectivity is not trivial, as humans possess a neural architecture, including the frontal lobes, that enables self-reflective cognition. Moreover, the presence of hormone-secreting glands influences our thought processes. Consequently, individuals are inherently predisposed to formulating subjective perceptions of their surroundings. While one may attribute value to their personal presuppositions, expecting others to adopt these singular paradigms is unrealistic. In essence, each individual possesses a distinct worldview, necessitating an objective approach to the scientific process.

4.1.2 The Empirical Nature of Predictions and the Pink Elephant

For a prediction of any physical theory to be considered empirical, it must be capable of being measured. Suppose, for instance, someone claims the existence of a pink elephant in the heart of Times Square. However, given that this particular elephant is invisible, intangible, odorless,

and inaudible, it is essentially undetectable. As a consequence, the hypothetical prediction of the existence of the pink elephant can not be validated empirically. In addition, information regarding its location, velocity, and weight should not be considered part of its entropy, as they are not empirically measurable. The idea behind this hypothetical example can be extended to other instances where certain features of physical systems are not possible to measure empirically. In general, such unattainable information should not play any part in the delineation of entropy.

4.1.3   The Role of Physics

Physics seeks to describe mathematical relationships between empirical measurements in order to make predictions about future observations. It should not be concerned with hypothetical predictions, but rather with constructing models that result in physically observable predictions. If some aspect of a prediction cannot be measured, it is not possible to claim to possess information about it. Our definition of entropy only encompasses information that has been obtained through empirical experiments. In other words, entropy represents the uncertainty in the measurable states of a system. Setting the entropy of a state of a system to be a specific value requires an action, i.e. a physical measurement.

Classical physics endeavors to describe the 'actual' idealized evolution of a system, including all of its immeasurable finer details of infinite precision. Classical physics therefore has an inherent entropy problem involving an infinite amount of immeasurable information regarding the physical systems it characterizes. However, information and entropy should not be focused on the 'actual' state of a system at these finer scales, but instead on what is theoretically measurable in practice. It is important to recognize that the term 'actual' is devoid of meaning, akin to the notion of a pink elephant, as neither is rooted in empiricism. Only empirical measurements grounded in physical reality can be objectively described. Therefore, the information pertaining to the entropy of a system should be restricted to solely encompass empirical measurements, i.e. what information can be obtained about a system through empirical experimentation in principle.

4.1.4   Uncertainties in Measurements

From a pragmatic perspective, each measurement, irrespective of the employed measuring instrument, inherently encompasses uncertainties. Utilizing more advanced instruments may result in reduced, albeit non-zero, uncertainties. However, eventually a threshold is reached, determining the extent to which the degree of precision in measurements is attainable. Beyond this scale, further enhancement of a state's precision becomes infeasible, and the physical theory should refrain from predicting such an overly precise state as an actual measurable state.

4.1.5   Mathematical Constructs and Reality

In scientific inquiry, it is important to recognize that many of the theories and models used are not actual representations of reality itself, but instead serve as useful mathematical constructs that provide physical predictions. This can be said to apply to fields, which are not real entities, but instead predict observations on a measuring instrument with the mathematical field serving merely as a tool for this purpose only. When considering such mathematical constructs, it is crucial to focus on what is actually measurable, namely the probability density of the physically measurable states used in the delineation of entropy.

Therefore, when presented with two equivalent theories, i.e. theories that yield the same physical predictions, it may be the case that one theory has a more complex inherent mathematical structure compared to the other. Despite this difference in mathematical complexity, the entropy of a particular system, given its state, should be independent of the choice of theory. This holds true even if the more complex theory appears to contain more information pertaining to its intricate mathematical structure. It is therefore essential that any theory establishes a clear connection between its mathematical structure and actual, real-world empirical measurements.

4.1.6 The Significance of Entropy in a Measurement Context

This marks a transition from asking questions about the true state of a hypothetical system to instead asking what can be learned about a system through empirical measurements in principle. It is important to remember that the only things we can observe are the results of experimental observations, and any inquiry beyond this is not productive. From this perspective, the concept of entropy is only meaningful when considered within a measurement context. Without the presence of a measurement, the notion of entropy becomes devoid of meaning.

In conclusion, acquiring particular information about any system necessitates collecting data via empirical measurements. The theoretical limit delineating the precision with which a system can be measured, in principle, establishes the size of the pixel for a continuous entropy representation. In order to even contemplate the concept of entropy for continuous state spaces necessitates the inclusion of a pixel size. Under our definition, entropy represents the measurable information pertaining to a physical system, implying that any physical theory should connect its theoretical and mathematical framework to real world empirical measurements, especially at smaller scales.

4.2 Understanding Entropy in Quantum Mechanics

In the context of this thesis, entropy is redefined to solely encompass empirical measurements, excluding any immeasurable entities. The following text aims to clarify the *measuring spin* example in quantum mechanics and establish a connection between the physical theory and empirical measurements, as opposed to describing the 'true' nature of things, which is typically done in classical physics.

4.2.1 Measuring Quantum Spin

Consider the typical example of measuring the spin of a particle using a detection apparatus. Upon setting the orientation of the apparatus, the measured spin on the apparatus can either display *up* or *down*, corresponding to values of -1 or 1, respectively. The quantum mechanical description of this scenario involves the wave function $|\Psi\rangle$, which can be expressed as a superposition of the up and down spin states

$$|\Psi\rangle = c_1|\uparrow\rangle + c_2|\downarrow\rangle. \tag{4.1}$$

Here, c_1 and c_2 are complex coefficients. The probabilities of measuring the spin up or down are given by the squared magnitudes of the coefficients, $|c_1|^2$ and $|c_2|^2$, respectively. It is crucial to note that the wave function Ψ does not represent the actual spin of the particle; rather, it describes the possible *measurement outcomes* that can be observed on the apparatus. Therefore, the state of the system is concerned with measurements and not the particle's spin itself.

Therefore, in this context, entropy is associated with the measurements 1 and -1, and not with any 'actual' spin state, whatever it might be, if there even is one. The true nature of the spin is irrelevant under the present definition of entropy, as the mathematical model should only be connected to empirical measurements. Attempting to describe the 'actual' spin of the particle is analogous to trying to describe the 'actual' position and mass of the hypothetical pink elephant. The primary focus should be on understanding the world through empirical measurements and not on uncovering the immeasurable inherent nature of things, which is what classical physics attempts to do. This shift in focus is essential for addressing the intrinsic entropy problem associated with classical approaches.

Again, revealing the true nature of things can only be accomplished through empirical measurements, and thus, uncovering nature is limited by the precision of the corresponding empirical measurements available. Therefore, entropy quantifies the variability of potential measurable states of a system. Since we have established that in the case of continuous state spaces, a continuous definition of entropy inherently demands a finite pixel size. This implies that the introduction of entropy to continuous state spaces automatically sets a limit on the precision of measurements at smaller scales, determined by the resolution of the pixel, however small it might be.

4.3 The Physics of the Pink Elephant

In the realm of classical physics, a notable issue arises concerning entropy. This challenge can be considered a defining characteristic of classical theories, as it results in a disconnect between the theoretical framework and empirical measurements. This challenge is most pronounced at smaller scales where classical physics predicts an infinite amount of immeasurable information (including immeasurable pink elephants), which can supposedly be measured independently of other factors, including the external environment. As the scale increases, the effective pixel size appears to approach zero ($\hbar \to 0$ implying infinitely small pixel size), rendering classical physics a seemingly reasonable approximation.

4.3.1 The Infinite Immeasurable States of Classical Physics

Within the purview of classical physics, it is indirectly postulated that an infinite number of immeasurable states are present within a minuscule region of phase space, denoted as $\mathrm{d}p\,\mathrm{d}x$. This premise stems from the assumption that the specified region contains an infinite number of points, implying the presence of an infinite amount of immeasurable information in the aforementioned phase space region. To quantify this immeasurable information associated with the continuous region, a continuous definition of entropy is required, which necessitates a pixel size, a notion not present in classical physics.

4.3.2 The Limitations of Classical Physics

This entropy issue results in the inability of classical theories to accurately predict physical measurements, ultimately relegating them to purely mathematical frameworks lacking any physical significance on smaller scales. To bridge this gap and enable a mathematical framework to describe physical phenomena, the definition of entropy, or measurable information (i.e., the physical measurements predicted by the theory), must be specified. This necessitates the inclusion of a finite pixel size, which is not an optional feature but rather a fundamental requirement for the continuous delineation of entropy.

4.3.3 The Emergence of Quantum Mechanics

The genesis of quantum mechanics can thus be perceived as a natural progression in addressing the entropy problem inherent in classical theories as will be discussed in more detail in Section 7. The introduction of a finite pixel size enables the mathematical framework to describe physical phenomena through the quantification of measurable information through entropy. This leads to the development of quantum mechanics as a means to address the limitations of classical physics.

Indeed, most endeavors in physics are driven by the ambition to sculpt mathematical models that faithfully represent empirical 'measurements'. However, it is the understanding of the fundamental concept of 'measurement' itself that gives birth to the foundations of quantum theory.

Part II

Bitemporal Causality and the Microcosm

The objective of this part is to utilize our consistent definition of entropy to analyze microscopic systems by examining Hamiltonian systems in phase space. We will demonstrate that Hamiltonian systems are inherently *deterministic* and *reversible*, with their time evolution characterized by the conservation of entropy and energy. Following this, we will delve into the nature of closed systems, demonstrating that entropy, according to our definition, cannot increase in a completely isolated system. Subsequently, we will explore the macroscopic notion that entropy appears to increase in systems. To unify these concepts, we introduce the Wigner-Moyal formalism—a Hamiltonian phase space framework that inherently incorporates the concept of a pixel in the theory as we will show. This formalism yields a mathematical construct equivalent to conventional quantum mechanics in Hilbert space. Understanding this framework becomes essential when discussing bitemporal electromagnetism and the antiphoton in subsequent sections. Lastly, we conclude this section by presenting the case of bitemporal causality in microscopic systems.

5 The Evolution of Hamiltonian Systems: Reversibility, Determinism and Entropy Conservation

This section will expand upon the concepts of Hamiltonian mechanics and phase space, introduced in Section 2.2, and integrate them with the new definition of entropy presented in Section 3. The objective is to demonstrate that a Hamiltonian system is characterized by *determinism* and *reversibility*, where both energy and entropy are conserved.

5.1 Determinism and Reversibility for Discrete and Continuous Systems

In this section, we provide definitions of the terms *determinism* and *reversibility* when describing the temporal evolution of systems. These concepts are important for understanding the behavior of physical systems over time, as they determine how the state of a system at a future time depends on its state at the present time, and vice versa. We first define these concepts for systems with discrete state spaces.

Definition 5.1. *Discrete Deterministic System: Let $r(t) = (x(t), p(t))$ be the phase space state representation of a discrete system at time $t \in \mathbb{Z}$. Furthermore, let $r(t_i)$ be the initial state of the system at time t_i and $r(t_f)$ the final state at time t_f, where $t_i < t_f$. A discrete system undergoing temporal evolution is considered to be deterministic iff, any final state $r(t_f)$, can be determined from an initial state $r(t_i)$ via a surjective function F, such that $F : r(t_i) \to r(t_f)$ which represents a mapping from an initial state to a final state.*

Definition 5.2. *Discrete Reversible System: Let $r(t) = (x(t), p(t))$ be the phase space state representation of a discrete system at time $t \in \mathbb{Z}$. Furthermore, let $r(t_i)$ be the initial state of the system at time t_i and $r(t_f)$ the final state at time t_f, where $t_i < t_f$. A discrete system is considered to be reversible iff, any initial state $r(t_i)$, can be determined from a final state $r(t_f)$ via a surjective function G, such that $G : r(t_f) \to r(t_i)$ which represents a mapping from an final state to a initial state.*

These definitions are limited to discrete systems. If equivalent definitions were to apply to systems with continuous state spaces, this would entail certain problems related to the earlier discussion on classical physics's assumption of infinite precision and the connection between entropy and empiricism.

Therefore, since every empirical measurement has an inherent uncertainty, determinism and reversibility are thus defined in relation to these uncertainties for systems with continuous state spaces,

as given by the following definitions:

Definition 5.3. *Continuous Deterministic System: A system in a continuous state space is defined as deterministic iff, any final finite element state $\hat{\rho}(\hat{x},\hat{p})\,\mathrm{d}\hat{x}\,\mathrm{d}\hat{p}$ at time t_f can be determined from an initial finite element state $\rho(x,p)\,\mathrm{d}x\,\mathrm{d}p$ via a surjective function F, such that $F: \rho(x,p)\,\mathrm{d}x\,\mathrm{d}p \to \hat{\rho}(\hat{x},\hat{p})\,\mathrm{d}\hat{x}\,\mathrm{d}\hat{p}$. Additionally, the differential phase space area of the final state must be less than or equal to that of the initial, i.e., $\mathrm{d}\hat{x}\,\mathrm{d}\hat{p} \leq \mathrm{d}x\,\mathrm{d}p$. This requirement implies that the probability density must satisfy $\hat{\rho}(\hat{x},\hat{p}) \geq \rho(x,p)$ in order for the integral of the probability density over all phase space to equal unity.*

Definition 5.4. *Continuous Reversible System: A system in a continuous state space is defined as reversible iff, any initial finite element state $\rho(x,p)\,\mathrm{d}x\,\mathrm{d}p$ at time t_i can be determined from a final finite element state $\hat{\rho}(\hat{x},\hat{p})\,\mathrm{d}\hat{x}\,\mathrm{d}\hat{p}$ via a surjective function G, such that $G: \hat{\rho}(\hat{x},\hat{p})\,\mathrm{d}\hat{x}\,\mathrm{d}\hat{p} \to \rho(x,p)\,\mathrm{d}x\,\mathrm{d}p$. Additionally, the differential phase space area of the final state must be greater than or equal to that of the initial, i.e., $\mathrm{d}\hat{x}\,\mathrm{d}\hat{p} \geq \mathrm{d}x\,\mathrm{d}p$. This requirement implies that the probability density must satisfy $\hat{\rho}(\hat{x},\hat{p}) \leq \rho(x,p)$ in order for the integral of the probability density over all phase space to equal unity.*
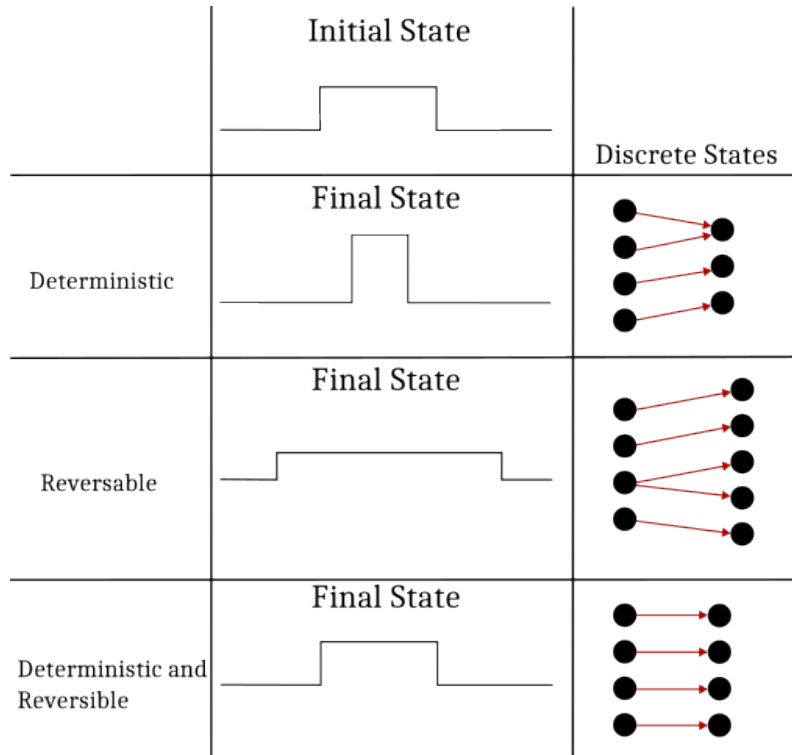
Figure 10: The time evolution of a system from an initial state to a final state can be characterized as either deterministic, reversible or both. For a deterministic system, any final state can be uniquely determined from the initial state via a surjective function. For a reversible system, on the other hand, any initial state is uniquely determined from the final state by a surjective function. If the system is both deterministic and reversible, the initial and final states are connected by a bijective function, i.e. a function that is one-to-one. In the middle column, an illustration of a continuous system is given by an initial state (represented as a uniform density function) at the top, followed by the final state for a deterministic system, reversible system and a both deterministic and reversible system, respectively. In the rightmost column, the relation between the initial state (dots to the left) and final state (dots to the right) is illustrated for a discrete system that is either deterministic, reversible or both. Here, the arrows represent the state mapping function.

The concepts of determinism and reversibility are illustrated in Figure 10 for continuous and discrete systems. For continuous systems, as illustrated in column in the middle, determinism and reversibility are defined in relation to uncertainties and the differential phase space area of the final and initial states represented by informal uniform distributions. A system represented in a continuous state space is considered to be deterministic if a unique mapping from its initial to final

state exists and the differential phase space area of the final state is less than or equal to that of the initial. Conversely, a system in a continuous states space is considered to be reversible if a unique mapping from its final to initial state exists and the differential phase space area of the final state is greater than or equal to that of the initial. Moreover, a system in a continuous state space is both deterministic and reversible if a *bijective* mapping between the initial and final state exists and the differential phase space area of the initial state and final state is equal. The equivalent of these concepts for discrete systems are illustrated in the rightmost column, where the dots to the left represent the initial state and the dots to the right represent the final state. The initial and final states are related by a mapping function, represented by the red arrows in the figure.

5.2 Reversibility and Determinism in Physical Systems

The principles of reversibility and determinism are central to the study of microscopic systems. In order to fully comprehend these properties, it is necessary to examine the requirements that must be met in order to truly exhibit them.

5.2.1 Requirements for Exhibiting Reversibility and Determinism

Consider a system represented by a distribution in the phase space $\rho(x, p)$. If the system is both reversible and deterministic, then the final distribution $\hat{\rho}(\hat{x}, \hat{p})$ must be a direct function of the initial distribution. However, this is not a sufficient condition for demonstrating the true nature of reversibility and determinism.

To truly exhibit these properties, it is necessary to also track each individual component of the distribution $\rho(x, p) \, \mathrm{d}x \, \mathrm{d}p$. This entails not only specifying the overall mapping of the distribution over time, but also the mapping of each specific element from the initial $\rho(x, p) \, \mathrm{d}x \, \mathrm{d}p$, to the final distribution $\hat{\rho}(\hat{x}, \hat{p}) \, \mathrm{d}\hat{x} \, \mathrm{d}\hat{p}$. The final state of each infinitesimal component must be uniquely linked to the initial state of each component.

Furthermore, the ability to track each component must be maintained throughout the evolution of the system. The information required to identify each component in the initial distribution must be equivalent to that required to identify the same component in the final distribution. This information can be quantified in terms of entropy.

5.2.2 Conservation of Distribution and Entropy

In the transformation of an infinitesimal component, two crucial elements must be conserved. The first is the contribution to the distribution, which must remain unchanged. If an initial element $\rho(x, p) \, \mathrm{d}x \, \mathrm{d}p$ in an infinitesimal area $\mathrm{d}x \, \mathrm{d}p$ constitutes a specific fraction of the entire distribution, this same fraction must be preserved in the final state distribution $\hat{\rho}(\hat{x}, \hat{p}) \, \mathrm{d}\hat{x} \, \mathrm{d}\hat{p}$.

Additionally, the contribution to the total entropy must also be conserved. The infinitesimal component must retain the same contribution to the total entropy in both the initial and final states.

This is due to the fact that, if the area were to expand, meaning $\mathrm{d}x \, \mathrm{d}p \leq \mathrm{d}\hat{x} \, \mathrm{d}\hat{p}$, then it is necessary that the probability density $\hat{\rho}(\hat{x}, \hat{p})$ decreases. However, if the probability density decreases, it would result in a change in its contribution to the entropy from its initial to final state. On the other hand, if the area were to contract, meaning $\mathrm{d}x \, \mathrm{d}p \geq \mathrm{d}\hat{x} \, \mathrm{d}\hat{p}$, the probability density $\hat{\rho}(\hat{x}, \hat{p})$ would increase, altering its contribution to the total entropy.

The only scenario in which both the contribution to the distribution and the contribution to the total entropy can be conserved is if the probability density remains constant, i.e. $\rho(x, p)$ evaluated at $\mathrm{d}x \, \mathrm{d}p$ equals $\hat{\rho}(\hat{x}, \hat{p})$ evaluated at the area of $\mathrm{d}\hat{x} \, \mathrm{d}\hat{p}$, and the area remains unaltered, meaning $\mathrm{d}\hat{x} \, \mathrm{d}\hat{p} = \mathrm{d}x \, \mathrm{d}p$. This underscores the significance of ensuring that the distribution and entropy are both conserved in a reversible and deterministic system.

5.2.3 Liouville's Theorem: The Evolution of the Phase Space Probability Density

Liouville's theorem, which is mathematically represented by Liouville's equation, governs the evolution of the probability density $\rho(x, p, t)$ in phase space. The equation is expressed as

$$\frac{\mathrm{d}}{\mathrm{d}t}\rho(x, p, t) = \frac{\partial}{\partial t}\rho(x, p, t) + \left(\frac{\partial \rho}{\partial x}\frac{\partial H}{\partial p} - \frac{\partial \rho}{\partial p}\frac{\partial H}{\partial x}\right) = 0, \tag{5.1}$$

where $\rho(x, p, t)$ is the probability density in phase space, t is time, $H(x, p)$ is the Hamiltonian of the system, and (x, p) are the phase space coordinates.

The equation can be rearranged and written in terms of the Poisson bracket as follows

$$\frac{\partial}{\partial t}\rho(x, p, t) = -\left(\frac{\partial \rho}{\partial x}\frac{\partial H}{\partial p} - \frac{\partial \rho}{\partial p}\frac{\partial H}{\partial x}\right) = -\{\rho, H\}. \tag{5.2}$$

These equations are often used to demonstrate the conservation of phase space volume along any trajectory following Hamilton's equations. The preservation of phase space volume in Hamiltonian systems will be further explored in the next section where we show the conservation of entropy, which is a stronger result. This is because it implies the conservation of information.

5.3 Conservation of Entropy

Here, the relationship between entropy and Hamiltonian mechanics is analyzed in order to show that entropy is conserved in *isolated system*.
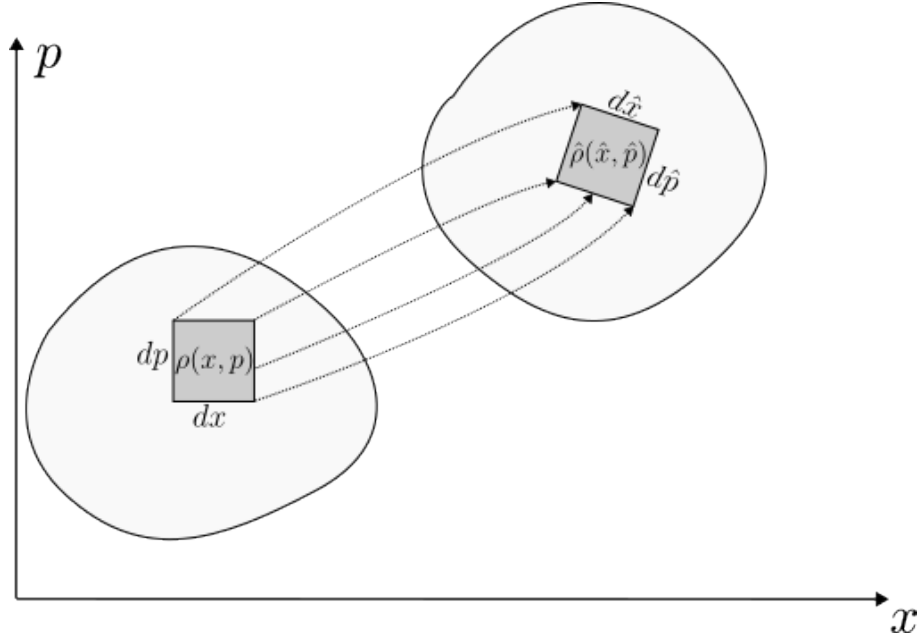
Figure 11: Time evolution of a system in phase space, represented by the evolution of the probability density $\rho(x, p)$ in each infinitesimal area $\mathrm{d}x\,\mathrm{d}p$ in the region of compact support to the time evolved distribution $\hat{\rho}(\hat{x}, \hat{p})$ in the area $\mathrm{d}\hat{x}\,\mathrm{d}\hat{p}$.

5.3.1 Hamiltonian Mechanics and Isolated Systems

Let a system be characterized by a probability density in phase space, denoted as $\rho(x, p)$, which is evolved over a time interval $\mathrm{d}t$, resulting in a transformed distribution $\hat{\rho}(\hat{x}, \hat{p})$, as illustrated in

Figure 11. The dynamics of the system are defined by the movement of each region in phase space, as determined by Hamilton's equations.

The fraction of the distribution that is contained within a small region $\mathrm{d}x\,\mathrm{d}p$ is quantified as $\rho(x,p)\,\mathrm{d}x\,\mathrm{d}p$. Following a brief time step $\mathrm{d}t$, the new coordinates resulting from Hamiltonian evolution are given by the following equations

$$
\begin{aligned}
\hat{x} &= x + \frac{\mathrm{d}x}{\mathrm{d}t}\,\mathrm{d}t = x + \frac{\partial H}{\partial p}\,\mathrm{d}t,\\
\hat{p} &= p + \frac{\mathrm{d}p}{\mathrm{d}t}\,\mathrm{d}t = p - \frac{\partial H}{\partial x}\,\mathrm{d}t.
\end{aligned}
\tag{5.3}
$$

The density and volume change according to the Jacobian of the transformation, represented by $|\boldsymbol{J}|$, is given by

$$
|\boldsymbol{J}| = \left\|\begin{matrix} \frac{\partial \hat{x}}{\partial x} & \frac{\partial \hat{x}}{\partial p} \\ \frac{\partial \hat{p}}{\partial x} & \frac{\partial \hat{p}}{\partial p} \end{matrix}\right\| = \frac{\partial \hat{x}}{\partial x}\frac{\partial \hat{p}}{\partial p} - \frac{\partial \hat{p}}{\partial x}\frac{\partial \hat{x}}{\partial p} = \{\hat{x}, \hat{p}\},
\tag{5.4}
$$

where $\{\cdot,\cdot\}$ is the Poisson bracket. The final density and volume are given by

$$
\mathrm{d}\hat{x}\,\mathrm{d}\hat{p} = |\boldsymbol{J}|\,\mathrm{d}x\,\mathrm{d}p, \qquad \hat{\rho}(\hat{x},\hat{p}) = \frac{\rho(x,p)}{|\boldsymbol{J}|}.
\tag{5.5}
$$

Combining the Jacobian definition in Equation (5.4) with the time-evolved coordinates in (5.3), yielding

$$
\begin{aligned}
|\boldsymbol{J}| &= \left\|\begin{matrix} \frac{\partial x(t+\mathrm{d}t)}{\partial x} & \frac{\partial x(t+\mathrm{d}t)}{\partial p} \\ \frac{\partial p(t+\mathrm{d}t)}{\partial x} & \frac{\partial p(t+\mathrm{d}t)}{\partial p} \end{matrix}\right\| = \left\|\begin{matrix} 1 + \frac{\partial}{\partial x}\left(\frac{\mathrm{d}x}{\mathrm{d}t}\right)\mathrm{d}t & \frac{\partial}{\partial p}\left(\frac{\mathrm{d}x}{\mathrm{d}t}\right)\mathrm{d}t \\ \frac{\partial}{\partial x}\left(\frac{\mathrm{d}p}{\mathrm{d}t}\right)\mathrm{d}t & 1 + \frac{\partial}{\partial p}\left(\frac{\mathrm{d}p}{\mathrm{d}t}\right)\mathrm{d}t \end{matrix}\right\| \\
&= 1 + \left(\frac{\partial}{\partial x}\frac{\partial H}{\partial p} - \frac{\partial}{\partial p}\frac{\partial H}{\partial x}\right)\mathrm{d}t + \mathcal{O}(\mathrm{d}t^2) \approx 1.
\end{aligned}
\tag{5.6}
$$

It is demonstrated that the phase space volume element $\mathrm{d}\hat{x}\,\mathrm{d}\hat{p} = \mathrm{d}x\,\mathrm{d}p$ remains unchanged and the final density is equal to the initial density $\hat{\rho}(\hat{x},\hat{p}) = \rho(x,p)$. The calculation of the entropy of the final distribution shows that it is equal to the entropy of the initial distribution

$$
\begin{aligned}
-\iint \hat{\rho}(\hat{x},\hat{p})\ln\left(\hat{\rho}(\hat{x},\hat{p})I_x I_p\right)\mathrm{d}\hat{x}\,\mathrm{d}\hat{p} &= -\iint \frac{\rho(x,p)}{|\boldsymbol{J}|}\ln\left(\frac{\rho(x,p)}{|\boldsymbol{J}|}I_x I_p\right)|\boldsymbol{J}|\,\mathrm{d}x\,\mathrm{d}p \\
&= -\iint \rho(x,p)\ln\left(\rho(x,p)I_x I_p\right)\mathrm{d}x\,\mathrm{d}p + \underset{0}{\underbrace{\iint \rho(x,p)\ln(|\boldsymbol{J}|)\,\mathrm{d}x\,\mathrm{d}p}}.
\end{aligned}
\tag{5.7}
$$

This equation shows that the entropy of the final distribution is equal to the entropy of the initial distribution, plus the expectation of the logarithm of the Jacobian. Since the evolution is Hamiltonian, the Jacobian is unitary and its logarithm is therefore zero. Thus, the entropy of the final distribution is that of the initial distribution. The entropy is therefore conserved, as expressed by the equation

$$
S(\rho(x(t), p(t), t)) = S(\rho(x(t+\mathrm{d}t), p(t+\mathrm{d}t), t+\mathrm{d}t)).
\tag{5.8}
$$

5.3.2 From Entropy Conservation to Hamiltonian Systems

Conversely, given that the evolution of a system $\rho(x, p)$ is such that the entropy is conserved. This hold true if and only if the logarithm of the Jacobian is equal to zero everywhere, which occurs when the Jacobian is equal to one. This can be observed in Equation (5.6) where the condition for entropy conservation is given by the following condition

$$\left(\frac{\partial}{\partial x} \frac{\partial H}{\partial p} - \frac{\partial}{\partial p} \frac{\partial H}{\partial x} \right) = \boldsymbol{\nabla} \cdot \boldsymbol{S} = 0. \tag{5.9}$$

This implies that the displacement vector field $\boldsymbol{S}$ is divergence-free, admitting a potential $H(x, p)$, resulting in Hamilton's equations (2.15) where energy is also conserved as all trajectories are contours of $H(x, p)$. Therefore, the conservation of entropy implies energy conservation and vice versa. In summary, we have shown that the evolution of a distribution over position and momentum in phase space according to Hamiltonian mechanics conserves entropy. Conversely, if a system conserves entropy, it must have a unitary Jacobian, which is the case for Hamiltonian systems, which in turn conserve energy.

Therefore, we have shown that conservation of energy in isolated systems can be traced back to the conservation of entropy. The entropy, quantifying the information content, remains constant in an isolated system. This constancy results in a specific relationship between the system's temporal evolution and the information it contains. This relationship results in the evolution of the system according to Hamiltonian mechanics, where energy conservation is an intrinsic property. This result highlights the fundamental connection between entropy and Hamiltonian mechanics in isolated systems and the importance of entropy conservation in understanding their behavior. It should be noted that the concept of entropy conservation can be extended to systems with multiple independent degrees of freedom [14].

5.3.3 Classical Physics and the Problem of Unmeasurable Information

The conservation of entropy is synonymous with the conservation of information. This concept highlights a major drawback of classical physics, which is the assumption of an infinite amount of information content and infinite precision within a system. This assumption leads to internal inconsistencies, since the additional immeasurable information pertaining to an arbitrary *mathematical model* that describes the evolution of the system cannot be measured and is therefore non-empirical. It is imperative that mathematical models of physical systems be based on empirical inputs and hence produce empirical predictions as outputs. Any additional details pertaining to the physical model that does not result in empirical predictions should not be considered as physical information that is inherent to the system. Making predictions about something that cannot be measured is akin to predicting the presence of a pink elephant in the heart of Times Square.

5.4 Unraveling the Past of Hamiltonian Systems

In the preceding sections, it was established that once the state of the system, represented by $\rho(x, p)$, is established, its future evolution can be obtained deterministically, while conserving its entropy, i.e. the degree of uncertainty in the knowledge of the system. This progression is uniquely specified by Hamilton's equations.

It is equally possible to determine the past state of the system through the same approach, as illustrated in Figure 12. By transforming $t \to -t$, the backwards Hamilton's equations, given by

$$\frac{\mathrm{d}x}{\mathrm{d}t} = -\frac{\partial H}{\partial p}, \qquad \frac{\mathrm{d}p}{\mathrm{d}t} = \frac{\partial H}{\partial x}, \tag{5.10}$$

can be solved for a past state of the system. This is because a time reversal leads to $\frac{\partial}{\partial t} \rightarrow \frac{\partial}{\partial(-t)} = -\frac{\partial}{\partial t}$. Although these equations are distinct from Eqs. (2.15), they nonetheless produce the same dynamic system by retracing the same pre-existing trajectory in phase space. The notion of causality becomes meaningless in this context.

It is worth noting that the backward Hamilton's Eqs. (5.10), can be obtained through either time reversal or by solving the regular Hamilton's equations, Eqs. (2.15), with negative energy such that $H \rightarrow -H$. This also means that the system in question propagates in the opposite direction of the momentum. This concept will be a recurrent theme throughout this thesis.
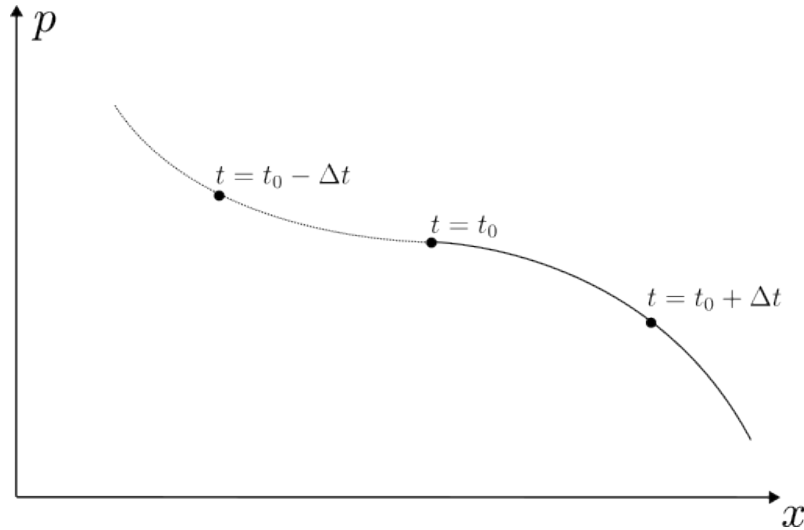
Figure 12: A Hamiltonian system entails both determinism and reversibility. Thus, knowing a point in phase space allows us to both predict future states and 'retrodict' (predict backwards in time) past states.

6 Unraveling the Mystery of Loschmidt's Paradox

The conservation of entropy in Hamiltonian systems has been established in the previous section. Yet, this result contradicts our common perception of entropy, which is that entropy seems to increase with the progression of time. This apparent discrepancy is commonly referred to as Loschmidt's paradox. The conundrum of Loschmidt's paradox arises upon consideration of the deterministic and reversible nature of microscopic physical systems and the observed increase in entropy throughout the universe. The paradox suggests that if the laws of physics are both predictable and capable of reversal, it would seem that the temporal progression of a physical system could be reversed, leading to a reduction in entropy, in contradiction to the second law of thermodynamics.

In order to comprehend the underlying mechanism behind this phenomenon, we will conduct an analysis through selected examples. This examination will facilitate the differentiation between microscopic and macroscopic entities, allowing for the formulation of definitions of concepts such as *microscopic systems*, *quasi-microscopic systems*, and *macroscopic interveners*. These definitions will give us an intuition that will be valuable in the remaining sections of the thesis. Finally, we examine the fundamental challenges pertaining to completely isolating a physical system from its surrounding environment.

6.1 The Unlikelihood of Time Reversal in Physical Phenomena

In this section, the phenomenon of reversing time in various physical systems is discussed with the aid of several examples.

6.1.1 Wine Glass Example

Take, for instance, a scenario in which a video depicts a wine glass being shattered on a floor surface. When the video is played in reverse, it displays a situation where the shock wave on the floor converges, resulting in the pieces of the glass reconstituting into its original form. While most physicists concur that such a sequence of events does not violate the established laws of physics, they highlight the minuscule probability of spontaneous reconstitution, given the precise arrangement and velocity of the pieces required for such an unlikely event. In simpler terms, the likelihood of a shattered wine glass reassembling into its original form spontaneously is highly unlikely, due to the vast number of ways in which the glass can be broken compared to the limited possibilities of reassembly.

6.1.2 Pool Game Example

Similarly, in a scenario of a frictionless pool game without pockets, in which the balls are initially arranged in a stationary triangular configuration (Figure 13), the observed spreading of the balls across the board can be reversed. While such a reversal does not contravene the known laws of physics, it is crucial to point out that the scenario where all balls reassemble into a stationary triangular shape with the proper distribution of kinetic energy has a low probability of occurring. That is, the number of initial configurations that result in a failure to reconstitute the balls into the original triangular formation in a pool game far exceeds the limited configurations that result in successful reconstitution.
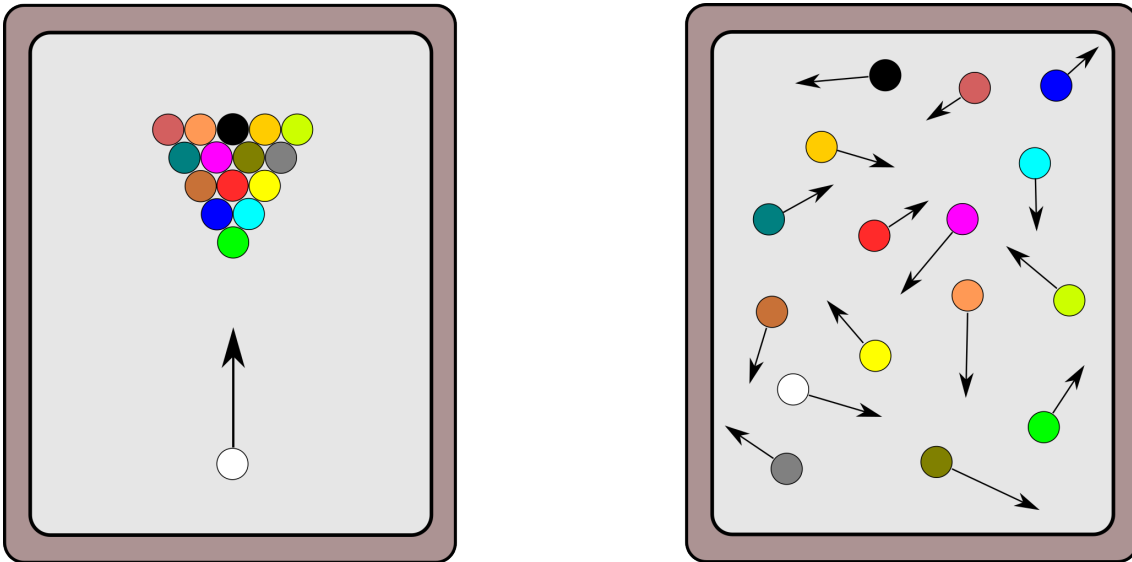
Figure 13: Frictionless pool game without pockets. **LEFT:** The balls are initially arranged in a stationary triangular configuration before the white ball hits them. **RIGHT:** Spreading of the balls across the board. Reconstruction into the initial state from a final state is possible, but has a low probability of happening.

The two examples illustrate that reversing the evolution of a system is often not in violation with the established laws of physics. These time reversed systems are instead rather improbable to observe.

6.2 Sliding Slab and Closed Systems

The concept of a closed system and the challenges in achieving it in practice are examined below.

6.2.1 The Naive Approach to the Sliding Slab System

In the study of physical systems, the dynamics of a sliding slab on a surface with friction can be characterized by a volume in phase space. Suppose that the slab consists of N particles which results in a $6N$-dimensional phase space in this particular example. As the exact state of the constituents of the slab is not known exactly, the phase space volume therefore encompasses the multiple potential states the slab can occupy. In the final state, the slab reaches a state of rest where the phase space volume ends up confined to the horizontal axis in phase space (where momentum is zero) since friction is involved in this example. Due to the final state being confined to the horizontal axis, the phase space volume must be reduced as a consequence. At first glance, this phenomenon may appear to contradict Liouville's theorem that was discussed in Section 5.2.3 which mandated the conservation of phase space volume along a trajectory. However, this apparent discrepancy can be reconciled by recognizing that the slab is not a closed system, and that some of the initial phase space volume pertaining to the slab has been dissipated to the surface, which was not initially a part of your system.

6.2.2 Revised Approach: Incorporating the Environment into the Hamiltonian System

The naive approach was flawed because it assumed the slab was an isolated system, failing to account for the surface's role within the Hamiltonian system. More specifically, the slab, comprised of N particles in a $6N$-dimensional phase space, was erroneously assumed to be a closed system. However, this model neglected the M particles that constitute the surface and their respective $6M$ extra phase space dimensions. As a result, in the extended $6(N + M)$-dimensional phase space

diagram, which now includes both the slab and the surface, the initial phase space volume does not decrease as the slab grinds to a halt. Instead, part of the volume initially contained in the $6N$ dimensions is now transferred to the additional $6M$ dimensions associated with the surface. As these extra dimensions are now a part of our system, the initial phase space volume in the expanded phase space does not decrease.

However, as some of the kinetic energy is transferred to the surface, causing it to heat up, the surface radiates some of this energy as thermal emission, or black body radiation, to the surrounding room in which the experiment is conducted. Therefore, the surrounding room, which receives the radiated energy, should also be incorporated into our system. The room, in turn, is not an isolated system, suggesting the need for a successive incorporation of additional surroundings. Therefore, it can be argued that the apparent lack of entropy conservation arises from the difficulty in isolating a system.

In order for the entropy to be conserved, the system, described by Hamilton's equations of motion, must be isolated from its environment. Consider an initial state of the slab described by a probability density $\rho_{6N}(x_i, p_i)$ in $6N$ dimensions. The entropy S_{6N} associated with this state can be calculated. However, as the slab interacts with the surface, the system ceases to be deterministic and reversible, leading to changes in both entropy and energy. As already discussed, to maintain the deterministic and reversible properties of the system, the extra $6M$ dimensions of the surface must be included, resulting in a $6(N+M)$ dimensional phase space. The entropy of the initial state $S_{6(N+M)}$ is greater than the entropy only considering S_{6N}, as the information initially provided by $\rho_{6N}(x_i, p_i)$ only described the uncertainty in the $6N$ dimensions associated with the slab and not the surface. Since we had limited knowledge of the state of the surface, the surface naturally has a high entropy S_{6M} associated with it. Therefore, the entropy of the slab alone, i.e. S_{6N}, must be lower than the entropy of the combined system $S_{6(N+M)}$. This is because the expanded phase space with $6(N+M)$ dimensions encompasses information or uncertainty of the probability density $\rho_{6(N+M)}(x_i, p_i)$ with the additional $6M$ dimensions that was known to a lesser degree initially. Thus, entropy appears to increase as the Hamiltonian system couples with the environment, which has a higher entropy due to its higher level of uncertainty due to the extra uncertainty of the surface when it is combined with the slab. However, if the system were examined initially in terms of a combined system of the surface and the slab, then the entropy $S_{6(N+M)}$ would naturally be conserved. Therefore, as time evolves, more and more of the environment must be included as part of the system, leading to an *apparent* increase in entropy.

In summary, this analysis demonstrates how a seemingly simple system — a slab sliding on a surface — can reveal the complex, interconnected nature of physical systems. This analysis also underscores the importance of appropriately defining the boundaries of the system. The implications of this understanding extends to the next topics of discussion.

6.3   Entropy Leakage

In instances where the system is not properly isolated from its environment, the entropy of the system may effectively appear to increase or decrease as the extra phase space dimensions associated with the environment are not incorporated into the Hamiltonian system. This phenomenon is referred to as entropy leakage.

6.3.1   Inward and Outward Entropy Leakage

Inward entropy leakage occurs when the entropy of a Hamiltonian system appears to *decrease* over time due to the influx of information from the environment. Conversely, *outward entropy leakage* occurs when the entropy of the Hamiltonian system appears to *increase* as information is displaced to the surrounding environment.

6.4 The Macroscopic Intervener

In this section, we define the concept of a *Macroscopic Intervener* through an illustrative example involving a game of pool. This definition will serve as a basis for the subsequent definitions of microscopic and quasi-microscopic systems.

6.4.1 Example: Frictionless Pool

Consider a frictionless game of pool on a table without any pockets. At a specific instant in time, if the positions and momenta of all the balls are known exactly, the future and past evolution of the system can be exactly determined. The balls move along straight paths until they collide with each other or the walls of the pool table. The walls of the pool table provide the boundary conditions for this Hamiltonian system. It is noteworthy that the walls of the container are *not* considered to be part of the environment as they do not have corresponding phase space dimensions. Additionally, the walls simply impose restrictive conditions on the motion of the balls at the boundary, and do not follow Hamilton's equations themselves.

The precise description of the walls' microscopic constituents' is not crucial in this context, as long as their macroscopic effect on the balls is specified. Given that the walls are macroscopic and therefore not part of the Hamiltonian system, they can be referred to as a *macroscopic intervener*. These interveners are not considered to be microscopic as their actual constituents' evolution is not incorporated into the microscopic Hamiltonian system. Nonetheless, since their macroscopic overall impact on the evolution of the Hamiltonian system is described, the term macroscopic intervener arises. In this specific example, the walls can also be considered as the system's macroscopic boundary conditions.

Suppose that a person physically intervenes in the game by striking a ball with a cue stick. If this particular action is precisely described, the person can similarly be considered as a macroscopic intervener. In the context of the microscopic framework, it would be highly impractical to incorporate the precise atomic configuration and the state of all the electrical impulses in the brain and body of the person striking the ball into the microscopic system.

The person's microscopic configuration would inherently have an extremely high entropy. As the person intervenes in the game, the game's entropy would significantly increase because the microscopic constituents of the player, possessing high entropy, must now be incorporated into the system.
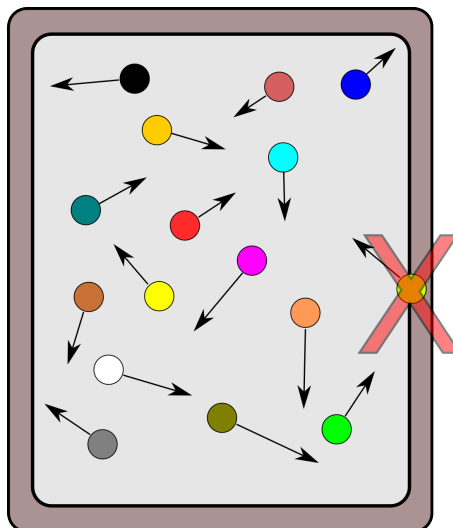
Figure 14: Pool game example continued. A state is depicted that violates the boundary conditions of the system. It is not possible for a ball to be partially inside a wall.

6.5 Boundary Conditions and Entropy

The boundary conditions play a crucial role in determining the entropy of a system. In order to calculate the entropy, it is necessary to obtain the probability density associated with a specific state. However, claiming that the probability density pertaining to the state of a system is represented by a particular function also implies certain restrictions on the boundary conditions. This is demonstrated in Figure 14, where an invalid scenario in the pool game example is depicted, in which a ball is partially inside a wall. This scenario cannot occur, and as a result, the probability of all initial conditions that violate the boundary conditions must be excluded.

Therefore, when specifying the entropy of a state, i.e. the information we have pertaining to the state of the system, one is simultaneously indirectly implying certain aspects about the boundary conditions of the system. Thus, specifying a system's entropy inherently involves defining some aspects of its boundary conditions. The boundary conditions must be inherently macroscopic in nature, as these signify the system's macroscopic interaction with its surrounding environment. This will be discussed in the forthcoming sections involving electromagnetism.

6.6 Microscopic and Quasi-Microscopic Systems

In this thesis, we classify Hamiltonian systems into two categories: microscopic and quasi-microscopic.

6.6.1 Microscopic System

A microscopic system is a closed system that adheres to the principles of determinism and reversibility and is isolated from its environment by macroscopic boundary conditions. These boundary conditions must preserve the conservation of energy and entropy. By specifying the impact of these macroscopic boundary conditions on the microscopic system, we can ensure the conservation of entropy.

6.6.2 Quasi-Microscopic Systems

On the other hand, a quasi-microscopic system, while still exhibiting determinism and reversibility, may involve macroscopic interveners. These interveners can transfer energy into or out of the system, provided that the manner in which this occurs is precisely described so that entropy is conserved. By treating these interveners as macroscopic entities and considering only their macroscopic impact on the system, the entropy leakages associated with them are disregarded. Consequently, the quasi-microscopic system may not conserve energy due to the particular interactions with the macroscopic intervener.

It's important to note that preserving entropy in a quasi-microscopic system requires accurate information about the impact of the macroscopic intervener on the microscopic system. This information can be acquired through a comparison of successive measurements of the system, conducted at its initial and final states.

6.6.3 Boundary Conditions

For microscopic Hamiltonian systems, the macroscopic boundary conditions play a pivotal role in determining the entropy of the system. The precise specification of these boundary conditions, which conserve energy, ensures the preservation of entropy. Calculating the entropy of a microscopic system requires determining the probability density of a specific state, considering the restrictions imposed by the boundary conditions.

6.7 Boundary Interactions and the Inadequacy of Classical Mechanics

In this section, we delve into the limitations of classical mechanics and make a compelling argument for its replacement with quantum mechanics. Despite its popularity, classical mechanics fails to accurately predict empirical observations at all scales. Classical mechanics' insufficiency stems from its flawed underlying assumptions, which, though seemingly accurate in some situations, prove untenable. The physical foundations of classical mechanics are problematic, despite the mathematical robustness of the theory.

6.7.1 Boundary Conditions

It is imperative to understand the shortcomings of classical mechanics to appreciate the significance of quantum mechanics. In any system's study, whether classical or thermodynamic, defining its boundaries and understanding the occurrences at these boundaries are crucial. This process influences the definable states for the system, revealing specific aspects that can be studied and examined.

Consider, for instance, the motion of a cannonball and a speck of dust through the air. The air molecules scatter off the surface of the cannonball, causing a negligible effect, allowing its state to be described precisely in terms of position and momentum. On the other hand, the effect of air molecules scattering off the surface of the speck of dust is substantial, causing it to jostle in different directions, resulting in a state that is described as a probability distribution over position and momentum. Finally, consider the scenario of a cannonball on the surface of the sun, where the plasma surrounding the sun scatters off its surface, causing the melting of the cannonball. This makes it challenging to identify which particles are part of the original cannonball. This example underscores the importance of considering boundary interactions when defining a system.

6.7.2 Classical Physics and the Infinitely Small Pixel

Classical mechanics assumes that objects can be isolated by neglecting the interaction with their surrounding environment. This leads to the description of the system as an infinitely precise quantity. However, as we consider smaller and smaller parts of the system, chaotic thermal fluctuations of its immediate surrounding environment begin to become more pronounced. Thus, the impact of boundary interactions of these smaller systems becomes increasingly significant, ultimately rendering the idea of isolation untenable. Classical mechanics is flawed because it is impossible to fully isolate a system at all scales, and there will always be some interaction with the environment that cannot be eliminated. Shielding against gravitational interaction or eliminating thermal radiation is theoretically impossible, meaning that complete isolation means that the system cannot be interacted with or measured empirically. From an empirical perspective, it then becomes akin to an empty system.

Consequently, the most accurate description must be statistical and probabilistic in nature, abandoning the classical notion of states being described as infinitely precise quantities. This argument aligns with the scientific method and our redefined definition of entropy. As we saw in Section 3.4, entropy lower than zero corresponds to a more refined and precise description than an empty system, which is logically inconsistent. Quantum mechanics resolves this issue by introducing pixel size, leading all pure states, including the vacuum or empty system, to have zero entropy. It is important to note that these entropic arguments are not separate from the isolation argument. These arguments all stem from the same fundamental issue - the inability to fully isolate a system. Classical mechanics fails to consider the impact of boundary interactions on the definition of a system's state and its experimentally accessible features. In certain situations, it may be possible to approximate that a system is perfectly isolated at a larger scale, but this is only a simplifying assumption.

In conclusion, classical mechanics must be disregarded due to its flawed assumptions, which result in logically inconsistent and experimentally flawed descriptions of the world. To fully understand the significance of quantum mechanics, it is crucial to comprehend the limitations of classical

mechanics and why it must be abandoned. The more accurate description of the world must be statistical and probabilistic in nature, as classical mechanics' notion of infinitely precise states containing infinite information is no longer valid. The inability of classical mechanics to fully isolate a system and account for boundary interactions highlights the importance of considering the impact of these interactions at the boundary upon defining a system's state and its experimentally accessible features. This shift towards a statistical and probabilistic description of the world aligns with the scientific method and our revised definition of entropy. This marks a crucial step towards a deeper understanding of quantum mechanics.

6.7.3 Summary

In conclusion, microscopic systems are Hamiltonian systems that conserve both energy and entropy due to the macroscopic boundary conditions that theoretically isolate them from their environment. In contrast, quasi-microscopic Hamiltonian systems may contain macroscopic interveners that conserve entropy but may not conserve energy. The distinction between these two types of systems is crucial for comprehending the behavior and evolution of Hamiltonian systems in the context of electromagnetism.

6.8 Integrating Key Concepts From Parts I and II

In this section, we will summarize the key points from the previous sections, specifically Parts I and II.

6.8.1 Hamiltonian Systems

In this thesis, it was demonstrated that Hamiltonian systems are characterized by deterministic and reversible evolution while conserving both entropy and energy. The challenge in the study of Hamiltonian systems lies in their isolation from the environment, which is deemed impossible. As a result, macroscopic boundary conditions are required to describe the interaction between the Hamiltonian system and its surroundings. In the case of quasi-microscopic systems, macroscopic interveners can affect the system, even though they are not described within the microscopic Hamiltonian framework. However, the effect of these interveners is specified in such a manner that the conservation of entropy is maintained.

6.8.2 Extension of Shannon's Entropy

Extending Shannon's entropy from discrete to continuous random variables required a precisely defined entropy concept, which was a complex challenge. The entropy of a continuous state demanded an infinite level of precision, which was infeasible due to the infinite amount of information it would contain, most of which would not be measurable. To resolve this issue, a pixel size was introduced as the smallest quantifiable unit in phase space, which represented an interval in which the defining of a state sufficed without the need for further precision. Nevertheless, this approach posed two additional difficulties: coordinate dependence and the issue of negative entropy.

6.8.3 Coordinate Dependence and Entropy Conservation

The coordinate dependence was addressed by introducing a sympathetic manifold (phase space), where the determinant of the Jacobian was equal to unity for both canonical transformations and transformations between different times. This ensured that the entropy became coordinate-independent and was conserved over time for Hamiltonian systems. In a similar manner, we will observe that quantum mechanics leverages Hilbert space, conserving entropy through unitary

transformations, analogous to canonical transformations. Additionally, quantum mechanics employs unitary evolution, preserving entropy during the temporal evolution of the wave function, as will be further discussed in the subsequent section.

6.8.4 Redefining Entropy

The definition of entropy was rooted in empiricism, considering only the measurable information within a system. This redefinition of entropy, as the Shannon entropy of measurable information, excluded non-measurable information from contributing to the system's entropy, distinguishing it from the thermodynamic definition that only pertains to equilibrium state entropies. Science is centered on making predictions, and all physical theories should strive to use mathematical models to relate empirical observations made at some point in time to predict future empirical observations. The redefined entropy only considered empirical observations and excluded hypothetical ones.

6.8.5 Negative Entropy, Quantum Mechanics and the Phase Space Pixel

The issue of negative entropy was more complex, pertaining to the theoretical possibility of making a state's phase space distribution narrow enough, compared to an arbitrarily chosen pixel size, to yield negative entropy. However, this did not imply that it was feasible to achieve this narrow distribution in practice. Assuming the existence of a minimum theoretical pixel size in phase space for which all measurements have positive entropy, quantum mechanics emerges as a natural consequence. This requirement can be satisfied by introducing a wave function of position and its Fourier transform of which was linked to momentum, as dictated by the Hirschman uncertainty relation. As the wave function of position becomes narrower, the momentum wave function broadens due to the inherent properties of the Fourier transform. Therefore, the inclusion of a pixel size was a necessary and natural step in extending entropy to the continuous domain. By assuming a minimum pixel size, the entropy problem in classical physics was solved and the emergence of quantum mechanics was facilitated for Gaussian distributions. In the next section, we generalize this to non-Gaussian distributions with the introduction of the Wigner-Moyal formalism.

7 The Phase Space Wigner-Moyal Formulation

In the present section, we will delve deeper into the entropy problem of classical physics, and demonstrate how our resolution efforts, outlined in previous sections, culminate in the emergence of quantum mechanics through the introduction of the Wigner-Moyal formulation. This formulation will be highly relevant in the subsequent part of the thesis where we will illustrate how electromagnetism is plagued by a similar entropy predicament and how its resolution gives rise to the bitemporal electromagnetic theory along with its prediction of the antiphoton.

In Section 3.4.4, we demonstrated that a connection between a phase space formulation of a state and its Hilbert space representation can be established for Gaussian distributions by introducing $\psi(x)$ and its Fourier transform in Hirschman's uncertainty relation to ensure $S_I \geq 0$. To meet this positive entropy requirement in the context of the symplectic manifold formulation, the equations of classical mechanics must be modified appropriately to take into account the constraint of $S_I \geq 0$. This leads to a transition towards non-commutative geometry, particularly the Wigner-Moyal formalism. However, our earlier analysis was limited to Gaussian distributions only. However, the general case necessitates a more intricate treatment, which we undertake in the present section by considering a two coin example before introducing the Wigner transform and its inverse, the Weyl transform. The Wigner transform enables the mapping of a given wave function in Hilbert space to its phase space counterpart, represented by a quasi-probability density function.

The Wigner-Moyal formalism was initially introduced to find classical counterparts to quantum evolution in phase space. To the best of our knowledge, there is no record in the scientific literature of the Wigner-Moyal formalism being discussed in relation to the entropy constraint of $S \geq 0$ in accordance with our definition. Finally, we compare the Von-Neumann definition of entropy in Hilbert space to our definition.

7.1 Generalizing to Non-Gaussian Distributions

This section extends our earlier results that came from the assumption of a theoretical limit on the pixel size, the consequences of which, were only applied Gaussian distributions. We shall witness that generalizing this result to non-Gaussian distributions marks the transition to non-commutative geometry involving the Moyal product. This gives rise to the Wigner function in framework of Wigner-Moyal formalism to describe physical states. Understanding this formalism will be crucial for the understanding bitemporal electromagnetism and its resolution of the entropy problem inherent in classical electromagnetism.

Let's expand our formalism to physical states represented by non-Gaussian distributions with zero entropy. This is not as straight forward process as it might first appear. This is because the reader might recall that we witnessed that Hirschman uncertainty was minimal and thus saturated for zero entropy states when the entropy is computed by

$$S_I = - \iint \rho(x,p) \ln \left(\rho(x,p) \hbar \pi e \right) \, \mathrm{d}x \, \mathrm{d}p, \tag{7.1}$$

for Gaussian distributions only. At first, this might appear to imply that non-Gaussian states must have an entropy larger than zero. However, as these non-Gaussian states represents the smallest possible states irreducible states, their entropy should under our definition be equal to zero.

The reason for this discrepancy has to do with the limit on the empirically accessible information within a state, which is limited by our proposition of the pixel having a smallest theoretical value. That is, for a zero entropy state defined by a pixel size, the Gaussian distribution will not only be the distribution that minimizes product of standard deviations of position x and momentum p, but the marginal distributions $\rho_x(x)$ and $\rho_p(p)$ will also be independent of one another so that the total distribution $\rho(x,p)$ can be expressed as $\rho(x,p) = \rho_x(x)\rho_p(p)$. This means that that within this assumed zero entropy theoretical pixel size, the position x and momentum p can be measured independently. This implies that this information can be empirically determined through experiment for these variables. In order to see what happens for zero entropy states represented

by non-Gaussian distributions, we examine an example involving coins in a box, where we witness a situation where reconstructing certain random variables with information that we do not have direct access to leads to a peculiar situation which lays the foundation for understanding the Wigner function in phase space.

Extended Probability Framework and Negative Probabilities

A variety of studies have demonstrated that the conventional understanding of probability can be extended to include non-standard numerical values, such as negative probabilities [7]. While the utilization of this unconventional viewpoint is not a necessity, it has been shown to offer advantages under specific conditions. It is crucial to emphasize that negative probabilities must be combined with positive probabilities to yield meaningful results in practical applications. This suggests that the emergence of negative probabilities in quantum theory is a manifestation of the mathematical disaggregation of states or systems that physically exist only as composites.

Thought Experiment: Two Coins in a Black Box

This text presents a thought experiment involving a black box containing two coins [65], with the aim of understanding how negative probabilities can emerge in the context of possessing partial or unobtainable information about a system.

Consider a black box containing two coins being tossed, and the box reports one of three possible outcomes at random:

1. Outcome of the first coin (heads or tails).

2. Outcome of the second coin (heads or tails).

3. Whether the outcomes of the two coins matched or were distinct.

The objective here is to reconstruct the joint probability distribution for the four possible outcomes of the coin pair: HH, TT, HT, TH. Note that the information of this joint probability distribution is not given to us directly from the three possible outcomes.

Upon conducting numerous trials, it is observed that:

Each coin displays heads two-thirds of the time when measured individually such that $P(H) = 2/3, P(T) = 1/3$ for each coin. The coins never match when compared, implying that $P(HH) + P(TT) = 0$. A distribution that reflects this correlation and adheres to the desired marginal distributions of each coin needs to be identified.

The information provided above implies that the probabilities satisfying the marginal distributions must be found based on the following information:

$$P(HH) + P(TT) = 0, \tag{7.2}$$

$$P(HT) + P(HT) = 1, \tag{7.3}$$

$$P_1(H) = P(HH) + P(HT) = \frac{2}{3}, \tag{7.4}$$

$$P_2(H) = P(HH) + P(TH) = \frac{2}{3}, \tag{7.5}$$

$$P_1(T) = P(TT) + P(TH) = \frac{1}{3}, \tag{7.6}$$

$$P_2(T) = P(TT) + P(HT) = \frac{1}{3}, \tag{7.7}$$

where $P_i(H)$ is the probability of the ith coin being heads, with $i \in 1, 2$. As anticipated, each coin has a $2/3$ probability of showing heads and a $1/3$ probability of showing tails. Additionally, the normalization condition must be satisfied, stating that the sum of all probabilities must equal 1:

$$P(HH) + P(HT) + P(TH) + P(TT) = 1. \tag{7.8}$$

Solving the aforementioned equations, a joint probability distribution, presented in Tab. 1, is obtained, which includes negative values.

Table 1: The joint probability distribution for the coin pair within the black box. The table contains negative probabilities, illustrating the hidden correlations and the quasi-probability distribution that arises due to the lack of access to certain information pertaining to the individual joint outcomes.

		Coin 1:	
		H	T
Coin 2:	H	$\frac{1}{6}$	$\frac{1}{2}$
	T	$\frac{1}{2}$	$-\frac{1}{6}$

This distribution appears counter intuitive because the only way to satisfy the marginal distributions and the coins never matching is by assigning a negative value to the joint probability $P(TT)$. This occurs because we are attempting to essentially reconstruct a joint probability distribution without having direct empirical access to the individual joint outcomes of these coins since this information was not provided to us from the experiment. We only possess information about sums of joint probabilities, i.e. $P(HT) + P(TH) = 1$ or $P(HH) + P(HT) = 2/3$.

One possible interpretation is to consider a joint 'quasi-probability' distribution, which may serve as a useful bookkeeping tool. This distribution characterizes the hidden correlations within the black box while preserving the inherent information pertaining to the marginal probabilities of the individual coins. In this scenario, negative probabilities emerge when separating a composite system because we are attempting to reconstruct joint probabilities without access to individual joint outcomes.

The negative probability in this example arises from attempting to construct a joint probability distribution for a composite system using only partial information. The provided information describes sums of joint probabilities (i.e. marginal probabilities), but not the actual joint probabilities themselves. In this particular instance, the composite system is the black box with the correlated coin tosses, and the partial information we have includes the marginal probabilities of each coin and the fact that the coins never match.

When we try to reconstruct the joint probability distribution from this partial information, we discover that the only way to satisfy both the marginal probabilities and the correlation constraints is to assign a negative probability to the $P(TT)$ event. This negative probability reflects the *hidden* correlations within the black box and can be considered a 'quasi-probability' in this context. It is crucial to note that negative probabilities are not probabilities in the classical sense, as probabilities should always be non-negative. Negative probabilities are an artifact that arises when trying to describe quantum systems or, in this case, a composite system with hidden correlations using classical probability theory.

In the context, entanglement can be conceptualized as an irreducible composite quantum system that cannot be decomposed into smaller, independent subsystems. This is due to the fact that such systems possess zero entropy and are thus irreducible. Therefore, it follows that it is not possible to describe one particle without concurrently describing the other in the entangled pair.

7.1.1 Generalization of Coin Example

Consider a black box in which two stochastic variables, X_1 and X_2, reside in a hidden state. The variables are defined as taking values in the set $\{H, T\}$. Direct measurement of both variables is not feasible. However, after a realization of (X_1, X_2), we have access to the following information where either

- The value of X_1 is revealed, or

- The value of X_2 is revealed, or

- The match or mismatch of the values of X_1 and X_2 is indicated.

Let Y_1, Y_2, and Y_3 be stochastic variables with values in $-1, 1$, such that the relationship between Y_j and X_j is defined as follows: $Y_j = -1$ if $X_j = H$ and $Y_j = 1$ if $X_j = T$, $j = 1, 2$, while $Y_3 = -1$ if the values of X_1 and X_2 match, and $Y_3 = 1$ otherwise. Through experimentation, we estimate the following probabilities:

$$P(Y_1 = -1) = a_1, \quad P(Y_2 = -1) = a_2, \quad P(Y_3 = -1) = a_3.$$

Given the probabilities for Y_1, Y_2, and Y_3, is it possible to construct a probability distribution for (X_1, X_2), even though its value cannot be directly measured? Let us assign probabilities $P(HH)$, $P(HT)$, $P(TH)$, and $P(TT)$ to the outcomes of (X_1, X_2). Then,

$$P(HH) + P(HT) = a_1, \quad P(HH) + P(TH) = a_2, \quad P(HH) + P(TT) = a_3,$$

and to satisfy the requirement that the probabilities sum to unity,

$$P(TH) + P(TT) = 1 - a_1.$$

The unique solution to the above set of equations is given by

$$P(HH) = \frac{a_1 + a_2 + a_3 - 1}{2}, \quad P(HT) = \frac{1 + a_1 - a_2 - a_3}{2},$$

$$P(TH) = \frac{1 + a_2 - a_1 - a_3}{2}, \quad P(TT) = \frac{1 + a_3 - a_1 - a_2}{2}.$$

It is possible that some of these probabilities may be negative, depending on the values of a_1, a_2, and a_3. In such a case, (X_1, X_2) is described by a quasi-probability distribution. The concept of negative probabilities is not a real concern as the variables (X_1, X_2) cannot be directly measured. However, let us calculate the moments $E[Y_j^n]$, $j = 1, 2, 3$ and $n = 0, 1, 2, \ldots$ of Y_j. We have

$$E[Y_j^n] = (-1)^n a_j + 1^n (1 - a_j) = 1 - (1 - (-1)^n) a_j, \quad j = 1, 2, 3.$$

Instead, using the quasi-probability distribution, we find

$$E[Y_1^n] = (-1)^n (P(HH) + P(HT)) + 1^n (P(TH) + P(TT)) = 1 - (1 - (-1)^n) a_1,$$

$$E[Y_2^n] = (-1)^n (P(HH) + P(TH)) + 1^n (P(HT) + P(TT)) = 1 - (1 - (-1)^n) a_2,$$

$$E[Y_3^n] = (-1)^n (P(HH) + P(TT)) + 1^n (P(TH) + P(HT)) = 1 - (1 - (-1)^n) a_3.$$

Therefore, while the quasi-probability distribution cannot be used in general to assign individual probabilities to hidden events, it can be used to evaluate the moments of the observable variables Y_1, Y_2, and Y_3.

7.2 Moyal Star Product

In the Hilbert space framework, the presence of non-commuting operators allows the non-negative entropy constraint $S \geq 0$ to be indirectly satisfied. In order to preserve this property in the phase space formulation, the introduction of the non-commutative Moyal product, embodied in the Moyal bracket, is required. The Poisson bracket is recovered in the classical limit $\hbar \to 0$ of the Moyal bracket as the pixel is effectively removed.

The Moyal star product is therefore a non-commutative multiplication operation between phase space functions, defined as

$$A \star B = A(x, p) \exp\left(\frac{i\hbar}{2} \left(\overleftarrow{\partial_x} \overrightarrow{\partial_p} - \overleftarrow{\partial_p} \overrightarrow{\partial_x} \right) \right) B(x, p). \tag{7.9}$$

Here, $\overleftarrow{\partial}$ and $\overrightarrow{\partial}$ denote left and right partial derivatives, respectively such that

$$A(x,p)(\overleftarrow{\partial_x}\overrightarrow{\partial_p})B(x,p) = \frac{\partial A(x,p)}{\partial x}\frac{\partial B(x,p)}{\partial p}. \tag{7.10}$$

The Moyal product can thus be computed by Taylor expanding the exponential containing the differential operators,

$$\exp(x) = 1 + x + \frac{x^2}{2!} + \frac{x^3}{3!} + \cdots, \tag{7.11}$$

where $x = \frac{i\hbar}{2}\left(\overleftarrow{\partial_x}\overrightarrow{\partial_p} - \overleftarrow{\partial_p}\overrightarrow{\partial_x}\right)$. The Moyal star product is associative but not commutative, which means that, in general, $A \star B \neq B \star A$ for conjugate variables. Lastly, note that the Moyal star product contains an inherent length scale to it with the presence of $\hbar$ in its definition.

7.3 Moyal Bracket and Moyal-Liouville Evolution Equation

The Moyal bracket is a mathematical construction in phase space formulation of quantum mechanics that extends the concept of the Poisson bracket in classical mechanics in order to account for the positive entropy condition imposed by the introduction of the phase space pixel, as the Moyal bracket includes $\hbar$ in its definition. We will later show that the Moyal bracket reduces to the Poisson bracket as $\hbar \to 0$.

7.3.1 Moyal Bracket

The Moyal bracket of two phase space functions $A(x,p)$ and $B(x,p)$ is defined

$$\{A,B\}_M = \frac{1}{i\hbar}(A \star B - B \star A) = \{A,B\}_P + \mathcal{O}(\hbar^2), \tag{7.12}$$

where $\{A,B\}_P$ represents the Poisson bracket of two classical phase space functions $A(x,p)$ and $B(x,p)$ is given by

$$\{A,B\}_P = A(x,p)\left(\overleftarrow{\partial_x}\overrightarrow{\partial_p} - \overleftarrow{\partial_p}\overrightarrow{\partial_x}\right)B(x,p). \tag{7.13}$$

More explicitly, the Moyal bracket is expressed as

$$\{A,B\}_M = \frac{2}{\hbar}A(x,p)\sin\left(\frac{\hbar}{2}\left(\overleftarrow{\partial_x}\overrightarrow{\partial_p} - \overleftarrow{\partial_p}\overrightarrow{\partial_x}\right)\right)B(x,p). \tag{7.14}$$

7.3.2 Relation to the Poisson Bracket

We start by Taylor expanding sine term of the Moyal bracket Equation (7.14) as

$$\begin{aligned}
\sin\left(\frac{\hbar}{2}\left(\overleftarrow{\partial_x}\overrightarrow{\partial_p} - \overleftarrow{\partial_p}\overrightarrow{\partial_x}\right)\right) &= \frac{\hbar}{2}\left(\overleftarrow{\partial_x}\overrightarrow{\partial_p} - \overleftarrow{\partial_p}\overrightarrow{\partial_x}\right) - \frac{1}{3!}\left(\frac{\hbar}{2}\right)^3\left(\overleftarrow{\partial_x}\overrightarrow{\partial_p} - \overleftarrow{\partial_p}\overrightarrow{\partial_x}\right)^3 + \dots \\
&= \frac{\hbar}{2}\left(\overleftarrow{\partial_x}\overrightarrow{\partial_p} - \overleftarrow{\partial_p}\overrightarrow{\partial_x}\right) + \mathcal{O}(\hbar^3).
\end{aligned} \tag{7.15}$$

Plugging this result back into Equation (7.14) we obtain

$$\begin{aligned}
\{A,B\}_M &= \frac{2}{\hbar}A(x,p)\left[\frac{\hbar}{2}\left(\overleftarrow{\partial_x}\overrightarrow{\partial_p} - \overleftarrow{\partial_p}\overrightarrow{\partial_x}\right) + \mathcal{O}(\hbar^3)\right]B(x,p) \\
&= A(x,p)\left[\left(\overleftarrow{\partial_x}\overrightarrow{\partial_p} - \overleftarrow{\partial_p}\overrightarrow{\partial_x}\right) + \mathcal{O}(\hbar^2)\right]B(x,p).
\end{aligned} \tag{7.16}$$

This shows that the Moyal bracket reduces to the Poisson bracket Equation (7.13) in the limit $(\hbar \to 0)$ of diminishing pixel size

$$\{A,B\}_M \xrightarrow{\hbar\to 0} A(x,p)\left[\left(\overleftarrow{\partial_x}\overrightarrow{\partial_p} - \overleftarrow{\partial_p}\overrightarrow{\partial_x}\right)\right]B(x,p) = \{A,B\}_P. \tag{7.17}$$

7.3.3 Moyal-Liouville Evolution Equation

The corresponding evolution equation in phase space is called the Moyal-Liouville equation:

$$\frac{\partial W(x,p,t)}{\partial t} = -\{H,W\}_M, \tag{7.18}$$

where $H(x,p)$ is the Hamiltonian function in phase space. It describes the time evolution of the of a phase space distribution $W(x,p,t)$, which will later be identified as the Wigner distribution. This equation is the phase space analogue of the Schrödinger equation in quantum mechanics.

In summary, the Moyal bracket is expressed directly in terms of a pixel size and its non-commutative nature functions to preserve the pixel size by limiting the accessible information of a physical state to the information that can be obtainable through actual empirically experiments. In the classical limit of the vanishing pixel size, the Moyal bracket reduces to the classical Poisson bracket.

7.4 Wigner and Weyl Transforms in Quantum Mechanics

Classical mechanics relies on the symplectic manifold representation of phase space, where canonical transformations have unit Jacobian determinants [68]. In contrast, quantum mechanics employs Hilbert space as the mathematical framework, utilizing unitary transformations and unitary evolution, which ensure the conservation of a wave function's entropy [73].

The Wigner and Weyl transforms serve as indispensable tools for transitioning between symplectic manifolds and Hilbert space, facilitating the analysis of quantum systems in both phase space and Hilbert space. The Wigner transform offers a quasi-probability distribution in phase space, uncovering vital information about the quantum state [94]. Concurrently, the Weyl transform enables the examination of quantum systems in Hilbert space using operators that are functions of position and momentum [92].

7.4.1 The Wigner Transform

The Wigner transform establishes a link between the quantum wave function in Hilbert space and phase space, allowing for a seamless transition between these two domains [94]. It has been determined that constraints originating from the phase space pixel complicate the concept of the temporal evolution equation in phase space. Owing to the restriction of precisely localizing a state more accurately than the permitted pixel resolution, both the conventional phase space probability distribution and the traditional Liouville's equation are unsuitable. Consequently, the Wigner transform and Wigner function are introduced.

Wigner initially devised the Wigner quasiprobability distribution as an alternate representation of a quantum mechanical state in phase space, derived from the Hilbert space representation. The Wigner quasiprobability distribution acts as an equivalent replacement for the standard density matrix in Hilbert space, operating within phase space. Wigner's representation is invaluable for converting states from Hilbert space into a phase space formalism. In this representation, any state in Hilbert space corresponds to a Wigner function $W(x,p)$ in phase space. The Liouville-Moyal equation provides an evolution equation for $W(x,p)$ in phase space, analogous to the quantum Liouville equation in Hilbert space.

The Wigner function $W(x,p)$ can be obtained the density matrix $\hat{\rho}$ of a quantum *mixed* state as

$$W(x,p) = \frac{1}{2\pi\hbar} \int_{-\infty}^{\infty} \langle x + \frac{y}{2}|\hat{\rho}|x - \frac{y}{2}\rangle e^{-\frac{ipy}{\hbar}} dy, \tag{7.19}$$

or similarly a wave function $\Psi(x)$ for a *pure* quantum state as

$$W(x,p) = \frac{1}{2\pi\hbar} \int_{-\infty}^{\infty} \Psi^*(x + \frac{y}{2})\Psi(x - \frac{y}{2}) e^{-\frac{ipy}{\hbar}} dy. \tag{7.20}$$

The Wigner function is real and normalized to unity. The Wigner function yields the correct marginal distributions for position and momentum such that $\int W(x,p)\,\mathrm{d}p = \langle x|\hat{\rho}|x \rangle = |\psi(x)|^2$ or $\int W(x,p)\,\mathrm{d}x = \langle p|\hat{\rho}|p \rangle = |\phi(p)|^2$ when integrated over p and x, respectively. Additionally, the Wigner distribution can be utilized in order to calculate averages of any dynamical variable of the system. Suppose we have a dynamical variable $G(x,p)$, then its ensemble average can be computed $\langle G(x,p) \rangle = \iint W(x,p)G(x,p)\,\mathrm{d}x\,\mathrm{d}p$. However, we can't interpret the Wigner distribution as a probability distribution outright, given its potential to take on negative values in specific phase space regions. This outcome is anticipated, considering the pixel's inclusion to guarantee positive entropy precludes the excessive pinpointing of both location and momentum. This result is expected, as the introduction of the pixel to ensure positive entropy prohibits overly precise localization of both position and momentum.

In quantum optics, the Wigner function has been used to analyze non-classical states of light, including squeezed states and photon-number states [87]. In quantum information theory, the Wigner and Weyl transforms have been employed to study entanglement and other quantum correlations between subsystems. The Wigner function's ability to take on negative values can serve as an indicator of non-classicality and entanglement in composite systems [61]. This property has been used to develop criteria for entanglement detection and to analyze multipartite entangled states [82].

7.4.2 The Weyl Transform

The Weyl transform, which acts as the reverse of the Wigner transform, maps physical states in symplectic manifolds back to Hilbert space [92]. This transformation plays a crucial role in connecting classical and quantum mechanics. It is achieved by first calculating the ordinary Fourier transform of a phase space distribution, then replacing the classical variables with quantum operators, and ultimately generating a version of the function within Hilbert space.

Hilbert space is a complete inner product space that serves as the state space for quantum systems. In this space, quantum states are represented by vectors, and observables are represented by Hermitian operators acting on these vectors [73]. The time evolution of a quantum system is described by the Schrödinger equation, which is formulated in Hilbert space [79].

The Weyl transform links classical and quantum mechanics by establishing a connection between symplectic manifolds and Hilbert space. Specifically, the Weyl transform is the inverse of the Wigner transform, which associates quantum states with phase space distributions.

The transformation is applied to a function in a two-dimensional Euclidean phase space, defined by coordinates (x,p). The canonical commutation relations are satisfied using operators $\hat{P}$ and $\hat{X}$. The Weyl transform, or the quantization of the function, is represented as follows

$$\Phi[f] = \frac{1}{(2\pi)^2} \iint \iint f(x,p) \left(e^{i(a(\hat{X}-x)+b(\hat{P}-p))} \right) \mathrm{d}x\mathrm{d}p\mathrm{d}a\mathrm{d}b. \tag{7.21}$$

Initially, the p and x integrals are computed, yielding the ordinary Fourier transform $\tilde{f}$ of f while retaining the operator $e^{i(a\hat{X}+b\hat{P})}$ [6]. Consequently, the Weyl transform can be expressed as

$$\Phi[f] = \frac{1}{(2\pi)^2} \iint \tilde{f}(a,b) e^{ia\hat{X}+ib\hat{P}} \mathrm{d}a\mathrm{d}b. \tag{7.22}$$

Understanding the Weyl transform involves two steps: first, computing the ordinary Fourier transform of the phase space distribution $f(x,q)$, and then substituting the classical variables p and x with some desired conjugate quantum operators $\hat{P}$ and $\hat{Q}$ in the Fourier inversion formula. This procedure generates a Hilbert space version of the function.

Additionally, the non-commutativity of the Moyal star product parallels the non-commutativity of operators in Hilbert space. Specifically, the commutator of two quantum operators $\hat{A}$ and $\hat{B}$ is given by

$$[\hat{A}, \hat{B}] = \hat{A}\hat{B} - \hat{B}\hat{A}. \tag{7.23}$$

This is because the Moyal transform of

$$\Phi[A(x,p) \star B(x,p)] = \Phi[A(x,p)]\Phi[B(x,p)], \tag{7.24}$$

serves as a bridge between same operations in Hilbert space.

The Moyal bracket is a central concept in the phase space formulation of quantum mechanics, extending the classical Poisson bracket and connecting to the commutation relations of quantum operators through the Weyl transform. The Moyal-Liouville evolution equation describes the time evolution of the Wigner function, while the non-commutative Moyal star product parallels the non-commutativity of quantum operators, providing a bridge between classical and quantum mechanics.

In summary, the Weyl transform is an essential tool in linking classical and quantum mechanics, as it maps symplectic manifolds back to Hilbert space. This is accomplished by calculating the ordinary Fourier transform of a phase space distribution and replacing classical variables with quantum operators, eventually creating a version of the function within Hilbert space.

7.5 The Wigner Function as Probability Density

The Wigner function represents a quasi-probability distribution in phase space, which is essential for analyzing quantum systems [94]. Nevertheless, the function is known to exhibit negative values, a consequence of mathematically separating a composite system [59]. Although counter intuitive, these negative values do not infringe upon probability rules, as $W(x, p)$ is not a genuine probability distribution [61].

The negative values of the Wigner function complicate its interpretation in a manner analogous to classical physics, particularly in the context of phase space and entropy. Interpreting $W(x, p)$ along quasi-classical trajectories is further hindered by the constraints introduced by the pixel size. The negative values in the Wigner function suggest that it does not provide a direct interpretation of a classical probability distribution. This issue originates from the possibility of entangled states, which can introduce interference terms associated with the surrounding environment. In order to regard $W(x, p)$ as a classical probability distribution, it is imperative to first incorporate these environmentally induced interference terms into the system. However, under our definition of entropy, which is linked to empirical measurements, this is considered unattainable.

This situation bears similarities to the measurement problem in quantum mechanics, a fundamental issue concerning the transition between quantum states and classical measurements. Resolving the measurement problem would imply the elimination of the interference terms in $W(x, p)$.

7.6 Hudson's Theorem

Hudson's theorem is an important result in the field of quantum mechanics, particularly in the context of the Wigner function. The theorem establishes a criterion for determining when the Wigner function of a pure quantum state is non-negative, implying that the state is Gaussian and can be described entirely by classical mechanics [59]. This accounts for the fact that our earlier discussion was restricted to Gaussian distributions only.

7.6.1 Hudson's Theorem Statement

Hudson's theorem can be stated as follows:

A pure quantum state has a non-negative Wigner function if and only if the state is a Gaussian state [59].

A Gaussian state is a quantum state whose wave function is characterized by a Gaussian function in position and momentum space. Gaussian states can be fully described by classical mechanics, as they do not exhibit non-classical features such as quantum superposition or entanglement. Gaussian states also happen to saturate the uncertainty relation as previously discussed.

7.6.2 Implications of Hudson's Theorem

Hudson's theorem has significant implications for the study of quantum mechanics and the interpretation of the Wigner function. It establishes that non-classical features, such as superposition and entanglement, can only be observed in quantum states with negative values in their Wigner functions. Non-classical states are those that cannot be described entirely by classical mechanics and exhibit quantum features such as superposition, entanglement, and quantum uncertainty. Thus, the presence of negativity in the Wigner function serves as an indicator of non-classical behavior in quantum systems [61].

In quantum optics, Hudson's theorem helps identify non-classical states of light. For instance, in the study of squeezed states, which exhibit reduced quantum uncertainty in one quadrature at the expense of increased uncertainty in the orthogonal quadrature [16], the Wigner function exhibits negativity. This negativity indicates the non-classical nature of squeezed states and their potential application in precision measurements and quantum communication [87].

In quantum information theory, Hudson's theorem aids in the analysis of non-classical correlations and entanglement between quantum systems. For example, when studying continuous-variable entanglement, the negativity of the Wigner function can serve as a criterion for detecting entanglement in composite systems [82].

7.7 Entropy of Phase Space Distributions

To compute the entropy of a Gaussian Wigner function $W_G(x, p)$, one can employ (3.20), yielding the following entropy expression

$$S_I = - \iint W_G(x,p) \ln \left(W_G(x,p) \hbar \pi e \right) \mathrm{d}x \, \mathrm{d}p = 0, \tag{7.25}$$

which implies that the pixel size $I_x I_p = \hbar \pi e$. A state is considered irreducible when it cannot be decomposed into smaller constituent states, while maintaining that the aggregate of these partitions accurately represents the original state. This characteristic arises from the zero entropy nature of the state, signifying that no further refinement can be achieved in describing the state. In other words, all available information about the state has been acquired. However, in the context of Hudson's theorem, determining the entropy from (7.25) for irreducible states can be challenging, as these states often exhibit negative values in their Wigner functions. Despite this, we have previously established the entropy of such states to be zero. The discrepancy observed previously can be attributed to the choice of coordinates employed to describe the state, which, in turn, determines the properties of the state to be measured. This concept can be better comprehended through a parallel discussion in Hilbert space in the subsequent section.

Now, let us consider the Wigner function for reducible states, i.e., $S_I = 0$. A reducible state, i.e. $S_I > 0$, constitutes a statistical combination of irreducible states; hence, the Wigner function of a reducible state is a weighted sum of the Wigner functions corresponding to the irreducible states comprising the reducible state. When combining the Wigner functions of individual irreducible states, their interference terms tend to average out and negate each other, leading to a more positive distribution. As a result, when more environmental factors are integrated into the phase space distribution, the reducible state typically loses coherence, and the interference terms in the Wigner function become less prominent. Consequently, the Wigner function tends to be more positive and closely approximates a classical probability distribution. In other words, as the quantum system interacts with and becomes entangled with its environment, the quantum features of the Wigner function (such as negative values) diminish when the surroundings are incorporated into the Wigner

function itself, causing the distribution to approach a classical-like behavior. This phenomenon is often referred to as decoherence and parallels our earlier discussion on closed systems in Section 6.

7.7.1 Pure Quantum States and Physical Observables

In this section, our objective is to show that all pure quantum state can satisfy the uncertainty relation. The uncertainty principle is often wrongly interpreted to suggest that certain pure states exhibit enhanced determinacy compared to other pure states.

To establish that all pure (irreducible) states exhibit equal determinacy, we point out that every irreducible state $|\psi\rangle$ constitutes an eigenstate of at least one observable. This is accomplished by contemplating two states $|\psi\rangle$ and $|\phi\rangle$ related to each other through a unitary transformation $\hat{U}$ such that $\hat{U}|\psi\rangle = |\phi\rangle$. This is because state space forms a vector space, with $|\psi\rangle$ and $|\phi\rangle$ representing two vectors that delineate a plane. There exists an angle α between these vectors, and the unitary operator $\hat{U}$ can be interpreted to rotate vectors within that plane by α, leaving vectors in the orthogonal directions unaltered.

Subsequently, we consider an operator represented by an observable $\hat{O}$ and presume that $|\phi\rangle$ is an eigenstate of $\hat{O}$ with eigenvalue o such that $\hat{O}|\phi\rangle = o|\phi\rangle$. We can then define another operator $\hat{A} = \hat{U}^\dagger \hat{O} \hat{U}$ that is self-adjoint (Hermitian) and possesses its own eigenstates corresponding to some observables. When $\hat{A}$ is applied to $|\psi\rangle$, we obtain

$$\hat{A}|\psi\rangle = \hat{U}^\dagger \hat{O} \hat{U}|\psi\rangle = \hat{U}^\dagger \hat{O}|\phi\rangle = o\hat{U}^\dagger|\phi\rangle = o|\psi\rangle. \tag{7.26}$$

Thus, we deduce that $\hat{A}|\psi\rangle = o|\psi\rangle$, signifying that $|\psi\rangle$ is an eigenvector of $\hat{A}$ with eigenvalue o. This demonstrates that being an eigenvector of some operator is not an exclusive attribute possessed by specific states; all states exhibit this property, indicating that all states have quantities that are perfectly prepared to measures in a specific way.

Furthermore, we prove that for every state $|\psi\rangle$, there exists a pair of observables $\hat{A}$ and $\hat{B}$ that saturate the uncertainty relation $\sigma_{\hat{A},\psi} \sigma_{\hat{B},\psi} = \frac{\hbar}{2}$, where $\sigma_{\hat{A},\psi}$ and $\sigma_{\hat{B},\psi}$ represent the standard deviations of $\hat{A}$ and $\hat{B}$, respectively, with respect to the state $|\psi\rangle$. To achieve this, we select $|\phi\rangle$ to be the Gaussian wave packet for x and p, which saturates the uncertainty relation. The unitary operator $\hat{U}$ relates $|\psi\rangle$ and $|\phi\rangle$, such that $|\phi\rangle = \hat{U}|\psi\rangle$. We then define $\hat{A} = \hat{U}^\dagger \hat{X} \hat{U}$ and $\hat{B} = \hat{U}^\dagger \hat{P} \hat{U}$. The expectation of $\hat{A}$ with respect to $|\psi\rangle$ can be calculated as follows

$$\langle \hat{A} \rangle_\psi = \langle \psi | \hat{A} | \psi \rangle = \langle \psi | \hat{U}^\dagger \hat{X} \hat{U} | \psi \rangle = \langle \phi | \hat{X} | \phi \rangle = \langle \hat{X} \rangle_\phi. \tag{7.27}$$

The expectation of $\hat{A}^2$ can be calculated similarly

$$\langle \hat{A}^2 \rangle_\psi = \langle \psi | \hat{A} \hat{A} | \psi \rangle = \langle \psi | \hat{U}^\dagger \hat{X} \hat{U} \hat{U}^\dagger \hat{X} \hat{U} | \psi \rangle = \langle \phi | \hat{X} \hat{X} | \phi \rangle = \langle \hat{X}^2 \rangle_\phi. \tag{7.28}$$

Analogous calculations can be conducted for $\hat{B}$, resulting in

$$\langle \hat{B} \rangle_\psi = \langle \hat{P} \rangle_\phi, \qquad \langle \hat{B}^2 \rangle_\psi = \langle \hat{P}^2 \rangle_\phi. \tag{7.29}$$

The standard deviations can then be expressed in terms of these quantities. Thus, $\sigma_{\hat{A},\psi}$ given $|\psi\rangle$ is

$$\sigma_{\hat{A},\psi} = \sqrt{\langle \hat{A}^2 \rangle - \langle \hat{A} \rangle^2} = \sqrt{\langle \hat{X}^2 \rangle - \langle \hat{X} \rangle^2} = \sigma_{\hat{X},\phi}, \tag{7.30}$$

and similarly,

$$\sigma_{\hat{B},\psi} = \sqrt{\langle \hat{B}^2 \rangle - \langle \hat{B} \rangle^2} = \sqrt{\langle \hat{P}^2 \rangle - \langle \hat{P} \rangle^2} = \sigma_{\hat{P},\phi}. \tag{7.31}$$

Since $|\phi\rangle$ is Gaussian and saturates the uncertainty relation, we obtain

$$\sigma_{\hat{A},\psi}\sigma_{\hat{B},\psi} = \sigma_{\hat{X},\psi}\sigma_{\hat{P},\psi} = \frac{\hbar}{2}. \tag{7.32}$$

Alternatively, we can use the commutation relation $[\hat{A},\hat{B}] = i\hbar$ to similarly show that

$$[\hat{A},\hat{B}] = \hat{A}\hat{B} - \hat{B}\hat{A} = \hat{U}^{\dagger}\hat{X}\hat{U}\hat{U}^{\dagger}\hat{P}\hat{U} - \hat{U}^{\dagger}\hat{P}\hat{U}\hat{U}^{\dagger}\hat{X}\hat{U} = \hat{U}^{\dagger}[\hat{X},\hat{P}]\hat{U} = i\hbar\hat{U}^{\dagger}\hat{U} = i\hbar. \tag{7.33}$$

In conclusion, we have demonstrated that for every state $|\psi\rangle$, there exists a pair of observables $\hat{A}$ and $\hat{B}$ that satisfies the uncertainty relationship, with $\sigma_{\hat{A},\psi}\sigma_{\hat{B},\psi} = \frac{\hbar}{2}$. This implies that each pure quantum state is a Gaussian state for some pair of non-commuting Hermitian operators. This substantiates that no state is more determined than another in terms of the uncertainty principle. All states have quantities that are perfectly prepared, and every state can be related to another state through a unitary transformation.

7.7.2   Entropy Continued

In the context of the Weyl transform, the operators in the exponent determine the basis in which the resulting wave function is expressed in. These operators correspond to observables that satisfy the uncertainty relation. A wave function $|\psi\rangle$ is said to be compatible with the Hermitian operators $\hat{A}$ and $\hat{B}$ if it satisfies the uncertainty relation with respect to these observables.

When the zero entropy phase space probability density $W(x,p)$ is Gaussian, it is compatible with the operators $\hat{X}$ and $\hat{P}$ in Hilbert space. This is because the Gaussian distribution for a zero entropy phase space probability density is strictly non-negative. If the operators $\hat{X}$ and $\hat{P}$ are used in the exponent of the Weyl transform, the resulting wave function will be compatible with these observables, corresponding to a set of physical measurements.

In the case of an irreducible non-Gaussian distributions, Hudson's theorem dictates that they must contain negative regions. As a result, the observables of position and momentum, represented by the Hermitian operators $\hat{X}$ and $\hat{P}$, are not compatible in this case. Consequently, calculating its entropy in phase space is not possible due to its negative values. This is consistent with the empirical definition of entropy, which loses its meaning outside of a measurement context. This is because the description of the state in phase space is formulated within a context in which a meaningful independent measurement can be made, avoiding entanglement or interference with the environment.

On the other hand, if an irreducible non-Gaussian Wigner function is compatible with a pair of conjugate Hermitian operators $\hat{A}$ and $\hat{B}$, then the use of these operators in the exponent of the Weyl transform will result in a Gaussian wave function expressed in the basis corresponding to the variables a and b.

The Wehrl entropy can be utilized to determine the entropy of measurable states in phase space without considering the specifics of the particular nature of the measurement process itself [88]. The calculation of entropy for a Wigner function involves the convolution of the function with a Gaussian followed by the application of the standard entropy integral. Further elaboration of the details will not be provided in this text. It is worth noting that the Von Neumann entropy serves a similar purpose in Hilbert space, providing a means of counting and quantifying the potential measurable information with disregard to how the state is intended to be measured. This is discussed in the next section where we similarly show that the Von Neumann entropy for any pure quantum state is always zero.

7.8   Von Neumann Entropy

Von Neumann entropy is a fundamental concept in quantum information theory, providing a measure of the uncertainty of a quantum state. It is defined for a given density matrix $\hat{\rho}$ as follows

$$S(\rho) = -\mathrm{Tr}(\hat{\rho}\ln(\hat{\rho})), \tag{7.34}$$

where $\mathrm{Tr}(\cdot)$ denotes the trace operation.

7.8.1   Pure and Mixed States

In quantum mechanics, states can be categorized into two types: pure states and mixed states. A pure state is represented by a wave function or a state vector and is described by a density matrix of the form $\rho = |\psi\rangle\langle\psi|$, where $|\psi\rangle$ is the state vector. A mixed state, on the other hand, is described by a density matrix that is a convex combination of pure states

$$\hat{\rho} = \sum_i p_i |\psi_i\rangle\langle\psi_i|, \tag{7.35}$$

where $p_i \geq 0$ and $\sum_i p_i = 1$.

7.8.2   Von Neumann Entropy of Pure States

For pure states, the von Neumann entropy is zero. To see this, consider a pure state with density matrix $\rho = |\psi\rangle\langle\psi|$. The von Neumann entropy is then given by:

$$S(\hat{\rho}) = -\mathrm{Tr}(\rho\ln(\hat{\rho})) \tag{7.36}$$
$$= -\mathrm{Tr}(|\psi\rangle\langle\psi|\ln(|\psi\rangle\langle\psi|)). \tag{7.37}$$

Since $\hat{\rho}^2 = |\psi\rangle\langle\psi|\psi\rangle\langle\psi| = |\psi\rangle\langle\psi| = \hat{\rho}$, we have $\ln(\hat{\rho}^2) = 2\ln(\hat{\rho})$, due to the fact that $\langle\psi|\psi\rangle = 1$ for pure quantum states. Since $\hat{\rho} = \hat{\rho}^2$, then it should follow that $S(\hat{\rho}) = S(\hat{\rho}^2)$. Therefore, the von Neumann entropy of a pure state is shown to be zero because,

$$S(\hat{\rho}) = S(\hat{\rho}^2) = -\mathrm{Tr}(\hat{\rho}^2\ln(\hat{\rho}^2)) = -2\mathrm{Tr}(\hat{\rho}\ln(\hat{\rho})) = 2S(\hat{\rho}) \implies S(\hat{\rho}) = 0. \tag{7.38}$$

This outcome is in agreement with our previous analysis of irreducible and reducible states, which correspond to pure and mixed quantum states, respectively. As previously noted, irreducible states exhibit zero entropy and set a fundamental lower bound on the information that can be known about a state.

7.8.3   Von Neumann Entropy of Mixed States

To show that the von Neumann entropy reduces to the Shannon entropy for mixed quantum states, let's first define the respective entropies and then consider a mixed quantum state.

The von Neumann entropy $S(\hat{\rho})$ of a quantum state in terms of its density matrix $\hat{\rho}$ is defined as

$$S(\hat{\rho}) = -\mathrm{Tr}(\hat{\rho}\ln(\hat{\rho})). \tag{7.39}$$

Let us consider a mixed quantum state $\hat{\rho}$ that is diagonal in some basis. A mixed state can be represented as a density matrix, which is a convex combination of pure states

$$\hat{\rho} = \sum_i \mathcal{P}_i |\psi_i\rangle\langle\psi_i|, \tag{7.40}$$

where $|\psi_i\rangle$ are the pure states and $\mathcal{P}_i$ are the probabilities associated with each state.

Assume that $\hat{\rho}$ is diagonal in the basis formed by the pure states $|\psi_i\rangle$. In this case, the density matrix $\hat{\rho}$ is given by

$$\hat{\rho} = \begin{pmatrix} \mathcal{P}_1 & 0 & \cdots & 0 \\ 0 & \mathcal{P}_2 & \cdots & 0 \\ \vdots & \vdots & \ddots & \vdots \\ 0 & 0 & \cdots & \mathcal{P}_n \end{pmatrix}. \tag{7.41}$$

To compute the von Neumann entropy, we need to calculate $\hat{\rho} \log \hat{\rho}$. Since the matrix $\hat{\rho}$ is diagonal, the logarithm of $\hat{\rho}$ is also a diagonal matrix, with the logarithm of the diagonal elements

$$\log \hat{\rho} = \begin{pmatrix} \log \mathcal{P}_1 & 0 & \cdots & 0 \\ 0 & \log \mathcal{P}_2 & \cdots & 0 \\ \vdots & \vdots & \ddots & \vdots \\ 0 & 0 & \cdots & \log \mathcal{P}_n \end{pmatrix}. \tag{7.42}$$

Now, we compute the product $\hat{\rho} \log \hat{\rho}$

$$\hat{\rho} \log \hat{\rho} = \begin{pmatrix} \mathcal{P}_1 \log \mathcal{P}_1 & 0 & \cdots & 0 \\ 0 & \mathcal{P}_2 \log \mathcal{P}_2 & \cdots & 0 \\ \vdots & \vdots & \ddots & \vdots \\ 0 & 0 & \cdots & \mathcal{P}_n \log \mathcal{P}_n \end{pmatrix}. \tag{7.43}$$

Taking the trace of the resulting matrix, we get

$$\mathrm{Tr}(\hat{\rho} \ln(\hat{\rho})) = \mathcal{P}_1 \ln \mathcal{P}_1 + \mathcal{P}_2 \ln \mathcal{P}_2 + \cdots + \mathcal{P}_n \ln \mathcal{P}_n = \sum_{i=1}^{n} \mathcal{P}_i \ln \mathcal{P}_i. \tag{7.44}$$

Finally, substituting this result back into the von Neumann entropy formula, we obtain

$$S(\hat{\rho}) = -\mathrm{Tr}(\hat{\rho} \ln \hat{\rho}) = -\sum_{i=1}^{n} \mathcal{P}_i \ln \mathcal{P}_i, \tag{7.45}$$

which shows that the von Neumann entropy reduces to the Shannon entropy for mixed quantum states when the density matrix is diagonal in the basis formed by the pure states.

If the density matrix is not diagonal in the basis of the pure states, we can still relate the von Neumann entropy to the Shannon entropy by diagonalizing the density matrix.

Suppose $\hat{\rho}$ is a density matrix representing a mixed quantum state, and it is not diagonal in the basis formed by the pure states $|\psi_i\rangle$. Then, we can always diagonalize $\hat{\rho}$ by finding a new orthonormal basis $|\phi_i\rangle$ such that the matrix representation of $\hat{\rho}$ in this basis is diagonal. This is possible because the density matrix is Hermitian, and Hermitian matrices can always be diagonalized by a unitary transformation.

Let $\hat{U}$ be the unitary matrix that diagonalizes $\hat{\rho}$, i.e.

$$\hat{\rho}' = \hat{U}\hat{\rho}\hat{U}^{\dagger} \begin{pmatrix} \mathcal{Q}_1 & 0 & \cdots & 0 \\ 0 & \mathcal{Q}_2 & \cdots & 0 \\ \vdots & \vdots & \ddots & \vdots \\ 0 & 0 & \cdots & \mathcal{Q}_n \end{pmatrix}. \tag{7.46}$$

where $\mathcal{Q}_i$ are the eigenvalues of $\hat{\rho}'$, which are also the probabilities associated with the new basis states $|\phi_i\rangle$. Since the trace operation is invariant under basis transformations, we have

$$S(\hat{\rho}) = -\text{Tr}(\hat{\rho}\ln(\hat{\rho})) = -\text{Tr}(\hat{U}^\dagger \hat{\rho}' \hat{U} \ln(\hat{U}^\dagger \hat{\rho}' \hat{U})). \tag{7.47}$$

Now, using the cyclic property of the trace, we can rewrite this as

$$S(\hat{\rho}) = -\text{Tr}(\hat{U}^\dagger \hat{\rho}' \hat{U} \hat{U}^\dagger \ln(\hat{\rho}') \hat{U}) = -\text{Tr}(\hat{\rho}' \ln(\hat{\rho}')) = S(\hat{\rho}'). \tag{7.48}$$

Since $\hat{\rho}'$ is a diagonal matrix, we can now follow the same procedure as before to show that the von Neumann entropy reduces to the Shannon entropy for the diagonalized density matrix $\hat{\rho}'$

$$S(\hat{\rho}) = -\text{Tr}(\hat{\rho}' \ln(\hat{\rho}')) = -\sum_{i=1}^{n} \mathcal{Q}_i \ln \mathcal{Q}_i. \tag{7.49}$$

In this case, the von Neumann entropy reduces to the Shannon entropy of the probability distribution $\mathcal{Q} = \{\mathcal{Q}_i\}$, which corresponds to the eigenvalues of the density matrix $\hat{\rho}'$.

The trace operation is a useful tool in this context as it exhibits basis invariance for square matrices. Specifically, the trace is equal to the sum of the eigenvalues of the density matrix, regardless of the chosen basis. This contrasts with our prior discussion of the negativity of the Wigner function, which is dependent on the choice of basis and thus corresponds to different observable measurements. The trace, however, circumvents this dependence on the choice of basis as it only considers the measurable states without reference to the method of measurement. Furthermore, the equivalence of the von Neumann entropy to the Shannon entropy for mixed states aligns with our particular redefinition of entropy.

This allows our definition of entropy to be considered as the phase space equivalent of the von Neumann entropy, differing in that our definition does care about how the measurement performed. Unlike the thermodynamic Gibbs entropy, which has units of Joules per Kelvin and represents the informational entropy of a state at equilibrium without a connection to empirical measurements or any form of a pixel, our definition of entropy is dimensionless and reflects the empirically measurable information of any state, whether in or out of equilibrium. As a result, our definition implies that the entropy of any closed system can never increase, while the thermodynamic equilibrium entropy may increase with volume expansions. This is due to the fact that the thermodynamic (equilibrium entropy) of a closed system can increase, where as the actual entropy cannot, as it would not only imply a loss of information, but would also violate energy conservation within the system.

In conclusion, the von Neumann entropy is equal to zero for pure states and is positive for mixed states. In the latter case, the von Neumann entropy reduces to the Shannon entropy.

7.9 Comparison of Koopman-von Neumann Theory and Wigner Formulation

Koopman–von Neumann theory, proposed by Bernard Koopman and John von Neumann in 1931 [63], is a classical-like description of quantum mechanics in phase space. Thus, Koopman–von Neumann theory and the Wigner-Moyal formulation are both phase space representations of quantum mechanics. While the Wigner formulation is a an non-commutative approach that incorporates a pixel size, the Koopman–von Neumann theory can be viewed as the limit of the Wigner formulation as the pixel size $\hbar \to 0$.

As a result, the Moyal-Liouville formalism is shown to encapsulate the phase space pixelation framework. As the phase space pixel size approaches zero ($\hbar\pi e \to 0$), the evolution of the Wigner function within the Moyal-Liouville formalism reduce to the classical Liouville's equation [12][10]. This results in the classical theory of Koopman–von Neumann mechanics, which is expectedly accompanied by an inherent entropy problem, causing it to inadequately describe quantum phenomena, such as the double-slit experiment [69][42][43].

The mismatch between the Koopman–von Neumann theory and empirical experiments is a consequence of this entropy issue. The Koopman–von Neumann formulation is unable to reproduce

certain key features of quantum mechanics, such as entanglement and quantum correlations, due to the inability to quantify the measurable information content in a particular experimental setup. This entropy problem stems from the fact that the theory does not preserve the Liouville measure, which is required to ensure a finite and constant entropy. Instead, the Koopman–von Neumann dynamics can generate infinite information, leading to an nonphysical divergence in entropy [95]. In contrast, the Wigner formulation does not suffer from the entropy problem, as it preserves the Liouville measure and maintains a finite and constant entropy. As discussed numerous times already, the continuous entropy delineation needed for accurately describing quantum phenomena requires a non-zero pixel size, which is absent in the classical theory.

In a specific theoretical framework, as the pixel size vanishes, represented by $\hbar \to 0$, the capacity for continuous entropy delineation does likewise, subsequently undermining the theory's predictive power at finer scales and limiting its efficacy in accurately describing quantum phenomena. In the context of comparing the Wigner-Moyal formalism, which has a non-zero pixel size ($\hbar$), to the Koopman–von Neumann formalism, which lacks the ability to predict quantum phenomena due to zero pixel size and absence of continuous entropy. The inherent non-commutative properties of the former framework serve to maintain a non-zero pixel size, thereby ensuring the potential for continuous entropy delineation.

In summary, while both Koopman–von Neumann theory and the Wigner formulation provide phase space representations of quantum mechanics, the Koopman–von Neumann theory is limited by its entropy problem and inability to match empirical experiments in certain cases. The Wigner formulation offers a more consistent semiclassical approach, converging to classical mechanics as the pixel size approaches zero and preserving the Liouville measure to ensure a finite and constant entropy.

7.10 Entropy Problem and Distinguishing Quantum Mechanics from Classical Mechanics

In phase space, which provides a symplectic manifold, entropy is coordinate invariant under canonical transformations with a Jacobian determinant equal to one. In contrast, in Hilbert space, unitary transformations are used to maintain this invariance.

The assumption of a minimal pixel size leads to the emergence of quantum mechanics through the Hirschman uncertainty relation. By employing a wave function of position and relating the momentum function through the Fourier transform, if either one of the functions is made too narrow, the other will widen to maintain positive entropy in phase space [60].

The Wigner function, $W(x,p)$, bears certain similarities to the probability density $\rho(x,p)$ in phase space, although this analogy is not entirely accurate. The Wigner function is a quasiprobability distribution, which implies that it can assume negative values, a characteristic that is evident from the requirement of pixel size to ensure the non-negativity of entropy, i.e., $S_I \geq 0$. Negative probabilities often arise from quantum interference, particularly when attempting to isolate a system that exists only as a composite. In this regard, we examined the interpretation of negative probabilities through various examples, shedding light on why the Gaussian case was initially easier to examine in the context of Hudson's theorem.

Incorporating phase space pixelation into classical physics necessitates alterations to the temporal evolution equations. An evolution equation akin to Liouville's equation, which accounts for the constraints imposed by phase space pixelation, is required to prevent simultaneous state localization, because describing a system with greater precision than the resolution of the pixel leads to negative entropy. The introduction of phase space pixel leads to a transition toward non-commutative geometry.

To connect a mathematical theory to empirical observations, entropy is essential for quantifying the potential measurable. In statistical physics, specifying entropy and energy for a given system suffices to determine the system's temporal evolution. A continuous entropy definition necessitates a pixel size; without it, quantification of the measurable states predicted by the theory becomes

impossible, particularly at smaller scales. Integrating a pixel size naturally arises when quantifying the information related to measurable states within a continuous state space. For continuous state spaces to possess entropy, a pixel size is indispensable. The absence of entropy in a physical theory involving continuous state spaces signifies an inability to describe and quantify the measurable states that could, in principle, be predicted by the theory.

The entropy of quantum states in Hilbert space were examined using Von Neumann entropy and subsequently compared to the phase space entropy addressed in earlier sections. It was be demonstrated that all quantum pure states possess zero entropy, corresponding to the imposition of an analogous phase space pixel size equivalent, in Hilbert space. Consequently, a pure quantum state represents the most accurate description of a state that can be measured and described within the imposed positive entropy constraint. These states are fundamentally irreducible, signifying that one cannot depict the state as a sum of smaller components. These hypothetical smaller components, resulting from partitioning the state, necessitate a more precise description than what is permitted by the phase space pixel, leading to negative entropy values.

8 A Philosophical Case for Bitemporal Causality

In this section, a philosophical argument for the concept of microscopic bitemporal causality is presented. This concept postulates that causality operates in both temporal directions, rendering the distinction between cause and effect meaningless. As a result, the state of a system at a given moment is determined by both past and future events. This idea is central to Wessel-Berg's bitemporal theory [91, p. 8], in which he asserts that:

> *Empirical facts involving single events of microscopic entities in the microcosm can not be explained by any objective causal theory.*

This leads to the inference that the universe cannot exhibit both causal and deterministic properties simultaneously.

One of the most successful theoretical frameworks, quantum field theory, fundamentally incorporates charge parity time symmetry, which is inconsistent with a unidirectional causal framework. Despite this fact, causality is still often assumed to be applicable in the microcosm. This assumption is intriguing, given that even in classical physics, it is believed that the world operates according to a reversible and deterministic framework where the state of a system at any given moment is determined not only by past events but also by future events, rendering the distinction between cause and effect irrelevant.

This is evident, for instance, in Hamiltonian mechanics in phase space, a framework employed to describe the behavior of systems in classical mechanics, which operates in a non-causal fashion. When a state in phase space is identified, both its future and past states can be ascertained, rendering the attribution of the origin of the state equally pertinent for future states as it is for past states. In this scenario, causality loses its significance.

In this discussion, we adopt a purely physical perspective on the universe and its contents, where everything evolves according to a set of evolution equations akin to the Hamiltonian formulation. From this perspective, humans are composed of the same mechanical and physical building blocks as everything else we study, all governed by the laws of physics. In this view, humans can be seen as complex algorithms based on matter that has evolved to ensure survival and reproduction.

Although humans exhibit complex behavior, it is essential to recognize that this behavior should also adhere to the laws of physics. It is unreasonable to suggest that humans possess an internal free will that allows them to defy the established laws of physics within their brains, unlike the rest of the matter in the universe. Consequently, if one could theoretically know the precise positions and interactions of all atoms and electrical impulses within a person and their environment, it would be possible to predict their future actions. In this framework, the concept of free will loses its meaning. In other words, humans are not distinct *ghosts* with free will in a deterministic and mechanical universe; rather, they are an integral part of the universe itself.

However, humans possess a unique operating system, the brain, that perceives the world in a way that is beneficial for survival. It is reasonable to assume that humans have evolved to perceive the world causally, which is favorable for survival and decision-making. The idea of causality is advantageous to us, as it allows us to make predictions and take actions rooted in past experiences. It is important to understand that the actual nature of the universe is independent of how we are programmed to perceive it. For example, our perception of time as a universal phenomenon is challenged by the theory of special relativity, which asserts that time is relative to the observer. This concept suggests that our understanding of time as a linear, unidirectional progression may not accurately represent reality.

From this perspective, the scientific process itself can be viewed as an expression of the universe's endeavor to comprehend itself. The present perspective posits that human beings do not possess a quasi-spiritual quality of volition in a deterministic and mechanistic cosmos, in which they are uniquely endowed with the ability to experimentally manipulate and observe the causal chain of events. Rather, humans are regarded as constituent elements of the universe, in no wise separate from the totality thereof. That is, humans are interconnected with the universe, and our under-

standing of it is ultimately an exploration of our own existence within this vast cosmic system.

In recent years, the application of the microscopic causal framework to quantum-related phenomena has resulted in numerous inconsistencies and paradoxes. One such phenomenon is quantum entanglement, which exhibits correlations between particles that appear to be independent of spatial and temporal constraints when viewed through a causal lens. This phenomenon, characterized by the instantaneous correlation of particle properties, regardless of their distance, has led some individuals to explore and adapt the concept of bitemporal causality.

Experimental evidence, such as the delayed-choice quantum eraser experiment conducted by Kim et al. (2000), supports the plausibility of bitemporal causality [62]. In this experiment, the decision to measure the path information or interference pattern of a photon was made after the photon had already passed through a double-slit apparatus. The results indicated that the decision to measure one property or the other determined the behavior of the photon, suggesting that causality may indeed operate in reverse.

In order to better understand the behavior of microscopic systems, it is essential to adopt a descriptive, rather than prescriptive, approach. As depicted in Figure 12, the state of the system simply exists and is not caused by anything else, either in its future or its past. It is merely a trajectory in phase space signifying the temporal evolutions of the universe, and the goal should be to describe the system as it is, without attributing causality to it. By avoiding the preconceived notion of cause and effect, one can gain a deeper understanding of the intricacies of the microscopic realm.

The conventional assumption of independence between measurements and the objects being measured is challenged by the recognition that each measurement process occurs in accordance with the laws of physics. As a result, the concept of independent measurements loses its meaning and becomes inapplicable in this context. This implies that the behavior of a quantum system is dependent on the manner in which it is measured, arising directly from the assumption of bitemporal causality.

The notion of free will posits that an individual has the ability to control and manipulate their own thoughts and actions in a manner that is not subject to the laws of physics, thereby allowing them to act as an autonomous entity in an otherwise deterministic universe and perform independent measurements. However, the assumption of bitemporal causality implies that the behavior of a quantum particle is contingent on the measurement that will take place. This is a necessary outcome if causality is rejected and an approach based on the bitemporal causality of phase space trajectories is adopted instead. This means that the probability of a quantum particle exhibiting a particular behavior is dependent on the detector settings at the time of measurement, which is to take place in the future.

The main argument put forth in Wessel-Berg's book is that the resolution of quantum paradoxes can be achieved by adopting bitemporal causality as a fundamental principle of the world. This approach entails a form of absolute determinism and the absence of free will. If the world operates according to deterministic principles, as implied by the bitemporal causality assumption, and this applies not only to inanimate objects but also to the behavior of physicists, including their beliefs and decisions regarding which experiments to perform, then many quantum paradoxes appear to resolve. This includes the predetermined choice by a physicist to perform a specific set of measurements rather than alternatives.

The rejection of determinism due to personal aversion to its implications is argued here to be poor scientific practice, as the role of the scientist is to attempt to create an objective description of the world irrespective of ones own feelings towards it. This thesis will operate under the assumption of bitemporal causality, as it is believed to be the correct explanation for quantum observations, which will be further explored in later sections.

Part III

Understanding the Antiphoton

Given the fact that the electromagnetic fields are represented in an inner product space, our exploration entails an in-depth comparison and generalization of specific quantum mechanics attributes within the Hilbert space, under both non-relativistic and relativistic frameworks. We then introduce the photon wave function, probing its inherent challenges related to the adequacy of position operators within the context of Hegerfeldt's theorem, particularly when negative energy solutions are disregarded. We conclude this section with a compelling example from Wessel-Berg's book, illustrating how the bitemporal theory effectively resolves the entropy issue. The insights gleaned from this part will prove instrumental as we delve into future discussions centered around bitemporal electromagnetism.

9 Relativistic and Non-Relativistic Wave Functions in Hilbert Space

In this section, we explore and compare both relativistic and non-relativistic equations within the framework of Hilbert space. However, prior to diving into this comparison, we find it crucial to elucidate the energy-time term that frequently surfaces within the exponentials of quantum formulations in Hilbert space.

9.1 The Origin of the Energy-Time Term

In the first part of this thesis we examined the nature of the $e^{\frac{i}{\hbar}\boldsymbol{r}\cdot\boldsymbol{p}}$ expansion vectors that formed a basis for any arbitrary quantum states in Hilbert space. However, when considering time evolution of these states, the expansion vector $e^{\frac{i}{\hbar}(\boldsymbol{r}\cdot\boldsymbol{p}-Et)}$ attains an additional term involving energy E times time t with a minus sign. The origin of the form of this exponential can be understood by first introducing Hamilton-Jacobi equations and Feynman's path integral formulation of quantum mechanics. The below discussion is based on a 2010 paper by J.H.Field (Ref. [35]) which is recommended to the curious reader that wishes to understand the topic at a greater depth.

9.1.1 Hamilton-Jacobi Equation and Action

First, let's start with the Hamilton's equations of motion for an n-dimensional classical system. We have a Hamiltonian $H(q_i, p_i, t)$, where q_i and p_i for $i = 1, 2, \ldots, n$ are the generalized coordinates and momenta, respectively. Hamilton's equations of motion are:

$$\frac{\mathrm{d}q_i}{\mathrm{d}t} = \frac{\partial H}{\partial p_i}, \qquad \frac{\mathrm{d}p_i}{\mathrm{d}t} = -\frac{\partial H}{\partial q_i}. \tag{9.1}$$

To derive the Hamilton-Jacobi equation, let's begin by considering a canonical transformation from the old coordinates (q_i, p_i) to the new coordinates (Q_i, P_i) that satisfy the following Hamiltonian equation

$$\frac{\mathrm{d}Q_i}{\mathrm{d}t} = \frac{\partial K}{\partial P_i}, \qquad \frac{\mathrm{d}P_i}{\mathrm{d}t} = -\frac{\partial K}{\partial Q_i}, \tag{9.2}$$

where the new Hamiltonian K of the transformed coordinates is related to H via a generating function F , such that

$$K(Q_i, P_i, t) = H(q_i, p_i, t) + \frac{\partial F}{\partial t}, \tag{9.3}$$

for any $F(q_i, Q_i, t)$, $F(p_i, Q_i, t)$, $F(q_i, P_i, t)$ or $F(q_i, P_i, t)$ $S \equiv$ [40]. The new Hamiltonian $K(Q_i, P_i, t)$ can be set to zero by defining the generating function $S = F(q_i, P_i, t)$ such that S satisfies

$$H(q_i, p_i, t) + \frac{\partial S}{\partial t} = 0, \tag{9.4}$$

where it is customary to call S as *Hamilton's principal function*. With this generating function S, the transformation equation become [40]

$$p_i = \frac{\partial S}{\partial q_i}, \qquad Q_i = \frac{\partial S}{\partial P_i}, \tag{9.5}$$

where upon substitution of the first equation into (9.4) yield

$$H\left(q_i, \frac{\partial S}{\partial q_i}, t\right) + \frac{\partial S}{\partial t} = 0, \tag{9.6}$$

which is the Hamilton-Jacobi equation. This equation can be used to solve for S which results in the equations of motion given by (9.5) for Q_i and p_i where the original spatial coordinate $q_i = q_i(Q_i, P_i, t)$ in these equations is given in terms of old coordinates [40]. This is is because the new momenta P_i in this canonical transformation must be constants which are fixed by the initial conditions in these transformed coordinates rendering $S(q_i, t)$ to be a function of q_i and t only [41]. This fact implies that that

$$dS = \sum_{i=1}^{n} \frac{\partial S}{\partial q_i} \, dq_i + \frac{\partial S}{\partial t} \, dt = \left(\sum_{i=1}^{n} p_i \frac{dq_i}{dt} - H\right) dt = \mathcal{L} \, dt, \tag{9.7}$$

where Equations (9.4) and (9.5) were utilized in the second last step that resulted in the identification of the Lagrangian function $\mathcal{L}$ for the dynamical system in the final step. The Hamilton's function S can be identified as an action of the Lagrangian by integrating (9.7) between two fixed times t_i and t_f along a given path

$$S = \int_{t_i}^{t_f} \mathcal{L} \, dt, \tag{9.8}$$

which is an important realization in our subsequent discussion of the Feynman path integral formulation of quantum mechanics.

9.1.2 Feynman Path Integral Formulation

The Feynman path integral method, also known as the path integral formulation of quantum mechanics, is an alternative approach to the standard wave function-based methods for describing quantum systems. It is based on the principle of least action, which states that the action of a classical system is minimized along the trajectory of a particle. The method was developed by Richard Feynman in the 1940s and is now a central tool in quantum field theory and statistical mechanics. The two main postulates of the Feynman path integral method are [33]:

I. **Superposition and Born's Probabilistic Interpretation:** The probability of finding a particle in a particular region of spacetime is given by the absolute square of the sum of complex contributions from each path in that region. The complex contributions are the probability amplitudes for each path. Mathematically, this can be expressed as

$$P(\mathcal{B}, \mathcal{A}) = \left|\sum_{\text{paths}} K_{\text{path}}\right|^2. \tag{9.9}$$

Here, $P(\mathcal{B}, \mathcal{A})$ is the probability of finding the particle in the spacetime region between points $\mathcal{A}$ at time t_i and $\mathcal{B}$ at time t_f, and K_{path} is the probability amplitude for each path.

II. Path Amplitude and Action: The amplitude for all paths between two points is given by a common real function, A, multiplied by the exponential of the classical action, in units of $\hbar$, contributing to phase differences between different paths. The classical action, $S([\boldsymbol{r}(t)]_i)$, is the time integral of the Lagrangian, $\mathcal{L}$, along the ith path $[\boldsymbol{r}(t)]_i$ in spacetime between some fixed times t_i and t_f between two fixed points defining the path, such that

$$K_{\text{path}} = A \exp\left(\frac{i}{\hbar} S([\boldsymbol{r}(t)]_i)\right), \tag{9.10}$$

where

$$S([\boldsymbol{r}(t)]_i) = \int_{t_i}^{t_f} \mathcal{L}([\boldsymbol{r}(t)]_i, t) dt. \tag{9.11}$$

Here, $\mathcal{L}$ is the classical Lagrangian of the system, and $[\boldsymbol{r}(t)]_i$ corresponds to a particular spacetime path between times t_i and t_f.

Combining both postulates, the probability of finding a particle in a particular region of spacetime is given by

$$P(\mathcal{B}, \mathcal{A}) = \left|\sum_{\text{paths}} A \exp\left(\frac{i}{\hbar} S([\boldsymbol{r}(t)])\right)\right|^2. \tag{9.12}$$

This expression highlights the key features of the Feynman path integral formulation: the superposition of probability amplitudes for each path and the dependence of the path amplitudes on the classical action. By considering all possible paths and summing their amplitudes, the Feynman path integral method provides a powerful way to compute the probability amplitudes and, ultimately, the probabilities for quantum systems to evolve from one state to another. Finally, notice from Equation (9.8) that S, in this case is actually the Hamilton's principle function.

9.1.3 Connection To Quantum Mechanics

By defining an arbitrary wave function

$$\Psi(\boldsymbol{r}, t) = e^{\frac{i}{\hbar} S(\boldsymbol{r}, t)}, \tag{9.13}$$

in this way can be shown that Ψ has all the required properties of a wave function of quantum mechanics [35]. Rearranging (9.13) yield

$$S = -i\hbar \ln(\Psi), \tag{9.14}$$

which results in the following quantities

$$\frac{\partial S}{\partial t} = -\frac{i\hbar}{\Psi}\frac{\partial \Psi}{\partial t}, \quad \frac{\partial S}{\partial x} = -\frac{i\hbar}{\Psi}\frac{\partial \Psi}{\partial x}, \quad \frac{\partial S}{\partial y} = -\frac{i\hbar}{\Psi}\frac{\partial \Psi}{\partial y}, \quad \frac{\partial S}{\partial z} = -\frac{i\hbar}{\Psi}\frac{\partial \Psi}{\partial z}. \tag{9.15}$$

Differentiating the three last term whilst using the fact that $\frac{\partial^2 S}{\partial x^2} = \frac{\partial^2 S}{\partial y^2} = \frac{\partial^2 S}{\partial z^2} = 0$ since for any $\frac{\partial^2 S}{\partial x^2} = \frac{\partial p_x}{\partial x} = 0$, we get

$$\left(\frac{\partial S}{\partial x}\right)^2 = -\frac{\hbar^2}{\Psi}\frac{\partial^2 \Psi}{\partial x^2}, \quad \left(\frac{\partial S}{\partial y}\right)^2 = -\frac{\hbar^2}{\Psi}\frac{\partial^2 \Psi}{\partial y^2}, \quad \left(\frac{\partial S}{\partial z}\right)^2 = -\frac{\hbar^2}{\Psi}\frac{\partial^2 \Psi}{\partial z^2}. \tag{9.16}$$

For a non-relativistic particle moving in a time-independent potential $V(\boldsymbol{r})$, the Hamilton-Jacobi Equation (9.6) becomes

$$\frac{1}{2m}\left[\left(\frac{\partial S}{\partial x}\right)^2 + \left(\frac{\partial S}{\partial y}\right)^2 + \left(\frac{\partial S}{\partial z}\right)^2\right] + V(\boldsymbol{r}) + \frac{\partial S}{\partial t} = 0, \tag{9.17}$$

where the first equation in (9.5) was used for the momentum and m represents the mass of the system. The substitution of the relevant quantities in Equations (9.15) and (9.16) results in the Schrödinger equation

$$i\hbar \frac{\partial \Psi}{\partial t} = -\frac{\hbar^2}{2m}\nabla^2 \Psi + V(\boldsymbol{r})\Psi. \tag{9.18}$$

The above result implies that any wave function Ψ of the Schrödinger equation is a path amplitude of the Feynman formulation. Relativistic equations can similarly be derived in this manner. We can now see that for free space in one dimension, the Hamilton's principle function S with energy E and momentum p can easily be obtained from Equations (9.5) and (9.6), i.e.

$$\frac{\partial S}{\partial x} = p, \qquad \frac{\partial S}{\partial t} = -H = -E \quad \implies \quad S = px - Et, \tag{9.19}$$

This Lorentz invariant quantity can be applied to (9.13) in thee dimensions which implies that

$$\Psi(\boldsymbol{r}, t) = e^{\frac{i}{\hbar} S(\boldsymbol{r}, t)} = e^{\frac{i}{\hbar} (\boldsymbol{r} \cdot \boldsymbol{p} - Et)}. \tag{9.20}$$

This result is quite general and can be applied to relativistic systems [35], where

$$\Psi(\tau) = e^{\pm \frac{i}{\hbar} mc^2 \tau}, \tag{9.21}$$

where c is the speed of light and $\tau = t\gamma$ represents proper time, where $\gamma = \left(1 - \frac{v^2}{c^2}\right)^{-1/2}$ is the Lorentz factor with v representing the magnitude of the velocity. In the next section we will demonstrate how this result can be used in order examine the behaviour of relativistic and non-relativistic systems.

9.2   Orthogonal Complex Exponentials in Quantum Mechanics

In standard quantum theory, wave functions are represented within the Hilbert space framework, allowing any given wave function to be decomposed into a linear combination of orthogonal complex exponentials in the form of the previous result. These exponentials $e^{i(\boldsymbol{r} \cdot \boldsymbol{p} - Et)/\hbar}$ form a basis that spans states represented as wave functions, where $\boldsymbol{p}$ and E denote momentum and energy, respectively. One particular convenience of these vectors stems from their eigenvector properties with respect to the differential operators

$$\hat{E} = i\hbar \frac{\partial}{\partial t} \qquad \hat{\boldsymbol{P}} = -i\hbar \nabla, \tag{9.22}$$

yielding the eigenvalue equations $\hat{E} e^{i(\boldsymbol{r} \cdot \boldsymbol{p}' - E't)/\hbar} = E' e^{i(\boldsymbol{r} \cdot \boldsymbol{p}' - E't)/\hbar}$ and $\hat{\boldsymbol{P}} e^{i(\boldsymbol{r} \cdot \boldsymbol{p}' - E't)/\hbar} = \boldsymbol{p}' e^{i(\boldsymbol{r} \cdot \boldsymbol{p}' - E't)/\hbar}$. Here, E' and $\boldsymbol{p}'$ serve as eigenvalues corresponding to the same eigenvector acted upon by the $\hat{E}$ and $\hat{\boldsymbol{P}}$ operators, respectively. The variables E' and $\boldsymbol{p}'$ are interdependent, as they are connected through an energy equation.

9.3   Non-Relativistic Case

In classical physics, the energy equation is typically expressed as $E = \frac{p^2}{2m} + V(\boldsymbol{r})$ as already discussed in the preceding subsection, with m representing mass and $V(\boldsymbol{r})$ denoting the potential energy as a function of position $\boldsymbol{r}$ of the system under consideration. By multiplying both sides of the aforementioned energy equation by a wave function $\Psi(x, t)$ and substituting the operators $\hat{E}$ and $\hat{\boldsymbol{P}}$ for E and $\boldsymbol{p}$, the Schrödinger equation is obtained:

$$i\hbar \frac{\partial \Psi(\boldsymbol{r}, t)}{\partial t} = -\frac{\hbar^2}{2m} \boldsymbol{\nabla}^2 \Psi(\boldsymbol{r}, t) + V(x) \Psi(\boldsymbol{r}, t). \tag{9.23}$$

9.4   Relativistic Case

In the relativistic scenario, wave equations must be Lorentz invariant to account for the effects of special relativity, and they should satisfy the Einstein energy-momentum relationship. The Einstein energy-momentum relationship is given by

$$E^2 = p^2 c^2 + m^2 c^4, \tag{9.24}$$

where p represents the magnitude of momentum. To derive a relativistic wave equation, we replace the energy and momentum values, E and p, with their respective quantum operators, $\hat{E}$ and $\hat{P}$, yielding

$$\hat{E}^2 = \hat{P}^2 c^2 + m^2 c^4. \tag{9.25}$$

Using the definitions of the operators, $\hat{E} = i\hbar \frac{\partial}{\partial t}$ and $\hat{P} = -i\hbar\nabla$, from (9.22), we obtain

$$\left(-\hbar^2 \frac{\partial^2}{\partial t^2}\right)\Psi(\boldsymbol{r}, t) = \left(-\hbar^2 c^2 \nabla^2 + m^2 c^4\right)\Psi(\boldsymbol{r}, t). \tag{9.26}$$

By rearranging and canceling terms, we obtain the Klein-Gordon equation

$$\frac{\partial^2 \Psi(\boldsymbol{r}, t)}{\partial t^2} - c^2 \nabla^2 \Psi(\boldsymbol{r}, t) = -\frac{m^2 c^4}{\hbar^2}\Psi(\boldsymbol{r}, t). \tag{9.27}$$

The Klein-Gordon equation is a relativistic wave equation that accommodates both positive and negative frequencies, as required by the Einstein energy-momentum relationship (9.24). This equation has plane wave solutions of the form

$$\Psi(\boldsymbol{r}, t) = A e^{i(\boldsymbol{p}\cdot\boldsymbol{r} - Et)}. \tag{9.28}$$

This is because the substitution of these plane waves into (9.27) yields $E^2\Psi = p^2 c^2 \Psi + m^2 c^4 \Psi$, meaning that they satisfy the Einstein energy momentum relation

$$E = \pm\sqrt{p^2 c^2 + m^2 c^4}, \tag{9.29}$$

which take on both positive and negative energies. Additionally, Equation (9.29) can be interpreted as a dispersion relation

$$\omega = \pm\sqrt{k^2 c^2 + \frac{m^2 c^4}{\hbar^2}}, \tag{9.30}$$

where both the energy and momentum are related to the angular frequency ω and the wave number $\boldsymbol{k}$ by

$$E = \hbar\omega, \qquad \boldsymbol{p} = \hbar\boldsymbol{k}. \tag{9.31}$$

This implies that both positive and negative frequencies, and any linear combination of the two, are valid solutions to the Klein-Gordon Equation (9.27). This notion contrasts with the traditional viewpoint in non-relativistic classical physics, where negative energy and frequency solutions are considered unphysical. Conversely, in the context of relativistic quantum mechanics, both positive and negative energy solutions are necessary to form a complete set of states, and the negative energy and frequencies cannot be disregarded [86].

The general solution of the Klein-Gordon equation can be expressed as a linear combination of plane wave solutions with a given $\boldsymbol{k}$

$$\Psi_k(\boldsymbol{x}, t) = A e^{i(\boldsymbol{k}\cdot\boldsymbol{r} - \omega_k t)}, \tag{9.32}$$

where $\omega_k = \pm\sqrt{k^2 c^2 + \frac{m^2 c^4}{\hbar^2}}$, or equivalently

$$\Psi_p(\boldsymbol{x}, t) = A e^{\frac{i}{\hbar}(\boldsymbol{p}\cdot\boldsymbol{r} - E_p t)}, \tag{9.33}$$

where $E_p = \pm\sqrt{p^2 c^2 + m^2 c^4}$ and A is some normalization constant. In contrast to the Schrödinger equation, the Klein-Gordon equation allows for two values of ω for each wave number $\boldsymbol{k}$: a positive and a negative value. To obtain a relativistic wave equation, the positive and negative frequency components must be isolated. To form a complete set of stationary solutions, both positive and negative frequency components must be considered

$$\Psi_p(\boldsymbol{r}, t) = \int \frac{d^3 p}{(2\pi\hbar)^3} e^{\frac{i}{\hbar}\boldsymbol{p}\cdot\boldsymbol{r}} \left[a(\boldsymbol{p})e^{-\frac{i}{\hbar}|E_p|t} + b(\boldsymbol{p})e^{\frac{i}{\hbar}|E_p|t}\right], \tag{9.34}$$

where $a(\boldsymbol{p})$ and $b(\boldsymbol{p})$ are complex coefficients for the positive and negative energies respectively. The integral represents a linear combination of positive frequency solutions (associated with $a(\boldsymbol{p})$) and negative frequency solutions (associated with $b(\boldsymbol{p})$). Both positive and negative frequency solutions are required to form a complete set of orthogonal stationary solutions, which is essential for representing any arbitrary initial condition for the field whilst preserving relativistic causality of physical observables. This idea will be further explored when discussing Hegerfeldt's Theorem in subsequent sections.

Negative Energy Solutions and Antiparticles

Special relativity is acknowledged for its symmetrical treatment of matter and antimatter. Antiparticles are recognized as having equivalent masses to their corresponding particles, yet exhibit negative energy and linear momentum that is opposite in direction to the velocity of propagation. This remains valid as long as the negative energy solutions are not reinterpreted as positive energy antiparticles, as is the case within the framework of conventional quantum field theory.

The energy-momentum relationship, given by (9.24), results in the following equations for particles and antiparticles, respectively

$$E = \gamma m c^2, \qquad E = -\gamma m c^2. \tag{9.35}$$

In accordance with the principles of special relativity, the relationship between a particle's energy E and linear momentum p is established as

$$\boldsymbol{p} = E \frac{\boldsymbol{v}}{c^2}. \tag{9.36}$$

The nature of Equation (9.36) can be further understood by considering the phase velocity $\boldsymbol{v}_{\text{phase}}$ and group velocity $\boldsymbol{v}_{\text{group}}$ for plane wave solutions, given by

$$\boldsymbol{v}_{\text{phase}} = \frac{\omega}{k} \hat{\boldsymbol{k}} = \frac{E}{p} \hat{\boldsymbol{p}} = \pm \frac{\sqrt{p^2 c^2 + m^2 c^4}}{p} \hat{\boldsymbol{p}}, \tag{9.37}$$

and

$$\boldsymbol{v}_{\text{group}} = \frac{\mathrm{d}\omega}{\mathrm{d}k} \hat{\boldsymbol{k}} = \frac{\mathrm{d}E}{\mathrm{d}p} \hat{\boldsymbol{p}} = \pm \frac{pc^2}{\sqrt{p^2 c^2 + m^2 c^4}} \hat{\boldsymbol{p}}, \tag{9.38}$$

where $\hat{\boldsymbol{k}}$ and $\hat{\boldsymbol{p}}$ are unit vectors such that $\boldsymbol{k} = k\hat{\boldsymbol{k}}$ and $\boldsymbol{p} = p\hat{\boldsymbol{p}}$, respectively. By utilizing Equation (9.29) and rearranging terms, Equation (9.36) can be derived from Equation (9.38).

Substituting the energies from (9.35) into (9.36) yields:

$$\boldsymbol{p} = \pm \gamma m \boldsymbol{v}, \tag{9.39}$$

which applies to both particles and antiparticles, indicating that negative energy solutions propagate in a direction opposite to the momentum vector. It is important to note that both particles and antiparticles have equivalent masses and interacting charges. An alternative perspective is that both entities exhibit the same mass, with the energy of the antiparticle considered positive while the sign of the charge and all other related quantum numbers are inverted. This alternative interpretation arises from the requirement that energy must be a positive observable quantity, as dictated by the reinterpretation of negative energies in quantum field theory.

For massless particles, the energy-momentum relationship derived from (9.24) for particles and antiparticles can be expressed as

$$E = pc, \qquad E = -pc. \tag{9.40}$$

This leads to the following expression for linear momentum for particle and anti-particle solutions, respectively

$$\boldsymbol{p} = p \left(\frac{\boldsymbol{v}}{c} \right) = p\hat{\boldsymbol{v}}, \qquad \boldsymbol{p} = -p \left(\frac{\boldsymbol{v}}{c} \right) = -p\hat{\boldsymbol{v}}, \tag{9.41}$$

where $\hat{\boldsymbol{v}}$ is the unit vector along the direction of propagation so that $\left(\frac{\boldsymbol{v}}{c} \right) = \hat{\boldsymbol{v}}$ because massless particles propagate at the speed of light such that $\boldsymbol{v} = c\hat{\boldsymbol{v}}$. It can be observed that the antiparticle exhibits negative energy and its linear momentum is in the opposite direction to its center of mass velocity. This concept is of utmost importance in the sections that follow, particularly in the discussion of the antiphoton.

However, it is crucial to emphasize that these negative energy solutions have been reinterpreted in the context of quantum field theory as antiparticles with positive energy. In this framework, antiparticles are described by positive energy solutions, and the energy, momentum, and velocity are related in the same way as for particles [86]. However, this thesis will not adopt this reinterpretation as it will be shown to be incompatible with photons and bosons in general, and

not as simply as a matter of flipping the charge as with fermions. Furthermore, avoiding this conventional reinterpretation will maintain consistency with the convention employed in Wessel Berg's book. Ultimately, the specific mathematical convention or reinterpretation employed is less significant than the manner in which the variables associated with each convention are related to actual empirical measurements.

Dirac and the Klein-Gordon Equation

Since the Klein-Gordon Equation (9.27) is a second-order partial differential equation in time, and as such, requires the specification of both the wave function $\Psi(\boldsymbol{r}, 0)$ and its derivative $\frac{\partial \Psi(\boldsymbol{r}, t)}{\partial t}$ at $t = 0$ to uniquely determine its solution. These initial conditions provide the necessary information to evolve the wave function in time and fully describe the dynamics of the system. With this in mind, we begin by presenting and examining the Dirac equation.

The Dirac equation is a relativistic wave equation that describes particles with spin-1/2, such as electrons. It was formulated by Paul Dirac in 1928 with the intention of reconciling the principles of quantum mechanics and special relativity [30]. The wave function in the Dirac equation is represented as 4-component spinors, and the equation is considered to be the square root of the Klein-Gordon equation, as the square root of the differential operators is obtained through the introduction of Dirac matrices with anti-commutative properties. These properties ensure that squaring the Dirac equation results in the Einstein energy-momentum relationship (9.24).

As the Dirac equation is a first-order equation in time, it only requires a single initial condition for its solution to be uniquely determined. This represents a significant advantage over the Klein-Gordon equation. However, the Dirac equation necessitates the use of negative frequency solutions as they are coupled to positive frequency solutions through the mass term as seen in a 2-component of left and right spinors

$$i\hbar \frac{\partial}{\partial t} \begin{pmatrix} \Psi_R \\ \Psi_L \end{pmatrix} = i\hbar c \begin{pmatrix} -\overrightarrow{\boldsymbol{\sigma}} \cdot \boldsymbol{\nabla} & 0 \\ 0 & \overrightarrow{\boldsymbol{\sigma}} \cdot \boldsymbol{\nabla} \end{pmatrix} \begin{pmatrix} \Psi_R \\ \Psi_L \end{pmatrix} + \begin{pmatrix} 0 & mc^2 \\ mc^2 & 0 \end{pmatrix} \begin{pmatrix} \Psi_R \\ \Psi_L \end{pmatrix}, \tag{9.42}$$

where $\overrightarrow{\boldsymbol{\sigma}} = (\boldsymbol{\sigma}_x, \boldsymbol{\sigma}_y, \boldsymbol{\sigma}_z)^{\intercal}$ are the Pauli matrices such that $\overrightarrow{\boldsymbol{\sigma}} \cdot \boldsymbol{\nabla} = \boldsymbol{\sigma}_x \partial_x + \boldsymbol{\sigma}_y \partial_y + \boldsymbol{\sigma}_z \partial_z$ and Ψ_L and Ψ_R represent left and right spinor components. The mass term m couples. Setting the mass term in the Dirac equation to zero decouples the left and right spinors and yields the Weyl equation

$$i\hbar \frac{\partial}{\partial t} \begin{pmatrix} \Psi_R \\ \Psi_L \end{pmatrix} = i\hbar c \begin{pmatrix} -\overrightarrow{\boldsymbol{\sigma}} \cdot \boldsymbol{\nabla} & 0 \\ 0 & \overrightarrow{\boldsymbol{\sigma}} \cdot \boldsymbol{\nabla} \end{pmatrix} \begin{pmatrix} \Psi_R \\ \Psi_L \end{pmatrix}, \tag{9.43}$$

due to the absence of off diagonal terms last term of (9.42). The Weyl equation has been used to describe massless spin-1/2 particles, such as neutrinos.

An additional obstacle arises when considering the negative frequency solutions associated with negative energy states of the Klein-Gordon equation. These solutions often lead to issues such as negative probabilities and probability currents. These problems are resolved in the Dirac equation, where negative frequency solutions are reinterpreted as positive frequency solutions for anti-particles, providing a physically meaningful interpretation of the theory.

To derive the probability density and probability current for the Klein-Gordon Equation (9.27), we first start with the equation itself. We can obtain the complex conjugate of the Klein-Gordon equation by taking the complex conjugate of both sides of (9.27)

$$\frac{\partial^2 \Psi(\boldsymbol{r}, t)^*}{\partial t^2} - c^2 \nabla^2 \Psi(\boldsymbol{r}, t)^* = -\frac{m^2 c^4}{\hbar^2} \Psi(\boldsymbol{r}, t)^*. \tag{9.44}$$

Next, we multiply Equation (9.27) by Ψ^* and Equation (9.44) by Ψ, and then subtract the resulting equations

$$\Psi^* \frac{\partial^2 \Psi}{\partial t^2} - \Psi \frac{\partial^2 \Psi^*}{\partial t^2} = \Psi^* \left(c^2 \nabla^2 \Psi - \frac{m^2 c^4}{\hbar^2} \Psi \right) - \Psi \left(c^2 \nabla^2 \Psi^* - \frac{m^2 c^4}{\hbar^2} \Psi^* \right). \tag{9.45}$$

Rearranging the terms and multiplying both sides by $i\hbar$ yields

$$\frac{\partial}{\partial t}\left[i\hbar\left(\Psi^*\frac{\partial\Psi}{\partial t}-\Psi\frac{\partial\Psi^*}{\partial t}\right)\right]+\nabla\cdot\left(\frac{\hbar}{i}\left(\Psi^*\nabla\Psi-\Psi\nabla\Psi^*\right)\right)=0. \tag{9.46}$$

Identifying the probability density $\rho(x,t)$ and probability current $\boldsymbol{J}(x,t)$ as

$$\rho(x,t)=i\hbar\left(\Psi^*\frac{\partial\Psi}{\partial t}-\Psi\frac{\partial\Psi^*}{\partial t}\right), \tag{9.47}$$

$$\boldsymbol{J}(x,t)=\nabla\cdot\left(\frac{\hbar}{i}\left(\Psi^*\nabla\Psi-\Psi\nabla\Psi^*\right)\right). \tag{9.48}$$

Equation (9.46) represents the continuity equation for the Klein-Gordon equation, ensuring the conservation of the current

$$\frac{\partial\rho}{\partial t}+\nabla\cdot\boldsymbol{J}=0. \tag{9.49}$$

In the case of the Klein-Gordon equation, the issue lies with the positivity of the probability density $\rho(x,t)$. Unlike the Dirac equation, the probability density in the Klein-Gordon equation can take on negative values, which complicates its interpretation as a probability density in the conventional sense.

The negative energy solutions can result in negative values for the probability density when considering the general solution of the Klein-Gordon equation. A closer examination of this phenomenon is necessary.

Let $\Psi_p^{(+)}(\boldsymbol{x},t)$ and $\Psi_p^{(-)}(\boldsymbol{x},t)$ be the positive and negative energy components of the general solution, respectively

$$\Psi_p^{(+)}(\boldsymbol{x},t)=\int\frac{d^3p}{(2\pi\hbar)^3}a(\boldsymbol{p})e^{\frac{i}{\hbar}(\boldsymbol{p}\cdot\boldsymbol{r}-|E_p|t)}, \tag{9.50}$$

$$\Psi_p^{(-)}(\boldsymbol{x},t)=\int\frac{d^3p}{(2\pi\hbar)^3}b(\boldsymbol{p})e^{\frac{i}{\hbar}(\boldsymbol{p}\cdot\boldsymbol{r}+|E_p|t)}, \tag{9.51}$$

so that a plane wave of Equation (9.33) yields the following

$$i\hbar\frac{\partial}{\partial t}\Psi_p^{(+)}(\boldsymbol{x},t)=|E_p|\Psi_p^{(+)}(\boldsymbol{x},t)\qquad i\hbar\frac{\partial}{\partial t}\Psi_p^{(-)}(\boldsymbol{x},t)=-|E_p|\Psi_p^{(-)}(\boldsymbol{x},t), \tag{9.52}$$

for the positive and negative energy (frequency) solutions respectively. The general solution is given by

$$\Psi_p(\boldsymbol{x},t)=\Psi_p^{(+)}(\boldsymbol{x},t)+\Psi_p^{(-)}(\boldsymbol{x},t) \tag{9.53}$$

Plugging this into the probability density expression

$$\rho(\boldsymbol{r},t)=i\hbar\left(\Psi_p^{(+)*}+\Psi_p^{(-)*}\right)\left(\frac{\partial\Psi_p^{(+)}}{\partial t}+\frac{\partial\Psi_p^{(-)}}{\partial t}\right)-i\hbar\left(\Psi_p^{(+)}+\Psi_p^{(-)}\right)\left(\frac{\partial\Psi_p^{(+)*}}{\partial t}+\frac{\partial\Psi_p^{(-)*}}{\partial t}\right) \tag{9.54}$$

Expanding this expression, we obtain four terms

$$\rho(\boldsymbol{r},t)=\rho^{(++)}+\rho^{(--)}+\rho^{(+-)}+\rho^{(-+)}, \tag{9.55}$$

where each term are defined as follows

1. $\rho^{(++)}=i\hbar\left(\Psi_p^{(+)*}\frac{\partial\Psi_p^{(+)}}{\partial t}-\Psi_p^{(+)}\frac{\partial\Psi_p^{(+)*}}{\partial t}\right)$, which corresponds to the positive energy component. For plane wave solutions of (9.33) yields $\rho^{(++)}=2|A|^2|E_p|$ and $\boldsymbol{J}^{(++)}=2A^2\boldsymbol{p}$.

2. $\rho^{(--)}=i\hbar\left(\Psi_p^{(-)*}\frac{\partial\Psi_p^{(-)}}{\partial t}-\Psi_p^{(-)}\frac{\partial\Psi_p^{(-)*}}{\partial t}\right)$, which corresponds to the negative energy component. For plane wave solutions of (9.33) yields $\rho^{(--)}=-2|A|^2|E_p|$. This negative energy component indeed contribute to negative probability densities.

73

3. $\rho^{(+-)} = i\hbar \left(\Psi_p^{*(+)} \frac{\partial \Psi_p^{(-)}}{\partial t} - \Psi_p^{(+)} \frac{\partial \Psi_p^{(-)*}}{\partial t} \right)$ and $\rho^{(-+)} = i\hbar \left(\Psi_p^{(-)*} \frac{\partial \Psi_p^{(+)}}{\partial t} - \Psi_p^{(-)} \frac{\partial \Psi_p^{(+)*}}{\partial t} \right)$ corres-

   pond to the cross terms. These cross terms can also yield both positive and negative values due to the interference between the positive and negative energy solutions as we shall soon see.

The Klein-Gordon equation's lack of a positive-definite probability density and real-valued probability current results in difficulties in interpreting these quantities physically, leading to the development of the Dirac equation, which resolves these issues. In the context of quantum field theory, the negative energy solutions can be reinterpreted in terms of antiparticles with positive energy.

9.5   Comparing Relativistic and Non-Relativistic Equations

The above discussion has demonstrated that relativistic equations differ from the non relativistic by the emergence of negative energy solutions which expands the Hilbert space used to describe relativistic states [70].

The Klein-Gordon equation is a second-order differential equation, and its solutions naturally include both positive and negative frequency components. To form a complete set of solutions, we need to consider both of these components, as they are orthogonal and allow us to represent any general solution to the Klein-Gordon equation as a linear combination of these components. This is essential for forming a complete set of stationary solutions that can describe any arbitrary initial condition for the field. These negative frequency solutions lead to issues such as negative probabilities and probability currents, which are resolved in the Dirac equation.

In order to avoid negative probabilities associated with the Klein-Gordon equation, one could in principle restrict oneself to only positive energy solutions. However, this approach is accompanied with its own set of problems that we shall see in when discussing Hegerfeldt's theorem in subsequent sections.

In relativistic systems, the Moyal-Liouville Equation (7.18) needs to be modified to describe relativistic dynamics to encompass both positive and negative frequency components [15] [57] [66]. This allows us to interpret the negative phase space densities of the Wigner function as negative energy antiparticles [28]. Consequently, in relativistic Wigner-Moyal formalism, Hudson's theorem no longer applies with the inclusion of the negative frequencies [13].

9.6   A Simplified Example: The Double Slit Experiment

The Wigner transform is applicable to both classical electromagnetic fields and quantum wave functions, rendering the Wigner-Moyal formalism a unifying link between bitemporal electromagnetic theory and standard relativistic quantum theory. This connection is established once the entropy issue associated with electromagnetism is identified and resolved.

Consider a double slit experiment with photons using the Wigner formalism [17]. The phase space Wigner function at three different times can be seen in Figure 15 along with its projections along the position axis and momentum axis. The two waves emanating from each slit can be represented as

$$\Psi_1(x) = \sqrt{\frac{RL}{2\pi/d}} \frac{1}{\sqrt{L^2 + (x + d/2)^2}} \exp\left[i \left(\frac{2\pi}{\lambda} \right) \sqrt{L^2 + (x + d/2)^2} \right], \qquad (9.56)$$

and

$$\Psi_2(x) = \sqrt{\frac{RL}{2\pi}} \frac{1}{\sqrt{L^2 + (x - d/2)^2}} \exp\left[i \left(\frac{2\pi}{\lambda} \right) \sqrt{L^2 + (x - d/2)^2} \right], \qquad (9.57)$$

where L represents the distance to the detection screen, d denotes the separation between the two slits, x is the distance to the screen's center, λ is the wavelength, and R is the photon rate that represents the number of photons emitted per unit time at the source. The amplitude of detecting

a photon at distance x from the screen's center is the sum of these two amplitudes emerging from each slit.
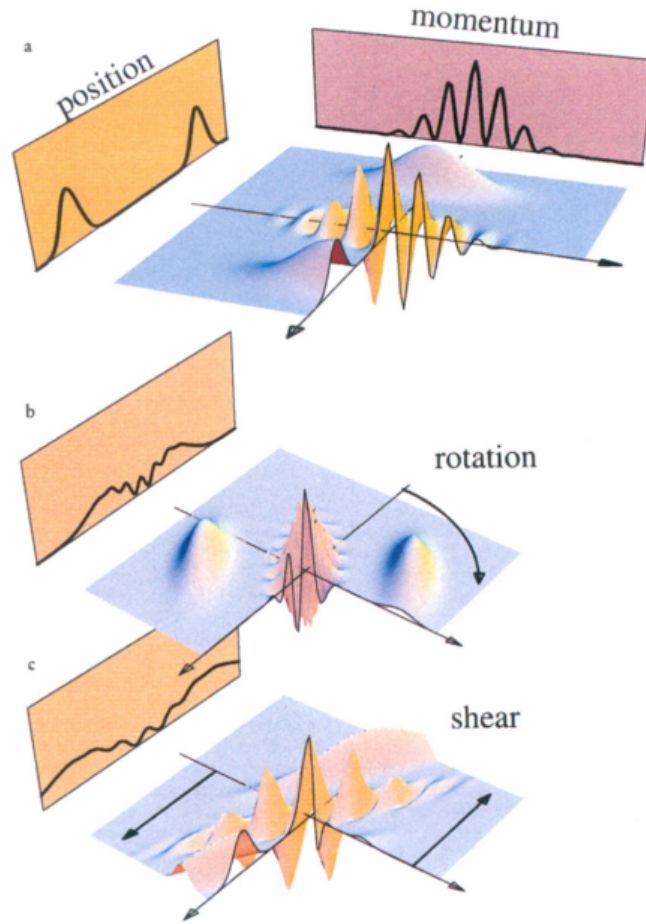
Figure 15: Wigner function in phase space at three different times, along with its projections along the position axis and momentum axis. Notice that it contains negative values.

Source: [65]

Consequently, the probability of detecting a photon at position x is given by the square of this sum

$$I(x) = |\Psi_1(x) + \Psi_2(x)|^2 = |\Psi_1(x)|^2 + |\Psi_2(x)|^2 + [\Psi_1^*(x)\Psi_2(x) + \Psi_1(x)\Psi_2^*(x)]\,, \tag{9.58}$$

This can be interpreted in terms of probability rules

$$\begin{aligned} P(\text{photon at } x \text{ via either slit}) = {} & P(\text{photon at } x|\text{via slit 1}) \cdot P(\text{via slit 1}) \\ & + P(\text{photon at } x|\text{via slit 2}) \cdot P(\text{via slit 2}) \\ & - P(\text{photon at } x \text{ via both slits}) \end{aligned} \tag{9.59}$$

The fact that we do not have knowledge of the slit from which the photon originated leads to the representation of partial information through negative energy solutions that propagate backward in time. This approach to examining the system contravenes the principle of unidirectional causality, as it necessitates that the photon has prior knowledge of its intended destination prior to its emission. This topic will be further explored in the subsequent discussions on electromagnetic reciprocity.
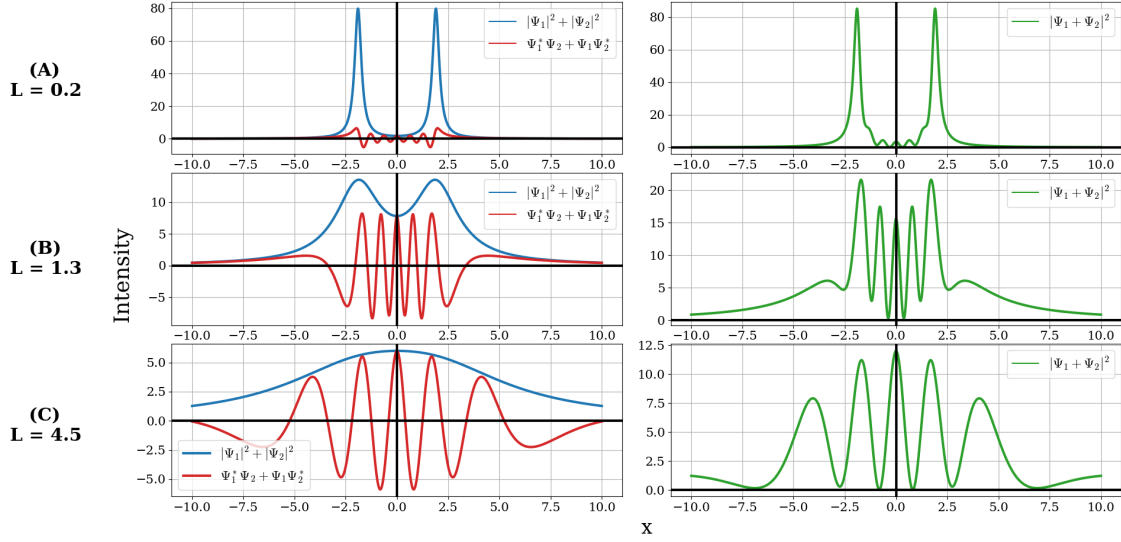
Figure 16: The Wigner function for the double-slit experiment projected along the position plane at 3 different distances from the slits. The plots in the left column display the different terms of (9.58) involving the square sum separately. The plots to the right display their superposition.

When either one of the slits is closed, forces the photon to pass through the other slit, so that the corresponding intensities are

$$I_1(x) = |\Psi_1(x)|^2 = \frac{1}{2\pi} \frac{RL}{L^2 + (x + d/2)^2}, \tag{9.60}$$

and

$$I_2(x) = |\Psi_2(x)|^2 = \frac{1}{2\pi} \frac{d}{L^2 + (x - d/2)^2}. \tag{9.61}$$

However, interpreting these terms in this manner, the probability of the cross terms exhibits negative peaks periodically approximately every $\lambda \frac{L}{d}$:

$$I_{12}(x) = [\Psi_1^*(x)\Psi_2(x) + \Psi_1(x)\Psi_2^*(x)] \tag{9.62}$$

$$= \frac{LR}{\pi\sqrt{L^2 + (x - d/2)^2}\sqrt{L^2 + (x + d/2)^2}} \cos\left[\frac{2\pi}{\lambda}(\sqrt{L^2 + (x + d/2)^2} - \sqrt{L^2 + (x - d/2)^2})\right]. \tag{9.63}$$

Figure 16 graphs the intensities $I_1(x) + I_2(x)$ and $I_{12}(x)$ separately (left column) as well as their superposition, $I(x)$ (right column) at three distinct distances L. This example of the double slit experiment presents a scenario where negative probabilities are not directly observable through empirical means. The information concerning the photon's passage through both slits requires interaction with the system, altering its dynamics. In light of our discussions on relativistic dynamics in the Wigner-Moyal formalism, this phenomenon implies the existence of negative energy antiparticles that traverse backwards in time, exerting a counteractive force by limiting certain emission modes of the light source, thereby giving rise to the observed interference pattern.

In general, the requirement for antiparticles in relativistic systems to abide by relativistic causality necessitates the incorporation of negative energy solutions and this concept applies not only to the double slit experiment but to numerous other systems as well. The incorporation of negative energy solutions in relativistic systems expands the Hilbert space and precludes certain no-go theorems, as demonstrated in Section 10 where single particle measurements are taken into account in solving the entropy problem of electromagnetism.

The Hegerfeldt theorem highlights the intrinsic non-locality present in one particle states composed solely of positive frequency components. The propagation of these states is found to be non-causal,

as an initial particle with compact support in a region tends to spread and occupy all space at a rate surpassing that of light, violating relativistic causality. Our future examination of Hegerfeldt's theorem will demonstrate that the propagation of positive and negative frequency components is non-causal when considered separately in a relativistic system. However, the combination of positive and negative frequency position eigenvectors results in the formation of covariant position eigenvectors exhibiting causal propagation. It has been established that no state characterized by strict localization and a finite number of particles can be composed solely of positive frequency terms.

9.7 Brief Note On Feynman Path Integral Method

For those well-versed in Feynman's path integral formulation, antiphotons can be readily understood without requiring an in-depth exploration of the subsequent sections. Readers unfamiliar with these topics can feel free to skip this subsection.

In perturbation theory, a space-time localized photon with a polarization is created by applying the free photon field operator at a specific space-time point. The propagator, which denotes the probability amplitude for a photon to propagate from one point in space-time to another, is obtained by summing over all space-time paths of a particle action. The connection between two-point functions in quantum field theory and particle paths is exemplified by the Feynman propagator. This fundamental concept in perturbation theory is derived from Feynman's path integral formulation [33]. It is worth noting that this perspective, emphasizing the particle-like behavior of photons, is not always thoroughly discussed in standard quantum field theory textbooks. These texts often concentrate more on the field-theoretic aspects of the subject.

The challenge lies in localizing photons—determining their positions at any given time. The position operator for a photon is not well-defined in the conventional sense because photon positions do not evolve causally. With path formulations, photons can travel back in time. This issue also arises for any relativistic particle when attempting to localize it within a region smaller than what is permitted by the pixel imposed by empirical observations. The Schrödinger position representation, using an operator, is only valid for non-relativistic massive particles.

There are two complementary resolutions to this problem. The standard approach involves discussing quantum fields and treating photons as excitations of the quantum field. In this context, localizing photons in space is not discussed.

The second method entails redefining the position of a photon in space-time rather than merely in space at one time. The photon trajectory is then defined as a sum over paths that extend both forward and backward in time. While this definition works well within perturbation theory, where it serves as an interpretation of Feynman's diagrams, it has not been used beyond perturbation theory due to the avoidance of negative energy solutions in contemporary quantum field theory. However, we will see that this formulation can be applied outside of perturbation theory for microscopic systems.

Localizing a photon to a specific point is not feasible due to the entropy pixel argument discussed earlier. A more precise assertion is that photons cannot be perfectly localized, akin to a delta function. A simple conceptual argument to support this claim is as follows:

Attempting to confine electrons within a region smaller than the constraints set by the pixel leads to significant consequences. The uncertainty principle dictates that the localized state must be composed of a range of energies considerably larger than mc^2, which represents the energy of the electron. As a result, this range must encompass negative-energy states, implying that any effort to measure an electron's position with such high precision inadvertently creates electron-positron pairs. Consequently, the state is no longer an eigenstate of particle number, and the concept of measuring the electron's position loses its meaning. This forms a good intuitive argument for the role of negative energy solutions in relativistic systems.

Brief Section Summary

The Hilbert formalism was investigated, examining how the equations governing the temporal evolution of states can be derived by enforcing energy conservation in both relativistic and non-relativistic scenarios. It was observed that, in relativistic cases, Hudson's theorem can be violated. Moreover, a stipulation was imposed on the dispersion relation, necessitating the inclusion of both positive and negative frequencies to not only define a zero entropy state (i.e., wave function) but also adhere to relativistic causality.

This discourse establishes the essential groundwork for identifying the entropy issue in classical electromagnetism, discussed later in Section 10. Addressing this problem entails ensuring Maxwell's theory complies with relativistic causality and then incorporating a pixel, namely, the zero entropy component of the electromagnetic field (i.e., the photon, the smallest measurable part of the electromagnetic field).

10 Hegerfeldt's Theorem and The Photon Wave Function

In this section, we employ the Riemann-Silberstein vector to derive a complex wave equation for a source-free electromagnetic field. The particular details of this approach is based on the 1996 paper by Iwo Bialynicki-Birula called *Photon Wave Function* [9]. The paper numerous interesting properties of the wave function that will not be discuss here, in particular, in relation to the Wigner transform.

The section utilizes the Riemann-Silberstein vector to establish a complex wave equation for the source-free electromagnetic field. The methodology employed is based on the seminal work by Iwo Bialynicki-Birula, titled *Photon Wave Function* published in 1996 [9]. While the paper explores various intriguing properties of the wave function, such as its relationship to the Wigner transform, they will not be addressed in this thesis. Given that electromagnetism is a Lorentz-invariant theory, we establish its connection to the principles of relativity discussed in the previous section. Subsequently, we examine the limitations of this approach in defining a position operator for the photon wave function and its relation to Hegerfeldt's theorem. Finally, we address the entropy problem in electromagnetism and demonstrate that the incorporation of negative energy solutions can rectify this issue with a simple example from Wessel Berg's book.

10.1 Maxwell's Equations and the Riemann Silberstein Vector

The Riemann-Silberstein vector is a complex representation that integrates the electric and magnetic fields into a single entity, thereby enabling a concise expression of the source-free Maxwell's equations. This vector provides a unified and compact description of the electromagnetic wave by combining the electric and magnetic fields. The Riemann-Silberstein vector was first introduced by Bernhardt Riemann in 1861 [77] and is defined as follows

$$\boldsymbol{F} = \boldsymbol{E} + ic\boldsymbol{B}, \tag{10.1}$$

where $\boldsymbol{E}$ represents the electric field, $\boldsymbol{B}$ represents the magnetic field, and i denotes the imaginary unit. We can utilize this complex vector in expressing Maxwell's equations given as

$$\nabla \cdot \boldsymbol{E} = \frac{\rho}{\epsilon_0}, \tag{10.2}$$

$$\nabla \cdot \boldsymbol{B} = 0, \tag{10.3}$$

$$\nabla \times \boldsymbol{E} = -\frac{\partial \boldsymbol{B}}{\partial t}, \tag{10.4}$$

$$\nabla \times \boldsymbol{B} = \mu_0 \boldsymbol{J} + \frac{1}{c^2}\frac{\partial \boldsymbol{E}}{\partial t}, \tag{10.5}$$

where $\boldsymbol{E}$ is the electric field, $\boldsymbol{B}$ is the magnetic field, ρ is the charge density, $\boldsymbol{J}$ is the current density, ϵ_0 is the vacuum permittivity, and μ_0 is the vacuum permeability. These equations in source free form cause $\rho = 0$ and $\boldsymbol{J} = 0$ so that multiplying (10.3) by ic and adding it to (10.2) yields

$$\nabla \cdot \boldsymbol{F} = 0, \tag{10.6}$$

which represents Equations (10.2) and (10.3) in a more compact form. Furthermore, by taking the curl of (10.4) and (10.5) and using the vector identity $\nabla \times (\nabla \times \boldsymbol{A}) = \nabla(\nabla \cdot \boldsymbol{A}) - \nabla^2 \boldsymbol{A}$, results in wave equation

$$\frac{1}{c^2}\frac{\partial^2 \boldsymbol{E}}{\partial t^2} - \nabla^2 \boldsymbol{E} = 0, \tag{10.7}$$

$$\frac{1}{c^2}\frac{\partial^2 \boldsymbol{B}}{\partial t^2} - \nabla^2 \boldsymbol{B} = 0, \tag{10.8}$$

for the electric and magnetic field respectively. Employing the same procedure as above where we multiply Equation (10.8) by ic and adding it to (10.7) enables us combine both equation using the Riemann-Silberstein vector yielding

$$\frac{1}{c^2}\frac{\partial^2 \boldsymbol{F}}{\partial t^2} - \nabla^2 \boldsymbol{F} = 0. \tag{10.9}$$

This equation represent Equations (10.4) and (10.5). However, one can obtain a first order equation instead considering the following quantity

$$c\nabla \times \boldsymbol{F} = c(\nabla \times \boldsymbol{E}) + ic^2(\nabla \times \boldsymbol{B}) = -c\frac{\partial \boldsymbol{B}}{\partial t} + i\frac{\partial \boldsymbol{E}}{\partial t} = i\frac{\partial \boldsymbol{F}}{\partial t}, \qquad (10.10)$$

where substitutions from (10.4), (10.5) and (10.1) have been made. Multiplying both sides of (10.10) by $\hbar$ yields

$$i\hbar\frac{\partial \boldsymbol{F}}{\partial t} = \hbar c \boldsymbol{\nabla} \times \boldsymbol{F}, \qquad (10.11)$$

which has some resemblance to quantum wave equations. We now introduce the following identity

$$\boldsymbol{\nabla} \times \boldsymbol{a} = -i(\overrightarrow{\boldsymbol{s}} \cdot \boldsymbol{\nabla})\boldsymbol{a}, \qquad \overrightarrow{\boldsymbol{s}} = \begin{pmatrix} \boldsymbol{s_1} \\ \boldsymbol{s_2} \\ \boldsymbol{s_3} \end{pmatrix}, \qquad (10.12)$$

which allows us to express $\nabla \times \boldsymbol{F} = -i(\overrightarrow{\boldsymbol{s}} \cdot \nabla)\boldsymbol{F}$ in terms of the a vector of 3x3 spin-1 matrices

$$\boldsymbol{s_1} = \begin{pmatrix} 0 & 0 & 0 \\ 0 & 0 & -i \\ 0 & i & 0 \end{pmatrix}, \quad \boldsymbol{s_2} = \begin{pmatrix} 0 & 0 & i \\ 0 & 0 & 0 \\ -i & 0 & 0 \end{pmatrix}, \quad \boldsymbol{s_3} = \begin{pmatrix} 0 & -i & 0 \\ i & 0 & 0 \\ 0 & 0 & 0 \end{pmatrix}. \qquad (10.13)$$

The source free Maxwell's equations can thus be given by the following two equations

$$i\hbar\frac{\partial \boldsymbol{F}}{\partial t} = c\left(\overrightarrow{\boldsymbol{s}} \cdot \frac{\hbar}{i}\boldsymbol{\nabla}\right)\boldsymbol{F}, \qquad \boldsymbol{\nabla} \cdot \boldsymbol{F} = 0. \qquad (10.14)$$

This equation resembles the quantum mechanical wave equation, one we identify $\hat{\boldsymbol{P}} = \frac{\hbar}{i}\boldsymbol{\nabla}$ so that $\boldsymbol{\nabla} \cdot \boldsymbol{F} = 0 \implies \hat{\boldsymbol{P}} \cdot \boldsymbol{F} = 0$ implies that the vector field is perpendicular to the propagation. It is important to note that normalization of the Riemann-Silberstein vector is necessary to establish its probabilistic interpretation. This is due to the fact that $|\boldsymbol{F}|^2 = \boldsymbol{F} \cdot \boldsymbol{F}^*$ is proportional to the energy density of the electromagnetic field. For further information, the reader is referred to the work of Bialynicki-Birula [9].

Further analysis of the photon wave function results in the following observation

$$i\hbar\frac{\partial \boldsymbol{F}}{\partial t} = \hat{H}\boldsymbol{F}, \qquad \boldsymbol{\nabla} \cdot \boldsymbol{F} = 0, \qquad (10.15)$$

where we set the Hamiltonian operator $\hat{H} = +c\overrightarrow{\boldsymbol{s}} \cdot \hat{\boldsymbol{P}}$ having cp as its eigenvalues, meaning that the wave propagates in the direction of the Pointing vector [85]. An *antiphoton* would correspond to a negative eigenvalue of the Hamiltonian operator, i.e. $-cp$, meaning that the wave would have negative energy and propagate in the opposite direction to the Poynting vector. That is, an antiphoton is a photon propagating backward in time. However, Equation (10.15) only describes photons of positive energies.

10.1.1 Position Operator For Photons

The position operator for the photon has been a long-standing challenge in the realm of quantum mechanics. Despite various attempts over the years, a satisfactory position operator for the photon has not been fully established. In the early 20th century, Newton and Wigner (1949) proposed a relativistic position operator for particles with mass but faced difficulties extending this to massless particles such as photons [72]. A major breakthrough occurred when Pryce (1948) proposed an alternative position operator for the photon; however, it still had limitations and was considered non-covariant [76]. The problem of photon position in quantum mechanics has also been closely tied to Hegerfeldt's theorem (1974), which imposes constraints on the localization of massless particles [50]. The theorem demonstrates that any covariant, localizable position operator for massless particles would lead to superluminal signaling when the Hamiltonian is strictly positive , which is

in conflict with the principles of relativity. The elusive nature of the photon position operator and its connection to Hegerfeldt's theorem exemplify the challenges inherent in reconciling quantum mechanics with relativistic principles. Consequently, the problem of the position operator for the photon remains an open question in quantum mechanics, with the Hegerfeldt's theorem posing a significant constraint on potential solutions.

In this thesis, we have shown that quantum mechanics resolves the entropy problem by establishing a connection between its mathematical formalism in Hilbert space, represented by the wave function, and empirical measurements through the use of Hermitian matrices. The eigenvalues of these matrices are real and correspond to physical observables, thereby establishing a connection between the wave function and physical measurements. However, the position operator problem for photons highlights a disconnect between the wave function and physical measurements, leading to an inherent entropy problem for the photon as we shall soon come to see.

The significance of this problem is discussed in the subsequent subsection, where the nature of the localization problem is examined in detail. The discussion of Hegerfeldt's theorem provides further insight into the challenges in determining a suitable localization operator for massless particles and is accompanied by an example from Wessel Berg's book.

10.2   Hegerfeldt's Theorem

Hegerfeldt's theorem is a type of no go theorem stating in quite general terms that in a theory where only positive (or negative) energy exists, localization of objects is problematic. The theorem was proposed by Gerhard Hegerfeldt in 1974, is a result in quantum mechanics that proves the impossibility of instantaneous, causal, and spatially compact signal propagation in relativistic quantum field theory [50]. The theorem demonstrates that any relativistic quantum field theory satisfying the requirements of microcausality and positive energy densities will unavoidably exhibit infinite spreading of wave packets in an arbitrarily short time, contradicting the intuitive notion of localized particles. The proof relies crucially on a certain property shared by bounded analytic functions defined in the lower complex half-plane (or upper half-plane in case of negative energy) [53]. We begin by establishing this crucial property. This is done by introducing Schwarz reflection principle and analytic continuation, and using these concepts to derive a general statement regarding bounded holomorphic functions that are restricted to the the lower (upper) half planes.

10.2.1   Schwarz Reflection Principle

The Schwarz Reflection Principle is a powerful tool in complex analysis that enables the extension of analytic functions across boundaries in the complex plane by reflecting them over a real or imaginary axis. In simpler terms, if a function is analytic (holomorphic) on one side of an axis and has nonsingular real values on the real line, we can 'reflect' it over that axis to obtain an analytic function on the other side.

Suppose we have an analytic function $f(z)$ in the lower half-plane (i.e., where $\text{Im}(z) \leq 0$), and $f(z)$ is continuous and real on the real axis. The Schwarz Reflection Principle asserts that we can define an extended function $F(z)$ that is analytic in both the upper and lower half-planes, according to the following:

1. For z in the lower half-plane ($\text{Im}(z) \leq 0$), the extended function is simply the original function, i.e., $F(z) = f(z)$.

2. For z in the upper half-plane ($\text{Im}(z) > 0$), the extension is given by $F(z) = f^*(z^*)$, where z^* denotes the complex conjugate of z.

Consequently, the Schwarz Reflection Principle allows the extended function $F(z)$ to be expressed as

$$F(z) = \begin{cases} f(z), & \text{for } \text{Im}(z) \leq 0 \\ f^*(z^*), & \text{for } \text{Im}(z) > 0. \end{cases} \tag{10.16}$$

This principle proves useful for extending analytic functions and solving boundary value problems in complex analysis.

10.2.2 Analytic Continuation

Analytic continuation is a technique employed in complex analysis to broaden the domain of a given analytic function. An analytic function can be locally represented by a convergent power series, and the objective of analytic continuation is to identify a unique analytic function that concurs with the initial function on a shared domain. In essence, it seeks a unique extension of a function, initially defined on a smaller domain, to a larger domain while preserving its analytic properties.

Consider an analytic function $f(z)$ defined on an open subset D of the complex plane $\mathbb{C}$. The analyticity of $f(z)$ guarantees that the function is differentiable at every point within D. Consequently, for every point $z_0 \in D$, a power series representation of $f(z)$ exists, as shown below:

$$f(z) = \sum_{n=0}^{\infty} a_n (z - z_0)^n, \tag{10.17}$$

where the series converges for all $z \in D$. The coefficients a_n are given by the Cauchy integral formula

$$a_n = \frac{1}{2\pi i} \oint_C \frac{f(z)}{(z - z_0)^{n+1}} dz. \tag{10.18}$$

In this case, C is a simple, closed contour within D that encompasses z_0. To carry out analytic continuation to a larger domain D', provided that $D \subset D'$, we must establish a new power series representation for $f(z)$ centered at a distinct point z_1 in the expanded domain D':

$$f(z) = \sum_{n=0}^{\infty} b_n (z - z_1)^n, \tag{10.19}$$

where the coefficients are given by

$$b_n = \frac{1}{2\pi i} \oint_{C'} \frac{f(z)}{(z - z_1)^{n+1}} dz. \tag{10.20}$$

Here, C' is a simple, closed contour in D' that encloses z_1. The contour C' should be chosen in such a way that it does not intersect the original domain D.

The function $f(z)$ is considered to be analytically continued from D to D' if the extended function aligns with the original function on the intersection of D and D'.

In summary, analytic continuation enables the extension of an analytic function's domain by constructing a new power series representation centered at a different point within the expanded domain.

10.2.3 Holomorphic Functions Restricted to the Lower Half-Plane

Suppose we have a holomorphic function $f(z)$ defined in the lower half-plane (i.e., $\text{Im}(z) \leq 0$), as in Figure 17a. Furthermore, suppose there is an interval $I \subset \mathbb{R}$ on the real axis, where $f(z)$ is real for all $z \in I$. This is in contrast to the setting in Section 10.2.1, where it was assumed that the function was real for the entire real axis and not only on an interval $I \subset \mathbb{R}$.

Since $f(z)$ is defined on the entire lower half-plane, it is also defined on $\Omega_I^- = \{z \in \mathbb{C} : \text{Im}(z) \leq 0, \text{Re}(z) \in I\}$. We can then apply the Schwarz Reflection Principle to reflect the values of $f(z)$ on Ω_I^- onto $\Omega_I^+ = \{z \in \mathbb{C} : \text{Im}(z) > 0, \text{Re}(z) \in I\}$ in the upper half-plane, thereby extending the function on the lower half-plane to Ω_I^+ as well. This is illustrated in Figure 17b.

The extended function, denoted by $F(z)$, can then be represented as

$$F(z) = \begin{cases} f(z), & \text{for Im}(z) \leq 0 \\ f^*(z^*), & \text{for Im}(z) > 0 \text{ and Re}(z) \in I. \end{cases} \qquad (10.21)$$

It is important to note that the reflection principle by itself only guarantees the extension of the function to the region directly above the interval I on the real axis. Since the reflected part on Ω_I^+ must similarly also be analytic, we can further extend this reflected part of the function to the rest of the upper half-plane by applying analytic continuation, as illustrated in Figure 17c. In this case, the reflected function on the domain Ω_I^+ serves as the starting point for this continuation.

(a)

(b)

(c)
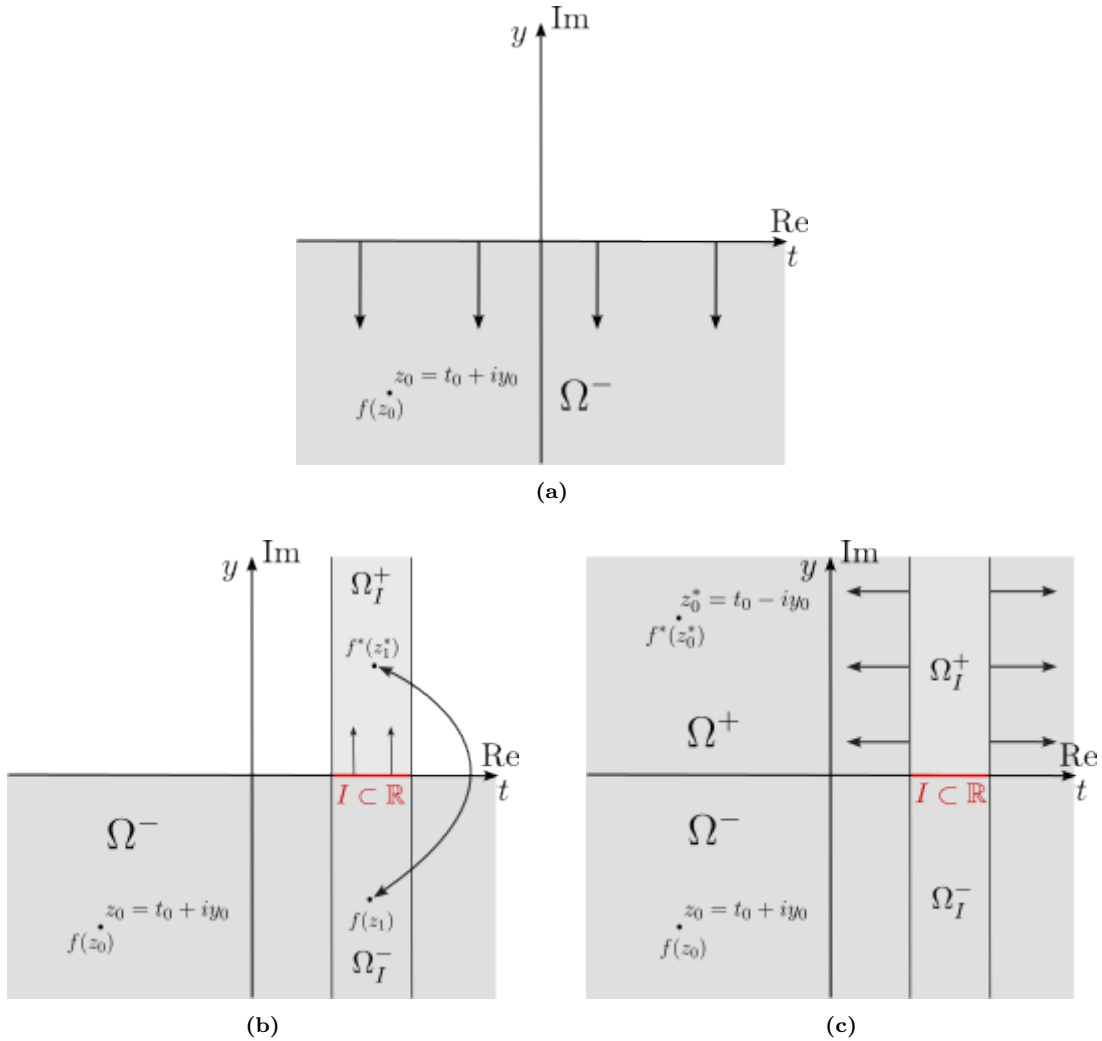
Figure 17: **(a)** An analytic function f in the lower half-plane, Ω^- (shaded region). **(b)** The function f is real on $I \subset \mathbb{R}$. Schwarz Reflection Principle is used to expand the function across the real axis, from Ω_I^- to the additional shaded region Ω_I^+. **(c)** The extended function f^* on Ω_I^+ is further extended to the rest of the upper half-plane by analytic continuation.

The entire process results in

$$F(z) = \begin{cases} f(z), & \text{for Im}(z) \leq 0 \\ f^*(z^*), & \text{for Im}(z) > 0. \end{cases} \qquad (10.22)$$

Through the implementation of these procedures, it becomes feasible to extend any holomorphic function $f(z)$ from the lower half-plane to encompass the entire complex plane, utilizing both the Schwarz Reflection Principle and Analytic Continuation.

In conclusion, the Schwarz Reflection Principle serves to expand a function across the real axis within the interval I. To achieve a more comprehensive extension of the function throughout the entire complex plane, the deployment of analytic continuation is essential.

10.2.4 Cases Involving Bounded Functions

Suppose we instead have a *bounded* holomorphic function $f(z)$ in the lower half-plane, with an interval I on the real axis where $f(z)$ is real whenever $z \in I$, we can again apply the Schwarz Reflection Principle and analytic continuation to define $F(z)$ over the whole complex plane using $F(z) = F(z^*)^*$ as done previously. However, this time the function is bounded. A bounded function is a function whose values are confined within a certain range or limit. In mathematical terms, a complex-valued function $f(z)$ is bounded if there exists a constant $M > 0$ such that for all z in its domain, $|f(z)| \leq M$. In other words, the magnitude of the function does not exceed a fixed positive constant M in its domain.

Since $f(z)$ is bounded in the lower half-plane, its extension $F(z)$ to the upper half-plane should also be holomorphic and bounded. The reason for this is that the extension $F(z)$ is simply the complex conjugate of $f(z)$ in the upper half-plane. Since the magnitude of a complex number and its complex conjugate are equal (i.e., $|z| = |z^*|$), the magnitude of $F(z)$ will be bounded in the upper half-plane by the same constant M that bounds $f(z)$ in the lower half-plane.

Liouville's theorem is a fundamental result in complex analysis that states every bounded entire (holomorphic in the whole complex plane) function must be constant. In other words, if a function is holomorphic everywhere in the complex plane and its magnitude is bounded by a constant M, then the function must be constant. Mathematically, if $F(z)$ is an entire function and there exists a constant M such that $|F(z)| \leq M$ for all z in the complex plane, then $F(z)$ must be constant, i.e., $F(z) = c$, where c is a complex constant.

Given our bounded holomorphic function $f(z)$ in the lower half-plane, with interval I on the real axis where $f(z)$ is real for all $z \in I$, we have shown that we can extend $f(z)$ to the entire complex plane by applying the Schwarz Reflection Principle and analytic continuation. The resulting function $F(z)$ is holomorphic and bounded in the entire complex plane. By Liouville's theorem, we can conclude that $F(z)$ must be a constant. Since $F(z)$ agrees with $f(z)$ in the lower half-plane, it follows that $f(z)$ must also be a constant in the lower half-plane.

This result can be stated more formally by the following lemma:

Lemma 10.1. *Let $\Omega^- = \{z \in \mathbb{C} : Im\, z \leq 0\}$, and let $f^- : \Omega^- \to \mathbb{C}$ be a bounded, continuous and analytic function in the interior of Ω^-. Assume $f^-(z)$ is real on a closed interval $I \subset \mathbb{R}$ of positive length. Then $f^-(z)$ is identically equal to a constant.*

Consequently, it becomes evident that possessing both analytic and bounded attributes in the lower half-plane imposes severe restrictions on the boundary values on the real axis. The existence of a finite interval on the real axis that yields real values enables us to extend the function to the upper half-plane using the Schwarz Reflection Principle. In doing so, we define a bounded analytic function across the entire complex plane, and Liouville's theorem then dictates that this function must be constant. where the merciless Liouville's theorem kills off everything, rendering the whole function to a constant! This outcome is a crucial aspect of the proof of Hegerfeldt's theorem.

10.2.5 Proof of Hegerfeldt's Theorem

We now show how a non-negative self-adjoint operator on a Hilbert space connects to bounded analytic functions in the lower half-plane. Let $\mathcal{H}$ be a Hilbert space over $\mathbb{C}$ with an inner product denoted as $\langle \cdot | \cdot \rangle$, and let $\hat{H} : \mathcal{D}(\hat{H}) \to \mathcal{H}$ be a non-negative, i.e. $\hat{H} \geq 0$, possibly unbounded, self-adjoint operator, where the domain of definition $\mathcal{D}(\hat{H}) \subset \mathcal{H}$ necessarily is proper a dense linear subspace in case $\hat{H}$ is unbounded. For temporal evolution equations of the form similar to (10.15), we define time translation of $\Psi(t) \in \mathcal{H}$ by

We now investigate the relationship between a non-negative self-adjoint operator on a Hilbert space and bounded analytic functions in the lower half-plane. Let $\mathcal{H}$ be a Hilbert space over $\mathbb{C}$ with inner product denoted as $\langle \cdot | \cdot \rangle$, and let $\hat{H} : \mathcal{D}(\hat{H}) \to \mathcal{H}$ be a non-negative, i.e. $\hat{H} \geq 0$, possibly unbounded, self-adjoint operator, where the domain of definition $\mathcal{D}(\hat{H}) \subset \mathcal{H}$ is a proper dense linear subspace in case $\hat{H}$ is unbounded. For temporal evolution equations similar to (10.15), we define time translation of $\Psi(t) \in \mathcal{H}$ by

$$i\hbar \frac{\partial \Psi(t)}{\partial t} = \hat{H}\Psi(t), \quad \Psi(0) = \Psi_0, \tag{10.23}$$

where $\hat{H}$ dictates the time evolution of a state $\Psi_0 \in \mathcal{H}$ with solutions of the form

$$\Psi(t) = e^{-\frac{i}{\hbar}\hat{H}t}\Psi_0, \quad \text{for } t \in \mathbb{R}. \tag{10.24}$$

We note that $\hat{U}(t) = e^{-\frac{i}{\hbar}\hat{H}t}$ is a unitary operator for $t \in \mathbb{R}$. Let $\hat{K}$ be a self-adjoint operator with a positive spectrum, i.e. $\hat{K} \geq 0$, and define

$$\mathcal{P}_K(t) = \langle \Psi(t) | \hat{K}\Psi(t) \rangle, \qquad \text{where } t \in \mathbb{R}, \text{ and } |\hat{K}| < \infty. \tag{10.25}$$

We can generally state that $\mathcal{P}_K(t) = 0 \Leftrightarrow \hat{K}^{\frac{1}{2}}e^{-\frac{i}{\hbar}\hat{H}t}\Psi_0 = 0$. This statement plays a crucial role in the proof of Hegerfeldt's Theorem and can be demonstrated as follows:

Since $\hat{K} \geq 0$, indicating that it contains a positive spectrum, its square root $\hat{K}^{\frac{1}{2}} \geq 0$ is uniquely defined, where $\hat{K}^{\frac{1}{2}}$ is also a self-adjoint operator. Consequently, the self-adjoint property of $\hat{K}^{\frac{1}{2}}$ allows us to derive the following result

$$\mathcal{P}_K(t) = \langle \hat{K}^{\frac{1}{2}}\Psi(t) | \hat{K}^{\frac{1}{2}}\Psi(t) \rangle = |\hat{K}^{\frac{1}{2}}\Psi(t)|^2 = |\hat{K}^{\frac{1}{2}}e^{-\frac{i}{\hbar}\hat{H}t}\Psi_0|^2. \tag{10.26}$$

Let $\mathcal{N}_0 \subseteq \mathbb{R}$ represent the zero set of $\mathcal{P}_K(t)$, such that $\mathcal{N}_0 = \{t \in \mathbb{R} \mid \mathcal{P}_K(t) = 0\}$. Consequently, for any given $t \in \mathcal{N}_0$, we can conclude that

$$\mathcal{P}_K(t) = |\hat{K}^{\frac{1}{2}}\Psi(t)|^2 = 0 \Leftrightarrow \hat{K}^{\frac{1}{2}}e^{-\frac{i}{\hbar}\hat{H}t}\Psi_0 = 0. \tag{10.27}$$

This further implies that $\hat{K}e^{-\frac{i}{\hbar}\hat{H}t}\Psi_0 = 0$ when both sides of the equation $\hat{K}^{\frac{1}{2}}e^{-\frac{i}{\hbar}\hat{H}t}\Psi_0 = 0$ are multiplied by $\hat{K}^{\frac{1}{2}}$.

Extension of the Unitary Operator to the Lower Half of the Complex Plane

The property $\hat{H} \geq 0$ implies that the Hamiltonian operator $\hat{H}$ possesses a positive spectrum, i.e.,

$$\langle \psi | \hat{H}\psi \rangle \geq 0, \qquad \forall \psi \in \mathcal{H}. \tag{10.28}$$

Consequently, extending the unitary operator $\hat{U}(t)$ to the lower half of the complex plane, Ω^-, by substituting $t \to z = t + iy$ with $y \leq 0$, results in $\hat{U}(z) = \hat{U}(t+iy) = e^{-i\hat{H}z} = e^{-\frac{i}{\hbar}\hat{H}t}e^{\hat{H}y}$ becoming a bounded operator for $z : \text{Im}(z) \leq 0 \subset \mathbb{C}$. It should be noted that a similar extension to the upper half-plane, $y \geq 0$, would lose its boundedness property due to the factor $e^{\hat{H}y}$ in the unitary operator $\hat{U}(z)$.

Furthermore, for arbitrary ϕ_1 and ϕ_2 in $\mathcal{H}$, the function

$$f(z) = \langle \phi_1 | U(z)\phi_2 \rangle = \langle \phi_1 | e^{-iHz}\phi_2 \rangle, \tag{10.29}$$

is continuous, bounded, and analytic on Ω^-. This property is crucial for the proof that will invoke Lemma 10.1. However, 10.29 is a very general result that becomes useful for proving Hegerfeldt's theorem by setting $\psi_0 = \hat{K}^{\frac{1}{2}}\phi$ for any arbitrary $\phi \in \mathcal{H}$, and $\phi_1 = \Psi_0$, and thereby defining

$$f_\phi(z) = \langle \hat{K}^{\frac{1}{2}}\phi | e^{-i\hat{H}z}\Psi_0 \rangle = \langle \phi | \hat{K}^{\frac{1}{2}}e^{-i\hat{H}z}\Psi_0 \rangle, \qquad \text{for } \text{Im}(z) \leq 0, \tag{10.30}$$

where we have utilized the Hermitian property of $\hat{K}^{\frac{1}{2}}$. In this case, ϕ is arbitrary, while Ψ_0 is predetermined, as it corresponds to the initial wave function of Equation (10.24), where $\Psi_0 = \Psi(0)$.

Since $f_\phi(z)$ is a specific instance of $f(z)$ in (10.29), we note that $f_\phi(z)$ is also continuous and bounded for $\text{Im}(z) \leq 0$ and analytic for $\text{Im}(z) < 0$. According to Lemma 10.1, the boundedness of $f_\phi(z)$ in the lower half-plane and the analyticity of $f_\phi(z)$ for $\text{Im}(z) < 0$ has been shown to impose severe restrictions on $f_\phi(z)$'s boundary values on the real axis.

Suppose that the zero set $\mathcal{N}_0$ encompasses an interval on the real line, i.e., $\mathcal{I} \subset \mathbb{R}$. This indicates that its complement $\mathcal{N}_0^c \in \mathbb{R}$ is not dense in $\mathbb{R}$, and that

$$f_\phi(z) = 0, \qquad \forall z \in \mathcal{I}. \tag{10.31}$$

It is worth noting that Lemma 10.1 generally holds whenever $f_\phi(z) \in \mathbb{R}$ for all $z \in \mathcal{I}$, indicating that the above is a special case. The 3 steps below provide a summary of the application of the procedure that has been discussed thus far in applying Lemma 10.1. The steps are as follows:

1. **Applying Schwarz Reflection Principle:** The restriction of $f_\phi(z)$ to the semi-strip

   $$\Omega_\mathcal{I}^- = \{z \in \mathbb{C} : \text{Im}(z) \leq 0, \text{Re}(z) \in \mathcal{I}\}, \tag{10.32}$$

   is continuous, bounded, and real for all $z \in \mathcal{I}$. Thus, by the Schwarz reflection principle, $f_\phi : \Omega_I^- \to \mathbb{C}$ extends to an analytic function on the strip

   $$\Omega_\mathcal{I} = \{z \in \mathbb{C} : \text{Re}(z) \in \mathcal{I}\},$$

   using (10.16), such that

   $$f_\phi(z) = f_\phi(z^*)^*, \qquad \text{for } \text{Im}(z) > 0. \tag{10.33}$$

2. **Applying Analytic Continuation:** This extended $f_\phi : \Omega_\mathcal{I} \to \mathbb{C}$ is bounded and continuous on Ω_I, and extends to a bounded and analytic function in the lower half-plane. Since $f_\phi(z)$ is in $\Omega_\mathcal{I}$, the analytic extension of f_ϕ is also bounded. Thus, if $\mathcal{N}_0$ contains an interval, the bounded function $f_\phi(z)$ in the lower half-plane can be extended by analytic continuation to a bounded analytic function on the entire complex plane $\mathbb{C}$.

3. **Applying Liouville's Theorem:** Liouville's theorem then states that $f_\phi(z) \equiv C$ for some constant C. Since $f_\phi(z) = 0$ for $z \in \mathcal{I}$, this implies that

   $$f_\phi(z) = \langle \phi | \hat{K}^{\frac{1}{2}} e^{-i\hat{H}z} \Psi_0 \rangle \equiv 0, \qquad \forall z \in \mathbb{C}. \tag{10.34}$$

Since $\phi \in \mathcal{H}$ is arbitrary, it follows that

$$\hat{K}^{\frac{1}{2}} e^{-\frac{i}{\hbar}\hat{H}t} \Psi_0 = \hat{K}^{\frac{1}{2}} \Psi(t) \equiv 0 \qquad \forall t \in \mathbb{R}. \tag{10.35}$$

Therefore, $\mathcal{P}_K(t) = \langle \Psi(t) | \hat{K} \Psi(t) \rangle = |\hat{K}^{\frac{1}{2}} \Psi(t)|^2$ either has

1. $\mathcal{P}_K(t) = 0$ for all $t \in \mathbb{R}$, i.e. $\mathcal{N}_0 = \mathbb{R}$ from the application of Liouville's theorem, or

2. $\mathcal{N}_0^C$ is dense in $\mathbb{R}$. This implies that $\mathcal{P}_K(t) = 0$ can only hold at single discrete points in $\mathbb{R}$.

In the second case, we demonstrate that the complement of the zero set $\mathcal{N}_0^C = \{t \in \mathbb{R} | \mathcal{P}_K(t) \neq 0\}$ must be dense in $\mathbb{R}$. For any $t \in \mathbb{R}$, let $|t - t_n| < 1/n$ for a $t_n \in \mathcal{N}_0^C$. This condition can always be satisfied, as $\mathcal{N}_0$ does not contain an interval. Consequently, $t_n \to t$ for $t_n \in \mathcal{N}_0^C$, which indicates that $\mathcal{N}_0^C$ is dense. Since $\mathcal{P}_K(t) = 0$ only at an instant, it follows from Equation (10.30) that $\hat{K}^{\frac{1}{2}} \Psi(t) \neq 0$ immediately after that instant, implying that $\mathcal{P}_K(t) > 0$. This is because $\mathcal{P}_K(t) = \langle \Psi(t) | \hat{K} \Psi(t) \rangle = 0 \Leftrightarrow \hat{K}^{\frac{1}{2}} \Psi(t) = 0$, as demonstrated in (10.27). The implications of this finding are explored in the subsequent section.

Probability of Belonging to a Set

Suppose $\Psi(t) = e^{-\frac{i}{\hbar}\hat{H}t}\Psi_0 \in \mathcal{H}$, with $|\Psi_0| = 1$, describes the time evolution of Ψ_0 with a self-adjoint operator $\hat{H} \geq 0$. We aim to perform a measurement on $\Psi(t)$, yielding mutually exclusive outcomes A or B, represented by two self-adjoint operators $\hat{A}$ and $\hat{B}$, respectively. Here, B represents the event of not observing A meaning that B is the complement of observing A such that $\mathcal{P}_A(t) = 1 - \mathcal{P}_B(t)$, where

$$\mathcal{P}_A(t) = \langle\Psi(t)|\hat{A}\Psi(t)\rangle, \tag{10.36}$$

$$\mathcal{P}_B(t) = \langle\Psi(t)|\hat{B}\Psi(t)\rangle, \tag{10.37}$$

denote the probabilities of measuring outcomes A and B, respectively. From (10.36), we deduce that since $\hat{A}$ and $\hat{B}$ represent the operators corresponding to probabilities, they must satisfy $\hat{A} \geq 0$ and $\hat{B} \geq 0$. Moreover, operators $\hat{A}$ and $\hat{B}$ are related to each other by

$$\hat{A} = \hat{I} - \hat{B}, \tag{10.38}$$

where $\hat{I}$ denotes the identity operator. Assuming that at the initial state (when $t = 0$), the probability of measuring A equals unity,

$$\mathcal{P}_A(0) = \langle\Psi_0|\hat{A}\Psi_0\rangle = 1. \tag{10.39}$$

Consequently, the probability of measuring B is

$$\mathcal{P}_B(0) = \langle\Psi_0|\hat{B}\Psi_0\rangle = 0, \tag{10.40}$$

implying that $\hat{B}\Psi_0 = 0$ by (10.27). Since $\hat{H} \geq 0$, Hegerfeldt's theorem applies, so that

$$\mathcal{P}_B(t) = \langle\Psi(t)|\hat{B}\Psi(t)\rangle > 0, \tag{10.41}$$

instantaneously for any $t > 0$ that can be arbitrarily close to $t = 0$. Similarly, this implies that

$$\mathcal{P}_A(t) = \langle\Psi(t)|\hat{A}\Psi(t)\rangle < 1, \qquad \forall t \in (0, \epsilon), \quad \text{for any } \epsilon > 0, \tag{10.42}$$

Thus, there is always a positive chance to measure B for any $t > 0$ as close to $t = 0$ as desired. The only other case (case 1 in Section 10.2.5) in which this conclusion does not hold would necessarily invoke Liouville's theorem, such that

$$\mathcal{P}_A(t) = \langle\Psi(t)|\hat{A}\Psi(t)\rangle = 1, \qquad \forall t \in \mathbb{R}, \mathcal{P}_B(t) = \langle\Psi(t)|\hat{B}\Psi(t)\rangle = 1, \qquad \forall t \in \mathbb{R}, \tag{10.43}$$

as a direct consequence of Lemma 10.1 in Hegerfeldt's theorem. This result indicates that the probabilities of measuring outcomes A and B remain constant throughout the entire real line, which is a highly unusual scenario in relativistic quantum mechanics, especially for massless particles propagating at the speed of light.

10.2.6 Example Demonstrating Violation of Relativistic Causality

Consider the initial wave function $\Psi_0 = \Psi(\boldsymbol{r}, 0)$ with compact support within an arbitrary region of space. Let $0 \leq \hat{A}_1 \leq 1$ represent a self-adjoint operator determining the probability of detecting the particle, described by $\Psi(t)$, inside a region V_1. The region V_1 is a sphere with radius R centered at the origin.

Although the above example is rather general, it can be made more concrete by representing the operator $\hat{A}_1$ with a function $A_1(\boldsymbol{r})$ defined as

$$A_1(\boldsymbol{r}) = \begin{cases} 1, & \text{for} \quad |\boldsymbol{r}| \leq R \\ 0, & \text{for} \quad |\boldsymbol{r}| > R. \end{cases} \tag{10.44}$$

Consequently, the operator $0 \leq \hat{B}_1 \leq 1$, given by $\hat{B}_1 = \hat{I} - \hat{A}_1$, which corresponds to measuring the particle outside region V_1, can be represented by

$$B_1(\boldsymbol{r}) = \begin{cases} 0, & \text{for} \quad |\boldsymbol{r}| \leq R \\ 1, & \text{for} \quad |\boldsymbol{r}| > R, \end{cases} \tag{10.45}$$

Suppose that at $t = 0$, the wave function is entirely contained within region V_1, so that the probability

$$\mathcal{P}_{A1}(0) = \langle \Psi(\boldsymbol{r}, 0) | \hat{A}_1 \Psi(\boldsymbol{r}, 0) \rangle = \int |\Psi(\boldsymbol{r}, 0)|^2 A_1(\boldsymbol{r}) \, \mathrm{d}^3 \boldsymbol{r} = \int_{|\boldsymbol{r}| \leq R} |\Psi(\boldsymbol{r}, 0)|^2 \, \mathrm{d}^3 \boldsymbol{r} = 1, \quad (10.46)$$

and likewise

$$\mathcal{P}_{B1}(0) = \langle \Psi(\boldsymbol{r}, 0) | \hat{B}_1 \Psi(\boldsymbol{r}, 0) \rangle = \int |\Psi(\boldsymbol{r}, 0)|^2 B_1(\boldsymbol{r}) \, \mathrm{d}^3 \boldsymbol{r} = \int_{|\boldsymbol{r}| > R} |\Psi(\boldsymbol{r}, 0)|^2 \, \mathrm{d}^3 \boldsymbol{r} = 0, \quad (10.47)$$

which implies that $\mathcal{P}_{A1}(t) = 1 - \mathcal{P}_{B1}(t)$ as previously discussed. The compact support of the initial wave function signifies that

$$\Psi(\boldsymbol{r}, 0) = 0 \qquad \text{for} \qquad |x| > R, \qquad (10.48)$$

in this particular concrete example. Nevertheless, to maintain generality, we observe that when $\mathcal{P}_A(t)$ is *non-constant* (in the case where Liouville's theorem has not been invoked), it is impossible for the probability to maintain the constant value $\mathcal{P}_{A1}(t) = 1$ for $t \in [0, \epsilon]$ for any arbitrarily small $\epsilon > 0$. This is because $\mathcal{P}_{B1} = \langle \Psi(\boldsymbol{r}, 0) | \hat{B}_1 \Psi(\boldsymbol{r}, 0) \rangle = 0$ can be used in conjunction with Lemma 10.1 in a similar manner as done previously.

Suppose we have another self-adjoint operator $0 \leq \hat{A}_2 \leq 1$ used to determine the probability of detecting the particle somewhere inside a region V_2. The point here is that V_2 encompasses V_1 but is orders of magnitude larger than V_1. For instance, V_2 could be as large as the observable universe, while V_1 might be just a single cubic meter. This implies that, at $t = 0$, both

$$\mathcal{P}_{A1}(0) = \langle \Psi(\boldsymbol{r}, 0) | \hat{A}_1 \Psi(\boldsymbol{r}, 0) \rangle = 1, \qquad (10.49)$$

and

$$\mathcal{P}_{A2}(0) = \langle \Psi(\boldsymbol{r}, 0) | \hat{A}_2 \Psi(\boldsymbol{r}, 0) \rangle = 1, \qquad (10.50)$$

where $\mathcal{P}_{A2}(t)$ represents the probability of detecting the particle inside V_2 at time t. Similarly, the self-adjoint $0 \leq \hat{B}_2 \leq 1$ would correspond to the probability, $\mathcal{P}_{B2}(t)$, of finding the particle outside region V_2 at time t, with $\mathcal{P}_{A2}(t) = 1 - \mathcal{P}_{B2}(t)$. By only considering positive energies, i.e. $\hat{H} \geq 0$, Hegerfeldt's theorem implies that at any time $t > 0$ that is arbitrarily close to $t = 0$, both probabilities immediately become

$$\mathcal{P}_{A1}(t) = \langle \Psi(\boldsymbol{r}, t) | \hat{A}_1 \Psi(\boldsymbol{r}, t) \rangle < 1 \quad \Leftrightarrow \quad \mathcal{P}_{B1}(t) > 0, \qquad \text{at any } t > 0, \qquad (10.51)$$

and similarly

$$\mathcal{P}_{A2}(t) \langle \Psi(\boldsymbol{r}, t) | \hat{A}_2 \Psi(\boldsymbol{r}, t) \rangle < 1 \quad \Leftrightarrow \quad \mathcal{P}_{B2}(t) > 0, \qquad \text{at any } t > 0, \qquad (10.52)$$

simultaneously. This means that a wave function initially contained entirely within V_1 has spread its tails outside V_1 and V_2 in an arbitrarily infinitesimal amount of time. Since V_2 can be orders of magnitude larger than V_1, this implies a violation of relativistic causality, as the probabilities spread faster than light, since t can be set arbitrarily close to $t = 0$.

10.2.7 General Physical Significance

Consider the Hamiltonian, $\hat{H}$, with a positive spectrum and suppose a measurement of a property of the state $\Psi(t)$ belongs to a specified set. Given the assumption that this property is known to belong to the set at $t = 0$, the formalism dictates that either the property will persistently belong to the specified set, or there will be an immediate positive probability for the property to deviate from the set.

Hegerfeldt's theorem, as we have seen, demonstrates a violation of relativistic causality in quantum mechanics when considering only positive energies. This result has profound implications on our understanding of causality and the nature of quantum systems. However, it's important to note that the theorem is built upon specific assumptions, and its conclusions may not apply under different circumstances.

10.2.8 Incorporating Both Positive and Negative Energies

If $\hat{H} \leq 0$ and $\Psi(t) = e^{-\frac{i}{\hbar}\hat{H}t}\Psi_0$, Hegerfeldt's argument is similarly applicable, but this time it pertains to the upper half-plane. However, by including both positive and negative energies, as in

$$\Psi(t) = (c_1 e^{-\frac{i}{\hbar}\hat{H}t} + c_2 e^{\frac{i}{\hbar}\hat{H}t})\Psi_0, \qquad c_1, c_2 \neq 0, \tag{10.53}$$

it becomes impossible to extend $c_1 e^{-\frac{i}{\hbar}\hat{H}t} + c_2 e^{\frac{i}{\hbar}\hat{H}t}$ in a half-plane to a bounded analytic function, rendering Hegerfeldt's argument inapplicable in this case.

Thus, one way to mitigate the violation of relativistic causality shown by Hegerfeldt's theorem is to include both positive and negative energies in the analysis, as demonstrated in the previous section. This approach is reminiscent of the concept of antiparticles in relativistic quantum mechanics, where particles and their corresponding antiparticles can be described by solutions with positive and negative energy components, respectively. It is for this reason that Hegerfeldt's theorem does not apply to the solutions to the Dirac equation, as these contain both positive and negative solutions [6].

As the particle evolves in time, the positive and negative energy components can interfere destructively, resulting in a wave function that remains localized and does not spread faster than the speed of light. This ensures that relativistic causality is preserved.

10.2.9 Significance Regarding Entropy

We have demonstrated in this thesis that quantum mechanics solves the entropy problem by connecting its abstract mathematics formalism in Hilbert space, i.e. the wave function, to empirical measurements through utilization of Hermitian matrices. The eigenvalues of these Hermitian matrices are real and correspond to physical observables.

However, in relativistic systems, we have shown that the attempt to create a physical observable for position, i.e. the position operator, using only positive energy solutions is hindered by Hegerfeldt's theorem. Negative energy solutions have been disregarded in the past due to their perceived inconvenience, as they imply negative time and thus violate the concept of unidirectional causality. For electrons, the sign of the charge can be flipped to reinterpret negative energies as positive energies. However, this procedure is not feasible for photons, which lack intrinsic charge, leading to the absence of a first quantized theory for the photon. This is due to no-go theorems such as Hegerfeldt's theorem, which hinder the connection of the wave function with some physical observables, resulting in an entropy problem.

One could argue that perhaps one just has to accept the fact that all photon localization operators must contain infinite exponentially decaying tails, in order to avoid negative energy solutions. However, Hegerfeldt's 1989 paper called *Difficulties With Causality In Particle Localization* and showed that this approach is flawed too concluding with the following [54]:

> *Positivity of the energy, or rather its boundedness from below, which is one of the axioms of quantum field theory, is the main ingredient of the results, not the appearance of a root. However, with arbitrarily negative energies one may have strict localization together with causal propagation, as in relativistic wave equations.*

The crucial insight from Hegerfeldt's theorem is that relativistic causality can only be preserved by including both positive and negative energy components. This is because the negative energy components can cancel out the unbounded tails of the wave function, allowing for a localized wave function that respects relativistic causality.

10.3 Introducing The Antiphoton

The antiphoton is characterized by a negative energy electromagnetic wave that travels in the opposite direction to its Poynting vector $\boldsymbol{S} = \boldsymbol{\mathcal{E}} \times \boldsymbol{\mathcal{H}}$, i.e. linear momentum. Unlike a regu-

lar photon, the antiphoton is not a solution of Maxwell's equations, but instead it is a solution of the backward Maxwell's equations. This implies that the antiphoton can be understood as a photon traveling backwards in time. The backward Maxwell's equations can be obtained by transforming the time variable, $t \to -t$, resulting in a set of quantities $\{\boldsymbol{E}(t), \boldsymbol{H}(t), \rho(t), \boldsymbol{J}(t)\} \to \{\boldsymbol{E}(-t), \boldsymbol{H}(-t), \rho(-t), -\boldsymbol{J}(-t)\} = \{\boldsymbol{\mathcal{E}}(t), \boldsymbol{\mathcal{H}}(t), \rho(t), -\boldsymbol{\mathcal{J}}(t)\}$ so that

$$\nabla \cdot \boldsymbol{\mathcal{E}} = \frac{\rho}{\epsilon_0}, \tag{10.54}$$

$$\nabla \cdot \boldsymbol{\mathcal{B}} = 0, \tag{10.55}$$

$$\nabla \times \boldsymbol{\mathcal{E}} = \frac{\partial \boldsymbol{\mathcal{B}}}{\partial t}, \tag{10.56}$$

$$\nabla \times \boldsymbol{\mathcal{B}} = -\mu_0 \boldsymbol{J} - \frac{1}{c^2} \frac{\partial \boldsymbol{\mathcal{E}}}{\partial t}. \tag{10.57}$$

The equations 10.54-10.57 represent the backward Maxwell's equations for the antiphoton. In these equations, the current density, $\boldsymbol{J}$, transforms as $\boldsymbol{J}(t) \to -\boldsymbol{J}(-t)$ due to its velocity component being a time derivative. The transformation $t \to -t$ results in $\frac{\partial}{\partial t} \to \frac{\partial}{\partial(-t)} = -\frac{\partial}{\partial t}$. It is noteworthy that the magnetic field, $\boldsymbol{B}$, does not change sign under this transformation, unlike in conventional electromagnetism under $t \to -t$. We shall later see that the latter kind of transformation corresponds to an *Advanced-Retarded* transformation, which is still a valid solution to the forward Maxwell's equations. In the *Photon-Antiphoton* transformation, with $t \to -t$, the magnetic field, $\boldsymbol{B}$, does not change sign as it is not a time derivative of anything.

The Riemann-Silberstein vector for the antiphoton is defined as follows

$$\boldsymbol{\mathcal{F}} = \boldsymbol{\mathcal{E}} + ic\boldsymbol{\mathcal{B}}. \tag{10.58}$$

By utilizing the backward Maxwell's equations for the antiphoton along with Equation (10.58), we obtain the antiphoton wave equation

$$i\hbar \frac{\partial \boldsymbol{\mathcal{F}}}{\partial t} = -c \left(\overrightarrow{\boldsymbol{s}} \cdot \frac{\hbar}{i} \boldsymbol{\nabla} \right) \boldsymbol{\mathcal{F}}, \qquad \boldsymbol{\nabla} \cdot \boldsymbol{\mathcal{F}} = 0, \tag{10.59}$$

which, when compared to the photon wave Equation (10.14), differs only by a sign.

By combining the wave equations for the photon and antiphoton, we can express the following

$$i\hbar \frac{\partial}{\partial t} \begin{pmatrix} \boldsymbol{F} \\ \boldsymbol{\mathcal{F}} \end{pmatrix} = i\hbar c \begin{pmatrix} -\overrightarrow{\boldsymbol{s}} \cdot \boldsymbol{\nabla} & 0 \\ 0 & \overrightarrow{\boldsymbol{s}} \cdot \boldsymbol{\nabla} \end{pmatrix} \begin{pmatrix} \boldsymbol{F} \\ \boldsymbol{\mathcal{F}} \end{pmatrix}, \tag{10.60}$$

in a similar fashion as Equation (9.43), where we have utilized spin-1 matrices $\overrightarrow{\boldsymbol{s}}$ instead of the spin-1/2 Pauli matrices $\overrightarrow{\boldsymbol{\sigma}}$. Equation (10.60) can thus be regarded as a spin-1 equation for bosons. It is worth noting that the lack of a mass term in these equations leads to decoupled systems. In contrast, the presence of mass terms in the Dirac equation results in coupling between negative and positive energy solutions, making the negative energy solution a requirement when solving the equations. However, this is not the case for the photon wave equations, which, owing to their uncoupled nature, do not show an explicit requirement for the incorporation negative energy solutions. Despite this, it will be demonstrated that the antiphoton solution is a crucial factor in resolving the entropy problem in electromagnetism and enabling strict localization of the photon.

It is noteworthy that by taking the curl of the last two Equations (10.56) and (10.57) of the backward Maxwell's equations, applying a vector identity, and using the first two Equations (10.54) and (10.55) in a manner similar to that described in Section 10.1, we obtain the equation

$$\frac{1}{c^2} \frac{\partial^2 \boldsymbol{\mathcal{F}}}{\partial t^2} - \nabla^2 \boldsymbol{\mathcal{F}} = 0, \tag{10.61}$$

which is identical to (10.9). Therefore, solutions of the form

$$\boldsymbol{\Psi} = \boldsymbol{F} + \boldsymbol{\mathcal{F}}, \tag{10.62}$$

which consist of both photon and antiphoton components, satisfy the equation

$$\frac{1}{c^2}\frac{\partial^2 \boldsymbol{\Psi}}{\partial t^2} - \nabla^2 \boldsymbol{\Psi} = 0, \tag{10.63}$$

which shares some resemblance to the the Klein-Gordon Equation (9.27) with $m = 0$. The fact that (10.63) has photon and antiphoton solutions can be seen by expressing (10.63)

$$\left(\frac{1}{c^2}\frac{\partial^2}{\partial t^2} - \nabla^2\right)\boldsymbol{\Psi} = \left(\frac{1}{c}\frac{\partial}{\partial t} + \overrightarrow{\boldsymbol{s}}\cdot\boldsymbol{\nabla}\right)\left(\frac{1}{c}\frac{\partial}{\partial t} - \overrightarrow{\boldsymbol{s}}\cdot\boldsymbol{\nabla}\right)\boldsymbol{\Psi} = 0, \tag{10.64}$$

as a factor of the photon and antiphoton wave equations respectively. In a similar fashion, we can rewrite the Klein-Gordon equation as the product of two first-order differential equations corresponding to the positive and negative energy solutions

$$\left(\frac{1}{c}\frac{\partial}{\partial t} + \sqrt{\nabla^2 - \frac{m^2 c^2}{\hbar^2}}\right)\left(\frac{1}{c}\frac{\partial}{\partial t} - \sqrt{\nabla^2 - \frac{m^2 c^2}{\hbar^2}}\right)\Psi(x,t) = 0. \tag{10.65}$$

The positive and negative energy solutions are given by (9.50) and (9.51), respectively.

Another aspect of the duality between photons and antiphotons can be seen by identifying the operators $\hat{E} = i\hbar\frac{\partial}{\partial t}$ and $\hat{\boldsymbol{P}} = (\hat{P}_x, \hat{P}_y, \hat{P}_z)^\intercal = \frac{\hbar}{i}\boldsymbol{\nabla}$, so that the Equation (10.14) can be re-written as

$$\hat{E}\boldsymbol{F} = c\overrightarrow{\boldsymbol{s}}\cdot\hat{\boldsymbol{P}}\boldsymbol{F}, \qquad \hat{\boldsymbol{P}}\cdot\boldsymbol{F} = 0. \tag{10.66}$$

By applying the operator twice, we get

$$\hat{E}^2\boldsymbol{F} = (c\overrightarrow{\boldsymbol{s}}\cdot\hat{\boldsymbol{P}})^2\boldsymbol{F} = \left(c^2\hat{\boldsymbol{P}}\cdot\hat{\boldsymbol{P}} - c^2\begin{bmatrix}\hat{P}_x\hat{P}_x & \hat{P}_x\hat{P}_y & \hat{P}_x\hat{P}_z \\ \hat{P}_y\hat{P}_x & \hat{P}_y\hat{P}_y & \hat{P}_y\hat{P}_z \\ \hat{P}_z\hat{P}_x & \hat{P}_z\hat{P}_y & \hat{P}_z\hat{P}_z\end{bmatrix}\right)\boldsymbol{F} = c^2(\hat{\boldsymbol{P}}\cdot\hat{\boldsymbol{P}})\boldsymbol{F}, \tag{10.67}$$

where it can be verified that the matrix of the tensor product of $\hat{\boldsymbol{P}}$ with itself is equal to zero by the divergence-less condition $\boldsymbol{\nabla}\cdot\boldsymbol{F} = 0$. This is because $(\hat{\boldsymbol{P}}\otimes\hat{\boldsymbol{P}})\boldsymbol{F} = -\hbar^2\boldsymbol{\nabla}(\boldsymbol{\nabla}\cdot\boldsymbol{F})$, which is zero. By denoting $\hat{\boldsymbol{P}}\cdot\hat{\boldsymbol{P}}$ as $\hat{P}^2$ we see that

$$\hat{E}^2\boldsymbol{F} = c^2\hat{P}^2\boldsymbol{F}, \tag{10.68}$$

has both positive and negative energies, i.e. $E = \pm pc$, as we would have obtained the same result of (10.68) if we had instead started with the wave equation for the antiphoton (10.59). In other words, the two Equations (10.7) and (10.8) of second order in time have *both* photon and antiphoton solutions.

In summary, Hegerfeldt's theorem demonstrates that a particle with a compactly supported wave function and only positive energies must spread faster than the speed of light, violating relativistic causality. The inclusion of both positive and negative energy components, as in the Klein-Gordon equation, allows for destructive interference that keeps the wave function localized and ensures that relativistic causality is preserved.

10.4 Incorporating the Antiphotons

The consequences of Hegerfeldt theorem can be seen more explicitly by considering the following wave function, representing the Fourier transform of (10.11)

$$i\hbar\omega\boldsymbol{F}(\boldsymbol{k}) = c\boldsymbol{k}\times\boldsymbol{F}(\boldsymbol{k}), \qquad \omega = c\sqrt{k_x^2 + k_y^2 + k_z^2}. \tag{10.69}$$

If the initial wave function $\boldsymbol{F}(\boldsymbol{r}, 0)$ is continuous and has compact support in a region V, its Fourier transform, loses this compact support property and becomes an entire function. This means that the right hand side of (10.69) is necessarily a holomorphic function of the variables k_x, k_y, k_z.

However, this is not the case for the left hand side that contains $\omega = c\sqrt{k_x^2 + k_y^2 + k_z^2}$. This is because its first derivative is not analytic at for $\boldsymbol{k} = 0$. This creates localization issues for the photon wave function using only positive energies.

$$\boldsymbol{\Psi}(\boldsymbol{r}, t) = \int \frac{\mathrm{d}^3 k}{(2\pi)^3} e^{i\boldsymbol{k} \cdot \boldsymbol{r}} (\boldsymbol{F}(\boldsymbol{k}) e^{-i\omega t} + \boldsymbol{\mathcal{F}}(\boldsymbol{k}) e^{i\omega t}) \tag{10.70}$$

$$i\omega \boldsymbol{\mathcal{F}}(\boldsymbol{k}) = -c\boldsymbol{k} \times \boldsymbol{\mathcal{F}}(\boldsymbol{k}), \qquad \omega = c\sqrt{k_x^2 + k_y^2 + k_z^2}. \tag{10.71}$$

$$i\omega(\boldsymbol{F}(\boldsymbol{k}) - \boldsymbol{\mathcal{F}}(\boldsymbol{k})) = c\boldsymbol{k} \times (\boldsymbol{F}(\boldsymbol{k}) + \boldsymbol{\mathcal{F}}(\boldsymbol{k})), \qquad \omega = \sqrt{k_x^2 + k_y^2 + k_z^2}. \tag{10.72}$$

where the same argument no longer holds because the functions on the right and left hand sides are not longer the same with the inclusion of the antiphoton solutions. The inclusion of negative energies is a necessary, but not sufficient condition [2].

Wessel-Berg's theory creates the sufficient framework in which utilizing these negative energies are used to solve the entropy problem of electromagnetism and thus yield predictions that accurately describe reality.

10.4.1   Overview of Recent Relevant Research

It is important to emphasize that the concept of negative energies is not novel and has been utilized by various authors in recent years to mitigate the problematic implications of Hegerfeldt's theorem. This approach has enabled the development of meaningful position operators for photons and other massless particles that are both Lorentz invariant and have a positive probability that satisfies a covariant continuity equation. Before delving into the main theory of bitemporal electromagnetism, this study provides a brief overview of the relevant literature on the subject.

The paper by Southall et al. [83] provides a more detailed discussion on the incorporation of negative frequencies in the second quantization of the electromagnetic field. The approach taken in the paper quantizes the field in position space, taking into account both negative and positive frequency solutions of Maxwell's equations. This leads to the construction of annihilation operators for highly-localized field excitations that follow bosonic commutator relations, enabling the formation of wave packets of light and a locally-acting interaction Hamiltonian. For those seeking an introductory material, a related paper by Hodgson et al. [55] can be used as a starting point.

In more recent literature, Hegerfeldt has demonstrated that the primary cause of spreading is the lower bound placed on the Hamiltonian of the system [51, 52]. Historically, these negative energy states have been largely ignored due to their violation of unidirectional causality. However, as already mentioned, the concept of adopting them to counteract the implications of Hegerfeldt's theorem is not a novel idea [54].

The significance of negative frequency components in a local description of photons has long been established. For example, Allcock emphasized that negative frequency modes are necessary to define states with a well-defined and measurable time of arrival [3–5]. Property 2 elucidates that a blip state's arrival at a specific position can be determined. Negative-frequency field solutions have also been explored in several other studies [11, 18–20, 29, 67]. The work of Margaret Hawton has demonstrated how the inclusion of negative frequencies, a biorthogonal description for meaningful position operators for photons can be achieved that contains all the appropriate properties in a relativistic theory [46–48].

The focus of these studies is the utilization of positive and negative frequency one-particle states for the description of photons. These states are formed by the field operator and its conjugate and exhibit biorthogonality as a consequence of their commutation relations. The position operator in these bases is covariant, and the Klein-Gordon wave function is localized [49].

In addition to the previous literature on negative energies, the recent PhD thesis by Daniel R. E. Hodgson, titled *A Theory of Local Photons with Applications in Quantum Field Theory* [56], provides an alternative approach to the quantization of the electromagnetic field. The author takes a different approach from the conventional method of describing photons as monochromatic waves with definite energy and momentum, which leads to limitations regarding the localizability and superluminal propagation of single photons.

Hodgson's approach is based on quantizing the free electromagnetic field in terms of perfectly localized quanta that propagate at the speed of light without dispersion. This approach overcomes earlier no-go theorems first by making a clear distinction between particles, which can always be localized, and the electric and magnetic fields, which cannot, and secondly by removing the lower bound on the Hamiltonian, thereby introducing negative-frequency photons. This thesis highlights the use of negative frequencies in overcoming earlier no-go theorems and describing photons dynamics in the presence of local interactions with specified boundary conditions.

In recent literature, the incorporation and application of negative frequencies to the double-slit experiment has been explored. The results obtained in these studies exhibit a high degree of similarity to those presented in the works of Wessel Berg [25, 26].

However, most of these studies do not mention negative energies nor antiphotons, and suggest that the incorporation of these negative frequencies is purely a mathematical trick. They also fail to mention that these negative frequency solution also fail to solve the forward Maxwell's equations.

10.5 Example: Reflection and Transmission at Normal Incidence

In this section, we discuss the first example from Wessel-Berg's book [91, p. 22-28], which explores the reflection and transmission of photons in the form of electromagnetic plane waves at normal incidence to a thin planar medium. This example highlights the limitations of conventional electromagnetic theory in accounting for single-photon measurements, revealing a discrepancy between the mathematical theory and actual empirical observations at finer scales.

10.5.1 Background Information

As discussed, Hegerfeldt's theorem establishes that localized states exhibit relativistic non-causal propagation. To circumvent the implications of this theorem and enable the connection between the theoretical framework and single zero-entropy measurements, the current study incorporates both positive and negative energy solutions of Maxwell's equations, effectively doubling the conventional Hilbert space. The entropy problem inherent to electromagnetism is addressed through the introduction of the concept of *photon doublets*, which consist of photon-antiphoton pairs, ultimately resolving the issue.

By first creating a microcosmic description of Maxwell's theory, Wessel-Berg's approach is found to be compatible with the standard version of the electromagnetism, only with the addition of the negative energy states of the antiphotons. The approach enables the theory to describe the individual photon measurement events, and thus, resolves the entropy problem in electromagnetism, as demonstrated by a 1D example involving reflection and transmission of electromagnetic waves in a thin plate of some medium.

It is crucial to mention that the initial presentation of this example in the book contains numerous errors, which can make comprehension challenging for first-time readers. It is only through the introduction of the general theory in later chapters that the author was able to correct the issues found in this initial example. Due to the sheer number of mistakes, discussing and explaining them here would likely only serve to confuse the reader.

10.5.2 Main Example

Consider the setup shown in Figure 18, which depicts a medium represented by the thick black line. Electromagnetic plane waves scatter on this medium at normal incidence, meaning they are perpendicular to the medium's surface. For simplicity, we assume the medium has negligible thickness. This assumption keeps the example straightforward, as the generalization to larger and non-negligible thicknesses does not significantly contribute to the understanding of this example. By assuming normal incidence, the problem is reduced to one spatial dimension, z, which is perpendicular to the medium's plane.

It is worth mentioning that despite the presence of multiple errors in the original example from Wessel-Berg's book, the following example offers a corrected and modified version that still conveys the same point. While there are significant differences between this revised example and the original, we will try to maintain much of the original notation.

One notable distinction is that the original example features only two terminals, while our revised example extends this to four terminals. Among these, two (T1 and T4) are referred to as *virtual* and depicted by dashed lines. These virtual terminals represent two imaginary planes in a vacuum, both parallel to the planar medium and situated at a distance l on each side of it. Specifically, terminal T1 is positioned above the medium, while T4 is located below it. The remaining two terminals (T2 and T3) are situated directly on the opposing sides of the medium's surfaces. Terminal T2 is on the upper surface of the medium, while T3 is on the lower surface, as illustrated in Figure 18. In the figure, the block arrows at any given terminal are separated along their plane for visualization purposes only, since this is a 1D example; in reality, they overlap.
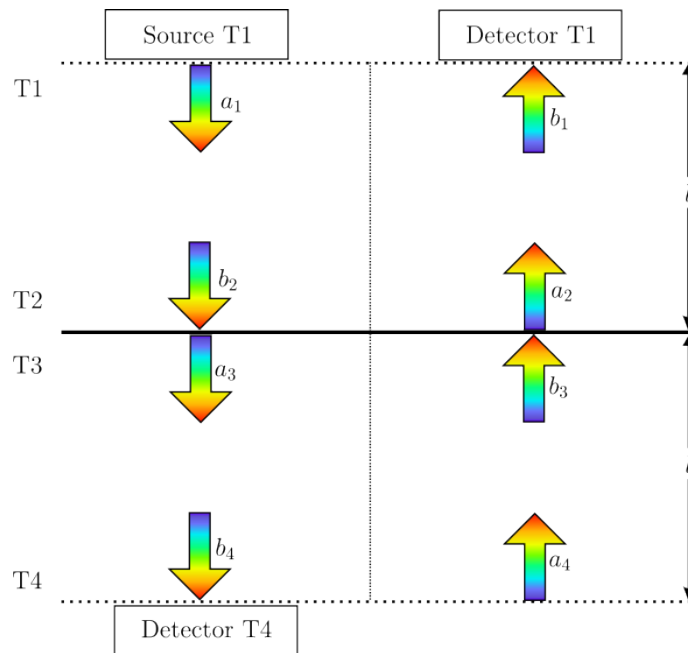
Figure 18: Revised example of reflection and transmission of photons in a one-dimensional thin medium in Wessel-Berg's book [91, p. 22-28]. A medium with negligible thickness, represented by the thick black line. Electromagnetic plane waves scatter on the medium at normal incidence, i.e. perpendicularly to the medium's surface. Four terminals are depicted, marked by T1, T2, T3 and T4. Two of these (T1 and T4) are *virtual* (dashed lines), and represent imaginary parallel planes in a vacuum at distance l from the planar medium. Each ith terminal has two components representing the amplitudes of the outgoing and incoming waves at the terminal, given by a_i and b_i, respectively. The direction of the wave propagation components at each terminal is indicated by the direction of the corresponding arrows.

All four terminals have two components, a_i and b_i, representing outgoing and incoming amplitudes of the electromagnetic field resulting in the powers flow in the form of electromagnetic waves at each terminal, where $i \in 1, 2, 3, 4$. These amplitude components essentially represent the square

root of the power flow for each plane wave.

In every component, there is a unique local coordinate system, the origin of which is situated at the location of each terminal. To mirror Wessel-Berg's original example as closely as possible, we introduce several modifications to the orientations of these local coordinate systems:

Examining Figure 18, we see that all components on the left have their local z axes directed downwards, whereas the components on the right orient their local z axes upwards. This is depicted in Figure 18, where each terminal's a_i and b_i components are represented by block arrows, with either the base or tip of each arrow marking $z = 0$ for the local coordinate of each component.

Furthermore, note that the arrow direction indicates the positive direction of each local z coordinate for the a_i and b_i components. The y axes for the left components point towards the left, while for the right components, they point to the right. The x axes for all components are directed outward from the figure.

A more comprehensive elucidation of electromagnetic wave transmission and reflection at normal incidence on a medium is provided in [44]. This reference presents an analogous example, exploring the true amplitudes and boundary conditions of the system within a global coordinate system.

In this example, the power of incoming waves is partially reflected, denoted by a reflection coefficient $\mathcal{R}$, with the residual portion transmitted, represented by a transmission coefficient $\mathcal{T}$. This can be expressed as

$$\mathcal{T} = 1 - \mathcal{R}, \tag{10.73}$$

which ensures a lossless setup. Considering that both sides of the medium plate exist in a vacuum, the reflection and transmission of the wave amplitudes, denoted by R and T respectively, correlate to the reflection coefficients as follows

$$\mathcal{R} = R^2, \qquad T = \sqrt{\mathcal{T}} = \sqrt{1 - R^2}. \tag{10.74}$$

This relationship ensures the conservation of energy.

It is important to note that this discussion is based on classical electromagnetic theory, which deals exclusively with the averages of a large number of photons. In examining Figure 18, if Source T1 emits N photons per second at a given frequency ω, with each photon having the same energy $\hbar\omega$, the number of photons detected at Detector T4 (N_T) and Detector T1 (N_R) would satisfy

$$\lim_{N \to \infty} \left(\frac{N_T}{N_R} \right) = \left(\frac{\mathcal{T}}{\mathcal{R}} \right), \tag{10.75}$$

where $N = N_T + N_R$. It is crucial to emphasize that Equation (10.75) demonstrates the average nature of classical electromagnetism. The classical theory only addresses the relationship concerning large number averages and provides no information on single-photon events.

Let the inward and outward components a_i and b_i be represented by vectors $\boldsymbol{a}$ and $\boldsymbol{b}$, such that the matrix $\boldsymbol{S}$ relates the two via

$$\boldsymbol{b} = \begin{bmatrix} b_1 \\ b_2 \\ b_3 \\ b_4 \end{bmatrix} = \boldsymbol{S}\boldsymbol{a} = \boldsymbol{S} \begin{bmatrix} a_1 \\ a_2 \\ a_3 \\ a_4 \end{bmatrix}. \tag{10.76}$$

Considering our earlier discussion about reflection and transmission coefficients, we know that

many of the components are related to one another. Therefore, $\boldsymbol{a}$ can be divided as follows:

$$
\begin{bmatrix} b_1 \\ b_2 \\ b_3 \\ b_4 \end{bmatrix} = \boldsymbol{S} \begin{bmatrix} \overline{a}_1 \\ \overline{a}_2 \\ \overline{a}_3 \\ \overline{a}_4 \end{bmatrix} + \boldsymbol{S} \begin{bmatrix} \hat{a}_1 \\ \hat{a}_2 \\ \hat{a}_3 \\ \hat{a}_4 \end{bmatrix}, \tag{10.77}
$$

where $\overline{\boldsymbol{a}}$ represents trivial input components inherent to the system, resulting exclusively from reflection and transmission from the external input column $\hat{\boldsymbol{a}}$. It is worth noting that, although $\hat{a}_2$ and $\hat{a}_3$ should intuitively be zero, we do not set them as such in order to maintain the generality of this discussion.
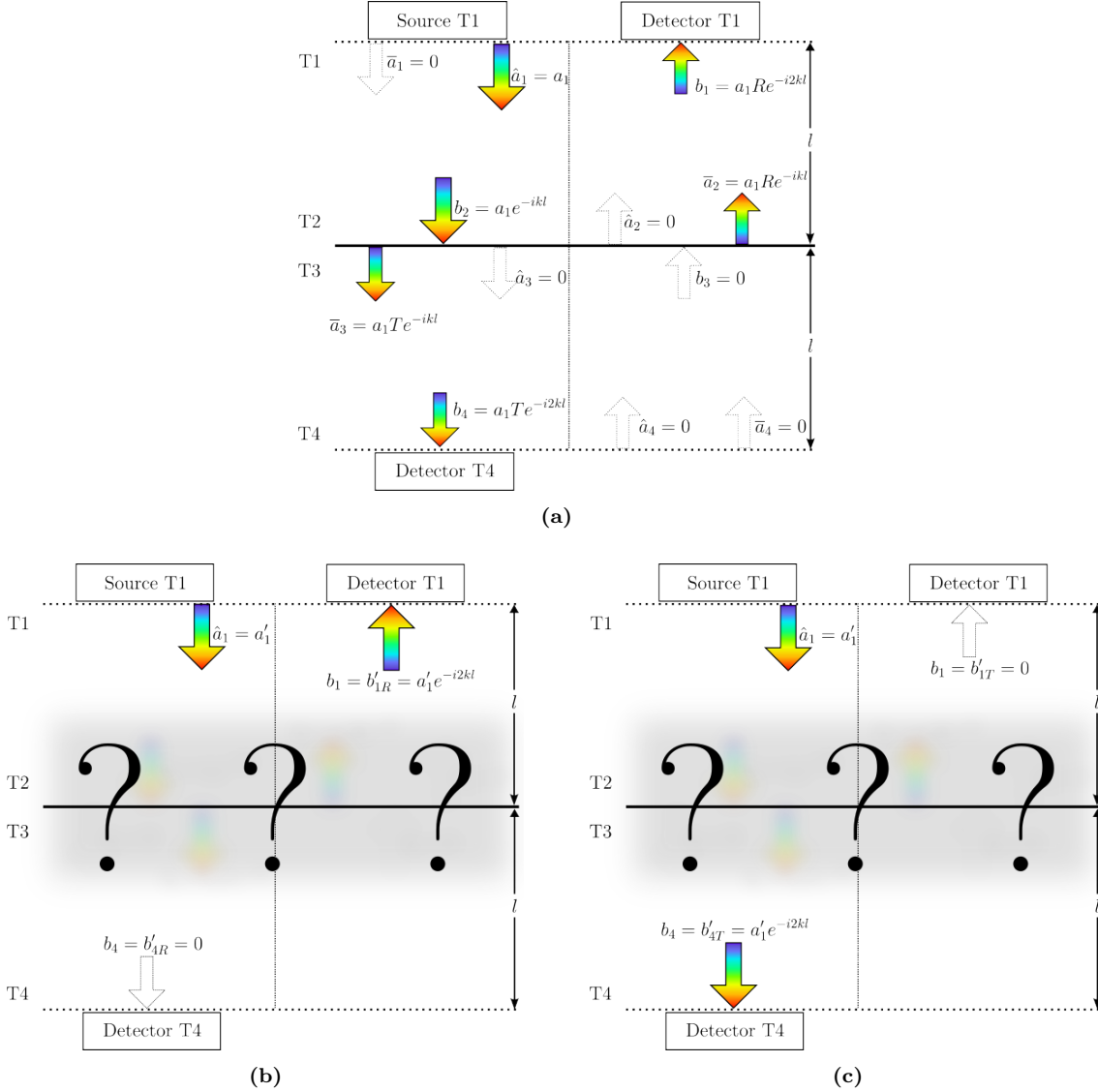
Figure 19: Revised example of reflection and transmission of photons in a one-dimensional thin medium in Wessel-Berg's book [91, p. 22-28] continued. **(a)** Situation where the external input is $\hat{\boldsymbol{a}} = (a_1, 0, 0, 0)^\mathsf{T}$. This results in $\boldsymbol{b} = (a_1 R e^{-i2kl}, a_1 e^{-ikl}, 0, a_1 T e^{-i2kl})^\mathsf{T}$. **(b)** Situation where only one photon is emitted from Source T1 and there is full reflection from the medium back to Detector T1. **(c)** Situation where only one photon is emitted from Source T1 and there is full transmission through the medium. The photon is then detected by Detector T4.

In a typical situation, the input from Source T1 would have $\hat{\boldsymbol{a}} = (a_1, 0, 0, 0)^\mathsf{T}$ and result in certain $\overline{\boldsymbol{a}}$ and $\boldsymbol{b}$ values. The relation between the trivial component $\overline{\boldsymbol{a}}$ and $\boldsymbol{b}$ can be expressed in terms of

a reflection matrix $\boldsymbol{R}$ as follows:

$$\bar{\boldsymbol{a}} = \begin{bmatrix} \bar{a}_1 \\ \bar{a}_2 \\ \bar{a}_3 \\ \bar{a}_4 \end{bmatrix} = \begin{bmatrix} 0 & 0 & 0 & 0 \\ 0 & R & T & 0 \\ 0 & T & R & 0 \\ 0 & 0 & 0 & 0 \end{bmatrix} \begin{bmatrix} b_1 \\ b_2 \\ b_3 \\ b_4 \end{bmatrix} = \boldsymbol{R}\boldsymbol{b}. \tag{10.78}$$

Substituting this relation into (10.77) and rearranging the terms, we obtain

$$\begin{bmatrix} b_1 \\ b_2 \\ b_3 \\ b_4 \end{bmatrix} = (\boldsymbol{S}^\dagger - \boldsymbol{R})^{-1}\hat{\boldsymbol{a}} = (\boldsymbol{S}^\dagger - \boldsymbol{R})^{-1} \begin{bmatrix} \hat{a}_1 \\ \hat{a}_2 \\ \hat{a}_3 \\ \hat{a}_4 \end{bmatrix}, \tag{10.79}$$

or equivalently

$$\hat{\boldsymbol{a}} = \begin{bmatrix} \hat{a}_1 \\ \hat{a}_2 \\ \hat{a}_3 \\ \hat{a}_4 \end{bmatrix} = (\boldsymbol{S}^\dagger - \boldsymbol{R})\boldsymbol{b} = (\boldsymbol{S}^\dagger - \boldsymbol{R}) \begin{bmatrix} b_1 \\ b_2 \\ b_3 \\ b_4 \end{bmatrix}, \tag{10.80}$$

which are expressions relating the inward components $\boldsymbol{b}$ to the outward components $\hat{\boldsymbol{a}}$.

Thus, the scenario where the external input $\hat{\boldsymbol{a}} = (a_1, 0, 0, 0)^\intercal$ from Source T1 results in $\boldsymbol{b} = (a_1 R e^{-i2kl}, a_1 e^{-ikl}, 0, a_1 T e^{-i2kl})^\intercal$, as depicted in Figure 19a. This result should be expected from our above discussion in the classical macroscopic case where the input a_1 from Source T1 represents a large number of photons N. Note that the $kl = \omega l/c$ in the exponentials accounts for the phase shift of the corresponding local coordinates of the length between T1 and T2, or equivalently, T3 and T4.

Let us further examine this macroscopic case involving a large number of photons where we express the power flow through the use Poynting's vector $\boldsymbol{S}$ by assuming the electric field to be oriented along the positive local x directions while assuming the magnetic field to be oriented along each y coordinate. This implies that $\boldsymbol{E}_j = a_i\hat{\boldsymbol{x}}_j$ or $\boldsymbol{E}_j = b_i\hat{\boldsymbol{x}}_j$ and $\boldsymbol{H}_j = a_i/Z\hat{\boldsymbol{x}}_j$ or $\boldsymbol{H}_j = b_i/Z\hat{\boldsymbol{y}}_j$ are the electric and magnetic fields the ingoing and outgoing components evaluated at their respective terminals, where $Z = \sqrt{\epsilon_0/mu_0}$. Here, each $\hat{\boldsymbol{x}}_j$ or $\hat{\boldsymbol{x}}_j$ represents the local coordinates of each of the 8 components. The energy flow can thus be expressed as

$$\boldsymbol{S}_j = \boldsymbol{E}_j \times \boldsymbol{H}_j. \tag{10.81}$$

For an incoming plane wave with $\hat{\boldsymbol{a}} = (a_1, 0, 0, 0)^\intercal$ with Poynting vector

$$\boldsymbol{S}_{1,a} = \frac{1}{Z}(a_1\hat{\boldsymbol{x}}_{1,a}) \times (a_1\hat{\boldsymbol{y}}_{1,a}), \tag{10.82}$$

where the wave consists of a large number of photons N in the macroscopic case. Here, the local coordinate unit vectors $\hat{\boldsymbol{x}}_{1,a}$ are double indexed where the first index specifies the terminal and the second differentiates between the ingoing and outgoing components. This wave of N photons is evaluated at terminal 2 at the planar surface

$$\boldsymbol{S}_{2,b} = \frac{1}{Z}(b_2\hat{\boldsymbol{x}}_{2,b}) \times (b_2\hat{\boldsymbol{y}}_{2,b}) = \frac{1}{Z}(a_1 e^{-ikl}\hat{\boldsymbol{x}}_{2,b}) \times (a_1 e^{-ikl}\hat{\boldsymbol{y}}_{2,b}). \tag{10.83}$$

The planar surface transmits and reflects these N photons such that the reflected power

$$\begin{aligned} \boldsymbol{S}_{2,a} &= \lim_{N\to\infty}\left(\frac{N_R}{N}\right)\left[\frac{1}{Z}(b_2\hat{\boldsymbol{x}}_{2,a}) \times (b_2\hat{\boldsymbol{y}}_{2,a})\right] = \mathcal{R}\frac{1}{Z}(b_2\hat{\boldsymbol{x}}_{2,a}) \times (b_2\hat{\boldsymbol{y}}_{2,a}) \\ &= \frac{1}{Z}(Rb_2\hat{\boldsymbol{x}}_{2,a}) \times (Rb_2\hat{\boldsymbol{y}}_{2,a}) = \frac{1}{Z}(Ra_1 e^{-ikl}\hat{\boldsymbol{x}}_{2,a}) \times (Ra_1 e^{-ikl}\hat{\boldsymbol{y}}_{2,a}), \end{aligned} \tag{10.84}$$

since $\mathcal{R} = R^2$ from (10.74). This means that the amplitude of the reflected electric field is $\boldsymbol{E}_{2,a} = Rb_2\hat{\boldsymbol{x}}_{i,a}$ and $\boldsymbol{H}_{2,a} = Rb_2/Z\hat{\boldsymbol{y}}_{i,a}$ for the magnetic field, such that $a_2 = Rb_2$. Likewise, the transmitted amplitude

$$
\begin{aligned}
\boldsymbol{S}_{3,a} &= \lim_{N \to \infty} \left(\frac{N_T}{N} \right) \left[\frac{1}{Z}(b_2\hat{\boldsymbol{x}}_{3,a}) \times (b_2\hat{\boldsymbol{y}}_{3,a}) \right] = \mathcal{T} \frac{1}{Z}(b_2\hat{\boldsymbol{x}}_{3,a}) \times (b_2\hat{\boldsymbol{y}}_{3,a}) \\
&= \frac{1}{Z}(Tb_2\hat{\boldsymbol{x}}_{3,a}) \times (Tb_2\hat{\boldsymbol{y}}_{3,a}) = \frac{1}{Z}(Ta_1e^{-ikl}\hat{\boldsymbol{x}}_{3,a}) \times (Ta_1e^{-ikl}\hat{\boldsymbol{y}}_{3,a}),
\end{aligned}
\tag{10.85}
$$

yielding $a_3 = Tb_2$. This means that out of the N photons, $N_R = \mathcal{R}N$ are reflected whilst the remaining $N_T = \mathcal{T}N$ are transmitted, as the incident power is split between the reflected and transmitted part. This macroscopic case is to be expected from the classical theory of electromagnetism.

Let us now consider a situation where the input from Source T1 is gradually decreased to the point where only one photon $N = 1$ at a time arrives at the absorbing plate, as illustrated in Figure 19b and Figure 19c, where this particular single photon input from Source T1 is denoted as a_1'. If we apply classical electromagnetic theory to these individual events, assuming that the photons are indeed electromagnetic waves, the theory would suggest that the photon energy $E = \hbar\omega$ should be divided into one reflected component and one absorbed component, as indicated in (10.73) and (10.79). However, this would mean that any photon could be split in as many indivisible components as desired, causing an entropy problem. We need to relate the theory at hand to the actual empirical measurements that dictate that the photon is the smallest measurable part (pixel) of the electromagnetic field.

This implies that a photon cannot partially transmit its energy within the medium and reflect the remaining portion, as doing so would require the part of the electromagnetic field corresponding to the photon (pixel) to be divided into smaller independent components than what can be empirically observed and verified. If such a division was possible, the frequency of the reflected part would have to decrease proportionally to the energy reduction. However, this frequency reduction is not possible in linear systems like those described by the classical theory.

Empirical observations show that a photon can either be completely absorbed or entirely reflected, suggesting that classical electromagnetic theory deviates from experimental results at smaller scales. At these scales, the classical theory starts describing entities like 'half photons' which do not align with empirical observations. Essentially, the classical theory predicts phenomena that cannot be observed, such as 'pink elephants'.

Classical electromagnetic theory lacks a non-commutative characteristic, similar to the Wigner formulation, which would prevent descriptions that are more refined than the allowed pixel size determined by actual empirical measurements. Unlike the Wigner formulation, this theory does not exhibit a non-commutative nature, which results in negative probabilities representing the limitations on empirically accessing certain aspects of the system.

As a consequence, the shortcomings of classical electromagnetic theory become more evident when partitioning the electromagnetic field into smaller independent parts. This division, taken to the extreme with infinite partitioning, leads to entropy issues, implying infinite precision of an infinite amount supposedly measurable information. This result highlights the need for a more refined theory that better aligns with empirical observations at smaller scales.

As a result, the classical relations expressed in Equations (10.75) and (10.73) are not applicable to individual photons. This limitation underscores the inadequacy of classical theory in explaining the behavior observed in the smallest empirical measurements, such as those involving single photons. This observation emphasizes the need for more sophisticated models to better describe these situations, as will be evident in the subsequent discussion.

Both Figure 19b and Figure 19c display actual empirical single photon measurements that would

be observed for single photon events represented by

$$
\boldsymbol{b}'_R = \begin{bmatrix} b'_{1R} \\ b'_{2R} \\ 0 \\ 0 \end{bmatrix} = \begin{bmatrix} a'_1 e^{-2ikl} \\ a'_1 e^{-ikl} \\ 0 \\ 0 \end{bmatrix}, \qquad \boldsymbol{b}'_T = \begin{bmatrix} 0 \\ b'_{2T} \\ 0 \\ b'_{4T} \end{bmatrix} = \begin{bmatrix} 0 \\ a'_1 e^{-ikl} \\ 0 \\ a'_1 e^{-2ikl} \end{bmatrix}, \tag{10.86}
$$

which correspond to the empirical inward components of a full reflection and a full transmission event, respectively. Finding the corresponding inputs that results in complete reflection $\hat{\boldsymbol{a}}_R$ and transmission $\hat{\boldsymbol{a}}_T$ requires solving the following two equations

$$
\hat{\boldsymbol{a}}_R = (\boldsymbol{S}^\dagger - \boldsymbol{R})\boldsymbol{b}'_R, \qquad \hat{\boldsymbol{a}}_T = (\boldsymbol{S}^\dagger - \boldsymbol{R})\boldsymbol{b}'_T. \tag{10.87}
$$

Before proceeding, we further divide the general input column vector $\hat{\boldsymbol{a}}$ into two parts: one representing the typical input and the other representing the *photon doublets*. This division is necessary because we lack empirical access to 'half photons', and thus negative energies are required according to the Wigner-Moyal formulation with Hegerfeldt's theorem in mind as the situation in Figure 19b and Figure 19c resemble the two coin example of Section 7.1. As we previously discussed in the context of the photon wave function formalism, probability is proportional to energy density, and negative energy corresponds to negative probability in optical phase space for relativistic systems. As a result, in accordance with the bitemporal electromagnetic theory, the standard single photon input a'_1 is supplemented as needed by extra plane wave solutions originating from the expanded Hilbert space. These supplementary solutions emerge due to the extension of classical electromagnetism into the bitemporal domain. The supplementary inputs take the form of photon doublet fluctuations, consisting of a photon-antiphoton pair. Let these additional inputs, which combine with the regular photon input, be represented by the vectors $\hat{\boldsymbol{\alpha}}_R$ for reflection and $\hat{\boldsymbol{\alpha}}_T$ for transmission. Consequently, the overall input vectors are given by

$$
\hat{\boldsymbol{a}}_R = \begin{bmatrix} a'_1 \\ 0 \\ 0 \\ 0 \end{bmatrix} + \begin{bmatrix} \hat{\alpha}_1 \\ \hat{\alpha}_2 \\ \hat{\alpha}_3 \\ \hat{\alpha}_4 \end{bmatrix}_R = \boldsymbol{a}'_1 + \hat{\boldsymbol{\alpha}}_R, \qquad \hat{\boldsymbol{a}}_T = \begin{bmatrix} a'_1 \\ 0 \\ 0 \\ 0 \end{bmatrix} + \begin{bmatrix} \hat{\alpha}_1 \\ \hat{\alpha}_2 \\ \hat{\alpha}_3 \\ \hat{\alpha}_4 \end{bmatrix}_T = \boldsymbol{a}'_1 + \hat{\boldsymbol{\alpha}}_T, \tag{10.88}
$$

where $\boldsymbol{a}'_1 = (a'_1, 0, 0, 0)^\intercal$. Using this new notation of (10.88), the required photon doublet supplements for routing the photon for the reflection and transmission cases can be found using (10.87) such that

$$
\hat{\boldsymbol{\alpha}}_R = (\boldsymbol{S}^\dagger - \boldsymbol{R})\boldsymbol{b}'_R - \boldsymbol{a}'_1, \qquad \hat{\boldsymbol{\alpha}}_T = (\boldsymbol{S}^\dagger - \boldsymbol{R})\boldsymbol{b}'_T - \boldsymbol{a}'_1. \tag{10.89}
$$

Now, let's assume that the stream consists of N well-separated photons $a'_{1,i}$ per second, with $i = 1, 2, \ldots, N$. Out of these, let N_T be transmitted, and N_R be reflected back. The total expenditure of photon supplements in the overall routing process is the sum of the respective constituents from Equation (10.89). By dividing the sum of reflected and transmitted doublet supplement parts given by Equation (10.89) by the square root of the total number of photons N (since we are dealing with amplitudes), we find

$$
\frac{1}{\sqrt{N}} \left(\sum_T \hat{\boldsymbol{\alpha}}_T + \sum_R \hat{\boldsymbol{\alpha}}_R \right) = (\boldsymbol{S}^\dagger - \boldsymbol{R}) \begin{bmatrix} \frac{1}{\sqrt{N}} \sum_R b'_{1R,i} \\ \frac{1}{\sqrt{N}} \sum_R b'_{2R,i} + \frac{1}{\sqrt{N}} \sum_T b'_{2T,i} \\ 0 \\ \frac{1}{\sqrt{N}} \sum_T b'_{4T,i} \end{bmatrix} - \begin{bmatrix} \frac{1}{\sqrt{N}} \sum_{R,T} a'_{1,i} \\ 0 \\ 0 \\ 0 \end{bmatrix}. \tag{10.90}
$$

If N becomes a very large number, the expressions on the right must be interpreted as macroscopic averages, according to the following

$$
\begin{bmatrix} \widetilde{b}_1 \\ \widetilde{b}_2 \\ \widetilde{b}_3 \\ \widetilde{b}_4 \end{bmatrix} = \begin{bmatrix} \frac{1}{\sqrt{N}} \sum_R b'_{1R,i} \\ \frac{1}{\sqrt{N}} \sum_R b'_{2R,i} + \frac{1}{\sqrt{N}} \sum_T b'_{2T,i} \\ 0 \\ \frac{1}{\sqrt{N}} \sum_T b'_{4T,i} \end{bmatrix}, \qquad \widetilde{a}_1 = \frac{1}{\sqrt{N}} \sum_{R,T} a'_{1,i}, \tag{10.91}
$$

where the tilde signifies macroscopic averages. Here, $\widetilde{a}_1$ represents the time-averaged photon flux of $a'_{1,i}$ leaving the configuration at terminal T1, while $\widetilde{b}_1$ and $\widetilde{b}_4$ correspond to the time-averaged classical reflected and transmitted parts, depicted as b_1 and b_4 in Figure 19a. As a result, the right-hand side of Equation (10.90) must be identified with the classical macroscopic relation found in Equation (10.80), implying that

$$(\boldsymbol{S}^\dagger - \boldsymbol{R}) \begin{bmatrix} \widetilde{b}_1 \\ \widetilde{b}_2 \\ \widetilde{b}_3 \\ \widetilde{b}_4 \end{bmatrix} = \begin{bmatrix} \widetilde{a}_1 \\ 0 \\ 0 \\ 0 \end{bmatrix}, \tag{10.92}$$

which shows that the left hand side of (10.90) vanishes with increasing number of detected photons

$$\lim_{N \to \infty} \frac{1}{\sqrt{N}} \left(\sum_R \hat{\boldsymbol{\alpha}}_{R,i} + \sum_T \hat{\boldsymbol{\alpha}}_{T,i} \right) = \boldsymbol{0}. \tag{10.93}$$

In summary, photon doublets vanish at the macroscopic scale when more components of the electromagnetic field are incorporated into the system. This results in an average description similar to that provided by the Wigner function.

10.5.3 Determining the Explicit Form of the Photon Doublets

To determine the form of the photon doublets in the above examples corresponding to Figure 19b and 19c, we must specify the $\boldsymbol{S}$ matrix for this particular configuration. It can be readily confirmed that the relevant matrices are as follows

$$\boldsymbol{S} = \begin{bmatrix} 0 & e^{-ikl} & 0 & 0 \\ e^{-ikl} & 0 & 0 & 0 \\ 0 & 0 & 0 & e^{-ikl} \\ 0 & 0 & e^{-ikl} & 0 \end{bmatrix}, \qquad \boldsymbol{R} = \begin{bmatrix} 0 & 0 & 0 & 0 \\ 0 & R & T & 0 \\ 0 & T & R & 0 \\ 0 & 0 & 0 & 0 \end{bmatrix}. \tag{10.94}$$

Moving forward in a similar manner, we find that the relevant matrix for the doublet computations and its inverse are

$$(\boldsymbol{S}^\dagger - \boldsymbol{R}) = \begin{bmatrix} 0 & e^{ikl} & 0 & 0 \\ e^{ikl} & -R & -T & 0 \\ 0 & -T & -R & e^{ikl} \\ 0 & 0 & e^{ikl} & 0 \end{bmatrix}, \qquad (\boldsymbol{S}^\dagger - \boldsymbol{R})^{-1} = \begin{bmatrix} Re^{-i2kl} & e^{-ikl} & 0 & Te^{-i2kl} \\ e^{-ikl} & 0 & 0 & 0 \\ 0 & 0 & 0 & e^{-ikl} \\ Te^{-i2kl} & 0 & e^{-ikl} & Re^{-i2kl} \end{bmatrix}. \tag{10.95}$$

It is worth noting that the above matrices are unitary, as the total energy is conserved in this lossless configuration. Utilizing the first matrix of (10.95), the form of the doublets for the cases of reflection and transmission, respectively, can be determined explicitly using (10.89) as follows

$$\hat{\boldsymbol{\alpha}}_R = (\boldsymbol{S}^\dagger - \boldsymbol{R})\boldsymbol{b}'_R - \begin{bmatrix} a'_1 \\ 0 \\ 0 \\ 0 \end{bmatrix} = \begin{bmatrix} 0 \\ a'_1 Te^{-ikl} \\ -a'_1 Te^{-ikl} \\ 0 \end{bmatrix}_R, \qquad \hat{\boldsymbol{\alpha}}_T = (\boldsymbol{S}^\dagger - \boldsymbol{R})\boldsymbol{b}'_T - \begin{bmatrix} a'_1 \\ 0 \\ 0 \\ 0 \end{bmatrix} = \begin{bmatrix} 0 \\ -a'_1 Re^{-ikl} \\ a'_1 Re^{-ikl} \\ 0 \end{bmatrix}_T. \tag{10.96}$$

From our earlier discussion involving Poynting vectors, we can infer that

$$\lim_{N \to \infty} \sum_R \hat{\boldsymbol{\alpha}}_{R,i} = R\sqrt{N}\hat{\boldsymbol{\alpha}}_R, \qquad \lim_{N \to \infty} \sum_T \hat{\boldsymbol{\alpha}}_{T,i} = T\sqrt{N}\hat{\boldsymbol{\alpha}}_R. \tag{10.97}$$

for identical photons with the same phase and frequency since $\sqrt{N_R} = \sqrt{\mathcal{R}N} = R\sqrt{N}$ and likewise $\sqrt{N_T} = \sqrt{\mathcal{T}N} = T\sqrt{N}$ as we are dealing with amplitudes. Figures 20a and 20b illustrate the full reflection and full transmission of single photons using these photon doublets, respectively. Observe that the negative values of the doublets indicate a reversal of the amplitude of the electric field whilst the magnetic field continues to propagate along the same direction meaning that the electromagnetic wave propagates in the opposite direction of the Poynting's vector. These antiphotons are depicted by greyscale block arrows pointing in the opposite direction of their propagation, as they represent photons traveling backward in time. These antiphotons are also paired with a regular photon, where the antiphoton cancels out the reflected or transmitted wave. Generally, when discussing photon doublets, it is assumed that the photon-antiphoton pairs have the same amplitude and shape, but not necessarily the same polarization. As a result, the photon doublet entity does not carry any net energy. The specifics of this concept will be explored in greater detail in subsequent sections and are also discussed in chapter 2 in Wessel-Berg's book.
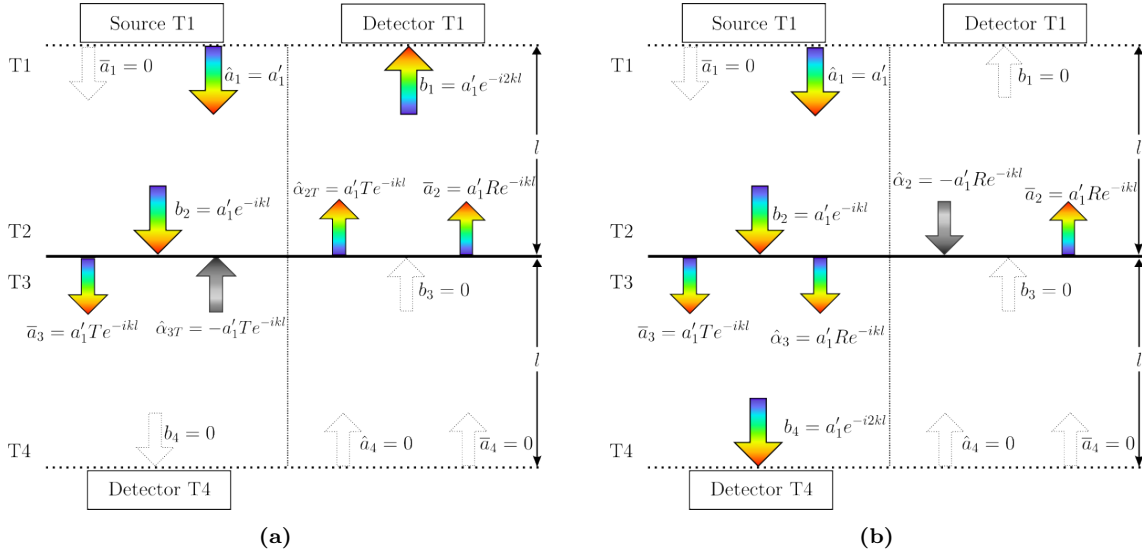
Figure 20: Revised example of reflection and transmission of photons in a one-dimensional thin medium in Wessel-Berg's book [91, p. 22-28] continued. Figures **(a)** and **(b)** correspond to the situations in Figures 19b and 19c, respectively. However, in addition, the form of the photon doublets is shown here. The grey arrows represent antiphotons which point in the opposite direction to their propagation.

Thus, in the words of Wessel-Berg [91, p. 26]:

> *The routing of individual photons to full absorption or to full reflection is orchestrated by the environmental photon doublet energy fluctuations so that the time average of the doublet energy supplement vanishes, a condition that also is the criterion for the time average ratio of transmission and reflection to equal the macroscopic ratio.*

The above statement is a central theme in the book where Wessel-Berg [91, p. 26] states that

> *The routing of the photons is organized by the environmental photon doublet energy fluctuations. A particular incident single photon, faced with two options-being fully absorbed or fully reflected is directed to the terminal minimizing the total time average photon doublet energy.*

In the following sections, we will discover that this innovative and potentially unexpected outcome arises as a fundamental principle of the bitemporal electromagnetic theory. This principle governs the behavior of individual photons in any lossless and reciprocal electromagnetic system, including free space.

10.6 Example After Math

Let us now examine the above example and relate it to relevant topics of this thesis to synthesize the information and gain a deeper understanding of the significance of the proposed theory in light of the previously discussed topics.

10.6.1 The Absence of The Pink Elephant in Bitemporal Electromagnetism

Photon doublets not only allow for localization by circumventing Hegerfeldt's theorem, thereby connecting the mathematical framework to empirical observations, but they also serve an additional crucial function. Photon doublets emerge when probing a system for finer details beyond the indivisible pixel (i.e. what is allowable through experiment), acting as a tool to prevent infinite precision of the field and serving a role of enforcing the pixel of the theory. This is similar to how the Wigner-Moyal formulation utilizes the non-commutative Moyal star product in the definition of the Moyal bracket or how quantum mechanics employs non-commutative operators.

Unlike classical electromagnetism, which allows for infinite precision of any state, these doublets create correlations with other parts of the electromagnetic field akin to the presence of negative values of the Wigner function. Consequently, the described state in question cannot be empirically measured independently of other parts of its environment, i.e., other parts of the electromagnetic field. Photons can therefore be viewed as indivisible components of a larger electromagnetic field functioning as the pixel of the bitemporal theory.

Without the restrictions imposed by photon doublets, nothing would stop us from consecutively partitioning the electromagnetic field into smaller and smaller parts to a point where the predictions of the theory would no longer align with actual physical observations. Consequently, not only would the theory face an entropy problem, but it would also cease to be an accurate description of reality at that scale. In other words, a disconnect between the predictions of the theory and actual empirical measurements would begin to emerge at that level.

10.6.2 Relating To Negative Probabilities and Coin Example

As previously discussed, photon doublets effectively prevent one from probing for specific questions about a physical system for which empirical answers are absent, such as certain features of a system that cannot be empirically measured. This scenario is analogous to the example of coins in Section 7.1, where only three variables were directly observable, and reconstructing the probability distribution presented in Table 1 required additional information that was not directly observable. The presence of photon doublets therefore represents a limitation on our ability to directly access certain information about a physical system through empirical means.

Recall that averaging the Wigner function over time, space, or by incorporating the environment's effects can smooth out the negative values, resulting in a non-negative quasi-probability distribution. However, it is essential to note that this process can also lead to a loss of information about the finer details of the quantum state, particularly its non-classical features.

10.6.3 Comparison to Book

These ideas are indirectly introduced in the first chapter of the book, where Wessel-Berg presents a relationship between bitemporal electromagnetism and classical electromagnetism.

Wessel-Berg highlights that the major result of his theory is the establishment of a new general principle governing the behavior of photons in all electromagnetic circuits and in lossless and reciprocal systems. This principle connects classical electromagnetism $(EM)_{\text{Classical}}$ with microscopic bitemporal electromagnetism $(EM)_{\text{Bitemporal}}$ through the formal relationship:

$$(EM)_{\text{Bitemporal}} = (EM)_{\text{Classical}} + (EM)_{\text{Doublet}}, \qquad (10.98)$$

where the last term $(\text{EM})_{\text{Doublet}}$ represents the photon doublets. In Wessel-Berg's book, a parallel is drawn between these doublets and the zero-point fluctuations of quantum field theory.

Wessel-Berg [91, p. 6] then states that if one were to take the ensemble average or similarly include more parts of the surrounding environment in the equation above, the result simplifies to

$$\langle\text{EM}\rangle_{\text{Bitemporal}} = \langle\text{EM}\rangle_{\text{Classical}}, \quad \Longrightarrow \quad \langle\text{EM}\rangle_{\text{Doublet}} = 0, \tag{10.99}$$

where we observe the disappearance of the photon doublets, analogous to the vanishing of the negative values of the Wigner function when including more parts of its surrounding environment.

The leftmost equation of (10.99) simply states that ordinary classical electromagnetics is the ensemble average of the bitemporal electromagnetics at the macroscopic scale. This is not particularly surprising, as the Wigner function also exhibits useful properties with regards to averages. This is because the average value of an observable, $O(x,p)$, can be calculated using the Wigner function, representing the quantum mechanical expectation value of that observable. The expectation value of $O(x,p)$ can be computed using the following equation

$$\langle O\rangle = \iint W(x,p)O(x,p)\,\mathrm{d}x\,\mathrm{d}p. \tag{10.100}$$

Here, the integral is taken over the entire phase space (all possible values of x and p). This expectation value corresponds to an ensemble average resulting from numerous consecutive measurements of identical states. If the Wigner function is time-dependent, then the average quantity represents the average measurement of the quantity O given the system's state at different times. Wessel-Berg states that the angle brackets signifying the average, $\langle\cdot\rangle$, represent the time average. In this context, he refers to how the Wigner function yields averages that have physical interpretations pertaining to multiple consecutive measurements of identically prepared systems.

The rightmost equation of (10.99) indicates that at the macroscopic scale, photon doublet energy fluctuations vanish. When photon doublets are incorporated and utilized at the microscopic scale, they possess predictive power similar to that of a state vector representing a quantum state that does not saturate the uncertainty relation for a given pair of observables expressed in a specific basis. As we have already mentioned, these antiphotons serve a purpose akin to the negative regions of the Wigner function in phase space. In fact, we have already established that for relativistic systems, the negative values of the Wigner function can correspond to antiparticles. The negative values of the Wigner function signify hidden correlations with the surrounding environment, preventing an overly precise description of a state that is entirely independent of its environment. This is because such a fine description would not be empirically feasible to measure or verify.

In a more general context, decoherence is the process by which a quantum system loses its quantum coherence and transitions to a more classical state, characterized by a decrease in the negative regions of the Wigner function. This transition primarily occurs due to interactions with the environment, which cause the system to become increasingly entangled with its surroundings. As the system interacts with the environment, its state expands to a mixed state by incorporating the surrounding environment, which, in quantum mechanics, can be described by a mixed state density matrix. In the Wigner-Moyal formulation, as more of the external environment is incorporated into the Wigner function, the negative regions average out, resembling a more classical state. Consequently, when decoherence occurs, the quantum state evolves towards a state that can be described by a classical probability distribution, even in the Wigner representation. This process is analogous to the vanishing of photon doublets as the number of examined photons, N, approaches infinity. In summary, on the macroscopic scale i.e. in the classical limit, Wessel Berg's doublets vanish in a similar fashion to the negative values of the Wigner distribution as more of the environment is incorporated into the system.

In summary, as more photons of the electromagnetic field are incorporated in the examination (i.e., larger parts of the electromagnetic field are included), the photon doublet fluctuations containing negative energies diminish. This is similar to how negative regions of the Wigner distribution vanish by involving more parts of the system as one approaches the classical limit (i.e., $\hbar \to 0$), giving the appearance that each individual part can be examined empirically in isolation from its environment.

10.6.4 Interpreting Negative Time

The presence of negative energy solutions does not imply that information can be sent back in time in a practical sense. Instead, the incorporation of these solutions makes sense on the microscopic scale where the absence of unidirectional causality is an inherent feature of these systems.

This is because the concept unidirectional causality never emerged in our discussion regarding microscopic systems in the previous sections. This is due to the nature of phase space trajectories, which possess both a future and a past. It is equally reasonable to attribute the cause of a trajectory's future state to its past state, as it is to attribute the cause of its past state to its future state. In other words, unidirectional causality loses its significance in microscopic systems.

As a result, although the inclusion of negative energies suggests negative time and a breach of unidirectional causality, applying these solutions to microscopic systems remains consistent. This is because such systems inherently exhibit bidirectional causality, which allows for the coexistence of both positive and negative energies.

The preceding discussion helps illuminate Wessel-Berg's perspective on antiphotons moving backward in time within a non-causal framework. To quote Wessel-Berg [91, p. 3]:

> *In the symmetric reference frame the 'cause' of a disturbance is not simply propagating forward in time but backward as well, governed by strict adherence to general boundary conditions in space and bidirectional time.*

Loosely speaking, this implies that a photon 'knows' its destination prior to its emission. This phenomenon results from the microscopic bidirectional causal structure in which emission is a reciprocal communication process between the emitter and the receiver. This will be discussed in greater depth in subsequent sections.

10.7 Comparison to Quantum Electrodynamics

Quantum electrodynamics, through the second quantization of the field, indirectly addresses a minor aspect of the entropy problem in classical electromagnetism. This is achieved by representing actual zero-entropy measurements using creation and annihilation operators corresponding to the respective fields pertaining to these measurements. However, it does not tackle the challenges posed by Hegerfeldt's theorem or the measurement problem inherent to quantum mechanics.

The second quantization is not a prerequisite for developing a theory that accurately describes reality at smaller scales, as will be demonstrated by the bitemporal theory. In this case, the first quantization is sufficient to resolve the entire entropy problem and bypass the adverse implications of Hegerfeldt's theorem.

Despite the fact that Wessel-Berg never mentions the word 'entropy' in his book, yet the following statement can be found in his work [91, p. 5]

> *The central theme in this new approach, which will be referred to as the Neoclassical Electromagnetic Theory, is the quoted hypothesis of bidirectional time at the photon or quantum level, together with additional conservational constraints imposed by the energy integrity of photons and charge conservation of electrons.*

The final portion of this quote implicitly highlights the need to align the theory with empirical observations, which serve as the 'constraints' mentioned. By addressing these constraints, the entropy problem in electromagnetism is indirectly resolved, enabling the theory to describe measurements at smaller scales effectively.

Moreover, by re-expressing conventional electromagnetism in a microscopic form using certain reciprocity relations, bitemporal electromagnetism will be demonstrated in subsequent sections to

address the measurement problem of electromagnetism. This is achieved by describing the photon wave function collapse in a classical manner.

Finally, it is worth noting that Wessel Berg's formulation does not suffer from the same infinity problems that result in renormalization as contemporary quantum field theory does. These issues are often encountered in calculations involving vacuum fluctuations. One type of infinity problem is infrared divergences, which occur when integrals diverge at low energies, which arise from the fact that the vacuum state has a non-zero energy due to zero-point fluctuations. Infrared divergences are typically associated with massless particles, such as photons, which can have arbitrarily long wavelengths. To deal with these infinities and in order to make meaningful predictions, quantum field theory employs a technique called renormalization. Renormalization is a mathematical procedure that removes the infinities by introducing counterterms and renormalizing the coupling constants (parameters) of the theory.

Part IV

Bitemporal Electromagnetism

Although the equations used in Wessel-Berg's simulations work exceptionally well in describing numerous real-world experiments, it is important to note that their derivations in the book heavily rely on a few unsupported theorems and proofs. This could potentially lead other readers to believe that the theoretical foundation of his theory is not well-founded. The author of this thesis has rectified these theorems and proofs, and it is suggested that the unsupported theorems and proofs used in the book are indirectly manifested in Wessel-Berg's unintentional attempts to create a microscopic theory of electromagnetism. His intuition, based on over 50 years of experience working with Maxwell's equations, likely played a significant role in this endeavor.

To present the bitemporal theory of electromagnetism, we need to draw upon our previous discussion in this thesis regarding microscopic systems. We then construct a microscopic theory of electromagnetism before extending it into the bitemporal domain. We initiate this process by arguing that traditional electromagnetism is fundamentally a macroscopic theory and follow up with a discussion of specific ideas that must be established and understood in order to create a deterministic, reversible microscopic theory of electromagnetism that conserves both energy and entropy. This is because negative energy solutions imply negative time and are, therefore, meaningful to employ in microscopic systems due to their lack of unidirectional causality, as these systems are inherently bitemporally causal.

We achieve this by transforming Maxwell's equations into the frequency domain and examining lossless and reciprocal systems while introducing specific reciprocity relations relating *advanced* and *retarded* solutions of Maxwell's equations. Additionally, we present useful theorems, such as the *noradiation* condition, which can be used to determine the entropy leakage within a system.

Finally, we discuss the content presented in Wessel-Berg's book in light of the theory developed in this thesis to evaluate the merits and shortcomings and its potential significance in contemporary physics, before concluding.

By constructing a theory that is both microscopic and free from the entropy problem traditionally associated with classical theories, we are setting the stage for a theoretical framework capable of predicting quantum phenomena.

11 Classical Electromagnetism is a Macroscopic Theory

Throughout this thesis, we have devoted considerable effort to exploring microscopic systems. These unique environments maintain conservation of energy and entropy, where causality is absent in its conventional sense. Instead, they display deterministic and reversible phase space trajectories, providing a bijective mapping of states through time.

Drawing from the definitions of microscopic systems established in Sections 6.6.1 and 6.6.2, we set out to introduce this section with a proposition: current classical electromagnetism does not meet the criteria of a microscopic theory. We shall unpack this assertion, laying the groundwork for introducing several pivotal concepts.

These concepts are essential to the construction of a microscopic theory of electromagnetism. This theory will stretch into the bitemporal domain, and crucially, the inclusion of the antiphoton will allow us to formulate the fundamental building block - the electromagnetic pixel - of our theory. This approach is pivotal in addressing the entropy problem that accompanies our proposed classical microscopic theory.

11.1 Microscopic Charges and Currents

In classical electromagnetism, we treat charged particles and currents as external inputs to Maxwell's equations. This is to say, we impose a charge distribution ρ or current distribution $\boldsymbol{J}$, and then we solve Maxwell's equations to find the resulting electric and magnetic fields. However, these charge and current distributions are treated as independent of the fields, i.e. macroscopic interveners in the microscopic system.

This is a simplification because, in reality, the motion of charged particles and currents in a microscopic system should respond to the electromagnetic fields produced by other particles as electromagnetism is a classical field theory. For example, if we have a region of space with a lot of positive charge, and we calculate the electric field, it will point away from that region. If we then place a positive test charge in that field, it should move away from the charged region due to the electric force. But in the simple treatment of electromagnetism, we don't include this effect; we treat the charge and current distributions as fixed and unchanging, rendering them macroscopic.

In the more complete treatment of electrodynamics, we must consider the feedback between the electromagnetic fields and the charged particles that create those fields. This is done by including the Lorentz force law, which describes how charged particles move in response to electric and magnetic fields. In this way, we get a coupled system of equations: Maxwell's equations tell us the fields given the charges and currents, and the Lorentz force law (combined with Newton's second law) tells us how the charges and currents move in response to the fields. We will elaborate more on this point through examples in the following section.

When we move to quantum electrodynamics (QED), things become even more complicated. Now, the charged particles are treated quantum mechanically, which means their motion is governed by the Schrodinger equation (or Dirac equation for relativistic particles) rather than Newton's laws. And the electromagnetic field itself can also have quantum effects, like the creation and annihilation of virtual particles. The interaction of charged particles and fields in QED is described by the so-called 'interaction Hamiltonian', which includes terms representing the absorption and emission of photons by charged particles.

The simple treatment of electromagnetism as a 'microscopic theory' is a simplification. In reality, electromagnetism is a macroscopic theory, which becomes even more complex when we consider quantum effects. The challenge of dealing with these complexities is one of the major tasks of theoretical physics. Consider the following illustrative example:

Example

Imagine a universe with just two electric charges, let's call them q_1 and q_2. In our initial setup, q_1 is stationary and q_2 is moving. According to the laws of electromagnetism, q_1, being a stationary charge, creates an electric field around it. When q_2, the moving charge, passes nearby, it experiences a force due to the electric field of q_1. This interaction causes q_2 to change its path – the classic principle of a force causing an acceleration.

However, there's another side to this interaction. The moving charge q_2 should also exert a force on q_1. The electric field of the moving charge q_2 should act upon q_1, causing it to accelerate and therefore move.

In our initial assumption, we considered q_1 to be fixed, stationary. It would be natural to ask, what is keeping q_1 in place? If q_2 can be affected by q_1, why can't q_1 be affected by q_2?

This assumption that q_1 remains stationary is, in reality, an imposed macroscopic boundary condition. We can justify this by imagining that q_1 is held in place by some external macroscopic mechanism that we haven't described – perhaps it's fixed to a large mass or held by some other forces that balance out the force exerted by q_2.

In the real world, such conditions often hold true. For instance, the electrons in a wire don't significantly move from their average positions when current flows because they are bound by the

forces from the atomic lattice of the conductor. But it's important to realize that these conditions are not fundamental to nature; they are macroscopic constraints that we impose to make the problem tractable.

A more complete treatment of this two-charge system would consider a microscopic system in which the mutual interactions and movements of both charges were taken into account, without any imposed external conditions. This more complete scenario reflects a microscopic perspective where every charge is dynamically involved, making for a richer and more complex behavior than what's often assumed in basic electromagnetism problems.

11.2 Microscopic Difficulties: The Case of Two-Electron Model

Furthermore, Eliezer's seminal paper *The Hydrogen Atom and the Classical Theory of Radiation* provides a compelling illustration of the challenges faced by classical electromagnetism when dealing with truly microscopic systems [32]. Co-authored with Dirac, the paper constructs a model of two electrons isolated in an otherwise empty universe – an idealized microscopic system without macroscopic factors.

Working with this model, Eliezer and Dirac found unexpected results when deriving the trajectories of the two electrons. The complications found point towards an inherent deficiency in classical electromagnetism: its inability to adequately simulate purely microscopic phenomena without the intrusion of macroscopic elements.

The authors' conclusion that there appears to be no solution allowing for a collision between the two electrons brings to light the inability of classical electromagnetism to fully encompass the dynamics of microscopic systems. This troubling result appears to point to an intrinsic deficiency in classical electromagnetism: namely, its inability to effectively simulate purely microscopic phenomena devoid of macroscopic elements.

Our thesis builds upon these insights by arguing for a new theoretical framework – a microscopic theory of electromagnetism that can handle scenarios such as the isolated two-electron system without introducing conceptual and computational inconsistencies. By explicitly addressing these kinds of small-scale, isolated systems, we hope to enhance the predictive power of electromagnetism beyond the macroscopic realm.

In conclusion, Eliezer and Dirac's two-electron model reinforces our motivation to develop a microscopic theory of electromagnetism that can accurately account for these scenarios. Their work provides a clear and compelling example of why it is necessary to delve beyond the traditional boundaries of classical electromagnetism and explore new, microscopic theories.

11.3 Further Reflections

This result of Dirac and Eliezer illustrates the difficulties inherent in treating electromagnetism as a fully microscopic theory. Classical electromagnetism, as encoded in Maxwell's equations, assumes that the sources of the electromagnetic fields (the charges and currents) are given and do not change due to the fields themselves. However, in a more complete treatment, the motion of charges should be influenced by the fields, leading to a mutual interaction that can have unexpected consequences, as shown in the Dirac-Eliezer model.

In a more complete theory, one would need to include the feedback between the charges and fields, leading to a system of coupled differential equations that describe the evolution of the charges and fields together. However, this is a much more complex problem, and solutions can be difficult to find, especially for systems with many charges. This is one of the challenges in developing a fully microscopic theory of electromagnetism.

The above examples are indeed touching on a key aspect of the difference between macroscopic and microscopic descriptions in electromagnetism, and more broadly, in physics.

When we're dealing with macroscopic descriptions, we usually handle 'idealized' or 'simplified' scenarios. For example, a point charge that is permanently fixed in space or a wire with a steady current running through it. These are not entirely accurate representations of reality, but they are close enough for most practical applications and they allow us to understand the fundamental principles involved.

In the first example above, we're assuming that charge q_1 is held fixed by some unspecified external mechanism, which could be a chemical bond, an electromagnetic trap, a large mass that resists acceleration, etc. We don't specify these details because we're focusing on the interaction between the moving charge and the fixed charge's electric field. This kind of simplification is common in physics, where we often isolate a particular aspect of a system to study it more thoroughly. This inevitably make the current or charge in question a macroscopic quantity.

However, in reality, charge q_1 would indeed be affected by the field of charge q_2. The stationary charge would experience a force due to the electric field of the moving charge, and if there were nothing else holding it in place, it would start to move as well. The entire system is interrelated, with every part affecting every other part since electromagnetism is a classical field theory at heart.

In a more microscopic description, we would take into account the forces experienced by each and every charged particle in the system due to the presence of every other charged particle as in a classical field theory. In the case of an electron in an atom, for example, we can't just consider the electron's interaction with the nucleus; we also need to consider its interactions with the other electrons in the atom.

In reality, nothing is truly 'fixed' in space; everything can move in response to forces. If we say that a charge is 'fixed', what we really mean is that there is some mechanism (e.g., a lattice of other charges) that prevents it from moving. In this sense, the 'fixed' charge is not an isolated system, but rather part of a larger system (e.g., a crystal lattice) that includes forces that balance the electric forces and keep the charge in place.

If we want to accurately describe the system's behavior on the smallest scales, we would need to include these microscopic interactions in our microscopic model. This is part of the challenge of moving from a macroscopic to a microscopic description: the complexity of the system increases dramatically. This is why for most practical applications, we use the macroscopic description which while an approximation, is usually sufficient. However, in order to adequately describe certain quantum phenomenon, it is imperative to establish a microscopic theory of electromagnetism that allows for the inclusion of the antiphoton.

In summary, the standard treatment of electrodynamics assumes that we know the distribution of charges and currents and that these are not affected by the electromagnetic fields they create. This can indeed be thought of as a macroscopic assumption, or what might be called a 'boundary condition' on the problem.

12 Towards a Microscopic Theory of Electromagnetism

In this section we discuss certain topics and ideas that are essential to establish in order to understand construct a microscopic theory of electromagnetism.

12.1 Origin of Electromagnetic Fields

In the context of our microscopic theory, it is posited that electromagnetic fields derive exclusively from charges in motion. The source of any field component can be precisely identified to a particular charge within the system, emphasizing the key role of charges in generating and modulating the system's electromagnetic environment. If any system has a particular field distribution of electric field $\boldsymbol{E}(\boldsymbol{r}, t)$ and a magnetic field $\boldsymbol{B}(\boldsymbol{r}, t)$, then in order for this field to be considered microscopic, these fields should be related back to the respective charges giving rise to these fields in the microscopic system. This implies that

$$\boldsymbol{E}(\boldsymbol{r}, t) = \sum_i \boldsymbol{E}_i(\boldsymbol{r}, t), \qquad \boldsymbol{B}(\boldsymbol{r}, t) = \sum_i \boldsymbol{B}_i(\boldsymbol{r}, t), \tag{12.1}$$

where the electric and magnetic fields in the system are the result of the superposition of the electric and magnetic fields of the different constituents within this microscopic system.

Crucial to our understanding of microscopic electromagnetism is the ability to decompose any electromagnetic field into its constituent parts, tracing each component back to its original source. This meticulous accounting process ensures that all field dynamics are directly linked to specific charge and current activities, reinforcing the deterministic nature of microscopic electromagnetism.

Fields that cannot be associated with a distinct source within our microscopic system are considered macroscopic. Macroscopic fields can be understood as those where the detailed origins are obscured or lost due to complexity or scale, thereby blurring the clear charge-to-field linkage that defines microscopic fields. These fields are thus simply imposed on the system and are not in any way affected by the dynamics of the system.

12.2 Fields from Charges

In order to see what fields are produced from moving charges, we examine the Lienard-Wiechert potentials for both advanced and retarded solutions. Although the advanced solutions can be disregarded in the macroscopic theory of electromagnetism, these solutions will prove to be vital to preserve the time-symmetry and entropy conservation in our microscopic theory. Therefore, we present them here to get an intuition for their nature.

12.2.1 Lienard-Wiechert Advanced and Retarded Potentials

We begin by deriving both the retarded and advanced potentials for point charges in the Lienard-Wiechert Potentials. Expressing the electromagnetic fields in terms of vector potential $\boldsymbol{A}$ and a scalar potential ϕ so that

$$\boldsymbol{E} = -\boldsymbol{\nabla}\phi - \frac{\partial \boldsymbol{A}}{\partial t}, \qquad \boldsymbol{B} = \boldsymbol{\nabla} \times \boldsymbol{A}, \tag{12.2}$$

we can express the Maxwell's equations in vacuum as

$$\left[\nabla^2 - \frac{\partial^2}{\partial t^2}\right] \boldsymbol{A} = -\mu_0 \boldsymbol{J}, \qquad \left[\nabla^2 - \frac{\partial^2}{\partial t^2}\right] \phi = -\frac{1}{\epsilon_0}\rho, \tag{12.3}$$

by using the Lorenz gauge condition

$$\boldsymbol{\nabla} \cdot \boldsymbol{A} + \frac{1}{c^2}\frac{\partial \phi}{\partial t} = 0. \tag{12.4}$$

In this gauge, the vector and scalar potential can be determined at any point in space $\boldsymbol{r}$ from any given current distribution $\boldsymbol{J}(\boldsymbol{r},t)$ and charge distribution $\rho(\boldsymbol{r},t)$ by evaluating the following integrals

$$\boldsymbol{A}(\boldsymbol{r},t) = \frac{\mu_0}{4\pi} \iiint \frac{\boldsymbol{J}(\boldsymbol{r}',t-\frac{|\boldsymbol{r}-\boldsymbol{r}'|}{c})}{|\boldsymbol{r}-\boldsymbol{r}'|} dV', \qquad \frac{\phi(\boldsymbol{r},t)}{c} = \frac{\mu_0}{4\pi} \iiint \frac{c\rho(\boldsymbol{r}',t-\frac{|\boldsymbol{r}-\boldsymbol{r}'|}{c})}{|\boldsymbol{r}-\boldsymbol{r}'|} dV', \qquad (12.5)$$

$$\widetilde{\boldsymbol{A}}(\boldsymbol{r},t) = \frac{\mu_0}{4\pi} \iiint \frac{\boldsymbol{J}(\boldsymbol{r}',t+\frac{|\boldsymbol{r}-\boldsymbol{r}'|}{c})}{|\boldsymbol{r}-\boldsymbol{r}'|} dV', \qquad \frac{\widetilde{\phi}(\boldsymbol{r},t)}{c} = \frac{\mu_0}{4\pi} \iiint \frac{c\rho(\boldsymbol{r}',t+\frac{|\boldsymbol{r}-\boldsymbol{r}'|}{c})}{|\boldsymbol{r}-\boldsymbol{r}'|} dV', \qquad (12.6)$$

where the tilde over the scalar and vector potentials signify the advanced solutions. The Lienard-Wiechert potentials are obtained by imposing a point charge q as the source of the current for the fields by utilizing the Dirac delta function so that

$$\rho(\boldsymbol{r}',t') = q\delta^3(\boldsymbol{r}'-\boldsymbol{r}_s(t')), \qquad \boldsymbol{J}(\boldsymbol{r}',t') = q\boldsymbol{v}_s(t')\delta^3(\boldsymbol{r}'-\boldsymbol{r}_s(t')), \qquad (12.7)$$

where $\boldsymbol{v}_s$ is the velocity of the point charge and $\boldsymbol{r}_s(t')$ is the trajectory of the particle as a function of time. By solving the integrals of (12.5) and (12.6) with sources given by (12.7) and utilizing (12.2) one obtains

$$\boldsymbol{E}(\boldsymbol{r},t) = \frac{q}{4\pi\epsilon_0} \left(\frac{\hat{\boldsymbol{n}}-\boldsymbol{v}_s/c}{|\boldsymbol{r}-\boldsymbol{r}_s|^2\gamma^2(1-\hat{\boldsymbol{n}}\cdot\boldsymbol{v}_s/c)^3} + \frac{\hat{\boldsymbol{n}}\times((\hat{\boldsymbol{n}}-\boldsymbol{v}_s/c)\times\boldsymbol{a}_s)}{|\boldsymbol{r}-\boldsymbol{r}_s|c^2(1-\hat{\boldsymbol{n}}\cdot\boldsymbol{v}_s/c)^3} \right) \Bigg|_{t'=t-\frac{|\boldsymbol{r}-\boldsymbol{r}'|}{c}},$$

$$\boldsymbol{B}(\boldsymbol{r},t) = -\boldsymbol{E}(\boldsymbol{r},t)\times\frac{\hat{\boldsymbol{n}}}{c}, \qquad (12.8)$$

$$\widetilde{\boldsymbol{E}}(\boldsymbol{r},t) = \frac{q}{4\pi\epsilon_0} \left(\frac{\hat{\boldsymbol{n}}+\boldsymbol{v}_s/c}{|\boldsymbol{r}-\boldsymbol{r}_s|^2\gamma^2(1+\hat{\boldsymbol{n}}\cdot\boldsymbol{v}_s/c)^3} + \frac{\hat{\boldsymbol{n}}\times((\hat{\boldsymbol{n}}+\boldsymbol{v}_s/c)\times\boldsymbol{a}_s)}{|\boldsymbol{r}-\boldsymbol{r}_s|c^2(1+\hat{\boldsymbol{n}}\cdot\boldsymbol{v}_s/c)^3} \right) \Bigg|_{t'=t+\frac{|\boldsymbol{r}-\boldsymbol{r}'|}{c}},$$

$$\widetilde{\boldsymbol{B}}(\boldsymbol{r},t) = +\widetilde{\boldsymbol{E}}(\boldsymbol{r},t)\times\frac{\hat{\boldsymbol{n}}}{c}, \qquad (12.9)$$

when we solve for both the advanced and retarded times denoted by $t+\frac{|\boldsymbol{r}-\boldsymbol{r}'|}{c}$ and $t-\frac{|\boldsymbol{r}-\boldsymbol{r}'|}{c}$, respectively. Here, γ is the Lorentz factor and $\boldsymbol{a}_s = \frac{\mathrm{d}\boldsymbol{v}_s}{\mathrm{d}t}$ is the acceleration. Additionally, $\hat{\boldsymbol{n}} = \frac{\boldsymbol{r}-\boldsymbol{r}'}{|\boldsymbol{r}-\boldsymbol{r}'|}$ is a unit vector pointing from the point source to the field point, $\boldsymbol{r}$, of interest. Notice that when transitioning from the retarded to the advanced potential we perform $t \to -t$ so that $\boldsymbol{v}_s \to -\boldsymbol{v}_s$. Additionally, we flip the orientation of the magnetic field as can be seen in the above equations so that the solution still satisfies Maxwell's equations. This means that as a charge accelerates, the retarded field expands from the source and outward into space where each Poynting vector in the field points away from the point source. On the other hand, the advanced solution converges toward the source instead which can easily be verified to be the case in a spacetime diagram, where all Poynting vectors with this advanced solution point toward the source. Notice that the Poynting vectors in both the advanced and retarded solutions point along the direction of propagation of the wave, meaning that these solutions are regular photons and satisfy Maxwell's equations. The advanced solutions are only disregarded because they are argued not to conform to our intuition regarding causality.

A close examination of Equation (12.8) will reveal that the first term of the electric field has a factor of $|\boldsymbol{r}-\boldsymbol{r}_s|^{-2}$ whilst the second term has a factor of $|\boldsymbol{r}-\boldsymbol{r}_s|^{-1}$ meaning that this term decays as the inverse of the distance. Since $\hat{\boldsymbol{n}}$ is a unit vector, the magnetic field will similarly contain two terms, where one decays as the inverse square of the distance whilst the other decays as only the inverse of the distance. The first terms are sometimes referred to as the Coulomb field, while the second terms are referred to as the radiation field. This is because the first term reduces to the known Coulomb field for $\boldsymbol{v}_s = 0$. The radiation field is zero when the velocity is constant, but becomes non zero when the charge undergoes acceleration. The reason why the second term is called the radiation field is due to the nature of the Poynting's vector defined as

$$\boldsymbol{S} = \frac{1}{\mu_0}\boldsymbol{E}(\boldsymbol{r},t)\times\boldsymbol{B}(\boldsymbol{r},t). \qquad (12.10)$$

By inserting for $\boldsymbol{E}(\boldsymbol{r},t)$ and $\boldsymbol{B}(\boldsymbol{r},t)$ from (12.8) we see that some terms in the resulting Poynting vector will decay as $|\boldsymbol{r}-\boldsymbol{r}_s|^{-2}$, whilst other terms will decay as $|\boldsymbol{r}-\boldsymbol{r}_s|^{-3}$ or as $|\boldsymbol{r}-\boldsymbol{r}_s|^{-4}$. By

integrating the Poynting vector field over a closed surface

$$\oiint \boldsymbol{S} \cdot \mathrm{d}\boldsymbol{A}, \tag{12.11}$$

for some surface, where $\mathrm{d}\boldsymbol{A} = \hat{\boldsymbol{n}}_\perp \, \mathrm{d}A$ so that $\hat{\boldsymbol{n}}_\perp$ represents the unit vector perpendicular and pointing out of the surface in question. Suppose we choose the surface to be a sphere centered at the charge. Then in order to measure the flux of energy out of this sphere, the area of the sphere is related to the radius by a factor $|\boldsymbol{r} - \boldsymbol{r}_s|^2$. This implies that as the radius of the sphere increases to infinity, the integral will vanish for all terms in the Poynting vector whose radial dependence decays more rapidly than $|\boldsymbol{r} - \boldsymbol{r}_s|^{-2}$. This means that acceleration of the point charge is necessary for result in radiation into the far field. However, we will later witness that certain accelerating current distributions can in some instances result in no radiation when we discuss the *noradiation condition*.

It is worth noting that since $\hat{\boldsymbol{n}}_\perp$ is pointing out of the closed surface, the integral (12.11) for the advanced solution will result in a negative value, meaning that energy is entering the closed surface, whilst in the retarded case, energy is leaving the volume enclosed by the surface.

In summary, all electromagnetic fields result exclusively from charges and current. If some electromagnetic radiation is detected at some place, this requires acceleration of charges. Although the advanced fields are often neglected, they constitute valid solutions to Maxwell's equations. For moving point charges, they converge, towards the point source. In the next sections we explore how these advanced fields can be used in conjunction with the retarded fields to create a microscopic theory of electromagnetism that is time-symmetric, i.e. it conserves entropy over time.

12.3   Interplay between Advanced and Retarded Fields

In our quest to create a more microscopic theory of electromagnetism we must create a framework where energy and entropy are conserved with the system, and where the system itself exhibits deterministic and reversible temporal evolution, implying a bijective mapping between future and past states. This implies that we need to construct a framework that is time symmetric, where the temporal evolution can be flipped at a final state to arrive back at the initial state. From a example involving a game of pool, at any particular final state, the balls can reverse their momentum and then arrive back at the initial state as time progresses.

In order to create a time symmetric theory, it is argued that we need to include both the advanced and retarded solutions to Maxwell's equations. The advanced solutions, although they are valid solutions of Maxwell's equations, are often neglected because they appear to violate our notion of unidirectional causality. However, in our microscopic formulation, where unidirectional causality is meaningless, these solutions will allow us to create a time symmetric theory and microscopic theory of electromagnetism.

12.3.1   Advanced Solutions and Microscopic Systems

The concept of advanced and retarded potentials in electromagnetism comes from the fact that electromagnetic interactions are not instantaneous, but instead propagate at the speed of light. The retarded potentials represent the 'causal' solution, in which the effect (the electromagnetic field at a certain point) follows the cause (the motion of the charge). Advanced potentials, on the other hand, represent a solution in which the effect seems to precede the cause, which is usually discarded as unphysical based on our everyday macroscopic experience of causality.

However, when we delve into quantum mechanics and quantum field theory, the notions of time and causality can become much less straightforward. For example, in the Feynman path integral formulation of quantum mechanics, a particle doesn't follow a single trajectory from point A to point B, but instead, all possible trajectories, including those that seemingly violate causality, contribute to the particle's path. This is encapsulated in Feynman's 'sum over histories' approach.

So, in a sense, advanced solutions do appear in the microscopic realm, but they're typically reinterpreted in a way that's consistent with causality. However, this doesn't necessarily mean that the concept of causality is violated or non-existent at the quantum level. Instead, it's more accurate to say that the quantum world allows for more complex and counterintuitive types of causal relationships compared to the macroscopic world.

Another example is the context of quantum field theory and its application to electromagnetic fields, where the advanced and retarded Green's functions play a role in describing propagators. The propagators in quantum field theory can be understood as the probability amplitudes for particles to propagate between two spacetime points. Both the advanced and retarded Green's functions contribute to these propagators, reflecting the fact that, in quantum mechanics, the distinction between past and future is less clear.

Our earlier discussions on phase space and defined futures and pasts is an interesting concept in this context. In deterministic systems, knowing the full phase space state at a given time allows one to predict the future and retrodict the past in the microscopic system in question.

In summary, we have raised an interesting point about microscopic systems, particularly in the context of phase space and time reversibility. In such systems, the distinction between the past and the future can become less clear, and time-reversal symmetry can play a significant role. In these cases, advanced and retarded solutions can be considered more on equal footing.

12.4   Wheeler-Feynman Absorber Theory

The Wheeler-Feynman Absorber Theory, also referred to as the Wheeler-Feynman Time-Symmetric Theory, is a conceptual framework conceived by physicists Richard Feynman and John Archibald Wheeler [34, 93]. This theory aims to interpret the fundamentals of electrodynamics with an emphasis on time-symmetry. In simpler terms, this theory suggests that the behaviors we observe in electromagnetism should look the same whether time is moving forward or in reverse. As this theory has many similarities to the theory of Wessel-Berg's formulation, we present briefly this theory and explore how the inherent time-symmetry is an essential component in any microscopic theory.

This assumption of time symmetry in the theory emerges from the observation that the mathematical equations governing electromagnetic fields, known as Maxwell's equations, remain unaltered when subjected to a time-reversal transformation when the magnetic fields are flipped. This reflects the principle that there seems to be no inherent reason for a distinction between past and future in these laws – there is no preferred direction of time apparent in the fundamental laws of physics. A theory preserving this time-reversal symmetry is perceived to be more consistent and elegant in microscopic formulations.

An intriguing implication that arises from this time-symmetric interpretation relates to the interaction of elementary particles. Following the philosophy of the Wheeler-Feynman Absorber Theory, these fundamental particles are not considered self-interacting. This notion harkens back to *Mach's Principle* and the ideas of physicist Hugo Tetrode, asserting that all forces on a particle result from interactions with other particles, not with itself. This has significant consequences, particularly in resolving the troubling concept of self-energies, which are infinite energies a particle would possess if it could interact with itself. This theory, thus, effectively circumvents the paradox of self-energies, contributing to a more coherent and logical understanding of the physical world [93].

Reconciling the principle of causality with time-reversal symmetry can be challenging. The governing equations for electromagnetic waves, known as Maxwell's equations, have two solutions. The first one is the *retarded* which is most often used and the solution *advanced* solution which is typically discarded due to causality reasons.

In order to get an intuition for the difference between advanced and retarded solutions, suppose we have a moving charged particle that generates an electromagnetic field at time $t_0 = 0$ and at point $\boldsymbol{r}_0 = \boldsymbol{0}$ which represents the origin of our coordinate system. As the electromagnetic field radiates,

it reaches a point $\boldsymbol{r}_1$ at a time $t_1 = |\boldsymbol{r}_1|/c$ after emission. This radiation field is called retarded because there is a lag, meaning that it takes time for the field to reach $\boldsymbol{r}_1$ as this process does not occur instantaneously. However, the electromagnetic field will also arrive at the same point at time $t_2 = -|\boldsymbol{r}_1|/c$, which is prior to the emission process of the charged particles. This radiation is called advanced as it is advanced in time. The advanced solution therefore contradicts the notion of causality, as it implies that the advanced waves know the specific behaviour of the charged particle in advance. This 'supposedly' opens up the possibility to detect the electromagnetic fields before their emission, causing these solutions to be discarded in the contemporary macroscopic theory of electromagnetism.

The Wheeler-Feynman absorber theory presents an intriguing perspective on charges, considering them as simultaneous absorbers and emitters of electromagnetic radiation. Within this theory, two types of fields are crucial: the time-retarded fields, which travel from the emitter to the absorber, and the time-advanced fields, which travel from the absorber to the emitter. By combining these two types of fields, seemingly causal waves emerge, even though the inclusion of time-advanced fields is a part of the theory's formulation.

Mathematically, Feynman and Wheeler proposed that all charged particles in the universe emit time-reversal symmetric fields, and thus creating the total field defined as

$$\boldsymbol{E}_{\text{tot}}(\boldsymbol{r}, t) = \sum_i \frac{\boldsymbol{E}_i(\boldsymbol{r}, t) + \widetilde{\boldsymbol{E}}_i(\boldsymbol{r}, t)}{2}. \tag{12.12}$$

Assuming the relation for the free field

$$\boldsymbol{E}_{\text{free}}(\boldsymbol{r}, t) = \sum_i \frac{\boldsymbol{E}_i(\boldsymbol{r}, t) - \widetilde{\boldsymbol{E}}_i(\boldsymbol{r}, t)}{2} = 0, \tag{12.13}$$

they could rewrite the total field as

$$E_{\text{tot}}(\boldsymbol{r}, t) = \sum_i \frac{\boldsymbol{E}_i(\boldsymbol{r}, t) + \widetilde{\boldsymbol{E}}_i(\boldsymbol{r}, t)}{2} + \sum_i \frac{\boldsymbol{E}_i(\boldsymbol{r}, t) - \widetilde{\boldsymbol{E}}_i(\boldsymbol{r}, t)}{2} = \sum_i \boldsymbol{E}_i(\boldsymbol{r}, t), \tag{12.14}$$

which is retarded, hence respecting causality. The zero 'free field' assumption is the essence of the absorber idea, suggesting all emitted radiation is fully absorbed by other particles in the universe. We will later come to see that the free field assumption has its own problems with energy conservation in larger systems and is effectively replaced with a reciprocity/energy theorem in Wessel-Bergs book which we will discuss in the subsequent sections. Additionally, it should be noted that the form of the free field formula (12.13) is not symmetric due to the minus sign in the formula so that when time is reversed, the advanced and retarded solutions changes places. Wessel-Bergs improved formulation with his reciprocity relation creates a more elegant solution to this.

Nevertheless, in the original theory of Feynman and Wheeler, this absorption mechanism is analogous to how common materials absorb incoming electromagnetic waves, which results in a zero outgoing field. The absorber theory just extends this concept to include both retarded and advanced waves.

Figure 21 presents a visual representation of the absorber theory as proposed by Wheeler and Feynman. It depicts the interaction between an emitter and an absorber in a space-time framework.

At the center of the diagram, there are two points representing the emitter and the absorber. A retarded wave is shown radiating out from the emitter, propagating towards the absorber, indicating the flow of time from past to future. Simultaneously, an advanced wave is illustrated as emanating from the absorber and moving towards the emitter, suggesting an influence that seemingly propagates backwards in time.
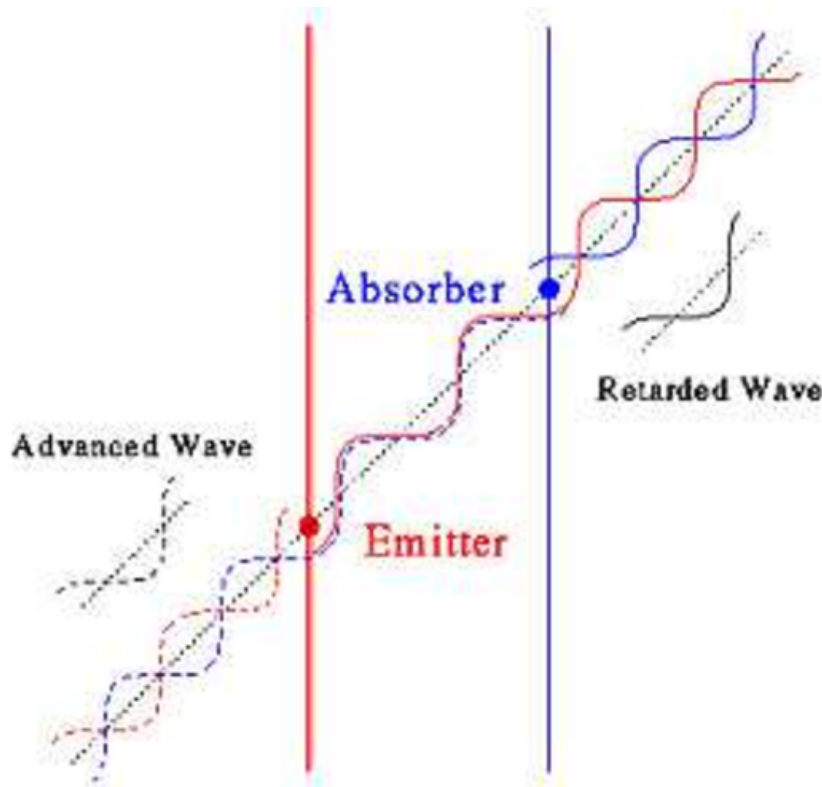
Figure 21: Illustration of Wheeler-Feynman absorber theory. The diagram depicts an emitter producing a retarded wave towards the absorber (from past to future), and an absorber emitting an advanced wave to the emitter (from future to past). The waves constructively interfere between the two, while destructively interfering elsewhere, demonstrating the core concept of absorber theory..

Source: [23]

The waves are shown to meet and constructively interfere between the emitter and the absorber, while they destructively interfere elsewhere, leading to a net zero radiation field. This demonstrates the crux of the Wheeler-Feynman absorber theory, which posits that the observable effects of electromagnetism are due to a balance of retarded and advanced waves between interacting charged particles.

In the Wheeler-Feynman absorber theory, the observed preferred time direction of the resulting field, which respects causality, is not a fundamental property of the system. Instead, it is a consequence of how we label the roles of "emitter" and "absorber." By simply switching these labels, we can effectively reverse the time direction. This indicates that the seemingly preferred time direction is an arbitrary artifact of our labeling convention, rather than an intrinsic characteristic of the system itself. It highlights the significance of context and perspective when interpreting the implications of the theory.

In summary, the Wheeler-Feynman Absorber Theory provides a time-symmetric perspective on electrodynamics, offering a logical framework that negates the possibility of self-interaction of particles, thereby resolving the self-energy problem.

12.5 Acceleration of Charges

When examining the Lienard-Wiechert potentials, we witnessed that acceleration of point charges resulted in radiation into the far field. However, one aspect which is often overlooked is the question pertaining to the cause of the acceleration of the charge to begin with. Charges do not spontaneously accelerate. They must be acted upon by a force from some field which is produced

by other charges. This implies that is our charge is performed work on by accelerating it, the energy increase of the charge of this process must be compensated for by a corresponding decrease of energy of the charges responsible the acceleration. If the system is assumed to be microscopic, then the field causing the acceleration must be able to be traced back to their respective charges. If the fields are rather given as an external imposed field, then the field must be considered macroscopic.

In our microscopic theory we propose the following: The emission of electromagnetic radiation into the far-field demands charge acceleration. However, charges cannot accelerate spontaneously; they require the influence of an advanced electromagnetic field. This advanced field—associated with a single charge—is a superposition of the retarded fields from other charges within the system, collectively driving the charge acceleration. This complex interaction between advanced and retarded fields is key to a comprehensive understanding of microcosmic electromagnetism. We will discuss the Lorentz force and its role in this microscopic formulation in later sections.

In essence, we are considering the advanced field as a sort of 'pre-emptive' field that acts on the charge, causing it to accelerate and emit the retarded wave. If we allow advanced waves (which, as we stated, could be thought of as waves propagating from the future to the past in the spacetime diagram), then indeed, one can imagine a scenario where an advanced wave from the future interacts with a charge, causing it to accelerate and emit a retarded wave.

This is a reversal of the usual cause-and-effect sequence that we're accustomed to in everyday life (and most physics), but it's not infeasible if we allow advanced waves. This is similar to the concepts explored in the Wheeler-Feynman absorber theory, as we mentioned earlier.

However, it's important to remember that this interpretation challenges our usual understanding of causality - the idea that causes must precede effects. In most of physics, and especially in the macroscopic world, we expect causes to precede effects, which is why we usually discard advanced solutions in classical electromagnetism.

In quantum mechanics, where cause and effect can become less distinct, this kind of time-reversed interpretation becomes more plausible. However, the full implications of such an interpretation in the context of quantum mechanics are still a topic of ongoing research.

In summary, while advanced potentials are usually discarded in classical electromagnetism to preserve causality, they can play a role in microscopic systems or quantum theories, where the concepts of causality and time reversibility are more nuanced. The advanced solutions can indeed represent radiation when looking at the system backwards in time, and their contributions can become relevant in specific contexts, such as absorber theory or quantum field theory.

12.5.1   Returning to Absorber Theory

The absorber theory argues as follows: An accelerating charge emits radiation, but the mechanism that causes the acceleration is typically another field or force. If we consider the interaction between two charges, each charge generates a field that influences the other. The interaction from the 'source' charge to the 'test' charge could be viewed as the retarded field, which travels forward in time from the source to the test charge.

Now, in response to this, the test charge also emits its own field, part of which travels back to the source charge. This is known as the advanced field. In the time-symmetric theory, the advanced field from the test charge is thought to be absorbed by the source charge, which then influences its motion.

In essence, the theory suggests that the total field experienced by a charge is a combination of the retarded fields from all other charges and the advanced fields that the charge itself produces in response to its acceleration, which are then absorbed by all the other charges in the universe.

While this picture, where advanced waves are interpreted as responses from the future, might seem unorthodox, it can provide a different perspective on electromagnetic interactions.

12.6   Breaking of Time Symmetry in Retarded-only Formulations

Time symmetry, a fundamental characteristic of microscopic systems, can be profoundly influenced by the type of electromagnetic solutions we adopt. In classical electromagnetism, we often resort to using only the retarded solutions to Maxwell's equations. While this simplifying assumption aligns well with our everyday experience of cause and effect, it can lead to a breaking of time symmetry when we consider the operation of antenna systems. Specifically, the one-sided focus on retarded radiation can impose an artificial asymmetry on a system that is naturally symmetric in time.

Consider a system involving two antennas, a transmitter and a receiver. In traditional electromagnetism, the transmitter emits a retarded wave that propagates through space and induces a current in the receiver. This implies that this retarded radiation happens at the upper light cone in a space time diagram only. This fits our typical understanding of cause (transmission) and effect (reception), occurring sequentially in time.

However, if we consider the time-reversed scenario, where we follow the wave from the receiver back to the transmitter, the wave that was initially retarded becomes advanced as it is emitted along the lower light cone in a space time diagram. In this reversed scenario, the wave appears to move backward in time, starting from the receiver and converging back on the transmitter. This highlights the time-symmetric nature of the radiation process, where the same physical phenomenon can be interpreted as retarded or advanced, depending on our temporal viewpoint.

By only considering the retarded solutions in our theory, we artificially break this time symmetry. We confine our perspective to a one-way temporal flow from transmitter to receiver, thus missing the symmetrical flow from receiver to transmitter in the reversed time frame. This omission is significant, as it neglects a fundamental aspect of the system's behavior.

In a truly time-symmetric description of the system, both the retarded wave from the transmitter and the advanced wave from the receiver should be included. When we include both of these components, the system's time symmetry is preserved, ensuring that the dynamics remain consistent whether we are moving forward or backward in time.

By prioritizing a causality-driven interpretation of electromagnetism, conventional theory may inadvertently ignore crucial aspects of time-symmetric behavior. Therefore, to maintain the microscopic time symmetry and thus entropy conservation (bijective state mapping) in our electromagnetic theory, it is essential to embrace both advanced and retarded solutions, thereby incorporating the full, bidirectional temporal dynamics of the system.

Including both advanced and retarded waves provides a more comprehensive and symmetric interpretation of electromagnetic interactions. This approach aligns with the time symmetry observed in microscopic systems, thereby creating a more consistent framework for understanding the fundamental behaviors of such systems. It marks an important step in developing a theory of electromagnetism that faithfully captures the rich complexity of the microscopic world.

The two antenna example is quite general and is directly analogous to a situation when a charged particle following a trajectory radiates a retarded field. This field is measured at a point away from the moving charge with an instrument. The moving charge could be seen as the first antenna, whilst the measuring instrument measuring the retreaded field could be seen as the receiving antenna. This is due to the fact that measuring the retarded field of a radiating current distribution implies having an instrument containing charges that interact with this field that result in a measurement. Thus, any measurement requires interaction with the field by charges within the measuring instrument. This interaction must be reciprocal in time if we assume the time-symmetry argument to hold.

Since the retarded field is measured by an instrument, the instrument in question is inherently measuring the field by letting the field interact with a charges within the instrument. The instrument can thus be considered to be a receiving antenna. In the time reversed case, the not only does the retarded field of the moving charge become the advanced field in this time reversed situation, but the measurement instrument must now emit retarded radiation (rather than than receiving it when measuring the field). Therefore, the result of this emission of the measuring instrument

would now interact in order to contribute to the overall trajectory of the charged particle in this time reversed situation. This is an essential concept to grasp when transitioning to a microscopic formulation of electromagnetism. We need to keep in mind that time symmetry and conservation of informational entropy are closely linked. If a temporal progression of a state can not be deterministically traced back to an earlier state implies a violation of time symmetry and that information has been lost. This means that entropy has not been conserved in this instance.

In summary, classical mechanics is deterministic and time-reversible, meaning if you perfectly know the initial state of a system (the positions and velocities of all particles), you can predict its future evolution as well as its past. The equations of motion are symmetric with respect to time. However, conventional electromagnetism is not as a single point particle undergoing acceleration and thus radiating a retarded field into the future light cone of a spacetime diagram does not have an analogue when the direction of time is reversed if one neglects the advanced solutions.

12.7 The Necessity of Advanced and Retarded Solutions in Microscopic Systems

The quest to comprehend microscopic systems through the lens of electromagnetism requires a departure from traditional, macroscopic electromagnetic theories. In these systems, the conventional tenets of classical electromagnetism, such as an explicit directional causality, must be reevaluated in light of the unique characteristics of the microscopic domain. As a result, a formulation of electromagnetic theory that incorporates both advanced and retarded solutions becomes an essential component of this exploration.

The significance of including both advanced and retarded solutions in the formulation lies in preserving the inherent time symmetry of microscopic systems. In such systems, determinism extends in both temporal directions. This means that a present state in a system's trajectory can be attributed equally to its past as well as its future states. This time symmetry is fundamentally distinct from our everyday experience of cause and effect, where the future is determined by the past but not vice versa. Yet, it is precisely this symmetry that is a key feature of microscopic systems and, therefore, must be embodied in a corresponding electromagnetic theory.

Furthermore, in microscopic systems, the conservation of energy and entropy, akin to their macroscopic counterparts, is imperative. The introduction of advanced solutions—representing waves that travel from future to past—facilitates the preservation of these conserved quantities. By treating the receiver and transmitter symmetrically, we ensure that energy and entropy are conserved across the entire system, embracing both its past and future states. Thus, the advanced solutions are not just mere mathematical artifacts, but rather they play a crucial role in constructing a coherent theoretical framework for electromagnetism at a microscopic level.

Causality, a bedrock principle in classical physics, often loses its conventional meaning in the microscopic domain. Unlike the macroscopic realm, where effects unidirectionally follow causes, microscopic systems exist as entities that aren't straightforwardly caused by anything. These systems' states relate just as much to their future as they do to their past, thereby questioning the applicability of classical causality. Hence, it is crucial to develop a microscopic electromagnetic theory that doesn't solely rely on causality as its guiding principle.

This proposal for an expanded electromagnetic theory finds echoes in existing scientific theories. The Wheeler-Feynman absorber theory, which considers both advanced and retarded waves, has been instrumental in understanding certain quantum phenomena which appear to violate causality. Furthermore, phenomena like quantum entanglement, where traditional causal relations are blurred, underline the need for this new perspective.

This perspective aligns with the time symmetry observed in quantum mechanics, where a state in the system trajectory can be attributed equally to its past as well as its future state before wave function collapse. Causality, in the classical sense, thus becomes an obsolete concept in our proposed microscopic framework. Systems simply exist, underlined by a deterministic bijective mapping to future and past points in their trajectory.

In conclusion, developing a microscopic electromagnetic theory that includes both advanced and retarded solutions is not just a theoretical exercise. It is a necessary endeavour to adequately capture the unique characteristics of microscopic systems. This endeavour pushes the boundaries of our understanding of the microscopic world and paves the way for a more comprehensive framework that can bridge the divide between classical and quantum electrodynamics.

12.8 Absorber Theory: A Step Towards a Microscopic Theory?

The Hamiltonian framework of classical mechanics is indeed a mathematical structure that is inherently time-symmetric. It describes the entire evolution of a system in a phase-space, where each point represents a possible state of the system, and trajectories in this space describe the evolution of the system over time. As we pointed out, in this picture, there's no inherent 'arrow of time' – we could just as well evolve the system backward in time.

The Wheeler-Feynman absorber theory brings this kind of time-symmetry to the realm of electromagnetism by considering both advanced (future-to-past) and retarded (past-to-future) electromagnetic waves. In this sense, it can indeed be seen as a more 'microscopic' or fundamental theory of electromagnetism, one that potentially digs deeper into the nature of electromagnetic interactions than the standard, macroscopic theory.

However, there are a few caveats and nuances to consider. First, even though the Wheeler-Feynman theory is time-symmetric, it is not devoid of causality, but is rather bitemporally causal. It's just that causality is understood in a different way: events can influence both the future and the past. This is quite a departure from our everyday experience and the usual way we understand physics, and it introduces its own complexities and paradoxes (e.g., how do we avoid causal loops?).

Second, it's important to note that the absorber theory, like the Hamiltonian formalism, is not a fully quantum mechanical theory. While it might offer a more 'microscopic' or fundamental perspective on electromagnetism, it does not predict measurements at smaller scales and therefore does not fully incorporate the features of quantum mechanics.

The Wheeler-Feynman absorber theory, on the other hand, is a deterministic theory and its time symmetry is expressed in the fact that both the future and the past can causally influence the present. In this theory, an accelerated charge emits both advanced and retarded waves, and the absorber response from the entire universe is what leads to the usual radiation reaction force. This theory also gives a unique answer for each event, just like classical physics, which is different from the probabilistic nature of quantum mechanics. This fact is reminiscent of the lack of the fundamental pixel in the absorber theory. Therefore, it would be more correct to say that the absorber theory is close to a classical microscopic theory of electromagnetism. This theory is deemed 'close' because it has certain nuances that need to be addressed to fulfill all of our criteria for a microscopic system. However, forming a time-symmetric formulation is the first and most important step in the formulation of any microscopic theory as this allows for the conservation of entropy.

While the Wheeler-Feynman absorber theory is sometimes considered a kind of 'microscopic' theory in the sense that it involves local interactions with the entire universe, it is not generally seen as a fundamental theory like quantum mechanics as it has problems at smaller scales due an inherent entropy problem that results from a lack of a pixel in the theory. Rather, it is often viewed as an interesting and somewhat unconventional interpretation of classical electromagnetism that can help to resolve some of the self-interaction problems. It should be mentioned that while it is indeed intriguing and has some notable advocates, it's not widely accepted as the standard interpretation of electromagnetism.

By forming a microscopic theory of electromagnetism, we can expand this theory to the bitemporal domain by introducing negative energies as a means to solve the entropy problem. Extending the Hilbert space to include negative energy solution allows us to form the pixel of the theory, i.e. the photon.

12.9 The Lorentz Force

The field of classical electromagnetism primarily revolves around two key components: Maxwell's equations and the Lorentz force law. While Maxwell's equations elegantly portray the origin and behavior of electric and magnetic fields arising from charges and currents, they do not elucidate how these fields reciprocally influence the charges and currents that gave rise to them. This crucial interplay between fields and their sources is captured by the Lorentz force

$$\boldsymbol{F} = q(\boldsymbol{E} + \boldsymbol{v} \times \boldsymbol{B}), \tag{12.15}$$

where $\boldsymbol{v}$ denotes the velocity of a charge carrier with charge q. For a continuous charge distribution, we substitute $\boldsymbol{J} = \rho \boldsymbol{v}$ (where $\boldsymbol{J}$ is the current density and ρ is the charge density) to transition from a discrete particle description to a continuous one, yielding the force density $\boldsymbol{f}$ (force per unit volume):

$$\boldsymbol{f} = \rho \boldsymbol{E} + \boldsymbol{J} \times \boldsymbol{B}. \tag{12.16}$$

Thus, to fully understand the dynamics of electromagnetic interactions, both these elements often must be considered in unison. However, in the context of our microscopic theory, we argue that the Lorentz force law is more suitably seen as a macroscopic approximation rather than a fundamental force law. This perspective will be illustrated through a dedicated example, following which we will propose a method for computing the microscopic force.

12.9.1 Limitations of the Lorentz Force Law

To illustrate the limitations of the Lorentz force law in our microscopic theory, let's consider the case of a charged particle moving into a homogeneous magnetic field as shown in Figure 22. According to the Lorentz force law, the force exerted on the particle would be perpendicular to its velocity, as encapsulated in the second term of the equation. Consequently, the particle trajectory would conform to a helical or spiral shape following the magnetic field lines, a phenomenon driven by centripetal acceleration.

Nevertheless, this picture is incomplete. As we have examined earlier in the thesis, the Lienard-Wiechert potentials assert that accelerating point charges must radiate and hence shed energy – a phenomenon known as cyclotron or synchrotron radiation. In the case of our spiraling particle, this energy must inevitably be siphoned off from the kinetic energy that sustains its helical motion.

The contradiction here is clear: if the Lorentz force is perpetually perpendicular to the particle's velocity, there should be no component of force working against the particle's kinetic energy. Yet, the process of radiation unequivocally indicates the depletion of this energy, suggesting a counteracting force parallel to the velocity.

This discrepancy signals that the Lorentz force law cannot fully encapsulate the dynamics at play within a homogeneous magnetic field. It lacks the mechanism to account for the radiation – losses in the energy of the charged particle. Therefore, the Lorentz force law, while useful in many macroscopic scenarios, may not provide a complete description for the interactions of particles with electromagnetic fields at a microscopic level. It is necessary to incorporate a more comprehensive force law that accounts for the effects of radiation and energy loss.

Addressing the intricacies of charged particle dynamics of the above example necessitates the introduction of the Abraham-Lorentz force [75]:

$$\boldsymbol{F} = \frac{2}{3} \frac{q^2}{4\pi\epsilon_0 c^3} \dot{\boldsymbol{a}}, \tag{12.17}$$

Here, $\dot{\boldsymbol{a}}$ denotes the time derivative of acceleration, or 'jerk'. While a relativistic counterpart to this force exists, it will not be discussed in the current context [75]. The centripetal nature of the acceleration means its direction aligns with the particle's motion, thereby inducing a force antiparallel to the particle's trajectory. This force, often labeled the 'self-force' or 'recoil-force', is thought to arise from the particle's interaction with its self-radiated field during radiation.
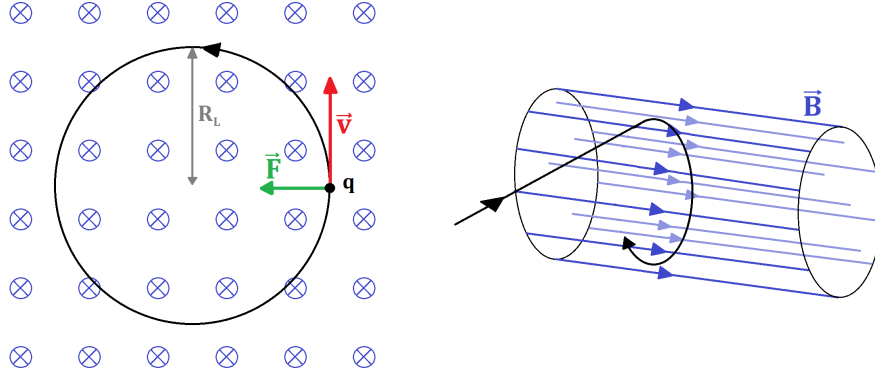
Figure 22: *Right Panel:* Illustration of a positively charged particle entering a locally homogeneous magnetic field, denoted by **B**. The trajectory of the particle is deflected due to the influence of the second term in the Lorentz force Equation (12.16). *Left Panel:* Depiction of the same positively charged particle undergoing circular motion when subjected to a static and homogeneous magnetic field **B**. Both scenarios demonstrate the impact of the Lorentz force on charged particles in magnetic fields.

It's noteworthy that this force isn't included in the original formulation of the Lorentz force. However, for accurate depiction of certain phenomena – such as the previously discussed example – it's frequently appended:

$$\boldsymbol{F} = q(\boldsymbol{E} + \boldsymbol{v} \times \boldsymbol{B}) + \frac{2}{3}\frac{q^2}{4\pi\epsilon_0 c^3}\dot{\boldsymbol{a}}. \tag{12.18}$$

Despite the addition of the Abraham-Lorentz force, this augmented force law remains incomplete. Consider a charged particle undergoing acceleration in a homogeneous electric field. The Lorentz force law suggests a constant acceleration parallel to the electric field, yielding $\dot{\boldsymbol{a}} = 0$. However, the Lienard-Wiechert potentials inform us that an accelerating particle should radiate, hence losing a portion of its kinetic energy. As the 'jerk' is zero in this scenario, the Abraham-Lorentz force can't account for this energy loss.

Moreover, the Lorentz force law omits a plethora of forces, such as the Casimir force and various other emergent forces from the realm of electromagnetism.

12.9.2   Lorentz Force and the Lagrangian Formulation of Electromagnetism

The complications demonstrated in the above examples arise from the distinct division of electromagnetism into two separate elements: Maxwell's equations and the Lorentz force law. A more comprehensive understanding emerges when we adopt the Lagrangian formulation of electromagnetism. This framework seamlessly blends the dynamics of charged particles and electromagnetic fields, making the Lorentz force law superfluous. The upcoming discussions will delve into this unified treatment of electromagnetism, revealing how trajectories and motion arise naturally from the Lagrangian description. We first derive the Lorentz force from macroscopic system where the fields are simply given and their origin is not considered.

The Lagrangian density for the electromagnetic field can be represented using the covariant indexed Faraday tensor $F_{\mu\nu}$ and the contra-variant four-current J^μ by utilizing the Einstein summation convention as follows

$$\mathcal{L}(A_\mu, \partial_n u A_\mu) = -\frac{1}{4\mu_0}F_{\mu\nu}F^{\mu\nu} - A_\mu J^\mu, \tag{12.19}$$

where the raising and lowering of indices is accomplished through the use of the pseudo Riemannian metric tensor and is defined by the Minkowski metric. Here, $F_{\mu\nu}$ is the electromagnetic field tensor, $A^\mu = (\frac{\phi}{c}, \boldsymbol{A})$ is the four-vector potential, and $J^\mu = (c\rho, \boldsymbol{J})$ is the four-current. The tensor $F_{\mu\nu}$ is constructed from A_μ via $F_{\mu\nu} = \partial_\mu A_\nu - \partial_\nu A_\mu$.

The dynamics of the electromagnetic field are then governed by the Euler-Lagrange equation for

fields, applied to this Lagrangian. The Euler-Lagrange equation for fields reads:

$$\frac{\partial}{\partial x^\nu}\left(\frac{\partial \mathcal{L}}{\partial\left(\frac{\partial A^\mu}{\partial x^\nu}\right)}\right) = \frac{\partial \mathcal{L}}{\partial A^\mu}. \tag{12.20}$$

Applying this to the Lagrangian of the electromagnetic field yields Maxwell's equations. Thus, the entire electromagnetic interaction, including the movement of charged particles and the dynamics of the electromagnetic field, is encapsulated in the above Lagrangian formulation through the principle of least action.

The elaboration from the Lagrangian viewpoint to the Lorentz force law forms a crucial bridge in the narrative of electromagnetism. This demonstrates the intertwined nature of Maxwell's equations and the Lorentz force, and underscores the seamless emergence of the latter from the foundational framework of the Lagrangian formalism.

Consider a charged particle of mass m and charge q moving in an external and macroscopic electromagnetic field. This is because the origin of this field is not specified. The Lagrangian of this system is given by:

$$\mathcal{L} = -mc^2\sqrt{1 - \frac{v^2}{c^2}} - qA_\mu u^\mu. \tag{12.21}$$

Here, $u^\mu = \gamma(c, \boldsymbol{v})$ signifies the four-velocity and A_μ denotes the four-potential.

The Euler-Lagrange equation,

$$\frac{d}{dt}\frac{\partial \mathcal{L}}{\partial \dot{x}^\mu} = \frac{\partial \mathcal{L}}{\partial x^\mu}, \tag{12.22}$$

is then applied to this Lagrangian, yielding the equation of motion for the particle. The left-hand side of this equation yields the force exerted on the particle, while the right-hand side computes the derivative of the Lagrangian with respect to the four-position x^μ.

Upon substituting the Lagrangian from (12.21) into (12.22), we find, after some rearrangements, the equation becomes

$$m\frac{d}{dt}\left(\frac{\dot{x}_n}{\sqrt{1 - \frac{v^2}{c^2}}}\right) = q\left(\frac{\partial A_0}{\partial x^p} - \frac{\partial A_p}{x_0}\right) + q\dot{x}^m\left(\frac{\partial A_m}{\partial x_n} - \frac{\partial A_n}{x_m}\right). \tag{12.23}$$

Multiplying both sides by $\frac{dct}{d\tau} = \frac{dx^0}{d\tau}$, while acknowledging that $\frac{\dot{x}_n}{\sqrt{1 - \frac{v^2}{c^2}}} = \frac{dx_n}{d\tau}$, where τ stands for proper time, we derive

$$m\frac{d^2 x_\mu}{d\tau^2} = q\frac{x^\nu}{d\tau}\left(\frac{\partial A_\nu}{\partial x^\mu} - \frac{\partial A_\mu}{\partial x^\nu}\right). \tag{12.24}$$

The spatial components of this equation can be recognized as the Lorentz force.

Furthermore, the temporal component, following the 'mostly plusses' convention for the Minkowski metric, of this equation forms

$$\frac{d(mu_\mu)}{d\tau} = \frac{d}{d\tau}\left(-\frac{mc^2}{\sqrt{1 - \frac{v^2}{c^2}}}\right) = q\frac{dx^\nu}{d\tau}\left(\frac{\partial A_\nu}{\partial x^0} - \frac{\partial A_0}{\partial x^\nu}\right) = -\boldsymbol{E}\cdot(q\boldsymbol{v}) = -\boldsymbol{E}\cdot\boldsymbol{J}. \tag{12.25}$$

Here, we utilize the fact $q\boldsymbol{E} = \boldsymbol{F}$, the force on the particle. This implies that the temporal component embodies an energy conservation law, to which we will return later. This principle dictates that the variation in kinetic energy equals the work performed on the system through the fields.

Through this exercise, we see the Lorentz force law as a fundamental consequence of the dynamics integrated into the Lagrangian formalism of electromagnetism, and not an independent construct.

It's important to note that the fields were assumed to be macroscopic and were superimposed on our particle, which is why the Lorentz force was derived from the Lagrangian without any correction terms. However, all fields are the outcomes of charges and currents. In our macroscopic scenario, it was assumed that the motion of our particle would not impact the charges and currents producing the macroscopic field.

12.9.3 Inclusion of Correction Terms: The Landau and Lifshitz Method

When our model is expanded to explore microscopic systems, we need to take into account the retardation time of the fields generated. A critical analysis by Landau and Lifshitz in their influential work, *Course On Theoretical Physics*, Vol. 2, [64] shines a light on this intricate detail.

Landau and Lifshitz focus on a temporal Taylor expansion of the sources $J^\mu = (c\rho, \boldsymbol{J})$ that considers the retardation effect in the generated fields

$$J^\mu\left(\boldsymbol{r}, t - \frac{|\boldsymbol{r} - \boldsymbol{r}'|}{c}\right) = \sum_{n=0}^{\infty} \frac{(-1)^n}{n!}\left(\frac{|\boldsymbol{r} - \boldsymbol{r}'|}{c}\right)^n \frac{\partial^n}{\partial t^n} J^\mu(\boldsymbol{r}, t). \tag{12.26}$$

The four-potential (A^μ) of Equation (12.5) can now be expressed as a simple series with these terms

$$\begin{aligned}
A^\mu(\boldsymbol{r}, t) &= \frac{\mu_0}{4\pi} \iiint_V \frac{J^\mu\left(\boldsymbol{r}, t - \frac{|\boldsymbol{r} - \boldsymbol{r}'|}{c}\right)}{|\boldsymbol{r} - \boldsymbol{r}'|} dV' \\
&= \frac{\mu_0}{4\pi} \sum_{n=0}^{\infty} \frac{(-1)^n}{n! c^n} \frac{\partial^n}{\partial t^n} \iiint_V J^\mu(\boldsymbol{r}, t)|\boldsymbol{r} - \boldsymbol{r}'|^{n-1} dV'.
\end{aligned} \tag{12.27}$$

Interestingly, it is shown by Landau and Lifshitz that the first few terms in the Taylor expansion result in the Lorentz force. Now, let's look at the subsequent terms. Consider the scalar potential (ϕ_3), which is first component of the fourth term $(n = 3)$ in Equation (12.27):

$$\phi_3 = -\frac{\mu_0}{4\pi c} \frac{1}{6} \frac{\partial^3}{\partial t^3} \iiint \rho|\boldsymbol{r} - \boldsymbol{r}'|^2 dV', \tag{12.28}$$

and the vector potential $(\boldsymbol{A}_1)$, which is the second term $(n = 1)$

$$\boldsymbol{A}_1 = -\frac{\mu_0}{4\pi c} \frac{\partial}{\partial t} \iiint_V \boldsymbol{J}(\boldsymbol{r}, t) dV'. \tag{12.29}$$

To simplify our analysis, we perform a gauge transformation: $A'_\mu = A_\mu + \frac{\partial f}{\partial x^\mu}$ for some scalar function $f(\boldsymbol{r}, t)$, and adjust the scalar function f to set the transformed scalar potential ϕ'_3 to zero

$$f(\boldsymbol{r}, t) = -\frac{\mu_0}{4\pi c} \frac{1}{6} \frac{\partial^2}{\partial t^2} \iiint \rho|\boldsymbol{r} - \boldsymbol{r}'|^2 dV'. \tag{12.30}$$

With this choice of $f(\boldsymbol{r}, t)$, the gauge-transformed vector potential simplifies to

$$\boldsymbol{A}'_1 = -\frac{\mu_0}{4\pi c} \frac{\partial}{\partial t} \iiint_V \boldsymbol{J}(\boldsymbol{r}, t) dV' - \frac{\mu_0}{4\pi c} \frac{1}{3} \frac{\partial^2}{\partial t^2} \iiint (\boldsymbol{r} - \boldsymbol{r}') \cdot \rho dV', \tag{12.31}$$

where we have used the fact that $\boldsymbol{\nabla}|\boldsymbol{r} - \boldsymbol{r}'|^2 = 2(\boldsymbol{r} - \boldsymbol{r}')$. Assuming that we are dealing with individual charges in our microscopic system, we can redefine the current and charge densities as sums over individual charges, i.e., $\boldsymbol{J} = \sum_i q\boldsymbol{v}_i\delta(\boldsymbol{r} - \boldsymbol{r}'_i)$ and $\rho = \sum_i q\delta(\boldsymbol{r} - \boldsymbol{r}'_i)$. Additionally, we observe that $\partial_t(\boldsymbol{r} - \boldsymbol{r}'_i) = -\dot{\boldsymbol{r}}'_i = -\boldsymbol{v}_i$. After substituting these quantities into Equation (12.31) and using the fact that $\mu_0 = 1/(c^2\epsilon)$, we arrive at:

$$\boldsymbol{A}'_1 = -\frac{2}{3} \frac{q}{4\pi\epsilon_0 c^3} \sum_i \dot{\boldsymbol{v}}_i, \tag{12.32}$$

Next, let's retrace the steps we previously took to find the force from the Lagrangian. We will find that $\boldsymbol{F} = -q\frac{\partial \boldsymbol{A}_1'}{\partial t}$. This holds because $\phi_3' = 0$ and $\boldsymbol{B} = \boldsymbol{\nabla} \times \boldsymbol{A}_1' = 0$, allowing us to express the force as:

$$\boldsymbol{F} = \frac{2}{3}\frac{q^2}{4\pi\epsilon_0 c^3}\,\dddot{\boldsymbol{d}}. \tag{12.33}$$

Here, $\dddot{\boldsymbol{d}}$ represents the third derivative of the dipole moment of the system, known as the 'jerk' of the system as a whole. This is due to Mach's principle, which states that if all charges jerk in the same direction, the jerk does not happen relative to anything else. However, if one of these charges jerks relative to the others, we simply get

$$\boldsymbol{F} = \frac{2}{3}\frac{q^2}{4\pi\epsilon_0 c^3}\dot{\boldsymbol{a}}. \tag{12.34}$$

This is the same as Equation (12.17). From these derivations, it is clear that the form of the force on charged particles in electromagnetic fields depends on the specific setup of the system. For instance, the jerk of individual charges in the system has a substantial effect on the force experienced by those charges. Thus, understanding the particular setup and dynamics of a system is crucial when dealing with microscopic systems and electromagnetic fields.

12.9.4 Further Examination

The interplay between the Lorentz force and Maxwell's equations, as well as the implications of a Lagrangian and the resulting equations of motion (inclusive of forces) it prescribes, compose the bedrock of classical field theory and our contemporary interpretation of physical laws.

It seems that the Lagrangian construct, encompassing both the fields and their interaction term, asserts a more fundamental role than the Lorentz force, which appears as a macroscopic special case. This is due to the Lorentz force's neglect of phenomena such as the Abraham-Lorentz force or the force that encapsulates Synchrotron radiation. As discussed, charged particles in a magnetic field, as directed by the Lorentz force, spiral at a constant velocity, and thus maintain constant kinetic energy. However, these spiraling particles experience centripetal acceleration. As the Lienard-Wiechert potentials suggest, accelerating charged particles must radiate, thereby losing kinetic energy and slowing down. This deceleration should be facilitated by a force. However, it cannot be attributed to the Lorentz force, which insists on the maintenance of a constant speed. This leads to the proposition that the Lorentz force functions as a macroscopic force in macroscopic fields.

Our examination has proven that the Abraham-Lorentz force can be deduced through a Lagrangian formulation, using a spatial derivative and subsequent Taylor expansion of the source terms. The initial terms of this expansion yield the Lorentz force, while subsequent terms account for the Abraham-Lorentz force.

The book of Landau and Lifshitz posits the resulting force as a product of the third derivative of the dipole moment, which manifests when one charge accelerates relative to others. This captures the essence of Mach's principle. As such, to ascertain the force exerted among multiple charges, one must compute only the cross-interaction term in the Lagrangian and then apply its derivative. Self-terms must be discarded since the charges should not exert forces on themselves via their own fields. This lends a time-symmetric approach to discern the microscopic force exerted by some charges on others, thereby providing a more inclusive explanation than the macroscopic Lorentz force.

The Lagrangian formulation of electromagnetism offers such a complete representation, accommodating these additional effects. With the Lagrangian, we address electromagnetism in a more unified and thorough way, capable of deriving the Lorentz force and integrating other effects like radiation reaction.

Thus, one might argue that the 'complete' version of electromagnetism is encapsulated by the appropriate Lagrangian. From this, not only the Lorentz force in the limit of non-accelerating charges can be derived, but also additional forces like the Abraham-Lorentz force, under conditions

of accelerating charges. This relegates the Lorentz force to a special, macroscopic case, with the Lagrangian formulation providing a more fundamental and encompassing description of the theory.

This demonstrates the power and ubiquitous usage of Lagrangian (and Hamiltonian) formalisms in theoretical physics. They offer a unified and comprehensive framework for describing physical systems, capable of incorporating a wide range of effects and phenomena, and are fully compatible with the principles of quantum and relativistic physics.

Yet, it's vital to acknowledge that the Lagrangian formulation, despite its fundamental and versatile nature, may seem more abstract and less intuitive than the force-based approach. Moreover, the specific form of the Lagrangian is contingent upon the particular model and theory at hand, often requiring meticulous derivation. Hence, the Lorentz force and Maxwell's equations retain significant importance and utility in numerous contexts, even though they can be derived from the more fundamental Lagrangian description.

12.9.5   General Structure

In any microscopic system encompassing N distinct components, the 4-current and 4-potential can be articulated as the summation of these individual elements. Mathematically, this is expressed as

$$A_\mu = \sum_{i=1}^{N} A_{\mu,i}, \qquad J^\mu = \sum_{i=1}^{N} J_i^\mu. \tag{12.35}$$

These individual components could be either discrete, point-like particles or they could manifest as continuous charge and current distributions that possess compact support in non-intersecting spatial regions.

Upon computing the interaction term in the Lagrangian, the straightforward approach yields

$$\sum_{\mu=0}^{3} A_\mu J^\mu = \sum_{\mu=0}^{3} \left(\sum_{i=1}^{N} A_{\mu,i} \right) \left(\sum_{j=1}^{N} J_j^\mu \right) = \sum_{\mu=0}^{3} \sum_{i,j} A_{\mu,i} J_j^\mu, \tag{12.36}$$

where $\sum_{i,j}$ denotes a double summation. We have temporarily abandoned the Einstein summation convention in order to show nature of the superposition more explicitly.

Nevertheless, as previously noted, we should exclude the 'self-interaction' term from our calculation. To be precise, a particle should not interact with the field it has radiated itself. This amendment results in the equation

$$\sum_{\mu=0}^{3} A_\mu J^\mu = \sum_{\mu=0}^{3} \sum_{i \neq j} A_{\mu,i} J_j^\mu. \tag{12.37}$$

The basis for this exclusion will be explored in depth in the upcoming sections. However, as a preliminary rationale, we could argue that a particle's interaction with its own radiated field often induces problematic scenarios in theoretical physics. For instance, the infamous 'self-interaction' issue often leads to divergences in classical field theories, which in turn can cause difficulties in determining the behavior of the system. Consequently, self-interaction terms are typically excluded when considering the dynamics of multiple particles or field sources. This approach offers a means to derive the microscopic force exerted by certain charges on others, thereby presenting a more inclusive explanation than the macroscopic Lorentz force.

This modification to the Lagrangian interaction term is one of many techniques utilized in classical field theory to rectify the divergences and inconsistencies introduced by self-interaction. The subsequent sections will delve further into these topics, elucidating the intricate dynamics and principles underlying these fundamental physical theories.

13 Delving into the Realm of Antennas

As we proceed to unfold our microscopic theory, it becomes imperative to incorporate a discourse on the phenomena of radiative energy transfer amidst separated but interactively correlated current distributions, more conventionally known as antennas. This investigation into the world of antennas is vital as it bridges our understanding from the macroscopic dynamics to the subtleties of the microscopic realm.

This examination will be undertaken by presenting an array of carefully selected examples that depict the fundamental and complex facets of antennas. By disentangling these instances, we shall illuminate the principles and mechanics that govern their operation and interplay.

Our exploration is not merely to understand antennas in isolation but to comprehend their relevance and contribution in the broader context of electromagnetic theory. The knowledge thus gained will serve as a powerful tool, enabling us to delve deeper into the microscopic formulation and unveiling the reciprocity relation as proposed by Wessel-Berg.

This comprehension is instrumental when discussing the microscopic formulation proposed by Wessel-Berg, especially with regards to his notable reciprocity relation. This principle lies at the heart of antenna theory, elucidating the essential symmetry in the interaction between antennas, regardless of whether they are transmitting or receiving signals.

This endeavor is not merely a detour; rather, it is a deliberate and essential part of our journey that fosters the comprehension necessary to grapple with the nuanced microscopic framework that we are on the cusp of examining.

13.1 A Study on Energy Distribution in Electromagnetic Field: Single Transmitter with Two Receivers

In electromagnetic systems, the energy distribution between various receiving bodies is an intricate phenomenon that relies heavily on factors such as distance, relative positioning, and the physical characteristics of the bodies involved. To understand the complexity of this energy distribution, consider a scenario involving a single transmitting antenna and two receiving antennas.

Our system comprises a transmitter that radiates a certain amount of energy, and two receivers denoted as Receiver 1 (R1) and Receiver 2 (R2). Without the presence of R1, R2 receives a proportion of energy radiated by the transmitter, based on its position, size, and the frequency of radiation.

In our investigation, we introduce R1 in the path of the radiated energy before it reaches R2. This physical positioning of R1 leads to the absorption of a portion of the radiated energy, which in turn induces a current in R1. This absorption of energy is not merely an interruption in the energy path; it significantly alters the energy distribution by reducing the amplitude of the electromagnetic wave around R1, effectively diminishing the energy that would otherwise reach R2 directly.

However, the dynamics of this system do not end here. The current induced in R1 due to absorbed energy also generates secondary electromagnetic fields, further complicating the energy distribution. These secondary fields can interact with the initial fields from the transmitter, leading to interference, the nature (constructive or destructive) of which depends on the relative phase and amplitude of these fields.

It is critical to note that the fields at R2's location are not identical in scenarios with and without R1. Contrary to an initial intuitive assumption, the fields at R2's location when R1 is present are not just the 'initial fields' from the transmitting antenna; they are the resultant of the interaction of initial fields and the secondary fields produced by R1. Thus, R1 not only 'blocks' the energy by physical obstruction but also alters the energy distribution through absorption and re-radiation of energy.

The discussion underlines the complexity of energy transfer in electromagnetic systems and em-

phasizes that the energy received by a receiver (such as R2) depends not only on the transmitter's fields but also on the impact of other bodies present in the system. To fully comprehend this, a detailed study taking into account the specific positions, sizes, and shapes of the antennas, as well as the frequency of radiation, is required.

Through this illustration, our thesis demonstrates the importance of understanding the intricacies of energy distribution in electromagnetic fields, paving the way for a more efficient and accurate design of systems involving multiple receivers.

13.2   Impacts of Load Disconnection on Energy Distribution: A Case Study of Two Receiver Antennas

In a typical electromagnetic system involving a transmitter and receivers, each component plays a crucial role in determining the final energy distribution. In this section, we investigate an intriguing scenario involving the disconnection of one of the receiver's load and study its impact on the energy distribution in the system.

Consider a system comprising a single transmitter and two receivers, Receiver 1 (R1) and Receiver 2 (R2), with R1 positioned between the transmitter and R2. Initially, R1 is connected to an electrical circuit (the load), and it absorbs a certain amount of energy from the radiated electromagnetic wave. The energy absorbed by R1 is then converted into electrical energy and transferred to the load. Consequently, the amplitude of the electromagnetic wave around R1 diminishes, which significantly impacts the energy reaching R2.

However, in our modified scenario, we explore the effects of disconnecting R1 from its associated load. When disconnected, R1 can no longer transfer the absorbed energy to the load. Yet, R1, a metallic structure, still interacts with the propagating electromagnetic wave. This interaction induces a current in R1, but unlike the previous case, this current has no destination as it is not connected to a circuit with a load as it is an open circuit.

This alteration in R1's operational state triggers it to behave akin to a scatterer or secondary source of electromagnetic waves, as the induced current oscillates within R1. The electromagnetic fields produced by this oscillating current will subsequently interfere with the original fields from the transmitter. However, with no continuous extraction of energy from R1 as was observed when connected to the load, the secondary radiation's characteristics change, leading to a new radiation pattern and possibly a different energy distribution at R2's location.

It is important to clarify here that while R1 no longer 'absorbs' energy in the conventional sense (conversion of electromagnetic energy into another form), it still interacts with the incoming wave and redirects its energy, which, in a broader sense, can be considered as a form of 'absorption'.

The scenario illustrates the crucial role of the receiver's operational state on energy distribution. Disconnecting R1 from its load not only alters its interaction with the incoming electromagnetic wave but also modifies the energy received by other receivers such as R2. A thorough understanding of these subtle interactions is pivotal in the efficient and accurate design of electromagnetic systems. The specific details of these changes would require complex calculations or simulations that take into account the unique characteristics of the antennas, their arrangement, and the frequency of radiation.

This case study underscores the critical need to investigate the intrinsic factors affecting the energy distribution in multi-receiver scenarios, highlighting the importance of system design considerations for optimized performance.

13.3   Exploring the Waveguide Aspect of Electric Circuits

Expanding on the insights gleaned from our analysis of antenna systems, we now turn our attention to the realm of electric circuits. Conventionally, the pedagogical understanding imparted is that conducting wires in a circuit are the medium through which current flows, thereby facil-

itating the transfer of energy throughout the system. But delving deeper into the intricacies of electromagnetism offers a more nuanced perspective.

In the grand schema of electromagnetic theory, energy transmission is orchestrated by the Poynting vector field. This concept implies that energy does not, in fact, flow directly through the conductive wires, but rather propagates through the surrounding electromagnetic field, that is, it flows through the space around the circuit, embodying an 'around-the-wire' model of energy transfer.

In this context, the role of the conducting wire transcends beyond being a mere conduit for current. Instead, it assumes the critical function of a waveguide, a director that governs the trajectory of the energy wave. The wire then guides these energy waves from the source, say a battery, to the corresponding load, steering the wave of energy to its intended destination.

13.4   Power Flow happens outside the Circuit

This idea is touching on some interesting aspects of electromagnetic theory and how it applies to electronic circuits. It's important to clarify that while the electrical energy indeed travels from source to receiver, it's not strictly correct to say that it 'technically travels through the air'.

Rather, the key is understanding how energy flows in an electric circuit from a more fundamental electromagnetic perspective, which involves the concept of Poynting vectors.

In an electrical circuit, we have both electric fields (from the voltage between points in the circuit) and magnetic fields (from the current flowing through the wires). This combination of electric and magnetic fields generates a Poynting vector that points from the power source to the load (e.g., from a battery to a resistor).

One might imagine that this vector 'travels' along the wire, but that's a bit of a simplification. What actually happens is that the electromagnetic field, and thus the energy, is primarily concentrated around the wire, in the space outside of the conductor.

This is because a conductor is effectively a guide for electromagnetic waves, in this case, the oscillations of the electric and magnetic fields due to the AC (alternating current) in the circuit. The fields are mostly confined to the region outside the wire because they cannot penetrate a good conductor at these frequencies.

So, in a sense, the wires guide the energy, much like how a fiber optic cable guides light, with the energy traveling around the wire rather than inside of it. This is a fact that's often overlooked in basic circuit theory, which tends to treat wires as ideal, lossless conductors with no electromagnetic fields outside them.

Finally, remember that this description applies most directly to AC circuits with rapidly oscillating currents and voltages. In a simple DC (direct current) circuit, the situation is less dynamic and the notion of 'energy flow' is not quite as apparent because the fields are static (not time-varying).

In both cases, though, the actual movement of electrical energy involves both the electric and magnetic fields, and the Poynting vector provides a way to quantify this.

13.5   Circuit Viewed as a Continuum of Small Antennas

We have now accurately described a more nuanced way to understand the energy transfer in an electric circuit, which is indeed due to the interaction of electromagnetic fields generated by accelerating charges. Let's further elaborate on this idea with regards to our examples involving antennas.

When a circuit is first energized (e.g., a switch is closed), charges in the battery (or other power source) do indeed accelerate, due to the electric field established by the potential difference (voltage) of the battery. This sudden acceleration of charges produces an electromagnetic field, which can be described by the Lienard-Wiechert potentials. The Lienard-Wiechert potentials are solutions

to Maxwell's equations (the fundamental equations of electromagnetism) that describe the electromagnetic field produced by a point charge moving arbitrarily (including acceleration). In this context, they provide a description of the electromagnetic field created by the accelerating charges in the battery.

When this electromagnetic field reaches a part of the circuit wire, it causes the charges in the wire to accelerate. This happens because the field exerts forces on the charges, which results in their acceleration. This moving charge creates its own electromagnetic field, leading to a sort of 'chain reaction' effect, causing further charges downstream to accelerate.

This process continues along the wire, with each part of the wire essentially acting as an antenna that both receives and transmits electromagnetic waves. The net effect is that an electromagnetic field is propagated along the circuit, even though individual electrons in the wire move quite slowly.

The energy flow associated with this process can be described by the Poynting vector. The Poynting vector points from the power source (e.g., battery) to the load (e.g., resistor), along the wire and in the surrounding space, indicating the direction of energy flow. At the resistor, energy is dissipated as heat. This happens because the resistor impedes the flow of charges, causing them to 'jostle' and transfer kinetic energy to the atoms in the resistor. This energy is then radiated away as heat.
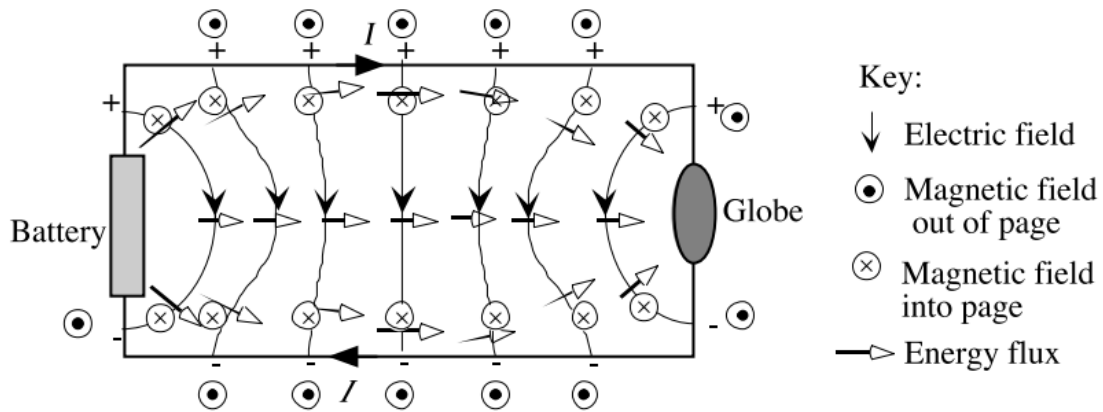
Figure 23: This figure, adapted from [80], provides a depiction of the energy flux in an electrical circuit. The white arrows represent the flow of energy from the battery to the resistor, manifesting as the Poynting vector field surrounding the wire. Notably, this energy flow is not confined to the conducting wires but propagates through the surrounding air, demonstrating the waveguide nature of electrical circuits. Additionally, the figure portrays the distribution of the electric field (curved lines) and the magnetic field (concentric circles) associated with the circuit.

The field-centric interpretation of energy transfer in electric circuits has been a subject of substantial investigation and discussion in the scientific community. Several scholarly articles and research papers [27] [38] [71] [80] have deeply explored this topic, shedding light on the intricate dynamics of field formulations in the context of energy transfer.

The illustration presented in Figure 23, extracted directly from one of these insightful studies [80], visually encapsulates the essence of this concept. These scholarly endeavors collectively illuminate the path to understanding how field formulations are pivotal to the process of energy transfer within electrical circuits, enhancing our comprehension of this fundamental phenomenon in the realm of electrical engineering.

The following is a more detailed picture of how electric fields and currents in a circuit give rise to electromagnetic waves and the associated Poynting vectors, which is be broken into a series of steps:

1. **Initial Acceleration of Charges in the Battery:** When a battery is connected to a circuit, the electric field established by the battery causes charges to accelerate. This happens due to the potential difference (voltage) across the terminals of the battery.

2. **Creation of Electromagnetic Fields:** These accelerating charges create an electromagnetic field, as described by the Lienard-Wiechert potentials. These potentials describe the electric and magnetic fields produced by a moving electric charge. The fields are dynamic, changing as the charge moves.

3. **Acceleration of Charges in the Wire:** The electromagnetic field created by the charges in the battery interacts with the charges in the wire. The electric field component of the electromagnetic field pushes and pulls on the charges in the wire, causing them to accelerate. The moving charges in the wire constitute an electric current.

4. **Propagation of the Electromagnetic Wave:** These accelerating charges in the wire create their own electromagnetic fields, which then influence charges further down the wire, causing them to accelerate as well. This cascading effect propagates the electromagnetic wave along the wire. This is similar to the way that waves propagate along a string when one end is shaken.

5. **Creation of the Poynting Vector:** All these electric and magnetic fields combine to form the Poynting vector field, which points in the direction of energy flow. In a simple circuit, the Poynting vector would point from the battery (the energy source) to the resistor (where the energy is dissipated as heat).

6. **Energy Dissipation in the Resistor:** Finally, when the electromagnetic wave reaches the resistor, it causes charges in the resistor to oscillate rapidly. These oscillating charges collide with atoms in the resistor, causing the atoms to vibrate more energetically—that is, to heat up. This converts the electrical energy carried by the electromagnetic wave into thermal energy, which is then dissipated.

This is a simplified explanation and the actual phenomena at the atomic and subatomic levels are quite complex, involving quantum mechanics and the intricate interplay of electrical charges and fields. However, it provides a good conceptual understanding of how electric circuits work from the perspective of electromagnetic fields and waves. Understanding this process will help us understand wave function collapse and the noradiation condition.

In summary, the energy flow in a circuit is a complex process that involves the propagation of electromagnetic fields along the wire. It's not simply a matter of 'current flowing', but rather a chain reaction of electromagnetic interactions involving accelerating charges and their associated fields. This energy transfer process can be captured by the concept of the Poynting vector.

14 Maxwell's Equations in the Frequency Domain

Maxwell's equations, originally expressed in the time domain, can also be expressed in the frequency domain. This formulation is particularly useful in dealing with problems involving harmonic oscillations, such as those in alternating current (AC) circuits, optics, and waveguides, among others.

The process of transforming these equations from the time domain to the frequency domain is achieved via a Fourier transformation. In general, the Fourier transformation of a function of time $f(t)$ is a function of frequency $\hat{f}(\omega)$ given by:

$$\hat{f}(\omega) = \int_{-\infty}^{+\infty} f(t)e^{-i\omega t}dt. \tag{14.1}$$

Now let's express Maxwell's equations in the frequency domain. The time domain Maxwell's equations are as follows (in the MKS system of units):

$$\nabla \cdot \boldsymbol{E}(\boldsymbol{r},t) = \frac{\rho(\boldsymbol{r},t)}{\varepsilon_0}, \tag{14.2}$$

$$\nabla \cdot \boldsymbol{H}(\boldsymbol{r},t) = 0, \tag{14.3}$$

$$\nabla \times \boldsymbol{E}(\boldsymbol{r},t) = -\mu_0 \frac{\partial \boldsymbol{H}(\boldsymbol{r},t)}{\partial t}, \tag{14.4}$$

$$\nabla \times \boldsymbol{H}(\boldsymbol{r},t) = \boldsymbol{J}(\boldsymbol{r},t) + \epsilon_0 \frac{\partial \boldsymbol{E}(\boldsymbol{r},t)}{\partial t}, \tag{14.5}$$

where $\boldsymbol{H} = \boldsymbol{B}/\mu_0$ results from the assumption that we are in vacuum. Applying the Fourier transformation to these equations, we obtain the frequency domain form of Maxwell's equations:

$$\nabla \cdot \boldsymbol{E}(\boldsymbol{r},\omega) = \frac{\rho(\boldsymbol{r},\omega)}{\varepsilon_0}, \tag{14.6}$$

$$\nabla \cdot \boldsymbol{H}(\boldsymbol{r},\omega) = 0, \tag{14.7}$$

$$\nabla \times \boldsymbol{E}(\boldsymbol{r},\omega) = -i\omega\mu_0 \boldsymbol{H}(\boldsymbol{r},\omega), \tag{14.8}$$

$$\nabla \times \boldsymbol{H}(\boldsymbol{r},\omega) = \boldsymbol{J}(\boldsymbol{r},\omega) + i\omega\varepsilon_0 \boldsymbol{E}(\boldsymbol{r},\omega). \tag{14.9}$$

Here $\rho(\boldsymbol{r},\omega)$, $\boldsymbol{J}(\boldsymbol{r},\omega)$, $\boldsymbol{E}(\boldsymbol{r},\omega)$, and $\boldsymbol{H}(\omega)$ are the Fourier transforms of charge density, current density, electric field, and magnetic field, respectively.

In the frequency domain, the temporal derivative has been replaced by a multiplication by $i\omega$. This can simplify the solution of problems involving wave propagation, especially when dealing with harmonic signals or linear media. Furthermore, the use of the frequency domain allows for the convenient analysis of phenomena such as retardation and advanced times in wave propagation, as well as the response of systems to specific frequency components.

14.1 Useful Properties of the Frequency Domain

Let us reconsider the field $\boldsymbol{E}(\boldsymbol{r},t)$ and its Fourier transform $\boldsymbol{E}(\boldsymbol{r},\omega)$. On substituting $-t$ in the original time-domain expression, we arrive at $\boldsymbol{E}(\boldsymbol{r},-t)$. The corresponding Fourier transform is obtained through the following substitution $-t$ in the Fourier transform integral:

$$\boldsymbol{E}(\boldsymbol{r},-t) = \frac{1}{2\pi} \int_{-\infty}^{+\infty} \boldsymbol{E}(\boldsymbol{r},\omega)e^{i\omega(-t)}\,\mathrm{d}\omega = \frac{1}{2\pi} \int_{-\infty}^{+\infty} \boldsymbol{E}(\boldsymbol{r},-\omega')e^{i\omega' t}\,\mathrm{d}\omega', \tag{14.10}$$

where we have performed the substitution $\omega = -\omega'$. This demonstrates that reversing the direction of time progression, i.e., $\boldsymbol{E}(\boldsymbol{r},t) \rightarrow \boldsymbol{E}(\boldsymbol{r},-t)$, directly corresponds to a similar reversal in the frequency domain, i.e., $\boldsymbol{E}(\boldsymbol{r},\omega) \rightarrow \boldsymbol{E}(\boldsymbol{r},-\omega)$. This is a widely applicable result.

Moreover, when $\boldsymbol{E}(\boldsymbol{r}, t)$ is a real-valued function, taking the complex conjugate of both sides of the Fourier transform results in:

$$\boldsymbol{E}(\boldsymbol{r}, t) = \boldsymbol{E}(\boldsymbol{r}, t)^* = \frac{1}{2\pi} \int_{-\infty}^{+\infty} \boldsymbol{E}^*(\boldsymbol{r}, \omega) e^{-i\omega t} \, \mathrm{d}\omega = \frac{1}{2\pi} \int_{-\infty}^{+\infty} \boldsymbol{E}^*(\boldsymbol{r}, -\omega') e^{i\omega' t} \, \mathrm{d}\omega', \qquad (14.11)$$

which leads to $\boldsymbol{E}(\boldsymbol{r}, -\omega) = \boldsymbol{E}^*(\boldsymbol{r}, \omega)$. However, it should be emphasized that this holds true only when $\boldsymbol{E}(\boldsymbol{r}, t)$ is a real quantity.

This scenario highlights a general property of Fourier transforms for real-valued functions. When the original function $\boldsymbol{E}(\boldsymbol{r}, t)$ is real – a common trait for many physical quantities – its Fourier transform satisfies the relation, $\boldsymbol{E}(\boldsymbol{r}, -\omega) = \boldsymbol{E}^*(\boldsymbol{r}, \omega)$.

This principle is particularly useful to keep in mind when investigating frequency domain phenomena in the next sections.

14.2   Time-Reversal Symmetries and the Frequency Domain

Consider the fields and sources $\boldsymbol{E}(\boldsymbol{r}, t), \boldsymbol{H}(\boldsymbol{r}, t), \boldsymbol{J}(\boldsymbol{r}, t), \rho(\boldsymbol{r}, t)$ in the time domain, which satisfy Maxwell's equations where $\boldsymbol{H} = \boldsymbol{B}/\mu_0$. Upon performing a time reversal transformation $t \to -t$, the sources and fields transform into $\boldsymbol{E}(\boldsymbol{r}, -t), \boldsymbol{H}(\boldsymbol{r}, -t), -\boldsymbol{J}(\boldsymbol{r}, -t), \rho(\boldsymbol{r}, -t)$. This transformed set, however, does not satisfy the original Maxwell's equations. The sign flip of the current is due to its time derivative, but the magnetic field $\boldsymbol{H}$ does not flip sign as it is not a time derivative of any quantity. Instead, these transformed fields and sources satisfy the equations for the antiphoton (10.54), (10.55), (10.56) and (10.57).

To ensure the time-reversed solutions still satisfy Maxwell's equations, we need to flip the sign of the magnetic field in the transformation: $\boldsymbol{H}(\boldsymbol{r}, t) \to -\boldsymbol{H}(\boldsymbol{r}, -t)$. Therefore, the overall transformation becomes: $\boldsymbol{E}(\boldsymbol{r}, t), \boldsymbol{H}(\boldsymbol{r}, t), \boldsymbol{J}(\boldsymbol{r}, t), \rho(\boldsymbol{r}, t) \to \boldsymbol{E}(\boldsymbol{r}, -t), -\boldsymbol{H}(\boldsymbol{r}, -t), -\boldsymbol{J}(\boldsymbol{r}, -t), \rho(\boldsymbol{r}, -t)$. This behavior was previously observed when discussing the retarded and advanced Lienard-Wiechert potentials, where a change of sign in the magnetic field in the advanced solution, along with the $t \to -t$ transformation, also resulted in $\boldsymbol{J} \to -\boldsymbol{J}$ due to the change of sign in the velocities.

Thus, performing a time reversal transformation $t \to -t$ and flipping the sign of the magnetic field effectively switches between the time-retarded and time-advanced solutions. Without the magnetic field inversion, the transformed sources and fields $\boldsymbol{E}(\boldsymbol{r}, -t), \boldsymbol{H}(\boldsymbol{r}, -t), -\boldsymbol{J}(\boldsymbol{r}, -t), \rho(\boldsymbol{r}, -t)$ become solutions to the Maxwell's equations for the antiphoton.

Let's now examine how these principles apply in the frequency domain. Due to the nature of the Fourier transform, both positive and negative frequencies are inherently present. The inverse Fourier transform that results in a real function $\boldsymbol{E}(\boldsymbol{r}, t)$ demonstrates this, as it includes both positive frequency components $\boldsymbol{E}(\boldsymbol{r}, \omega)$ and their complex conjugates representing negative frequency components $\boldsymbol{E}(\boldsymbol{r}, -\omega) = \boldsymbol{E}^*(\boldsymbol{r}, \omega)$:

$$\boldsymbol{E}(\boldsymbol{r}, t) = \frac{1}{2\pi} \int_{-\infty}^{+\infty} \boldsymbol{E}(\boldsymbol{r}, \omega) e^{i\omega t} \, \mathrm{d}\omega = \frac{1}{2\pi} \int_0^{+\infty} \left[\boldsymbol{E}(\boldsymbol{r}, \omega) e^{i\omega t} + \boldsymbol{E}^*(\boldsymbol{r}, \omega) e^{-i\omega t} \right] \mathrm{d}\omega, \qquad (14.12)$$

These negative frequency components, required by the Fourier transform, solve the complex conjugated form of Maxwell's equations

$$\nabla \cdot \boldsymbol{E}^*(\boldsymbol{r}, \omega) = \frac{\rho^*(\boldsymbol{r}, \omega)}{\varepsilon_0}, \qquad (14.13)$$

$$\nabla \cdot \boldsymbol{H}^*(\boldsymbol{r}, \omega) = 0, \qquad (14.14)$$

$$\nabla \times \boldsymbol{E}^*(\boldsymbol{r}, \omega) = +i\omega\mu_0 \boldsymbol{H}^*(\boldsymbol{r}, \omega), \qquad (14.15)$$

$$\nabla \times \boldsymbol{H}^*(\boldsymbol{r}, \omega) = \boldsymbol{J}^*(\boldsymbol{r}, \omega) - i\omega\varepsilon_0 \boldsymbol{E}^*(\boldsymbol{r}, \omega), \qquad (14.16)$$

which are trivially obtained, as $\boldsymbol{E}^*(\boldsymbol{r}, \omega)$ can be found by taking the complex conjugate of the already known $\boldsymbol{E}(\boldsymbol{r}, \omega)$.

In the Fourier integral of (14.12), $\boldsymbol{E}(\boldsymbol{r}, \omega)$ is paired with $e^{i\omega t}$, while $\boldsymbol{E}^*(\boldsymbol{r}, \omega) = \boldsymbol{E}(\boldsymbol{r}, -\omega)$ is paired with $e^{-i\omega t}$. As $\boldsymbol{E}(\boldsymbol{r}, -\omega)$ and $\boldsymbol{E}(\boldsymbol{r}, \omega)$ are intrinsically related in the Fourier transform, performing a time reversal transformation implies swapping their places

$$\boldsymbol{E}(\boldsymbol{r}, -t) = \frac{1}{2\pi} \int_0^{+\infty} \left[\boldsymbol{E}^*(\boldsymbol{r}, \omega) e^{i\omega t} + \boldsymbol{E}(\boldsymbol{r}, \omega) e^{-i\omega t} \right] \mathrm{d}\omega. \tag{14.17}$$

Applying this transformation to all sources and fields results in the solution of Maxwell's equations for the antiphoton when the magnetic field is not flipped. These ideas are essential to understand in order to understand the nature of the Bitemporal theory.

14.3 The Useful Harmonic Nature of Oscillations

The use of the frequency domain not only facilitates the decomposition and analysis of problems into individual frequencies but also establishes a relationship between the vector and scalar potentials in the Lorenz gauge condition from Equation (12.4). This relationship can be expressed as:

$$\phi(\boldsymbol{r}, \omega) = \frac{-c^2}{i\omega} \boldsymbol{\nabla} \cdot \boldsymbol{A}(\boldsymbol{r}, \omega), \tag{14.18}$$

which considerably simplifies many of the problems we will subsequently examine.

Furthermore, the predictable and harmonic character of the frequency domain allows for an effortless representation of both the vector and scalar potentials at retarded and advanced times, owing to the periodic and repeating nature of oscillations. As a result, the four-potential A^μ for the time-retarded and time-advanced solutions can be more succinctly expressed in the frequency domain than in the time domain of Equations (12.5) and (12.6). In the frequency domain, the four-potentials take the following forms

$$A^\mu(\boldsymbol{r}, \omega) = \frac{\mu_0}{4\pi} \iiint \frac{J^\mu(\boldsymbol{r}', \omega) e^{-i\omega \cdot \frac{|\boldsymbol{r} - \boldsymbol{r}'|}{c}}}{|\boldsymbol{r} - \boldsymbol{r}'|} \, \mathrm{d}V', \tag{14.19}$$

$$\widetilde{A}^\mu(\boldsymbol{r}, \omega) = \frac{\mu_0}{4\pi} \iiint \frac{J^\mu(\boldsymbol{r}', \omega) e^{+i\omega \cdot \frac{|\boldsymbol{r} - \boldsymbol{r}'|}{c}}}{|\boldsymbol{r} - \boldsymbol{r}'|} \, \mathrm{d}V', \tag{14.20}$$

respectively for time-retarded and time-advanced four potentials. The simplified nature of these expressions is due to the fact that a time translation in the time domain (as in retarded or advanced time translation) simply translates into a phase shift in the frequency domain, as illustrated by:

$$\boldsymbol{J}(\boldsymbol{r}, t \pm \frac{|\boldsymbol{r} - \boldsymbol{r}'|}{c}) = \frac{1}{2\pi} \int_{-\infty}^{+\infty} \boldsymbol{J}(\boldsymbol{r}, \omega) e^{i\omega \left(t \pm \cdot \frac{|\boldsymbol{r} - \boldsymbol{r}'|}{c} \right)} \, \mathrm{d}\omega = \frac{1}{2\pi} \int_{-\infty}^{+\infty} \left[\boldsymbol{J}(\boldsymbol{r}, \omega) e^{\pm i\omega \cdot \frac{|\boldsymbol{r} - \boldsymbol{r}'|}{c}} \right] e^{i\omega t} \, \mathrm{d}\omega. \tag{14.21}$$

The advantageous properties of these harmonic oscillations will be further explored and employed in the ensuing sections.

14.4 Power Flow in the Frequency Domain

The power flow in an electromagnetic field is described by the Poynting vector. In the time domain, this vector is defined as the cross product of the electric field $\boldsymbol{E}$ and the magnetic field $\boldsymbol{H}$ as

$$\boldsymbol{S}(\boldsymbol{r}, t) = \boldsymbol{E}(\boldsymbol{r}, t) \times \boldsymbol{H}(\boldsymbol{r}, t), \tag{14.22}$$

where $\boldsymbol{r}$ represents the position vector, and t is the time.

When examining a single frequency, the electric and magnetic fields can be represented as complex exponential functions, where the real part corresponds to the actual physical fields. Hence, we can express the electric and magnetic fields in terms of their frequency domain representations as

$$\boldsymbol{E}(\boldsymbol{r}, t) = \mathrm{Re}\left(\boldsymbol{E}(\boldsymbol{r}, \omega) e^{i\omega t} \right), \tag{14.23}$$

and

$$\boldsymbol{H}(\boldsymbol{r},t) = \text{Re}\left(\boldsymbol{H}(\boldsymbol{r},\omega)e^{i\omega t}\right). \tag{14.24}$$

Substituting these into the Poynting vector equation, we obtain

$$\boldsymbol{S}(\boldsymbol{r},t) = \text{Re}\left(\boldsymbol{E}(\boldsymbol{r},\omega)e^{i\omega t}\right) \times \text{Re}\left(\boldsymbol{H}(\boldsymbol{r},\omega)e^{i\omega t}\right). \tag{14.25}$$

We can further expand the real parts of $\boldsymbol{E}$ and $\boldsymbol{H}$ using Euler's formula to include the complex conjugate components, resulting in

$$\boldsymbol{S}(\boldsymbol{r},t) = \frac{1}{2}\left(\boldsymbol{E}(\boldsymbol{r},\omega)e^{i\omega t} + \boldsymbol{E}^*(\boldsymbol{r},\omega)e^{-i\omega t}\right) \times \frac{1}{2}\left(\boldsymbol{H}(\boldsymbol{r},\omega)e^{i\omega t} + \boldsymbol{H}^*(\boldsymbol{r},\omega)e^{-i\omega t}\right). \tag{14.26}$$

Expanding and rearranging, we finally arrive at

$$\boldsymbol{S}(\boldsymbol{r},t) = \frac{1}{2}\text{Re}\left(\boldsymbol{E}(\boldsymbol{r},\omega) \times \boldsymbol{H}^*(\boldsymbol{r},\omega)\right) + \frac{1}{2}\text{Re}\left(\boldsymbol{E}(\boldsymbol{r},\omega) \times \boldsymbol{H}(\boldsymbol{r},\omega)e^{2i\omega t}\right). \tag{14.27}$$

The first term on the right side represents the time-average power flow, which we are typically interested in, while the second term fluctuates with a frequency of 2ω, averaging to zero over any complete cycle. Therefore, the Poynting vector in the frequency domain is given by the real part of the cross product of the electric field and the complex conjugate of the magnetic field, scaled by a factor of one-half.

The term involving $e^{2i\omega t}$ is the rapidly oscillating part of the Poynting vector in the frequency domain. This term represents the rapid fluctuations in the instantaneous power flow at a frequency twice that of the original electromagnetic wave, due to the interaction between the complex electric and magnetic fields.

Mathematically, these fluctuations are due to the cross-product between the complex components of the electric and magnetic fields. Physically, it represents the rapid exchange of energy between the electric and magnetic fields, which is typical in an electromagnetic wave.

However, the important point to note is that these rapid fluctuations average out to zero over a complete cycle or over any time period encompassing multiple cycles. This is because the integral of a cosine or sine function over its period is zero. As a result, this term does not contribute to the net power transfer, which is often the quantity of interest.

Therefore, while this term is part of the complete description of power flow in the frequency domain, it is typically ignored in power calculations because it does not contribute to the average power flow. Instead, we focus on the first term, which represents the time-averaged power flow donoted here as $\boldsymbol{S}(\boldsymbol{r},\omega)$, as it gives us the net transfer of energy in the system

$$\boldsymbol{S}(\boldsymbol{r},\omega) = \frac{1}{2}\text{Re}\left(\boldsymbol{E}(\boldsymbol{r},\omega) \times \boldsymbol{H}^*(\boldsymbol{r},\omega)\right). \tag{14.28}$$

The necessity for the complex conjugation in the formulas in the frequency domain can be easier understood in light of Parseval's formula

$$\int\limits_{-\infty}^{\infty} F_1(t)F_2(t)dt = \int\limits_{-\infty}^{\infty} F_1(\omega)F_2(-\omega)\,\mathrm{d}\omega \tag{14.29}$$

for two functions $F_1(t)$ and $F_2(t)$ and their respective Fourier transforms $F_1(\omega)$ and $F_2(\omega)$. This representation in conjunction with Parseval's formula provides insights into the power flow in an electromagnetic wave in the frequency domain, highlighting the spectral composition of the energy transport.

14.5   The Complex Poynting Theorem

In the complex frequency domain, the Poynting theorem extends its powerful utility by dealing with the power flowing across the boundaries of a volume, the work done on the charges within the

volume, and the energy rate of change within a volume at specific frequencies. Here, we present the complex Poynting theorem

$$\frac{1}{2} \oiint_S \boldsymbol{E} \times \boldsymbol{H}^* \cdot \mathrm{d}\boldsymbol{S} = \frac{i\omega}{2} \iiint_V (\varepsilon_0 \boldsymbol{E} \cdot \boldsymbol{E}^* - \mu_0 \boldsymbol{H} \cdot \boldsymbol{H}^*)\, \mathrm{d}V - \frac{1}{2} \iiint_V \boldsymbol{E} \cdot \boldsymbol{J}^*\, \mathrm{d}V \tag{14.30}$$

The time-domain version of the Poynting theorem provides a real-time snapshot of the energy dynamics in a system, focusing on the immediate power flow across the volume's boundaries, the instantaneous work done on the charges, and the rate of energy change within that volume.

In contrast, the frequency-domain version brings a new dimension to our understanding, focusing on the flow of power for distinct frequency components rather than the whole spectrum at once. This formulation takes into account phase relationships between field components and their sources that may be crucial to understanding frequency-dependent phenomena.

This new perspective breaks down the energy dynamics into the contributions from each frequency separately. This detailed breakdown can offer valuable insights into the operation and design of frequency-dependent devices and systems. The complex Poynting theorem in the frequency domain is hence a fundamental tool in our exploration of electromagnetic phenomena in the spectral domain.

15 Wessel-Berg's Principle of Reciprocal Energy Conservation

The cornerstone of Wessel-Berg's theory is a particular reciprocity relation formulated in the frequency domain, providing the backbone for the systematic analysis of energy interactions in electromagnetic systems. This equation proposes a symmetry, or reciprocity, between two independent and non-overlapping current distributions $\boldsymbol{J}_1$ and $\boldsymbol{J}_2$ with compact support that engender the fields $\boldsymbol{E}_1, \boldsymbol{H}_1$ and $\boldsymbol{E}_2, \boldsymbol{H}_2$, respectively. Encapsulating a volume V enclosed by a surface S, the proposed relation is expressed as

$$\oiint_S (\boldsymbol{E}_1 \times \boldsymbol{H}_2^* + \boldsymbol{E}_2^* \times \boldsymbol{H}_1) \cdot \hat{\boldsymbol{n}} \, \mathrm{d}S = \iiint_V (-\boldsymbol{E}_1 \cdot \boldsymbol{J}_2^* - \boldsymbol{E}_2^* \cdot \boldsymbol{J}_1) \, \mathrm{d}V, \qquad (15.1)$$

where the integrals are over a surface, S, enclosing a volume, V, which encompasses both current distributions. Here, $\hat{\boldsymbol{n}}$ is a unit vector normal to the surface S.

Interestingly, Wessel-Berg further posits that the surface integral terms in this relation equate to zero, essentially implying that both sides of the reciprocity relation are zero. This assertion, however, lacks rigorous proof and has been subject to much debate. It's worth noting that the core tenets of Wessel-Berg's theory hinge heavily on this principle.

Throughout this thesis, attempts have been made to elucidate and rectify this postulation by Wessel-Berg, who has provided scant details on its underpinnings.

After a great deal of thought, it was determined that Wessel-Berg's relation must be viewed as an reciprocity relation between the advanced and retarded solutions in order for the surface integral term to vanish. As an example, $\boldsymbol{E}_1$ and $\boldsymbol{H}_1$ can be thought of as the retarded fields originating from the current distribution $\boldsymbol{J}_1$, while $\boldsymbol{E}_2$ and $\boldsymbol{H}_2$ represent the advanced fields induced by $\boldsymbol{J}_2$. This implies that the reciprocity relation of Wessel-Berg can be expressed

$$\oiint_S (\boldsymbol{E}_1 \times \widetilde{\boldsymbol{H}}_2^* + \widetilde{\boldsymbol{E}}_2^* \times \boldsymbol{H}_1) \cdot \hat{\boldsymbol{n}} \, \mathrm{d}S = \iiint_V (-\boldsymbol{E}_1 \cdot \boldsymbol{J}_2^* - \widetilde{\boldsymbol{E}}_2^* \cdot \boldsymbol{J}_1) \, \mathrm{d}V. \qquad (15.2)$$

where we have used the tilde notation for the advanced solutions $\widetilde{\boldsymbol{E}}_2$ and $\widetilde{\boldsymbol{H}}_2$. We will in general utilize this tilde notation to represent time advanced fields in the remainder of this thesis. In this conceptual framework, one might envisage $\boldsymbol{J}_1$ as a transmitting antenna with $\boldsymbol{J}_2$ acting as the receiver. Wessel-Berg's reciprocity relation thus describes the reciprocal relationship between the retarded field of $\boldsymbol{J}_1$ and the advanced field of $\boldsymbol{J}_2$ as depicted in a spacetime diagram in Figure 21. However, this reciprocity relation can likewise be used to describe the relationship between the advanced field of $\boldsymbol{J}_1$ and the retarded field of $\boldsymbol{J}_2$ as everything is interconnected in a field theory.

The reciprocity relation thus replaces the need for the formulation of the absorber theory's free field formula (12.13). Wessel-Berg's relation additionally equates the total power radiated by the retarded fields of one system into the advanced fields of another to the inverse process by utilizing the complex conjugates of the fields and current in the frequency domain.

Thus, this reciprocity relation serves dual roles as an energy conservation law and an embodiment of the time symmetry principle inherent in the Wheeler-Feynman theory which allows the entropy of the system to be conserved. It therefore replaces the need for the free field formula (12.13) as it lacks the energy conservation properties, whilst the minus sign in the formula breaks the symmetry in the theory. This is because when a time reversal transformation is performed, the time-retarded solutions now become the time-advanced solutions and vice versa in the formula. The free field formula is not invariant due to the minus sign under this process

$$\boldsymbol{E}_{\text{free}}(\boldsymbol{r}, t) = \sum_i \frac{\boldsymbol{E}_i(\boldsymbol{r}, t) - \widetilde{\boldsymbol{E}}_i(\boldsymbol{r}, t)}{2} = 0, \quad \xrightarrow{t \to -t} \quad \boldsymbol{E}_{\text{free}}(\boldsymbol{r}, t) = \frac{\widetilde{\boldsymbol{E}}_i(\boldsymbol{r}, t) - \boldsymbol{E}_i(\boldsymbol{r}, t)}{2} = 0. \quad (15.3)$$

Although this does not directly cause an issue due to the fact that the free field is zero, the minus sign technically breaks the time symmetry of the equation. The free field is used in the absorber theory to calculate the reaction force on a charged particle. According to this theory,

when a charged particle accelerates, it emits radiation, which is absorbed by all other charges in the universe. These charges then re-radiate the energy back to the original particle, producing a reaction force. The free field is the field that is directly produced by the particle's acceleration, and it is this field that is absorbed and re-radiated by the other charges.

The above reciprocity relation (15.2) can be seen as a manifestation of this principle. It provides a way to calculate the fields generated by a given current distribution without having to solve the wave equation directly, and it also ensures the conservation of energy.

The relation of Wessel-Berg (15.2) therefore has a similar function to the free field formula of the absorber Theory posited by Wheeler and Feynman, providing an alternative perspective by linking the advanced and retarded fields. The reciprocity relation, in this interpretation, serves as a testament to the time symmetry principle in the Wheeler-Feynman theory. It declares that the total power radiated by the retarded fields of one system into the advanced fields of another equals the power radiated by the retarded fields of the second system into the advanced fields of the first.

Furthermore, this reciprocity ensures energy conservation across the entire system, especially when more than two distributions are present. This is embodied in the volume integral of Equation (15.2), stating that the energy gain of one antenna due to the work done by the fields of the other equals the energy loss of the latter. It postulates that the energy gain of one antenna, attributed to the work performed by the fields of the other antenna, must balance the energy loss of the latter, as manifested in the volume integral of Equation (15.1). This is in harmony with the principle of energy conservation, securing energy balance in systems housing more than two distributions.

Despite the similarities, Wessel-Berg's theory diverges markedly from the Wheeler-Feynman absorber theory. Rather than adhering to the free field equation, Wessel-Berg replaces it with the reciprocity relation, thereby also ensuring energy conservation within the enclosed volume. While the Absorber theory describes the total field to be the sum of half of the field as advanced and the other half as retarded, Wessel-Berg regards the retarded and advanced fields as relative terms. This suggests that a specific field can be perceived as advanced when solving Maxwell's equations for one type of current distribution, while the identical field can be deemed a retarded field for another current distribution in solving the same equations. The retarded field from the transmitters must equal the advanced field of the receiver.

This scenario echoes the notion that an emitter's current density $\boldsymbol{J}_1$ and its corresponding fields $\boldsymbol{E}_1$ and $\boldsymbol{H}_1$ that satisfy Maxwell's equations do not satisfy Wessel-Berg's reciprocity relation by themselves. The reciprocity relation requires the simultaneous satisfaction of Maxwell's equations by *both* the emitter and the receiver. Hence, we also require that the current of the reciever $\boldsymbol{J}_2$ and its fields $\widetilde{\boldsymbol{E}}_2$ and $\widehat{\boldsymbol{H}}_2$ to conform to Maxwell's equations simultaneously. Consequently, it underscores the importance of delineating the theory strictly in terms of fields. The inference here is that the motion of charges merely serves as a tool to reveal the existing fields surrounding the charge.

Let's consider a scenario where a current distribution undergoes a certain kind of acceleration at a predetermined time. We can compute the resulting radiated (retarded) field using Maxwell's equations. However, since charges necessitate a field to induce acceleration, we can also determine the advanced field that would be required beforehand for this acceleration to occur in the first place through Maxwell's equations. In this situation, the advanced field's interaction with the current results in energy loss from the charges creating the advanced field. Consequently, Wessel-Berg's reciprocity relates the advanced and retarded fields to each other, whilst preserving energy conservation within the system. This advanced field can be conceptualized as a superposition of numerous retarded fields, each stemming from different moving charges responsible for accelerating the current distribution under consideration.

At its essence, the reciprocity relation encapsulates the principle of action and reaction, bearing a resemblance to Newton's Third Law. The work accomplished by the fields of one current distribution on another is counterbalanced by the reciprocal work conducted by the fields from the second distribution acting on the first. This reciprocity ensures time reversibility and consequently aids in the preservation of the system's entropy.

It's worth noting that the application of Newton's Third Law in classical electromagnetism is not straightforward. This complexity arises from the fact that not only particles but also electromagnetic fields are capable of carrying momentum. A more detailed exploration of this subject is provided in Section 15.6.

15.1 Significance of Lossless and Reciprocal Systems

Wessel-Berg's reciprocity relation is a fundamental feature of systems where $\varepsilon^\dagger = \varepsilon$ and $\mu^\dagger = \mu$. These conditions ensure losslessness and reciprocity, which are essential for the conservation of energy and entropy in physical systems. In this section, we elucidate the critical role of these properties in microscopic systems.

Properties of Lossless and Reciprocal Systems   In the frequency domain, a reciprocal system has an invariant relationship between input and output, regardless of the direction of the signal. This can we thought analogously to Newton's third law, where the state of the system can be traced back to its past, allowing time-symmetry in the system. This is an essential aspect to possess in order to conserve the entropy within the microscopic system. Reciprocity is thus mathematically represented by symmetric permittivity, ε, and permeability, μ, tensors. This symmetry implies that the transpositions of these tensors are equal to the tensors themselves, i.e., $\varepsilon^\mathsf{T} = \varepsilon$ and $\mu^\mathsf{T} = \mu$.

Losslessness refers to a system in which there is no dissipation of energy into heat or other non-recoverable forms. In such a system, permittivity and permeability tensors are purely real, implying they have no imaginary components. This property can be represented by $\varepsilon^* = \varepsilon$ and $\mu^* = \mu$.

Microscopic Systems: Inherent Losslessness and Reciprocity   Microscopic systems must fundamentally exhibit lossless and reciprocal properties, which are critical for the conservation of energy and entropy. The violation of these principles at this level would suggest a loss of information, which is inconceivable as it contravenes the law of energy conservation.

Any apparent deviation from losslessness and reciprocity at larger scales indicates a transition from a microscopic to a macroscopic view. These deviations often correspond with energy dissipation into heat, a predominantly macroscopic process where the information is lost, time symmetry is broken and the evolution of the state of the system is no longer reversible as a consequence. Therefore, seemingly non-lossless or non-reciprocal systems at macroscopic scales should be understood as large-scale manifestations of underlying microscopic systems that inherently embody these properties.

Significance of Hermitian Permittivity and Permeability   A system is both lossless and reciprocal when it satisfies $\varepsilon^\dagger = \varepsilon$ and $\mu^\dagger = \mu$. In such a system, electromagnetic waves propagate without energy loss, and their propagation characteristics remain invariant, regardless of the direction of propagation. This behaviour stems from the combination of two conditions: (1) the symmetry of the tensors ensuring reciprocity and (2) the purely real nature of the tensors ensuring losslessness.

In conclusion, the preservation of both reciprocity and losslessness in a microscopic system is essential for maintaining the conservation of both energy and entropy. This means that at the most fundamental level, physical systems must exhibit lossless and reciprocal behaviour, since energy cannot simply vanish.

15.2 Derivation of the Reciprocity Relation

The reciprocity relation in electromagnetism can be derived from Maxwell's equations. We start with the Maxwell's equations for two systems. For the first system, we have:

$$\nabla \times \boldsymbol{E}_1 = -i\omega\mu_0\boldsymbol{H}_1, \tag{15.4}$$

$$\nabla \times \boldsymbol{H}_1 = \boldsymbol{J}_1 + i\omega\varepsilon_0\boldsymbol{E}_1, \tag{15.5}$$

And for the second system (conjugated), we have

$$\nabla \times \boldsymbol{E}_2^* = +i\omega\mu_0\boldsymbol{H}_2^*, \tag{15.6}$$

$$\nabla \times \boldsymbol{H}_2^* = \boldsymbol{J}_2^* - i\omega\varepsilon_0\boldsymbol{E}_2^*, \tag{15.7}$$

We take the scalar product of $vecH_2^*$ and the first equation of the first system and the second equation of the second system by $\boldsymbol{E}_1$, and subtract the two resulting equations

$$\boldsymbol{H}_2^* \cdot (\nabla \times \boldsymbol{E}_1) - \boldsymbol{E}_1 \cdot (\nabla \times \boldsymbol{H}_2^*) = \boldsymbol{\nabla} \cdot (\boldsymbol{E}_1 \times \boldsymbol{H}_2^*) = -i\omega\mu_0\boldsymbol{H}_1 \cdot \boldsymbol{H}_2^* - \boldsymbol{J}_2^* \cdot \boldsymbol{E}_1 + i\omega\boldsymbol{E}_1 \cdot \boldsymbol{E}_2^*. \tag{15.8}$$

Similarly, we take the scalar product of the second equation of the first system with $\boldsymbol{E}_2^*$ and the first equation of the second system by $vecH_1$, and subtract the two resulting equations

$$\boldsymbol{H}_1 \cdot (\nabla \times \boldsymbol{E}_2^*) - \boldsymbol{E}_2^* \cdot (\nabla \times \boldsymbol{H}_1) = \boldsymbol{\nabla} \cdot (\boldsymbol{E}_2^* \times \boldsymbol{H}_1) = i\omega\mu_0\boldsymbol{H}_1 \cdot \boldsymbol{H}_2^* - \boldsymbol{J}_1 \cdot \boldsymbol{E}_2^* - i\omega\boldsymbol{E}_1 \cdot \boldsymbol{E}_2^*. \tag{15.9}$$

Adding the results of these two steps, we get

$$\nabla \cdot (\boldsymbol{H}_2^* \times \boldsymbol{E}_1 + \boldsymbol{H}_1 \times \boldsymbol{E}_2^*) = -\boldsymbol{E}_1 \cdot \boldsymbol{J}_2^* - \boldsymbol{E}_2^* \cdot \boldsymbol{J}_1 \tag{15.10}$$

Applying the divergence theorem to convert the volume integral to a surface integral, we obtain the desired reciprocity relation

$$\oiint_S (\boldsymbol{E}_1 \times \boldsymbol{H}_2^* + \boldsymbol{E}_2^* \times \boldsymbol{H}_1) \cdot \hat{\boldsymbol{n}}dS = \iiint_V (-\boldsymbol{E}_1 \cdot \boldsymbol{J}_2^* - \boldsymbol{E}_2^* \cdot \boldsymbol{J}_1)\,\mathrm{d}V \tag{15.11}$$

This completes the derivation of the reciprocity relation from Maxwell's equations in the frequency domain.

15.3 Lorentz Reciprocity and Surface-Term Cancellation

Lorentz reciprocity theorem is a foundational principle in electrodynamics that correlates the interactions of electric and magnetic fields generated by different sources. For a surface S enclosing a volume V, this theorem is mathematically represented as

$$\iiint_V [\boldsymbol{J}_1 \cdot \boldsymbol{E}_2 - \boldsymbol{E}_1 \cdot \boldsymbol{J}_2]\,\mathrm{d}V = \oiint_S [\boldsymbol{E}_1 \times \boldsymbol{H}_2 - \boldsymbol{E}_2 \times \boldsymbol{H}_1] \cdot \mathrm{d}\boldsymbol{S}. \tag{15.12}$$

A key aspect of Lorentz reciprocity involves showing that the surface integral term is zero under certain conditions, such as the case where the fields propagate in a medium that is sufficiently homogeneous and isotropic at far distances. This is where the Sommerfeld radiation condition, an important concept in the study of radiating electromagnetic fields, becomes significant.

To demonstrate the cancellation of the surface term, we first assume the medium to be homogeneous and isotropic far away. The radiated fields take the form of spherical waves, propagating radially outward, along the $\hat{\boldsymbol{r}}$ direction. It is noteworthy that the direction of propagation $\hat{\boldsymbol{r}}$ is orthogonal to both the electric field $\boldsymbol{E}$ and magnetic field $\boldsymbol{H}$, which results in $\hat{\boldsymbol{r}} \cdot \boldsymbol{E} = 0$. Moreover, the magnetic field $\boldsymbol{H}$ is given by $\hat{\boldsymbol{r}} \times \boldsymbol{E}/Z$, where Z denotes the scalar impedance of the surrounding medium, defined as $\sqrt{\mu/\epsilon}$.

Now, considering the individual terms of the surface integral, we have

$$\boldsymbol{E}_1 \times \boldsymbol{H}_2 = \frac{\boldsymbol{E}_1 \times (\hat{\boldsymbol{r}} \times \boldsymbol{E}_2)}{Z},$$

which, using a vector triple product identity $\boldsymbol{A} \times (\boldsymbol{B} \times \boldsymbol{C}) = (\boldsymbol{A} \cdot \boldsymbol{C})\boldsymbol{B} - (\boldsymbol{A} \cdot \boldsymbol{B})\boldsymbol{C}$, simplifies to

$$\boldsymbol{E}_1 \times \boldsymbol{H}_2 = \frac{\boldsymbol{E}_1 \cdot \boldsymbol{E}_2}{Z}\hat{\boldsymbol{r}}.$$

Similarly, we find

$$\boldsymbol{E}_2 \times \boldsymbol{H}_1 = \frac{\boldsymbol{E}_2 \cdot \boldsymbol{E}_1}{Z}\hat{\boldsymbol{r}}.$$

Since these two terms are equal, they cancel each other out when subtracted in the surface integral of the Lorentz reciprocity theorem (15.12).

The Sommerfeld radiation condition plays a vital role in this derivation. The condition states that there are no incoming waves from infinity. This is implicitly required here because for any wave propagating radially outward in the $\hat{\boldsymbol{r}}$ direction, an incoming wave would interfere with the radiation process and cause the surface integral not to vanish. Hence, to apply Lorentz reciprocity in this context, it is necessary to adhere to the Sommerfeld radiation condition in order for the solutions of Maxwell's equation to remain unique.

15.4 Wessel-Berg's Reciprocity and Surface-Term Cancellation

Unlike the Lorentz reciprocity theorem, the same proof for the surface term cancellation does not apply directly to Wessel-Berg's reciprocity. This difference stems from the unique characteristics of the electromagnetic fields involved in each theorem. In the case of Wessel-Berg's reciprocity, an additional assumption is required for the cancellation of the surface term, that is, one of these fields must be advanced and the other retarded.

An advanced field is characterized by its convergence towards the charge emitting the field, while a retarded field expands outward from the charge. This distinction in field propagation direction fundamentally influences the conditions for the surface term cancellation in Wessel-Berg's reciprocity.

To demonstrate this, let us consider $\boldsymbol{E}_1$ to be the retarded field and $\boldsymbol{E}_2^*$ to be the advanced field. As before, we assume the medium to be homogeneous and isotropic at far distances. The radiated fields take the form of plane waves, propagating along the $\hat{\boldsymbol{r}}$ direction. For the advanced field, the wave propagates radially inward with a flipped magnetic field, while for the retarded field, the wave propagates radially outward. This characteristic property of wave propagation flips the sign magnetic field in the Sommerfeld radiation condition for the advanced field, thus allowing for the cancellation of the surface term.

In mathematical terms, considering an advanced field (denoted with a tilde) and a retarded field, the critical relation becomes

$$\boldsymbol{H}_1 = \hat{\boldsymbol{r}} \times \boldsymbol{E}_2/Z, \quad \text{and} \quad \widetilde{\boldsymbol{H}}_2^* = -\hat{\boldsymbol{r}} \times \widetilde{\boldsymbol{E}}_2^*/Z. \tag{15.13}$$

From this, we find

$$\boldsymbol{E}_1 \times \widetilde{\boldsymbol{H}}_2^* + \widetilde{\boldsymbol{E}}_2^* \times \boldsymbol{H}_1 = \boldsymbol{E}_1 \times (-\hat{\boldsymbol{r}} \times \widetilde{\boldsymbol{E}}_2^*/Z) + \widetilde{\boldsymbol{E}}_2^* \times (\hat{\boldsymbol{r}} \times \boldsymbol{E}_1/Z). \tag{15.14}$$

Simplifying this, we find

$$\boldsymbol{E}_1 \cdot \widetilde{\boldsymbol{E}}_2^*\hat{\boldsymbol{r}}/Z - \widetilde{\boldsymbol{E}}_2^* \cdot \boldsymbol{E}_1\hat{\boldsymbol{r}}/Z = 0, \tag{15.15}$$

where $\hat{\boldsymbol{r}}$ denotes a unit vector. The negative sign from the advanced field cancels with the positive from the retarded field when subtracted in the surface integral of the Wessel-Berg's reciprocity theorem, leading to the cancellation of the surface term.

Thus, by carefully considering the distinct behaviors of advanced and retarded fields, we are able to establish the conditions under which the surface term in Wessel-Berg's reciprocity vanishes. This essential insight validates the reciprocity relation in this particular scenario and sheds light on the intricate interplay of different electromagnetic fields.

15.5 Reciprocity Between Retarded and Advanced Solutions: A Deeper Insight

The intriguing aspects of the reciprocity relation and energy conservation relation, as outlined in Equation (15.2), include not just the conservation of energy but also the inclusion of advanced and retarded fields and the vanishing of the surface term. These properties stem from the symmetry in the interaction term of the Lagrangian when analyzed in the frequency domain.

The 4-vector potentials for the first and second systems, which are retarded and advanced respectively, can be written as

$$
A_1^\mu(\boldsymbol{r},\omega) = \frac{\mu_0}{4\pi} \iiint \frac{J_1^\mu(\boldsymbol{r}',\omega) e^{-i\omega\cdot\frac{|\boldsymbol{r}-\boldsymbol{r}'|}{c}}}{|\boldsymbol{r}-\boldsymbol{r}'|}\, \mathrm{d}V', \tag{15.16}
$$

$$
\widetilde{A}_2^\mu(\boldsymbol{r},\omega) = \frac{\mu_0}{4\pi} \iiint \frac{J_2^\mu(\boldsymbol{r}',\omega) e^{+i\omega\cdot\frac{|\boldsymbol{r}-\boldsymbol{r}'|}{c}}}{|\boldsymbol{r}-\boldsymbol{r}'|}\, \mathrm{d}V'. \tag{15.17}
$$

Examining the interaction term in the frequency domain leads us to the following relations

$$
\begin{aligned}
\iiint_V A_{1,\mu}(\boldsymbol{r},\omega) J_2^{\mu*}(\boldsymbol{r},\omega)\, \mathrm{d}V &= \iiint_V \left[\frac{\mu}{4\pi} \iiint_V \frac{J_1^\mu(\boldsymbol{r}',\omega) e^{-i\omega\cdot\frac{|\boldsymbol{r}-\boldsymbol{r}'|}{c}}}{|\boldsymbol{r}-\boldsymbol{r}'|}\, \mathrm{d}V' \right] J_2^{\mu*}(\boldsymbol{r},\omega)\, \mathrm{d}V \\
&= \iiint_V \left[\frac{\mu}{4\pi} \iiint_V \frac{J_2^{\mu*}(\boldsymbol{r},\omega) e^{-i\omega\cdot\frac{|\boldsymbol{r}-\boldsymbol{r}'|}{c}}}{|\boldsymbol{r}-\boldsymbol{r}'|}\, \mathrm{d}V \right] J_1^\mu(\boldsymbol{r}',\omega)\, \mathrm{d}V' \\
&= \iiint_V \left[\frac{\mu}{4\pi} \iiint_V \frac{J_2^\mu(\boldsymbol{r},\omega) e^{+i\omega\cdot\frac{|\boldsymbol{r}-\boldsymbol{r}'|}{c}}}{|\boldsymbol{r}-\boldsymbol{r}'|}\, \mathrm{d}V \right]^* J_1^\mu(\boldsymbol{r}',\omega)\, \mathrm{d}V' \\
&= \iiint_V \widetilde{A}_{2,\mu}^*(\boldsymbol{r},\omega) J_1^\mu(\boldsymbol{r},\omega)\, \mathrm{d}V,
\end{aligned} \tag{15.18}
$$

This implies an inherent symmetry between advanced and retarded fields, signifying that a retarded field $A_{1,\mu}$ acting on J_2^μ can be equivalently expressed as the advanced field $\widetilde{A}_{2,\mu}$ acting on J_1^μ. Mathematically, this can be written as

$$
\iiint_V \left(\boldsymbol{A}_1 \cdot \boldsymbol{J}_2^* - \phi_1 \rho_2^* \right) \mathrm{d}V = \iiint_V \left(\widetilde{\boldsymbol{A}}_2^* \cdot \boldsymbol{J}_1 - \widetilde{\phi}_2^* \rho_1 \right) \mathrm{d}V, \tag{15.19}
$$

and similarly,

$$
\iiint_V \left(\boldsymbol{A}_1^* \cdot \boldsymbol{J}_2 - \phi_1^* \rho_2 \right) \mathrm{d}V = \iiint_V \left(\widetilde{\boldsymbol{A}}_2 \cdot \boldsymbol{J}_1^* - \widetilde{\phi}_2 \rho_1^* \right) \mathrm{d}V, \tag{15.20}
$$

allowing the reversal of time. The latter results follow the same derivation as the former. Upon rigorous examination, the author has found only a single paper discussing reciprocity between retarded and advanced solutions by Welsh (1960) [90]. This seminal paper extends the Lorentz reciprocity theorem to handle arbitrary time dependence. Uniquely, unlike the Wessel-Berg reciprocity relation, Welsh derived his reciprocity theorem in the time domain rather than the frequency domain. The resulting formula is given by

$$
\int_t \oiint (\boldsymbol{E}_1 \times \widetilde{\boldsymbol{H}}_2 + \widetilde{\boldsymbol{E}}_2 \times \boldsymbol{H}_1) \cdot \hat{\boldsymbol{n}}\, \mathrm{d}S\, \mathrm{d}t = \int_t \iiint_V (-\boldsymbol{E}_1 \cdot \boldsymbol{J}_2 - \widetilde{\boldsymbol{E}}_2 \cdot \boldsymbol{J}_1)\, \mathrm{d}V\, \mathrm{d}t \tag{15.21}
$$

where the time integral is performed over a specific interval $T_1 < t < T_2$. Here, T_1 denotes a time before the sources are activated, and T_2 represents the time after the sources are deactivated.

Alternatively, the time integral can also extend from negative to positive infinity, converting Equation (15.21) into a convolution. This yields a direct parallel between the Wessel-Berg's relation in the frequency domain and Welch's formula, illustrating the fundamental symmetry that exists between advanced and retarded solutions.

15.6 Energy Conservation and Self-Interaction Terms

Wessel-Berg's formula is marked by complex conjugates, which translate the reciprocity relation in terms of power flow. This is inherent in a microscopic system where the electric and magnetic fields in Poynting's vector (14.28) are synthesized from microscopic components. Specifically, we have $\boldsymbol{E}(\boldsymbol{r}, \omega) = \sum_{i=1}^{n} \boldsymbol{E}_i$ and $\boldsymbol{H}(\boldsymbol{r}, \omega) = \sum_{i=1}^{n} \boldsymbol{H}_i$, causing Equation (14.28) to evolve into

$$
\begin{aligned}
\boldsymbol{S}(\boldsymbol{r}, \omega) &= \frac{1}{4} \left(\boldsymbol{E} \times \boldsymbol{H}^* + \boldsymbol{E}^* \times \boldsymbol{H} \right) \\
&= \frac{1}{4} \left[\left(\sum_{i=1}^{n} \boldsymbol{E}_i \right) \times \left(\sum_{j=1}^{n} \boldsymbol{H}_j^* \right) + \left(\sum_{j=1}^{n} \boldsymbol{E}_j^* \right) \times \left(\sum_{i=1}^{n} \boldsymbol{H}_i \right) \right] \\
&= \frac{1}{4} \sum_{i,j} \left[\boldsymbol{E}_i \times \boldsymbol{H}_j^* + \boldsymbol{E}_j^* \times \boldsymbol{H}_i \right]
\end{aligned}
\tag{15.22}
$$

Interestingly, this term bears a resemblance to the surface integral in Wessel-Berg's reciprocity relation and would also be similar to Welsh's had we performed the same procedure in the time domain.

This implies that Wessel-Berg's reciprocity relation represents energy exchange within a system such that the work performed by one field (e.g., $\boldsymbol{E}_1$) on current $\boldsymbol{J}_2$ is equal to the work exerted by field $\boldsymbol{E}_2$ on $\boldsymbol{J}_1$ if the system remains unaffected by external influences. In this scenario, the volume integral of (15.2) should equal zero, consequently making the surface integral zero, which implies no energy escape from the closed surface S encapsulating the volume V. If energy transfer is only occurring within the microscopic system enclosed by surface S, then the volume integral of (15.2) would indeed be zero, resulting in zero surface integral of the power outflow from the system and thereby preserving the overall energy.

However, if the surface integral is non-zero, it suggests the presence of external factors influencing our system that are not part of our microscopic system. In this scenario, if we expand the surface S to include these external factors, the surface integral would become zero, implying that all energy exchange occurs within the microscopic system.

To illustrate this, consider two currents $\boldsymbol{J}_1$ and $\boldsymbol{J}_2$ where surface S only encloses $\boldsymbol{J}_1$, the transmitting antenna. Consequently, the volume integral within this confined volume would not equal zero, leading to a net energy outflow from the surface. This energy would, however, be directed towards current $\boldsymbol{J}_2$. Expanding surface S to include $\boldsymbol{J}_2$ would restore the zero state of the surface term, thereby conserving the system's energy.

Of note, Equation (15.22) contains self-interaction terms where $i = j$, namely $\boldsymbol{E}_i \times \boldsymbol{H}_i^* + \boldsymbol{E}_i^* \times \boldsymbol{H}_i$. These terms should be excluded, as was the case in our previous analysis of the Lorentz force and the interaction terms of the Lagrangian. These self-interaction fields are removed from both the Wessel-Berg and Welsh reciprocity relations, as they do not contribute to the total power flow on the surface of S. A similar procedure for the current and electric field would yield terms like $\boldsymbol{E}_i \cdot \boldsymbol{J}_i$, which would suggest the currents' self-produced fields perform work on themselves—an assertion incompatible with any microscopic theory. The exclusion of these self interaction terms are easily accomplished with the inclusion of the antiphoton solutions which are obtained by a time reversal of Wessel-Berg's reciprocity relation.

15.6.1 Interpretation of Macroscopic Field Energy and the Connection to Poynting's Theorem

An enlightening perspective on the essence of Wessel-Berg's reciprocity as a principle of energy conservation can be attained by examining Poynting's theorem in the frequency domain (Equation (14.30)).

Wessel-Berg postulates that the field energy, $u(\boldsymbol{r}, t) = \frac{1}{2}(\epsilon_0 \boldsymbol{E} \cdot \boldsymbol{E} + \mu_0 \boldsymbol{H} \cdot \boldsymbol{H})$ or its equivalent in the frequency domain, $u(\boldsymbol{r}, \omega) = \frac{1}{2}(\varepsilon_0 \boldsymbol{E} \cdot \boldsymbol{E}^* - \mu_0 \boldsymbol{H} \cdot \boldsymbol{H}^*)$, should be viewed as a macroscopic quantity by stating the following [91, p. 36-37]:

> *These properties, being entirely foreign in classical electromagnetism, are likely to cause wariness amongst readers familiar with electromagnetic theory. Some readers might feel compelled to outright reject these unfamiliar concepts, perhaps arguing that nonzero fields are always associated with a corresponding nonzero energy density u which in free space is specified by the usual formula:*
>
> $$u = \frac{1}{2}(\epsilon_0 \boldsymbol{E} \cdot \boldsymbol{E} + \mu_0 \boldsymbol{H} \cdot \boldsymbol{H}) \tag{15.23}$$
>
> *How is this formula to be reconciled with the concept of doublets having zero energy in spite of the fact that their fields are nonzero? The answer to this question is that (15.23) is a special case applicable to macroscopic electromagnetism only; the relation does not apply in the neoclassical formulation. In assessing these subtle differences it is well to keep in mind that a general procedure for determining energy density must be based on the excitation process itself, relating the buildup of energy to the required expenditure of power influx into the relevant volume of space. And for the plane wave doublets the result of such a process is zero energy density, as shown in (2.54, Wessel-Berg's book). In the macroscopic classical case the same process leads to the well known formula (15.23). Both formulae are correct in the model environments for which they are defined. For the comfort of the concerned readers these questions, relating to the build up of bitemporal electromagnetic energy, are discussed more thoroughly in the next chapter.*

Regrettably, Wessel-Berg does not provide a detailed explanation regarding why the field energy should be interpreted as a macroscopic quantity. Nonetheless, one may gain insights into its macroscopic nature by leveraging the microscopic superposition principle.

Before invoking this principle, it's crucial to acknowledge upfront that the very notion of an external macroscopic field energy loses its relevance in a microscopic context. Typically, an external field energy is predefined for any system under consideration. Given that all fields stem from moving charges, it logically follows that these moving charges must form a part of the microscopic system for the system as a whole to qualify as microscopic. Under these circumstances, it is no longer pertinent to enforce a macroscopic field onto the system. Instead, one could define this field as a superposition of individual fields each produced by their respective currents within the system.

To illuminate this point, consider applying the microscopic superposition principle to a modified form of Poynting's theorem in the frequency domain, wherein Equation (14.30) is multiplied by 2, leading to

$$\oiint_S \boldsymbol{E} \times \boldsymbol{H}^* \cdot \mathrm{d}\boldsymbol{S} = i\omega \iiint_V (\varepsilon_0 \boldsymbol{E} \cdot \boldsymbol{E}^* - \mu_0 \boldsymbol{H} \cdot \boldsymbol{H}^*) \, \mathrm{d}V - \iiint_V \boldsymbol{E} \cdot \boldsymbol{J}^* \, \mathrm{d}V. \tag{15.24}$$

Given that all fields arise from charges, the microscopic superposition principle necessitates that in a microscopic system, all fields $\boldsymbol{E}(\boldsymbol{r}, \omega) = \sum_i \boldsymbol{E}_i(\boldsymbol{r}, \omega)$ and $\boldsymbol{H}(\boldsymbol{r}, \omega) = \sum_i \boldsymbol{H}_i(\boldsymbol{r}, \omega)$ should be broken down, where each ith component is associated with the field produced by the ith constituent

within the microscopic system. Implementing this principle to Equation (15.24), we obtain

$$\oiint_S \left(\sum_i \boldsymbol{E}_i \right) \times \left(\sum_j \boldsymbol{H}_j^* \right) \cdot \hat{\boldsymbol{n}} \, \mathrm{d}S$$

$$= i\omega \iiint_V \left[\varepsilon_0 \left(\sum_i \boldsymbol{E}_i \right) \cdot \left(\sum_j \boldsymbol{E}_j^* \right) - \mu_0 \left(\sum_i \boldsymbol{H}_i \right) \cdot \left(\sum_j \boldsymbol{H}_j^* \right) \right] \mathrm{d}V - \iiint_V \left(\sum_i \boldsymbol{E}_i \right) \cdot \left(\sum_j \boldsymbol{J}_j^* \right) \mathrm{d}V.$$

$$(15.25)$$

In our microscopic system, the currents that produce the fields are contained within, thus allowing us to utilize Maxwell's equations to express the two fields as

$$\boldsymbol{E}_i = \frac{1}{i\omega\epsilon_0} (\boldsymbol{\nabla} \times \boldsymbol{H}_i - \boldsymbol{J}_i), \qquad \boldsymbol{H}_j^* = \frac{1}{i\omega\mu_0} (\boldsymbol{\nabla} \times \boldsymbol{E}_j^*). \qquad (15.26)$$

These two relationships can then be inserted into the energy density term, $\varepsilon_0 \boldsymbol{E} \cdot \boldsymbol{E}^* - \mu_0 \boldsymbol{H} \cdot \boldsymbol{H}^*$, deconstructing it into its microscopic constituents such that

$$\sum_{i,j} \oiint_S \boldsymbol{E}_i \times \boldsymbol{H}_j^* \cdot \mathrm{d}\boldsymbol{S} = \sum_{i,j} \iiint_V (\boldsymbol{E}_j^* \cdot (\boldsymbol{\nabla} \times \boldsymbol{H}_i - \boldsymbol{J}_i) - \boldsymbol{H}_i \cdot (\boldsymbol{\nabla} \times \boldsymbol{E}_j^*)) \, \mathrm{d}V - \sum_{i,j} \iiint_V \boldsymbol{E}_i \cdot \boldsymbol{J}_j^* \, \mathrm{d}V. \quad (15.27)$$

By utilizing the vector identity $\boldsymbol{\nabla} \cdot (\boldsymbol{A} \times \boldsymbol{B}) = \boldsymbol{B} \cdot (\boldsymbol{\nabla} \times \boldsymbol{A}) - \boldsymbol{A} \cdot (\boldsymbol{\nabla} \times \boldsymbol{B})$, invoking the divergence theorem, and rearranging terms, we arrive at

$$\sum_{i,j} \oiint_S (\boldsymbol{E}_i \times \boldsymbol{H}_j^* + \boldsymbol{E}_j^* \times \boldsymbol{H}_i) \cdot \mathrm{d}\boldsymbol{S} = \sum_{i,j} \iiint_V (-\boldsymbol{E}_i \cdot \boldsymbol{J}_j^* - \boldsymbol{E}_j^* \cdot \boldsymbol{J}_i) \, \mathrm{d}V. \qquad (15.28)$$

Here, the field energy term $\varepsilon_0 \boldsymbol{E} \cdot \boldsymbol{E}^* - \mu_0 \boldsymbol{H} \cdot \boldsymbol{H}^*$ that was initially present in Poynting's theorem (15.24) has vanished. This disappearance occurs as the term has been identified with and accounted for by the sources present within the microscopic system.

Equation (15.28) resembles Wessel-Berg's reciprocity relation when the self-interaction terms (where $i = j$) are disregarded. Additionally, some of these fields need to be advanced in order for the surface integral to be zero, although this is not a requirement. This means that Wessel-Berg's reciprocity relation is a special case of (15.28). Thus, we have demonstrated that the Wessel-Berg reciprocity theorem emerges as a special case of energy conservation from the application of Poynting's theorem.

Through this exploration, we have gained a deeper understanding of why the electromagnetic field energy, $u(\boldsymbol{r}, \omega) = \frac{1}{2}(\varepsilon_0 \boldsymbol{E} \cdot \boldsymbol{E}^* - \mu_0 \boldsymbol{H} \cdot \boldsymbol{H}^*)$, is considered as a macroscopic quantity. This is because, in a microscopic context, this field energy must originate from charges contained within the microscopic system. Consequently, these fields can be traced back to their originating currents within this microscopic system, allowing them to be re-expressed in terms of the underlying currents using Equations (15.26) of Maxwell's equations, leading to a modified Poynting theorem equation with the absence of the Wessel-Berg's Reciprocity relation.

15.6.2 Newton's Third Law and Conservation of Momentum

Newton's third law of motion states that for every action, there is an equal and opposite reaction. This law holds up quite well in a wide range of physical situations, including many in classical mechanics. However, in the context of electromagnetism and various other fields of modern physics like quantum mechanics or general relativity, its straightforward application may not be accurate or sufficient. This does not imply that Newton's third law is invalid in electromagnetism, but rather that the law must be applied in a more comprehensive manner.

The electromagnetic force doesn't act instantaneously at a distance, but instead, it propagates with the speed of light. This implies that the "reaction" to a changing electric or magnetic field isn't immediate, but takes some time to propagate, which seems to violate the instantaneity implied by Newton's third law.

Moreover, electromagnetic fields themselves can carry momentum. According to the theory of electromagnetism, changes in the distribution of electric charges and currents can produce electromagnetic fields that propagate outwards carrying energy, momentum, and angular momentum.

In the electromagnetic interaction between charged particles, for example, if a charged particle emits a photon (the pixel of the electromagnetic field) then both the particle and the photon will carry momentum. If the photon is absorbed by another charged particle, that particle will gain the photon's momentum, thus preserving the total momentum of the system. In this sense, if we consider the entire system including both particles and the electromagnetic field, the law of conservation of momentum is preserved, which is a more generalized interpretation of Newton's third law.

However, given that the microscopic version of electromagnetism presumes all radiation to be a reciprocal process between the emitter and absorber, whilst being able to account for and attribute the presence of the field energy term to within the microscopic system itself, Newton's third law becomes easier to conceptualize and apply in these scenarios. This is mainly due to the fact that there is no need to account for the momentum carried by the electromagnetic fields as their ultimate destination is predetermined. This further illustrates the usefulness of the reciprocity relation in conserving momentum in addition to energy within a microscopic system.

16 Understanding the Nonradiation Condition

The nonradiation condition, a fundamental principle in classical electromagnetism, illustrates scenarios where an accelerating charge distribution does not emit electromagnetic radiation. A single point charge undergoing acceleration will invariably radiate as per Larmor's formula and the Lienard-Wiechert potentials [45]. However, when dealing with multiple point charges—collectively referred to as a charge distribution—it's possible that radiation from some charges can be wholly absorbed by others, culminating in a net zero radiation from the system as a whole. This condition will be shown to be a useful tool in Wessel-Berg's theory.

In the contemporary understanding, pioneered by Hermann A. Haus [45], the nonradiation condition rests on the Fourier transform of the current distribution

$$\boldsymbol{J}(\boldsymbol{k}, \omega) = \iiiint\limits_{-\infty}^{\infty} \boldsymbol{J}(\boldsymbol{r}, t) e^{i(\boldsymbol{k} \cdot \boldsymbol{r} - \omega t)} \mathrm{d}t \mathrm{d}^3 \boldsymbol{r}, \tag{16.1}$$

nullifying for its light-like components, such that

$$\boldsymbol{J}(\boldsymbol{k}, \omega) = 0, \qquad \text{when} \qquad \omega^2 - c^2 |\boldsymbol{k}|^2 = 0, \tag{16.2}$$

where ω represents the frequency, c is the speed of light, and $\boldsymbol{k}$ is the wave vector of the Fourier component [39]. This means the nonradiation condition holds true when a charge distribution, even under acceleration, lacks any Fourier components that resonate with waves traveling at light speed.

16.1 Illustration: Particle with Constant Velocity

An intriguing application of the nonradiation condition comes in the case of a charge moving with a constant velocity. In this scenario there is an absence of acceleration, so that the charge doesn't radiate. This is not due to lack of acceleration but is instead attributed to the absence of any Fourier components that coincide with the speed of light [45].

To explore this, let us consider a particle with charge q moving along the trajectory $\boldsymbol{r}_s(t)$ as a function of time. The charge distribution and current distribution can be represented as

$$\rho(\boldsymbol{r}, t) = q \delta^3(\boldsymbol{r} - \boldsymbol{r}_s(t)), \qquad \boldsymbol{J}(\boldsymbol{r}, t) = q \dot{\boldsymbol{r}}_s(t) \delta^3(\boldsymbol{r} - \boldsymbol{r}_s(t)). \tag{16.3}$$

Taking the spatial Fourier transform of the current distribution yields

$$\boldsymbol{J}(\boldsymbol{k}, t) = \iiint\limits_{-\infty}^{\infty} \boldsymbol{J}(\boldsymbol{r}, t) e^{i(\boldsymbol{k} \cdot \boldsymbol{r})} \mathrm{d}^3 \boldsymbol{r} = q \dot{\boldsymbol{r}}_s(t) e^{i \boldsymbol{k} \cdot \boldsymbol{r}_s(t)}. \tag{16.4}$$

If we consider the velocity to be constant, we can express $\boldsymbol{r}_s(t) = \boldsymbol{v}t$ where $\boldsymbol{v}$ is a constant velocity vector. This assumption allows for

easy computation of the temporal Fourier transform:

$$\boldsymbol{J}(\boldsymbol{k}, \omega) = \int\limits_{-\infty}^{\infty} \boldsymbol{J}(\boldsymbol{k}, t) e^{i(-\omega t)} \mathrm{d}t = \int\limits_{-\infty}^{\infty} q \boldsymbol{v} e^{i(\boldsymbol{k} \cdot \boldsymbol{v}t - \omega t)} \mathrm{d}t = 2\pi q \boldsymbol{v} \delta(\boldsymbol{k} \cdot \boldsymbol{v} - \omega), \tag{16.5}$$

leading to the realization that nonzero components only exist when

$$|\boldsymbol{k}||\boldsymbol{v}| \cos(\theta) = \omega, \tag{16.6}$$

with θ being the angle between the arbitrary vectors $\boldsymbol{k}$ and $\boldsymbol{v}$. Given that $-1 \leq \cos(\theta) \leq 1$ and $|\boldsymbol{v}| < c$, it follows that

$$-|\boldsymbol{k}|c < |\boldsymbol{k}||\boldsymbol{v}| \cos(\theta) < |\boldsymbol{k}|c, \tag{16.7}$$

which implies that the particle with constant velocity $\boldsymbol{v}$ lacks components synchronous with the speed of light [45]. Hence, the particle doesn't radiate into the far field.

The nonradiation condition thus serves as a fundamental theorem for discerning whether a given current distribution will radiate. In this context, a charge moving at a constant velocity does not radiate, not because it's unaccelerated, but because it lacks Fourier components that resonate with light speed.

16.2   Another Example: The Rotating Charged Sphere

Abbott and Griffiths provide another fascinating instance of the nonradiation condition through their exploration of a charged, rotating sphere [1]. They reveal that, contrary to conventional expectations, it is feasible for an extended charged body, such as a spherical shell, to undergo acceleration without radiating.

If the sphere's center oscillates sinusoidally at certain frequencies satisfying $\sin(\omega R/c) = 0$, or equivalently $\omega_j = j\pi c/R$ (with j as an integer), the sphere will remain radiation-free. The nonradiation condition applies not only to these specific frequencies but also to any superposition of them. As such, any periodic motion with a duration of $2R/c$, which is the time it takes for light to travel across the sphere's diameter, results in no radiation.

Extending this concept to a spherical shell that rotates sinusoidally about a diameter, the sphere will not radiate if its frequency satisfies the condition $j_1(\omega R/c) = 0$, where $j_1(z)$ is the first-order spherical Bessel function.

These examples underscore the intriguing potential to manipulate extended charged bodies, even those experiencing acceleration, to prevent them from radiating. The nonradiation condition thus challenges conventional wisdom derived from simpler models and holds considerable relevance for the design of systems seeking to limit radiation losses. The understanding of such conditions has proved crucial in interpreting phenomena like Cherenkov radiation, where the speed of light in the medium is less than c [45]. The nonradiation condition emerges as a powerful tool when scrutinizing entropy leakage within a system, providing vital insights into the criteria for a system's closure. Moreover, this theorem paves the way for quantifying the role of photon doublets in any given electromagnetic setup.

17 Implications of Wessel-Berg's Formulation

The distinct perspectives brought forth by Wessel-Berg's theory and conventional electromagnetic theory can be best illustrated by a conceptual example. This exploration will allow us to delve into the peculiar notion of self-interaction terms and highlight their inherent inconsistencies.

A Theoretical Dilemma: The Lonely Star Imagine a solitary star in an otherwise empty universe. In such a scenario, one may question whether the star would radiate. Specifically, if a charge on the star's surface were to accelerate, would it emit radiation into the void? According to conventional theory, the self-interaction fields from the charge ($\boldsymbol{E}_1 \times \boldsymbol{H}_1$) should propagate throughout the universe, despite the lack of a receiver for this radiation.

This theoretical situation raises issues when considering time-reversed circumstances—advanced radiation fields converging from infinity towards the lone charge. Given that all fields originate from moving charges, these converging fields cannot stem from other charges, contradicting the fundamental premise that the universe is empty.

Self-interaction and Its Consequences Classical electrodynamics grapples with the challenge of self-interaction, which often leads to the emergence of infinities (self-energy problems). Although regularization techniques are employed to manage these issues, it's only within quantum electrodynamics (QED) that a comprehensive solution is offered, via renormalization.

This leads us to question the nature of radiation itself: If there's no charge to absorb a photon, can the photon genuinely be said to exist? Classical electrodynamics posits that an accelerating charge radiates irrespective of the presence of another charge to absorb the radiation, leading to the propagation of an electromagnetic wave carrying energy and momentum.

A Different Perspective: Wheeler-Feynman and Wessel-Berg In contrast, the Wheeler-Feynman absorber theory and Wessel-Berg's reciprocity theorem present a more interactive view of emission and absorption. They suggest that radiation must involve a reciprocal relationship between the emitter and the receiver. This concept indicates that electromagnetic radiation must 'know' its destination before emission, a notion that challenges our classical understanding.

Such a framework would suggest that in instances where this reciprocal relationship is not satisfied, self- interaction fields are reflected by an antiphoton, preventing the charge from emitting the intended radiation pattern, thus cancelling that radiation mode. A similar phenomenon is observed in the double slit experiment described in Wessel-Berg's book.

Repercussions on Our Lonely Star In the light of this, we might conclude that a solitary star in an otherwise empty universe might not radiate, as there is nothing to transfer energy towards. The self-interaction fields, which represent a charge's reaction to its own field, pose a complex issue in classical electrodynamics. In Wessel-Berg's reciprocity relation, these fields are notably absent, the focus instead being placed on the 'cross terms', signifying the interaction between different sets of fields and currents.

In contrast, conventional macroscopic electromagnetic theory holds that an isolated accelerating charge will radiate irrespective of the presence of a specific receiver for the radiation. This perspective, depicted by the Larmor formula in classical electrodynamics, manifests in various phenomena such as synchrotron radiation from charged particles in magnetic fields.

Delving Deeper: Absorber Theory and Transactional Interpretation These philosophical quandaries link closely to concepts like the Wheeler-Feynman absorber theory and the transactional interpretation of quantum mechanics [23]. Both propose radiation as a time-symmetric interaction between emitter and absorber.

The Wheeler-Feynman absorber theory, which considers both retarded and advanced solutions of Maxwell's equations (representing waves traveling forwards and backwards in time, respectively), suggests a time-symmetric transaction linking cause and effect. In this theory, for a particle to radiate, there must be an absorber somewhere in the future, implying a form of retrocausality.

This interpretation shares several similarities with the transactional interpretation of quantum mechanics, proposed by John G. Cramer [23]. It argues that the wave function involves a transaction between the emitter and the absorber, bringing a unique perspective to the radiation process.

Returning to our hypothetical scenario, our lonely star, as per these interpretations, would not radiate since there are no other charges to absorb the radiation. These would be nothing to radiate towards and nothing to transfer the energy towards. This conclusion, seemingly contradictory to our conventional understanding of radiation, highlights the intriguing concepts brought forth by these unconventional theories.

17.1 Unraveling Self-Interaction Fields

The Concept and Issues of Self-Interaction The concept of self-interaction fields arises when we consider a particle, such as an electron, moving in its own generated field. Within classical electrodynamics, this electron, while being the origin of an electric field, is also influenced by it, leading to the creation of a 'self-force'. This seemingly benign situation, however, poses a significant issue. As this self-force is singular at the electron's position, an infinite self-energy of the electron emerges, a stark contrast to the observed finite mass-energy of the electron. This apparent paradox is addressed through the process of renormalization.

Such complications are not unique to electrodynamics but also surface in other field theories. These complexities often indicate that the particular field theory, being an effective theory, is only valid below a certain energy scale and above a certain length scale. Beyond these scales, the theory may fail to accurately describe the physical phenomena. This emphasizes the fact that effective theories have their limitations and are not universally applicable across all energy scales and distances.

Wessel-Berg's Reciprocity Theorem and Self-Interaction Fields Within the framework of Wessel-Berg's reciprocity theorem, self-interaction fields, represented by terms such as $\boldsymbol{E}_1 \times \boldsymbol{H}_1^*$ and $\boldsymbol{E}_2 \times \boldsymbol{H}_2^*$ where fields and their sources belong to the same system, are conspicuously absent. This absence suggests that the theorem's primary concern lies in the interaction of distinct sources through their respective fields, sidelining self-interaction issues.

In many practical applications of electromagnetism, our focus often gravitates towards how one system, represented by $\boldsymbol{E}_1, \boldsymbol{H}_1, \boldsymbol{J}_1$, interacts with another system, described by $\boldsymbol{E}_2, \boldsymbol{H}_2, \boldsymbol{J}_2$. Consequently, the investigation of a system's self-interaction becomes less pertinent. This viewpoint aligns harmoniously with the reciprocity theorem, reinforcing its broader physical relevance.

As already discussed, the Wheeler-Feynman absorber theory assumes the presence of absorbers in the universe, which are needed to interact with the advanced and retarded waves produced by a radiating source removing the need for these self-interacting fields. This absorber concept is used to justify the time-symmetric aspects of the theory.

The idea that a photon 'knows' its destination prior to emission, or that a star would not radiate without an absorber, has profound implications that challenge our standard conceptions of cause and effect. These ideas are reminiscent of the *transactional interpretation* of quantum mechanics, which proposes that quantum processes are 'transactions' involving a backward-in-time wave (from the absorber to the emitter) and a forward-in-time wave (from the emitter to the absorber) which likewise avoids these self-interacting fields situations [22].

Radiation, Self-Acceleration, and Runaway Solutions Another puzzling manifestation of self-interaction emerges when contemplating a charged particle accelerating in its own electric field. Intuitively, this situation suggests the particle should radiate energy, leading to the dilemma of 'self-

acceleration' or 'runaway solutions'. In this scenario, particles appear to perpetually accelerate, culminating in absurd physical predictions.

Exclusion of self-interaction could be perceived as a convenient strategy to evade these associated issues. Yet, it also implies that the theorem provides a more specific insight than just the total system energy—it captures the energy transfer or interaction between different sources.

The Challenges and Implications of Self-Interaction Fields   The interpretation and handling of self-interaction fields pose significant challenges within the realm of theoretical physics, spanning both classical and quantum contexts. They raise profound physical and mathematical questions about the nature of particles and fields, the role of infinities in physics, and the limitations of our physical theories. This highlights the need for a more comprehensive understanding and effective resolution of self-interaction problems, an endeavor that remains an active area of research in theoretical physics.

17.2   Example: Wessel-Berg's Reciprocity and Perfect Conductors

In this section, we examine an intriguing application of the Wessel-Berg reciprocity relation

$$\oiint_S (\boldsymbol{E}_1 \times \widetilde{\boldsymbol{H}}_2^* + \widetilde{\boldsymbol{E}}_2^* \times \boldsymbol{H}_1) \cdot \hat{\boldsymbol{n}} \, \mathrm{d}S = \iiint_V (-\boldsymbol{E}_1 \cdot \boldsymbol{J}_2^* - \widetilde{\boldsymbol{E}}_2^* \cdot \boldsymbol{J}_1) \, \mathrm{d}V, \qquad (17.1)$$

to the case of a perfectly conducting boundary, which offers unique and remarkable properties.

Consider a transmitting antenna located inside a volume V, enclosed by a surface S. This antenna is characterized by the current $\boldsymbol{J}_1$ contained entirely within V and generates the retarded electromagnetic fields $\boldsymbol{E}_1$ and $\boldsymbol{H}_1$. In this particular example, the receiving antenna embodies a perfect conductor that takes the form the thin surface S enclosing the volume V. This antenna has surface electric and magnetic currents denoted as $\boldsymbol{J}_{S,2}$ and $\boldsymbol{M}_{S,2}$ respectively which are impressed on the surface. In our analysis, the magnetic current, $\boldsymbol{M}_{S,2}$, is an imaginary current, a mathematical construct for the application of the surface equivalence principle. Additionally, we focus on neutral currents, excluding Coulomb fields, and only consider radiation fields. These assumptions simplify our study without impacting the generality of our results.

Since the receiving antenna is a perfect conductor, the retarded electromagnetic fields emitted from $\boldsymbol{J}_1$ will induce surface currents on S whose fields superimpose with the original field to exactly cancel both the electric and magnetic fields inside the perfectly conducting material. The surface electric current $\boldsymbol{J}_{S,2}$ and surface magnetic current $\boldsymbol{M}_{S,2}$ in such a scenario can be determined using the surface equivalence principle with the following relations

$$\boldsymbol{J}_{S,2} = \hat{\boldsymbol{n}} \times (\boldsymbol{H}_{\mathrm{OUT}} - \boldsymbol{H}_{\mathrm{IN}}), \qquad \boldsymbol{M}_{S,2} = -\hat{\boldsymbol{n}} \times (\boldsymbol{E}_{\mathrm{OUT}} - \boldsymbol{E}_{\mathrm{IN}}). \qquad (17.2)$$

Here, $\boldsymbol{E}_{\mathrm{OUT}}$ and $\boldsymbol{H}_{\mathrm{OUT}}$ represent the total electric and magnetic fields immediately outside the surface S. Similarly, $\boldsymbol{E}_{\mathrm{IN}}$ and $\boldsymbol{H}_{\mathrm{IN}}$ represent these fields immediately inside the surface S.

Perfect conductors, in theory, do not permit electric fields to penetrate their surface. This is because the free electrons in the conductors can rearrange themselves in response to an external electric field, creating an induced electric field that exactly cancels out the external one. This effect happens extremely quickly, so for all practical purposes, the outside of this perfect conductor does not experience any of the electromagnetic fields resulting from the inside sources.

Additionally, perfect conductors are also perfect reflectors of electromagnetic waves. This is because an electromagnetic wave induces currents in the conductor, and these currents in turn radiate their own electromagnetic waves, out of phase with the original, which results in destructive interference and the cancellation of the incident wave.

Since we have a current inside a closed perfect conductor, the electromagnetic radiation it produces would not be able to penetrate or escape the conductor. The radiation would be reflected off the inner surface of the conductor.

Given that the surface S is a perfect conductor, the fields outside it $\boldsymbol{H}_{\text{OUT}} = \boldsymbol{E}_{\text{OUT}} = \boldsymbol{0}$. Furthermore, in this setup, the advanced fields arising from the surface currents $\boldsymbol{J}_{S,2}$ and $\boldsymbol{M}_{S,2}$, denoted as $\widetilde{\boldsymbol{E}}_2$ and $\widetilde{\boldsymbol{H}}_2$ respectively, must equal the retarded fields of $\boldsymbol{E}_1$ and $\boldsymbol{H}_1$ originating from within the surface such that the total field S

$$\boldsymbol{E}_{\text{IN}}(\boldsymbol{r}, t) = \boldsymbol{E}_1(\boldsymbol{r}, t) = \widetilde{\boldsymbol{E}}_2(\boldsymbol{r}, t), \qquad \boldsymbol{H}_{\text{IN}}(\boldsymbol{r}, t) = \boldsymbol{H}_1(\boldsymbol{r}, t) = \widetilde{\boldsymbol{H}}_2(\boldsymbol{r}, t), \qquad \forall \boldsymbol{r} \in V, \qquad (17.3)$$

implying that the actual field in V can be represented equivalently by either the retarded or advanced radiation fields, due to their relative nature.

This consideration underscores a fundamental paradigm shift in our understanding of electromagnetic interactions. Conventionally, we associate causality with field generation, often imagining fields as 'produced' by charges. This, however, is an oversimplification. A more nuanced perspective considers the co-existence of charges and fields, viewing charges' motion as unveiling the existing fields and vice versa.

In this non-causal framework, the existence of these fields and the motion of charges are interrelated, but not causal in nature. Measuring the charge's motion simply discloses the fields expected around the charge, both preceding (advanced) and following (retarded) its motion. Analogously, measuring a state in phase space neither 'causes' nor 'creates' its future or past trajectory. The trajectory simply exists in its entirety, and our measurements of a state at an instant merely reveals its future and past states via Hamilton's equations. In a similar vein, discerning the motion of a charge uncovers the fields before and after its motion, whilst discerning the fields uncovers the existing motion of charges.

Additionally, the retarded fields on the surface currents $\boldsymbol{E}_2$ and $\boldsymbol{H}_2$ that are generated *outside* the surface S destructively interfere with the retarded fields of $\boldsymbol{J}_1$, so such that the total field

$$\boldsymbol{E}_{\text{OUT}}(\boldsymbol{r}, t) = \boldsymbol{E}_1(\boldsymbol{r}, t) + \boldsymbol{E}_2(\boldsymbol{r}, t) = 0, \qquad \boldsymbol{H}_{\text{OUT}}(\boldsymbol{r}, t) = \boldsymbol{H}_1(\boldsymbol{r}, t) + \boldsymbol{H}_2(\boldsymbol{r}, t) = 0, \quad \forall \boldsymbol{r} \notin V.$$
$$(17.4)$$

This situation results in the total reflection of the electromagnetic fields generated inside V, resulting in the containment of the fields within the volume. This confinement naturally satisfies the noradiation condition which also implies that energy is dissipated from the system.

This example is essentially a 3D version of the 1D example of Figure 21, where we see that the advanced and retarded waves match one another in the region between them and interfere destructively elsewhere. However, unlike the absorber theory, which assumes that the total field is half retarded and half advanced, this formulation stipulates that these are relative terms. In this situation, the existing field inside S can either be found by examining the advanced field resulting from currents on the surface, or equivalently, the retarded fields from the current inside V, as these must match. Therefore, these two equivalent solutions both describe the same physical field. The motion of the charges can rather be thought of a useful tool that can be used to reveal the nature of this preexisting field in these bitemporally causal microscopic systems.

This equality showcases an elegant manifestation of the Wessel-Berg reciprocity relation and suggests a profound reciprocity between advanced and retarded fields under such conditions. In this context, the currents on the perfect conductor serve as an instructive metaphor for the particles, or 'absorbers', found in the remainder of the universe. These absorbers are typically omitted in smaller-scale microscopic system analyses, yet they play a significant role in engaging with self-interaction fields which are similarly excluded from these microscopic models. Despite their absence from the smaller system, their effects persist and are essentially negated by the antiphotons within the system, thereby giving rise to photon doublets. As a result, these particles are conceptualized as photon doublets within smaller systems in the theoretical architecture. This viewpoint provides a comprehensive framework that underscores the relevance and representation of particles in microscopic systems, deepening our understanding of their role within the wider landscape of electromagnetic interactions.

It is worth noting that these are idealized physics concepts. A truly "perfect" conductor does not exist in the real world, and electromagnetic radiation could leak out of or into a real-world conductor. Also, the behavior of the fields and currents would be more complex in real-world situations due to factors like resistive heating, impedance, etc. But for the purposes of a theoretical

question like the above scenario, the idealized principles are useful simplifications.

17.2.1   Example Aftermath

Recall that the system as a whole satisfies the noradiation condition as it does not radiate in its totality. Therefore this example exemplifies a situation where no self-interaction fields are required, as the system is entirely self-contained, incorporating all components that account for the system's behavior. This implies that, when viewed in its totality, all antiphotons in this system should mutually annihilate, making this system a classical analogue akin to the Gaussian distribution of the Wigner function. However, when dissecting the system into smaller partitions, the need for antiphotons and doublets arises due to the unavailability of hidden correlations to the outside that have been disregarded in the now reduced section of the system.

It is important to underscore that while the absorbers found throughout the universe are not always explicitly incorporated into the smaller microscopic models, their influence within the system is nonetheless encapsulated by the photon doublet concept. This can be conceived as a silent 'waveguide' role played by these external absorbers, orchestrating the electromagnetic flux from one region of the smaller microscopic system to another. In essence, this process culminates in the collapse of the photon wave function as the energy is directed from the point of emission and converges to the location where the wave collapse is anticipated. This intricate process appears to be effectively mediated through photon doublets.

The set of particles contained within the system's observable universe collectively fulfill the noradiation condition. However, this system may not exhibit time symmetry. This apparent asymmetry arises because, while the system doesn't radiate outwardly, it can accept incoming energy and information through its event horizon, thereby disrupting its inherent time symmetry. The integration of the photon doublet concept sheds light on phenomena such as Unruh radiation and Hawking radiation. This theory suggests that photon doublets, which previously symbolized external regions of the universe, join the observable universe as these 'virtual' photon doublets materialize into real particles.

When Wessel-Berg refers to the environmental doublet energy, he is specifically addressing the doublets within the event horizon of the universe that satisfy the no-radiation condition. However, these doublets do not form part of the smaller, more immediate microscopic system under study.

The photon doublet concept proves instrumental in deciphering the Casimir effect, providing unique insights into how different constituents of a system can possess distinct boundaries for their event horizons. The concept of an observable universe associated with a point in space is crucial here. In this context, the observable universe comprises all particles that collectively form the 'no radiation condition'. Given that electromagnetism is a field theory, a charge undergoing acceleration generates a field that permeates throughout its observable universe and not beyond.

Notably, the boundaries of the observable universe vary for different observers located at distinct positions. When a large object is placed in proximity to an observer, it effectively restricts certain modes of field oscillations, consequently altering the event horizon forming the observer's observable universe. This effectively reduces the distance to the horizon in the direction of the object, creating a 'shadow' effect on the observable universe from the observer's perspective.

This asymmetry or anisotropy in the event horizon, due to the non-uniform shadowing, engenders a difference in the doublet energy across the horizon. This energy difference is experienced as a pressure difference, which then manifests as a force. The pressure difference arises from the shift in doublet energy distribution due to the alteration of the event horizon. Consequently, this alteration and its consequent force represent a pivotal mechanism in the manifestation of the Casimir effect.

Intriguing parallels can be drawn between the mechanisms discussed above and the Unruh effect, wherein an observer accelerating through a vacuum perceives a temperature, known as Unruh temperature, as opposed to an inertial observer who perceives it as pure vacuum. A key aspect of the Unruh effect is the creation of a Rindler horizon for the accelerating observer, effectively a boundary beyond which events are unobservable, similar to how a massive object introduced near

an observer changes the event horizon in the context of the Casimir effect.

The comparison of the acceleration-induced Rindler horizon to the dynamic changes in the event horizon experienced during the Casimir effect offers a compelling framework. It posits that an observer's acceleration transforms their respective event horizon, in turn giving rise to the perceived thermal bath of particles known as Unruh radiation. This paradigm may offer a unique perspective on inertia. It suggests that the presence of this observable universe within the event horizon plays a vital role in causing inertia. Specifically, the hypothesis implies that any acceleration-driven alteration in the event horizon may generate a reactionary force. This force, potentially, could be understood as the inertia experienced by the observer in a similar sense to the Abraham Lorentz force in its derivation through the Lagrangian formulation. It should be noted that the derivation utilized Mach's principle, which indirectly assumes the presence of the observable universe.

This phenomenon can be understood within the framework of photon doublet theory. As an observer accelerates, the boundary of the observer's observable universe, or event horizon, changes. This is similar to the Casimir effect where a change in event horizon occurs due to the placement of a large object. The changes in event horizons in both scenarios result in pressure differences stemming from shifts in the doublet energy distribution.

In the context of the Unruh effect, this results in the perception of Unruh radiation. The doublet energy is redistributed due to the change in the event horizon, leading to an isotropic bath of radiation being perceived by the accelerating observer. Therefore, Unruh radiation can be considered an observable manifestation of the changes in the photon doublet energy distribution due to acceleration-induced changes in the observer's event horizon.

Thus, we see that the photon doublet concept has the potential to provide profound insights into not only static quantum effects such as the Casimir effect, but also dynamic relativistic phenomena such as the Unruh effect.

The intricate mechanics of these phenomena, while fascinating, lie beyond the scope of this thesis. A more detailed exposition will be reserved for subsequent publications to delve deeper into the transformative implications of these theories.

The predictive power of these photon doublets is notable. As Wessel-Berg elucidates in Chapter 9 of his book [91, p. 233], they are thought to be accountable for the enigmatic $\frac{1}{f}$ noise observed in electrical circuits, a puzzling phenomenon that, to this day, remains shrouded in mystery. Intriguingly, antiphotons appear to be crucial actors in this process, as Wessel-Berg's analytical derivation of the empirically observed noise from his theory involves the use of photon doublets. This implies a significant role for antiphotons in the genesis of this mysterious noise implying potential indirect empirical evidence for their existence.

In addition to the above discussion, this example underscores the utility of invoking the surface equivalence principle in electromagnetism. By utilizing Equation (17.2) in Wessel-Berg's reciprocity relation, this principle allows us to recast the surface integral into a form closely resembling the volume integral

$$\oiint_S (-\boldsymbol{E}_1 \cdot \boldsymbol{J}_{S,2}^* - \widetilde{\boldsymbol{E}}_2^* \cdot \boldsymbol{J}_{S,1}) \, \mathrm{d}S = \iiint_V (-\boldsymbol{E}_1 \cdot \boldsymbol{J}_2^* - \widetilde{\boldsymbol{E}}_2^* \cdot \boldsymbol{J}_1) \, \mathrm{d}V, \qquad (17.5)$$

where we have used the fact that $(\boldsymbol{E}_1 \times \boldsymbol{H}_2^*) \cdot \hat{\boldsymbol{n}} = \boldsymbol{E}_1 \cdot (\hat{\boldsymbol{n}} \times \boldsymbol{H}_2^*) = -\boldsymbol{E}_1 \cdot \boldsymbol{J}_{S,2}^*$. The above equation delineates a parallel between the dynamics taking place inside the volume and their surface equivalent counterparts. This transition is particularly handy in scattering theory, a domain where Wessel-Berg's reciprocity theory finds substantial application in his book. Application of the above equivalence principle is extremely useful in situations where the microscopic system in its totality does not satisfy the noradiation condition but where energy and entropy are both conserved. In these situations, the absorbers external to the system but within the event horizon of the noradiation condition can be viewed as equivalent surface currents impressed on the surface S of the microscopic system that act as a waveguide that route the energy within the microscopic system in the *frequency domain*.

The fact that the system does not satisfy the radiation condition implies that the system radiates as a whole. However, this radiation of advanced and retarded fields now effectively interacts with

these surface currents imprinted on S, essentially reflecting the radiation back inside the surface, contributing to routing the energy within the system. This makes it 'appear' as if the system is closed so that energy and entropy are conserved. This involves the use of photon doublets, which are discussed in the following section.

In summary, through the lens of a perfectly conducting surface and Wessel-Berg's reciprocity, we observe a remarkable interplay between advanced and retarded electromagnetic solutions. This scenario illustrates how total system self-containment leads to a cancellation of antiphotons, resembling the Gaussian distribution of the Wigner function. Moreover, this setup illuminates the critical role of surface equivalence in offering an alternate perspective on electromagnetic interactions and furthering our understanding of scattering phenomena.

17.3   The Integration of the Antiphoton

In this section, we will focus on the integration of antiphoton solutions into the framework of Wessel-Berg's theory. An interesting approach to arriving at the formulation of antiphoton solutions is by applying time reversal to Wessel-Berg's reciprocity Equation (15.2) without inverting the magnetic field. This maneuver results in the following equation

$$-\oiint_S (\boldsymbol{\mathcal{E}}_1 \times \widetilde{\boldsymbol{\mathcal{H}}}_2^* + \widetilde{\boldsymbol{\mathcal{E}}}_2^* \times \boldsymbol{\mathcal{H}}_1) \cdot \hat{\boldsymbol{n}} \, \mathrm{d}S = \iiint_V (-\boldsymbol{\mathcal{E}}_1 \cdot \boldsymbol{J}_2^* - \widetilde{\boldsymbol{\mathcal{E}}}_2^* \cdot \boldsymbol{J}_1) \, \mathrm{d}V. \tag{17.6}$$

Alternatively, we could derive this equation directly from Maxwell's equations for the antiphoton. In this case, Maxwell's equations for the antiphoton could be employed to derive Poynting's theorem for the antiphoton. This results in a peculiar situation where a flux of antiphotons into a closed surface S effectively *decreases* the energy enclosed within the surface

$$-\oiint_S \boldsymbol{\mathcal{E}} \times \boldsymbol{\mathcal{H}}^* \cdot \mathrm{d}\boldsymbol{S} = i\omega \iiint_V (\varepsilon_0 \boldsymbol{\mathcal{E}} \cdot \boldsymbol{\mathcal{E}}^* - \mu_0 \boldsymbol{\mathcal{H}} \cdot \boldsymbol{\mathcal{H}}^*) \, \mathrm{d}V - \iiint_V \boldsymbol{\mathcal{E}} \cdot \boldsymbol{J}^* \, \mathrm{d}V. \tag{17.7}$$

In this equation, we have replaced the photon fields with the antiphoton fields, while simultaneously transforming $\omega \to -\omega$ and $\boldsymbol{J} \to -\boldsymbol{J}$. Wessel-Berg delves into this aspect in Chapter 3 of his book [91, p. 44-56]. The unique energy flux behavior of the antiphoton is attributed to its propagation direction being opposite to its Poynting vector, leading to the interpretation of the antiphoton as a photon journeying backwards in time.

This behavior contrasts sharply with Poynting's theorem, where an inward flux of photons entering a region enclosed by S increases the energy in the fields.

Wessel-Berg ingeniously integrates both the reciprocity theorem for the photon (15.2) and the time-reversed relation for the antiphoton (17.6) to formulate the concept of the photon doublet, which comprises a photon-antiphoton pair. This elucidates that in Wessel-Berg's theory, there exist *four* categories of solutions - retarded and advanced for both the photon and the antiphoton. It's noteworthy, however, that the terms 'retarded' and 'advanced' lose their conventional meanings when applied to the antiphoton.

17.4   An Illustrative Demonstration of Wessel-Berg's Reciprocity Relation

Having delved into the theoretical aspects of Wessel-Berg's reciprocity relation, we are now equipped to illustrate these concepts with a practical example. To give the reader a better intuition of the underlying mechanics of Wessel-Berg's reciprocity relation, this example plots the 3D vector field in the *frequency domain* of the power flow terms $\boldsymbol{E}_1 \times \widetilde{\boldsymbol{H}}_2^* + \widetilde{\boldsymbol{E}}_2^* \times \boldsymbol{H}_1$ which arise from two separated Dirac delta currents

$$\boldsymbol{J}_1(\boldsymbol{r}, \omega) = \delta^3(\boldsymbol{r} - \boldsymbol{r}_1)\boldsymbol{d}, \qquad \boldsymbol{J}_2(\boldsymbol{r}, \omega) = \delta^3(\boldsymbol{r} - \boldsymbol{r}_2)\boldsymbol{d}, \tag{17.8}$$

where the emitter $\boldsymbol{J}_1(\boldsymbol{r}, \omega)$ is located at the origin of our coordinate system, i.e. $\boldsymbol{r}_1 = \boldsymbol{0}$ whilst the receiver $\boldsymbol{J}_2(\boldsymbol{r}, \omega)$ is located at $\boldsymbol{r}_2 = \boldsymbol{a}$. Here, $\boldsymbol{d}$ is a vector signifying the magnitude and

orientation of these currents. This vector points along the z-axis, where both currents are parallel. Additionally, $\boldsymbol{a}$ is a displacement vector separating the currents and is parallel to the x-axis. The selection of vectors $\boldsymbol{d}$ and $\boldsymbol{a}$ must be carefully considered due to the energy and momentum conservation restrictions of the system. These aspects are analyzed in greater detail in the example aftermath section below.

Figure 24 depicts the resulting Poynting vector field the dynamics of the Poynting vector field $\boldsymbol{E}_1 \times \widetilde{\boldsymbol{H}}_2^* + \widetilde{\boldsymbol{E}}_2^* \times \boldsymbol{H}_1$ in Wessel-Berg's reciprocity relation. This vector field therefore illustrates the energy transfer from the emitter $\boldsymbol{J}_1$ (left), to the receiver $\boldsymbol{J}_2$ (right). The reader may recall that the fields $\boldsymbol{E}_1$ and $\boldsymbol{H}_1$ denote the retarded fields of the emitter $\boldsymbol{J}_1$ while $\widetilde{\boldsymbol{E}}_2$ and $\widetilde{\boldsymbol{H}}_2$ represent the advanced field of the absorber $\boldsymbol{J}_2$.
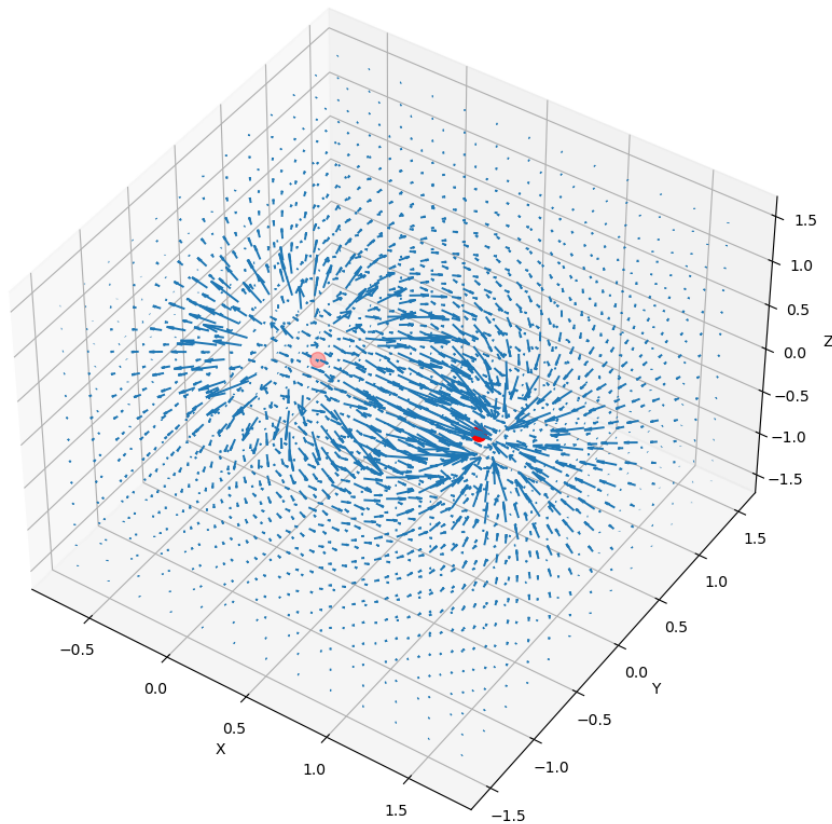
Figure 24: A 3D representation of Wessel-Berg's Reciprocity Power Flow in the frequency domain. Two point currents given by (17.8) are illustrated as red points where the left one is serving as the transmitter and the right one as the receiver. The blue arrows signify the Poynting vector field $\boldsymbol{E}_1 \times \widetilde{\boldsymbol{H}}_2^* + \widetilde{\boldsymbol{E}}_2^* \times \boldsymbol{H}_1$ in the frequency domain, emanating from the transmitter and converging on the receiver, thus depicting the energy transfer between the two charges in the system.

This visual power flow pattern in Figure 24 embodies a form of wave function collapse as the energy is routed and effectively dumped at the absorber. This illustrative depiction intends to provide readers with a hands-on comprehension of Wessel-Berg's reciprocity relation's core nature and its fundamental mechanism of action. Our understanding of the energy flow, as depicted in Figure 24, finds striking similarities with an illustration in Wessel-Berg's book [91, p. 112]. We

present this illustration here as Figure 25, featuring both the original figure description and our own elaboration for clarity.

Figure 25 comprises three subfigures marked as (a), (b), and (c). Subfigure (a) informally portrays the energy flow from atom A to atom B, encapsulating the essence of Wessel-Berg's reciprocity relation. The energy flow depicted here parallels what we observe in Figure 24, the latter being a more formal, plotted representation than a drawing. In addition to atom A and atom B, subfigure (a) includes auxiliary absorbers labeled C dispersed throughout the universe. These absorbers act as waveguides shaping the observed radiation pattern. Notably, arrows denoted as 'Doublet routing admixture' represent photon-antiphoton doublets, which represent the absorbers not directly included in the atom A and atom B system but contribute to guiding the observed energy flow. These absorbers interact with the self-interaction field, which spread in space until the no-radiation condition is met, as demonstrated in the perfect conductor example. Wessel-Berg's concept of 'Photon Routing' refers to this waveguide behavior that facilitates energy transmission within a system. It should be noted that the energy flow of Figure 25 resembles Figure 23 as both figures illustrate the waveguide nature of directed power flow.

Interestingly, the properties of Wessel-Berg's reciprocity theorem necessitate the assumption that reciprocity occurs between the retarded and advanced fields. However, an apparent gap in his book is a lack of any mention of the word 'advanced' in his entire book, let alone a small discussion on advanced solutions of Maxwell's equations. Yet, on the same page as Figure 25, Wessel-Berg draws a parallel between his theory and the absorber theory of Feynman and Wheeler with a poignant remark [91, p. 112]:

> According to this interpretation, the emission and absorption processes are tied together in an intimate fashion. The emission does not happen unless the prospective absorber is in the right constellation for minimization of the PDE time average. The process has the character of a 'handshaking' operation. The atoms must be in mutual consent between the two of them, as well as in agreement with the environmental sea of photon doublets. This interpretation eliminates the quantum mechanical concept of absolute randomness in the basic emission process. Still the process is of course random, but the random outcome is a deterministic phenomenon associated with objective randomizing factors that are unknown to us due to our ignorance of the instantaneous condition of the environmental sea of doublets governing the process. The shared responsibility of emitter and absorber is reminiscent of the Wheeler-Feynman 'Absorber Theory', but their description differs from the present one in that it does not in any sense describe the wave to particle transition affected through the intermediacy of photon doublets.

Wessel-Berg's acknowledgement that his theory shares similarities with the absorber theory of Feynman and Wheeler is indeed notable, particularly concerning the time symmetric component and the 'hand-shake' process between the transmitter and receiver. These 'hand-shake' occurrences in the emission process are depicted vividly in Figures 21 and 26, reflecting the transactional interpretation of John Cramer, which is in turn rooted in the absorber theory of Feynman and Wheeler. These figures portray a 'hand-shake' interaction between the receiver (with a retarded wave) and the transmitter (with an advanced wave), ensuring the conservation of overall energy and symmetry of time. Despite its merits, this theory falls short in resolving the entropy problem at smaller scales. Wessel-Berg alludes to this in his quote, stating that it doesn't employ negative energy solutions and photon doublets, crucial components for the pixel in his theory. Regrettably, Wessel-Berg's omission of advanced solutions in his discourse inevitably adds layers of complexity to readers attempting to understanding his theory.

Turning to subfigure (b) in Figure 25, it portrays atom A and atom B in a state where the energy transmitted from atom A in the form of retarded fields doesn't align with the advanced fields necessary for absorption at atom B. This misalignment may result from the transmitter wave being of an incorrect frequency or the energy of the transmitter wave being insufficient for an electron in atom B to transition between orbitals. The misdirected field from the transmitter gets reflected back in time by the antiphoton, resulting in a photon doublet. This photon doublet, having its electric and magnetic fields parallel, carries no net energy. Consequently, atom B declines atom A's transmission attempt with an antiphoton that permeates space and redirects the energy wave

of the transmitter to another atom. This process helps preserve the atom's integrity, ensuring it cannot split between two atoms with both absorbing half a photon.
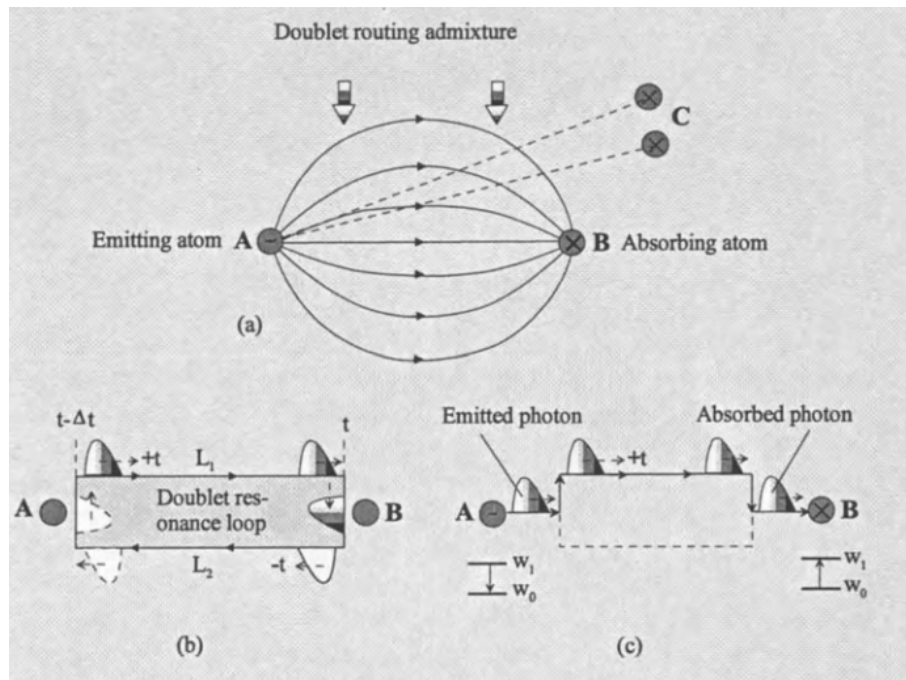
Figure 5.3. Illustration of the emission-absorption process. **(a)** Atom **A** is the emitter, atom **B** the absorber. Atoms **C** represent some of the available auxiliary absorbers in the universe. **(b)** State of no emission: The two atoms are in a passive handshaking state because the overall environmental doublet energy balance is not conducive to emission. The atoms are tied together in a doublet resonance loop with time average energy equal to zero. **(c)** State of emission and absorption: The environmental balance of time average energy is improved through emission from atom **A** of a regular photon which is subsequently absorbed by atom **B**.

Figure 25: A depiction of the complexities and interactions in the emission-absorption process, highlighting the role of doublet resonance loops and wave function collapses.

Source: [91, p. 112]

In contrast, subfigure (c) demonstrates a successful transmission attempt, where the emitted wave aligns with the advanced wave required for an electron to transition between orbitals. Consequently, the wave isn't reflected back by an antiphoton, facilitating energy transfer from atom A to atom B. In this process, several other absorbers partake in the 'wave function collapse,' aiding in routing the energy from atom A to atom B as shown in subfigure (a). This captures the interaction between retarded and advanced fields, as well as between photon and antiphoton, in the energy exchange process.

As we have seen in subfigure (b) of Figure 25, the energy transmitted from atom A doesn't align with the advanced fields necessary for absorption at atom B. This misalignment leads to a reflection of the field back in time and results in a photon doublet that carries no net energy. As such, atom B declines the transmission attempt from atom A.

This intricate concept of energy transfer and retrocausality in quantum mechanics is further visualized in Figure 26. This figure depicts the transactional interpretation of quantum mechanics using a polarization-entangled 2-photon source. The source is situated at the bottom center and sends out offer waves, Ψ_R and Ψ_L, to two polarization measuring devices located on the upper right and left, respectively. Each device responds with a confirmation wave, Ψ_R^* and Ψ_L^*, respectively. This figure aptly illustrates the 'handshake' concept, a reciprocal communication process between the photon source and the measuring devices, thus involving retrocausality.
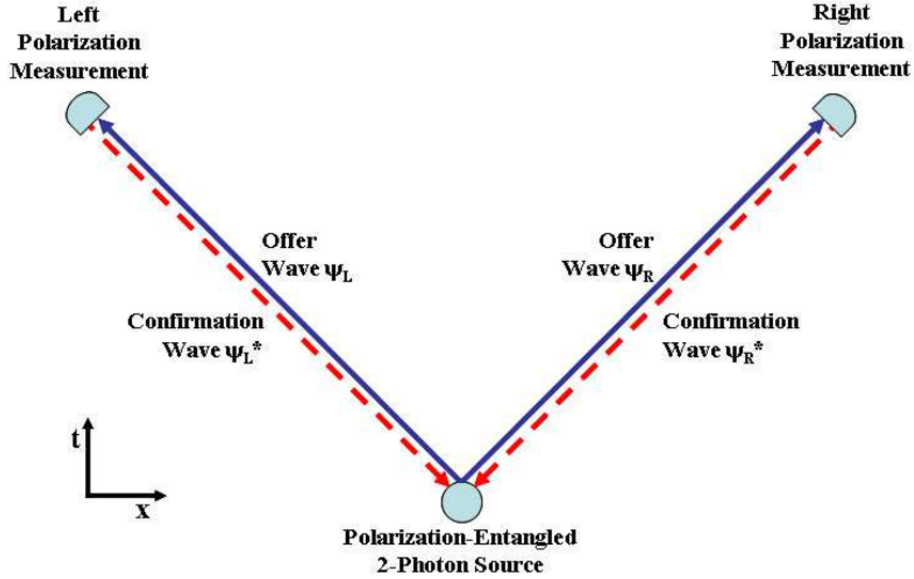
Figure 26: Transactional interpretation of quantum mechanics with polarization-entangled 2-photon source. A central source emits two entangled photons towards two polarization measuring devices. Offer waves Ψ_R and Ψ_L are sent from the source to the measuring devices, which in turn send confirmation waves Ψ_R^* and Ψ_L^*, indicating a 'handshake' interaction. Retrocausality is represented by the reverse flow of the confirmation waves.

17.4.1 Example Aftermath: Invoking the Noradiation Condition

To reanalyze the example illustrated in Figure 24, we apply the noradiation condition from Section 16 to a similar example in the time domain. This example only varies so slightly from the former due to the time domain aspect. This is because every vector in the frequency domain represents a harmonic oscillation of a field along that direction and at a given frequency. Therefore, the point current vectors must now be represented by moving point charges in order to satisfy the continuity equation. Therefore, we start with the initial setup of the simulation which consists of two oscillating charges denoted as $\boldsymbol{r}_1(t)$ (on the left) and $\boldsymbol{r}_2(t)$ (on the right).

In the first stage, we solely apply the noradiation condition to the first charge ($\boldsymbol{r}_1(t)$) before analyzing the implications of introducing the second charge. The center of oscillation and its velocity for the first charge is located at the origin of our coordinate system and can be expressed mathematically as

$$\boldsymbol{r}_1(t) = \boldsymbol{d}\sin(\omega_0 t), \qquad \dot{\boldsymbol{r}}_1(t) = \omega_0 \boldsymbol{d}\cos(\omega_0 t). \tag{17.9}$$

Here, ω_0 represents the oscillation frequency, and the vector $\boldsymbol{d}$ describes both the amplitude (through its magnitude) and the direction of oscillation. Consequently, the charge and current distributions become

$$\rho_1(\boldsymbol{r}, t) = q\delta^3(\boldsymbol{r} - \boldsymbol{r}_1(t)), \qquad \boldsymbol{J}_1(\boldsymbol{r}, t) = q\dot{\boldsymbol{r}}_1(t)\delta^3(\boldsymbol{r} - \boldsymbol{r}_1(t)). \tag{17.10}$$

We then proceed by executing the spatial Fourier transform, leading to

$$\boldsymbol{J}_1(\boldsymbol{k}, t) = q\iiint\limits_{-\infty}^{\infty} \dot{\boldsymbol{r}}_s(t)\delta^3(\boldsymbol{r} - \boldsymbol{r}_1(t))e^{i\boldsymbol{k}\cdot\boldsymbol{r}}\,\mathrm{d}^3\boldsymbol{r} = q\omega_0\boldsymbol{d}\cos(\omega_0 t)e^{i(\boldsymbol{k}\cdot\boldsymbol{d})\sin(\omega_0 t)}. \tag{17.11}$$

The following step involves applying the temporal Fourier transform to the expression above. However, it is not a straightforward process and necessitates the application of the Jacobi-Anger expansion

$$e^{iz\sin(\theta)} = \sum_{n=-\infty}^{\infty} J_n(z)e^{in\theta}, \tag{17.12}$$

where $J_n(z)$ stands for the n-th Bessel function of the first kind. Utilizing this expansion to the exponent in (17.11), we obtain

$$\boldsymbol{J}_1(\boldsymbol{k},t) = \frac{q\omega_0\boldsymbol{d}}{2}(e^{i\omega_0 t} + e^{-i\omega_0 t}) \sum_{n=-\infty}^{\infty} J_n(\boldsymbol{k}\cdot\boldsymbol{d})e^{in\omega_0 t}. \tag{17.13}$$

This simplified expression allows us to easily execute the temporal Fourier transform

$$\boldsymbol{J}_1(\boldsymbol{k},\omega) = \int_{-\infty}^{\infty} \boldsymbol{J}(\boldsymbol{k},t)e^{-i\omega t}\,\mathrm{d}t. \tag{17.14}$$

Finally, this results in the expression

$$\boldsymbol{J}_1(\boldsymbol{k},\omega) = \frac{q\omega_0\boldsymbol{d}}{2} \sum_{n=-\infty}^{\infty} J_n(\boldsymbol{k}\cdot\boldsymbol{d})[\delta(\omega - (n-1)\omega_0) + \delta(\omega - (n+1)\omega_0)]. \tag{17.15}$$

As one would expect, $\boldsymbol{J}_1(\boldsymbol{k},\omega)$ has non-vanishing light-like components when $\omega = c|\boldsymbol{k}|$. This is hardly surprising considering it's a point charge undergoing oscillatory motion, leading to acceleration. This becomes more apparent for small $\boldsymbol{k}\cdot\boldsymbol{d}$, where all Bessel functions go to zero, excluding the zeroth, which becomes $J_0(\pm(\omega_0/c)\hat{\boldsymbol{k}}\cdot\boldsymbol{d}) \approx 1$ for the light-like components satisfying $\omega = c|\boldsymbol{k}|$, where $\hat{\boldsymbol{k}} = \boldsymbol{k}/|\boldsymbol{k}|$.

Next, let's examine the situation when the second charge is introduced. The position and velocity of the second charge can be described as

$$\boldsymbol{r}_2(t) = \boldsymbol{a} + \boldsymbol{d}\sin(\omega_0 t), \qquad \dot{\boldsymbol{r}}_2(t) = \omega_0\boldsymbol{d}\cos(\omega_0 t). \tag{17.16}$$

Assuming for simplicity that the oscillations are in phase, occur in a parallel direction, and share the same frequency. The vector $\boldsymbol{a}$ denotes the displacement vector of the second charge from the first. Though a more general example could be examined with differing directions of oscillations and a phase difference between them, this simplified example adequately demonstrates the principle of this section.

In the specific case of Figure 24, $\boldsymbol{a}$ is oriented along the x-axis. Following similar steps as before, we find

$$\boldsymbol{J}_2(\boldsymbol{k},t) = q\omega_0\boldsymbol{d}\cos(\omega_0 t)e^{i(\boldsymbol{k}\cdot\boldsymbol{d})\sin(\omega_0 t)}e^{i\boldsymbol{k}\cdot\boldsymbol{a}}. \tag{17.17}$$

This differs from (17.11) by a phase factor $e^{i\boldsymbol{k}\cdot\boldsymbol{a}}$, which aligns with the Fourier transform's nature. Similarly, we derive

$$\boldsymbol{J}_2(\boldsymbol{k},\omega) = \frac{q\omega_0\boldsymbol{d}e^{i\boldsymbol{k}\cdot\boldsymbol{a}}}{2} \sum_{n=-\infty}^{\infty} J_n(\boldsymbol{k}\cdot\boldsymbol{d})[\delta(\omega - (n-1)\omega_0) + \delta(\omega - (n+1)\omega_0)]. \tag{17.18}$$

This differs from (17.15) by a phase factor in this simplified example.

The total current distribution $\boldsymbol{J}(\boldsymbol{r}, t)$ is the sum of the two components

$$\boldsymbol{J}(\boldsymbol{r}, t) = \boldsymbol{J}_1(\boldsymbol{r}, t) + \boldsymbol{J}_2(\boldsymbol{r}, t). \tag{17.19}$$

This describes the current distribution of our two-charge system. As the Fourier transform has a linear property, the Fourier transform of the total current distribution is the sum of its two charges' Fourier transforms:

$$\boldsymbol{J}(\boldsymbol{k}, \omega) = (1 + e^{i\boldsymbol{k} \cdot \boldsymbol{a}}) \frac{q\omega_0 \boldsymbol{d}}{2} \sum_{n=-\infty}^{\infty} J_n(\boldsymbol{k} \cdot \boldsymbol{d})[\delta(\omega - (n-1)\omega_0) + \delta(\omega - (n+1)\omega_0)]. \tag{17.20}$$

Firstly, we acknowledge the presence of a factor $(1 + e^{i\boldsymbol{k} \cdot \boldsymbol{a}})$ in the derived function, which gives us insights into the presence and absence of certain wave number components. Specifically, for light-like components, we need to enforce

$$\boldsymbol{J}(\frac{\omega}{c}\hat{\boldsymbol{k}}, \omega) = (1 + e^{i\frac{\omega}{c}\hat{\boldsymbol{k}} \cdot \boldsymbol{a}}) \frac{q\omega_0 \boldsymbol{d}}{2} \sum_{n=-\infty}^{\infty} J_n(\frac{\omega}{c}\hat{\boldsymbol{k}} \cdot \boldsymbol{d})[\delta(\omega - (n-1)\omega_0) + \delta(\omega - (n+1)\omega_0)]. \tag{17.21}$$

An important observation is that no light-like Fourier components exist in all directions $\hat{\boldsymbol{k}}$ that satisfy $\frac{\omega}{c}\hat{\boldsymbol{k}} \cdot \boldsymbol{a} = \pi$ for a given $\boldsymbol{a}$. This suggests that some radiation emitted by the first charge gets absorbed by the second charge. However, the presence of non-vanishing light-traveling components implies that the system, as a whole, radiates. This radiation persists until it reaches the rest of the charges in the observable universe, satisfying the no-radiation condition. Consequently, the energy transfer between the two charges is contingent upon the presence of external charges, an action represented by the photon doublets.

The scenario in Figure 24 inherently contains these photon doublets. Given Hegerfeldt's theorem, which applies to photon wave functions with compact support, this is unsurprising. The theorem implies that a photon's behavior is completely contained within a region, independent of its surroundings. As we see in this example, this is not strictly the case in field theories such as electromagnetism, where we must consider the entire system.

It's noteworthy that the future behavior of charge 2 can be determined through the 'advanced field' concept. Given the known trajectory of a charge, we can predict the fields it will produce using the retarded potential. However, since this trajectory is known in advance, the advanced fields that need to act on the charge for this trajectory to occur must also be known. This provides temporal symmetry, creating a seemingly 'closed' system.

Considering phase differences and different oscillation directions could lead to varied and intriguing scenarios, further showcasing this principle's power. Different configurations, in turn, radiate as a combined system to varying degrees. If a particular setup radiates more, it requires more surrounding charges for the energy routing process.

Figure 27: Depiction of the vector potential handshake, demonstrating the primary paths contributing to the observed potential.

The Wessel-Berg reciprocity relation is critical for ensuring energy conservation across the system by mapping effective energy transfers between different parts. When applied to a volume V enclosed by a surface S, it allows the charges on the universe participating in energy routing to be equivalently expressed on the surface S using the surface equivalence principle, all the while maintaining energy conservation.

Although the fields produced by the transmitter $\boldsymbol{J}_1(\boldsymbol{r}, \omega)$ impact all other charges in the universe (given electromagnetism's field theory nature), energy is routed effectively to the receiver in the frequency domain, with the remaining charges acting as wave guides. The fact that the two charges alone can't satisfy the no-radiation condition necessitates the other charges' indirect action present in the universe for energy routing. Even though this is a simple scenario, it exhibits the general applicability of the no-radiation condition, an important tool not explicitly discussed in Wessel-Berg's book.

17.4.2 Comparing Results

The concept of using advanced waves in tandem with retarded waves is not a novel idea. A significant example of this can be found in the research paper titled *Symmetry, Transactions, and the Mechanism of Wave Function Collapse* by John Cramer and Carver Andress Mead [24]. In this paper, the authors executed similar simulations that utilized advanced and retarded waves in harmony with the transactional interpretation of quantum mechanics. Although their approach did not fully leverage Wessel-Berg's reciprocity relation, they manually ensured global energy conservation to execute their simulations. This procedure, interestingly, yielded results that mirrored those from our examples, as depicted in Figures 27 and 28. The parallelism in the outcomes, achieved with less effort using Wessel-Berg's reciprocity relation, underscores its practical utility.
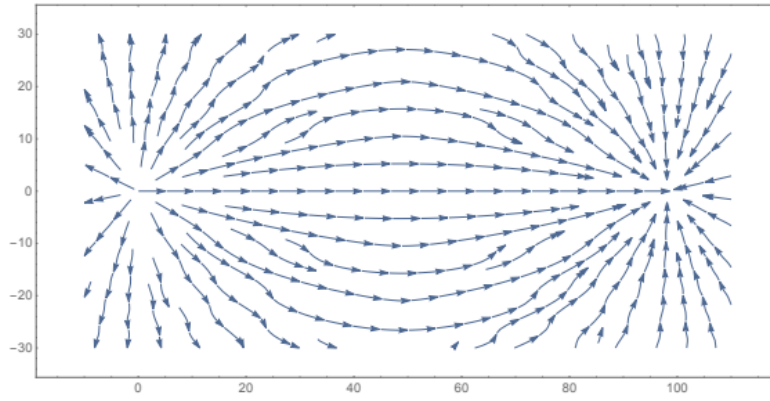
Figure 28: Streamlines of the quantum handshake, providing visual representation of the energy transfer process.

Furthermore, Cramer and Mead demonstrate, in their paper, an energy transition characterized by a 'handshake' motion between two atoms. This is reminiscent of the process described by Wessel-Berg, as shown in Figure 25 (c), further illustrated in Figure 29 in Cramer and Mead's work.
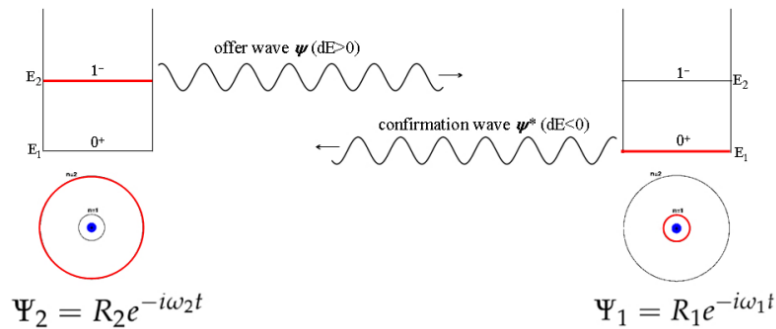
Figure 29: Model of energy transition between two atoms, illustrating the 'handshake' phenomenon in relation to Wessel-Berg's reciprocity relation. This resembles Figure 25 (c).

In summary, using advanced and retarded solutions of Maxwell's equations, we've developed a microscopic theory of electromagnetism that conserves both energy and entropy, akin to Hamiltonian mechanics. Yet, these formulations remain classical, as they don't confront the entropy problem directly.

Addressing the entropy challenge in Hamiltonian mechanics gives rise to the Wigner-Moyal phase space formalism, inherently integrating a pixel. Consequently, this formulation produces the Wigner function, which necessitates the inclusion of negative probabilities.

Similarly, confronting the entropy dilemma in our microscopic theory of electromagnetism leads to the bitemporal theory, which intrinsically incorporates the antiphoton. This inclusion arises due to the association of the negative probabilities within the Wigner function with negative energy solutions in relativistic theories in Hilbert space.

18 Discussion

18.1 A Critique of Wessel-Berg's Bitemporal Theory

This section provides an analytical discussion of Wessel-Berg's book to facilitate a comprehensive understanding for future readers, highlighting both its merits and flaws.

18.1.1 General Overview

Wessel-Berg's introductory chapters serve as an informative primer on his bitemporal theory, which he refers to as 'Neoclassical.' The use of 'classical' can be seen as ambiguous, considering it traditionally implies a theory grappling with entropy problems. If we adhere to this definition, his theory would not qualify as 'classical.' Nevertheless, Wessel-Berg's presentation of his theory is intuitive, offering logically consistent explanations of intricate concepts like wave function collapse or EPR paradoxes, compared to the standard Copenhagen interpretation.

18.1.2 Dissecting the First Chapters

The book's second chapter often confuses readers as it appears more akin to a draft than a finished piece. Wessel-Berg defines concepts loosely and includes numerous mathematical inaccuracies in his equations. These issues are particularly evident in his reflection-transmission example, originally intended to spark interest in his more generalized theory.

In the third chapter, where one might expect the establishment of the theoretical framework, advanced fields are conspicuously absent following the introduction of his reciprocity relation. Instead, Wessel-Berg employs a problematic Green's function method to illustrate surface term cancellation. The fundamental flaw here is that the nature of his Green's function is under-defined, relying solely on his attributed properties. This issue with surface term cancellation is addressed comprehensively in this thesis. Wessel-Berg overlooks the need to discuss the reciprocity relation's significance and plunges into a microwave description of electromagnetism. He proposes that orthogonal solutions of Maxwell's equations, derived using Sturm-Liouville theorem properties, form a complete basis for all fields. This approach both underplays the theory's intricacies and overcomplicates matters prematurely.

Wessel-Berg uses an admittance matrix, $\boldsymbol{Y}$, to relate the orthogonal electric and magnetic field bases through a linear transformation. He makes an error in discussing the properties of the admittance matrix, insisting it is both symmetric ($\boldsymbol{Y}^{\mathsf{T}} = \boldsymbol{Y}$) and skew-Hermitian ($\boldsymbol{Y}^{\dagger} = -\boldsymbol{Y}$), implying a pure imaginary nature. This isn't accurate since this property isn't invariant under unitary transformations. While this doesn't impact the main scattering formulation, it's crucial to understand this detail, as Wessel-Berg uses it to argue that $\boldsymbol{Y}(-\omega) = -\boldsymbol{Y}(\omega)$ for his antiphoton relation. Instead, the admittance matrix should possess purely imaginary eigenvalues as energy isn't lost in a microscopic system. These inaccuracies can lead to considerable confusion for first-time readers.

The book's fourth chapter ventures into speculative territory, particularly when it suggests that electrons might also exhibit bitemporal characteristics. However, it is lacking in detail and supportive arguments, resulting in an array of unfounded claims.

Chapter 5, dealing with the nature of photon wave function collapse, offers useful insights despite several initial flaws that do not impact the discussion later on.

The first of Wessel-Berg's assumptions, and a primary point of contention, is the assertion that any closed surface S can be partitioned into N distinct sections. Each section supposedly functions as an orthogonal solution of Maxwell's equation. The basis for this assumption is his definition of orthogonality through a surface integral

$$\oiint\limits_{S} \boldsymbol{e}_i \cdot \boldsymbol{e}_j \, \mathrm{d}S = \delta_{ij}, \qquad \forall i, j = 1, 2, 3, \ldots N \tag{18.1}$$

where $\boldsymbol{e}_i$ are the normalized orthogonal independent solutions of Maxwell's equations within the confines of S and $\delta_{ij} = 0$ for $i \neq j$ and $\delta_{ij} = 1$ for $i = j$. Partitioning the surface into non-overlapping N areas is, theoretically, possible. The rationale is that any given field can be equated to equivalent surface currents on the surface S. These currents, when applied with Huygens principle and Maxwell's equations, generate the required fields. These surface currents can then be segmented into non-overlapping areas to satisfy Wessel-Berg's orthogonality relation.

In principle, it's possible to partition the surface enclosing a volume into many smaller patches and consider each patch as a separate secondary Huygens source, or as separate surface currents under the surface equivalence principle. Each patch would generate its own electromagnetic fields, and each of these field distributions should satisfy Maxwell's equations. This is because Maxwell's equations are local laws, i.e., they hold at every point in space. Therefore, the field resulting from each patch, being an electromagnetic field, should satisfy Maxwell's equations. When we then superpose the fields from all patches to get the total field, the resulting field will also satisfy Maxwell's equations. This is because Maxwell's equations are linear differential equations, and the superposition of solutions to a linear differential equation is also a solution.

However, the tricky part in this process is dealing with the edges of the patches, as the fields may not match up perfectly at these edges. This is a well-known difficulty in numerical methods for solving differential equations, known as the patching problem. In practice, this issue is typically handled by using overlapping patches and some method for blending the solutions in the overlap regions, or by using special techniques to ensure that the solution is smooth at the edges of the patches.

Another important point to note is that, while the fields due to individual patches would satisfy Maxwell's equations, this doesn't necessarily mean that the sources (i.e., currents and charges) associated with each patch would individually satisfy the continuity equation for charge, which is a global conservation law. This is because the sources on one patch can affect the fields on another patch. The full system of sources and fields must satisfy the continuity equation. Therefore, partitioning the surface and considering each patch separately is conceptually possible and can be a useful approach in some cases. However, it also brings its own complications, especially when it comes to handling the edges of the patches and ensuring global conservation laws are respected.

In summary, as these partitioned areas of the closed surface S are independent, the surface currents in each must satisfy the continuity equation independently, just as the actual currents within the volume V, enclosed by S, must do. This stipulation necessitates careful management of the boundaries between these surfaces to restrict the flow of surface currents between them. Consequently, only a limited set of scenarios could meet these conditions, indicating a lack of generality in Wessel-Berg's assumption.

The second issue arises from Wessel-Berg's mistake in expressing the electric and magnetic fields at every point on the surface are parallel to each other, meaning that the first part of his chapter's logical structure falls apart. This is obviously a mistake on his part.

Despite these inaccuracies, the remainder of the chapter is free from such flaws and provides a thorough demonstration of how photon wave collapse occurs in his theory. As such, readers should navigate the initial sections of this chapter with caution and awareness of these discrepancies, but can confidently rely on the later sections for an understanding of photon wave collapse within the context of Wessel-Berg's bitemporal theory.

Chapter 6 builds a general scattering formulation extensively used in his book's simulations. The highlight of this chapter, are the formulation of his equations that he then uses throughout the entire book which result in the accurate depiction of various quantum experiments.

It is argued in this thesis that the demonstration and explanation of the $1/f$ noise in electronic circuits as a direct consequence of antiphoton's effect on circuit is the crown jewel of his book.

To put it into perspective, the $1/f$ noise, or pink noise, is a signal with a power spectral density inversely proportional to its frequency, often represented as $S(f) \propto 1/f^{\alpha}$, where α is close to 1 [31]. Despite its prevalence in numerous systems, including electronic devices and biological processes, the origin of $1/f$ noise is not fully understood [58]. This noise has been observed since the 1920s, with various theories proposed, from charge trapping/detrapping in conductive materials to number fluctuation models, yet a comprehensive theory remains elusive [89].

His other simulations of the double-slit experiment, the EPR paradox, the wave function collapse and the delayed choice quantum eraser are also major highlights of his book, illustrating the theory's predictive power when incorporating the antiphoton.

18.1.3   The Stern-Gerlach Experiment

Lastly, Chapter 10 of Wessel-Berg's book critically examines the Stern-Gerlach experiment, a cornerstone experiment often cited in introductory texts to highlight the peculiarities of quantum mechanics. The Stern-Gerlach experiment, performed by Otto Stern and Walther Gerlach in 1922, aimed to investigate the angular momentum of silver atoms [84]. The experiment involved passing a beam of silver atoms through an inhomogeneous magnetic field. Instead of exhibiting a continuous spread, as predicted by classical physics, the beam split into two distinct paths. These unexpected results provided key evidence for the quantum property of spin and had far-reaching implications for quantum mechanics, validating the concept of quantization of atomic properties and spurring the development of the spin quantum number in atomic theory [36, 78].

What sets the discussion in Chapter 10 apart from the rest of Wessel-Berg's book is its independence from the bitemporal theory. Wessel-Berg makes an intriguing argument that the Stern-Gerlach experiment's results can be elucidated solely through classical electromagnetism, sidestepping the need for quantum mechanics or the bitemporal theory. He identifies the underlying issue as the assumption of an inhomogeneous magnetic field produced by the experimental setup's magnets, which supposedly exert a force on the passing silver atoms. However, this presumption overlooks the divergence-free nature of magnetic fields, i.e., $\boldsymbol{\nabla} \cdot \boldsymbol{B} = 0$, a property not accommodated in the experimental design. Once this property is incorporated, simulations yield results comparable to empirical observations.

Building upon this, the author of this thesis conducted an enhanced simulation of the experiment, integrating additional factors. A Maxwell-Boltzmann distribution was enforced for the velocity profile for the silver atoms, and a slight angular spread was also introduced in the atom emissions from their source. The magnetic field was also meticulously replicated to match the original experiment more closely using a Python library called magpylib. This improved simulation achieved results more in line with the actual empirical findings of Stern and Gerlach, as opposed to the simpler model proposed by Wessel-Berg.

Though the concept of spin is an established fixture in physics, the Stern-Gerlach experiment, frequently utilized in introductory texts as a demonstration of spin, may not be aptly suited for this role. Despite its historical prominence, this experiment doesn't intrinsically demonstrate the quantum nature of spin, potentially leading to misconceptions when used to illustrate such a crucial aspect of quantum mechanics. Textbooks would greatly benefit from featuring more robust experiments that effectively demonstrate the concept of spin. Consequently, Wessel-Berg's dissection of the Stern-Gerlach experiment presents another intriguing facet of his book.

In summary, while Wessel-Berg's book serves as a rich source of innovative ideas, its effectiveness is somewhat hampered by mathematical inaccuracies in the first chapters, speculative statements, and lack of detail in certain areas. Future readers must approach it with these caveats in mind to accurately grasp the potential implications of his bitemporal theory.

18.2 Wessel-Berg's Antiphoton Concept

As discussed throughout this thesis, the energy-momentum relation for massless particles like photons, derived from Einstein's relation $E^2 = (pc)^2 + (mc^2)^2$ takes the form $E = \pm pc$ when the mass is zero. The positive root corresponds to the normal photon solutions we see, while the negative root is interpreted, under our proposal, as the antiphoton or negative-energy solution.

The argument of this thesis is a proposal to utilize the negative energy solutions for photons directly, in order to circumvent issues like those raised by Hegerfeldt's theorem. We have seen that this theorem essentially suggests that localized states with strictly positive energy can lead to immediate action at a distance, which conflicts with locality in quantum field theory.

As already discussed, Hegerfeldt's theorem highlights the tension between two seemingly incompatible features of relativistic quantum theories: the strict localization of states (they exist in a finite region of space at a given time) and their evolution over time in a way that preserves this localization while also preserving causality (effects cannot propagate faster than light). In the context of quantum field theory, which is often used to describe particles such as the photon, the conventional approach to resolve this tension has been to accept that states are not strictly localizable. This is reflected in the ubiquitous use of field operators that create or annihilate particles at every point in space, rather than in a finite region.

We are suggesting that the Hegerfeldt's theorem's challenge to the principle of locality can be circumvented in Wessel-Berg's theory by the direct or indirect incorporation of negative energy solutions, and since we cannot reinterpret negative energy solutions for the photon due to its charge neutrality, we must use these solutions directly.

Inclusion of antiphotons introduces an intriguing element into the conversation, paving the way towards a resolution of the entropy problem in classical electromagnetism and thus opening doors for statistical mechanics. In statistical physics, once the energy E and entropy S of a system are established, the statistical evolution of the system can be determined. Consequently, an accurate depiction of entropy could potentially unearth novel, large-scale, emergent forces of a statistical nature deriving from electromagnetism. The entropic force represents one such instance, which can be expressed as

$$\boldsymbol{F} = T\boldsymbol{\nabla}S, \tag{18.2}$$

where T signifies the system's temperature. The reader may recollect our discussion from Section 2.1.4, wherein the definition of temperature provided in Equation (2.11) involves the energy and entropy of the system and was stated as

$$\frac{1}{T} = \frac{\partial S}{\partial E}. \tag{18.3}$$

This resolution of the entropy problem in electromagnetism invites potential advancements in the field of statistical physics. It underlines another drawback of negating the antiphoton by declaring the photon as its own antiparticle—doing so could hinder the possibility of novel discoveries.

Under our proposal, instead of reinterpreting negative energy solutions as positive energy states of a separate particle, we would have to find a way to include these negative energy states directly in the theory as Wessel-Berg has done so successfully in his theory. This would require a non-standard interpretation of the energy of these photons, and how they relate to time which has been discussed in this thesis. It might also necessitate changes to the way we understand the propagation of light, its interactions with matter on microscopic scales.

That being said, Wessel-Berg's idea prompts further exploration into the nature of time, causality, and the very essence of quantum fields. Despite the challenges of in his book, such novel thinking has often led to paradigm shifts in our understanding of the universe, and it would indeed be intriguing to see where this line of reasoning could lead.

18.3 The Death of the Pink Elephant

The discussion thus far has revealed that the initial motivating inquiry of this thesis concerning the reason behind bitemporal electromagnetism's capacity to seemingly predict quantum phenomena may not have been the most pertinent question after all. A more appropriate question to consider is the reason why bitemporal electromagnetism yields predictions that accurately correspond to empirical observations. The resolution to this inquiry parallels that of quantum mechanics: both theoretical frameworks address the entropy problem. In order to solve this entropy problem, which entails connecting abstract mathematical frameworks to empirical observations, relativistic theories necessitate the incorporation of negative frequencies at their core, which gives rise to the antiphoton. It appears that entropy has ironically been the pink elephant in the room in attempts of bridging classical and quantum physics.

The whole emphasis on entropy in this thesis to distinguish between classical and quantum physics may strike some people as a revolutionary idea that has the potential to have a drastic impact on the way of thinking and perceiving the natural world. However, these ideas are not novel nor revolutionary, but instead are simply flat out common sense, and are used extensively in numerous other fields. There is one particular field in mind that comes to mind which relies heavily on the use of entropy to make predictions, and this is the field of artificial intelligence and its use of neural networks. These kind of AI models do not assume absolute truths, or their existence, nor do they attempt to find how things 'actually' are. They create progressively better predictive models through iterative methods based on the limited information they have access to. Similarly, these algorithms often quantify this information using Shannon entropy. In these AI models, zero entropy represents the best information the AI can possibly possess using the data it has access to. These algorithms do not have access to perfect infinite information, including hypothetical pink elephants. They utilize the information they have access to and form a model based on this information, and subsequently link this model back to actual predictions. The neural network model serves solely as a means to that end. This is analogous to the mathematical models utilized in physics. The process of linking these models back to actual physical states at finer scales is where classical mechanics falls short and quantum mechanics comes to its aid.

Additionally, reinforcement learning algorithms, differ slightly from other simpler AI algorithms in that they are endowed with the ability to interact with their designated environment. This is also the field where terms like *entropy gain* are used quite frequently, where algorithms are designed to take actions that result in the greatest amount of information gain regarding the state of their environment. At no point during the information gathering process, do the algorithms assume that they can acquire information without affecting the environment. Information gathering is a process in itself and inherently necessitates interactions with the environment, which inevitably alters it. Therefore, it becomes apparent that employing models reminiscent of classical physics, where measurements are presumed to be independent of what is being measured, would be not only nonsensical but outright foolish in these situations.

Thus, a crucial question remains: In what way is the world that we inhabit and interact with any different to the one of the aforementioned AI examples? Our access is limited to empirical data from the physical realm, which we must process meaningfully to develop models with predictive power of the natural world. Are we to suggest that the quest for the 'true' nature of the pink elephant should be of primary concern of every physicist? To phrase it differently, what value does the 'true' description of the world hold if parts of its finer details cannot be empirically measured nor verified? All we have access to is empirical information from the physical world that we have to process in a meaningful way, to create models that have predictive power of the natural world.

Physicists should therefore refrain from delving into questions of how things 'actually' are, pertaining to the 'true' nature of the world, as such questions resemble asking for the 'true' weight and position of the pink elephant. These types of questions ultimately cause more harm than good. Instead, physicists should shift their attention to asking questions regarding what one could possibly hope to learn about the natural world through empirical means, following in the footsteps of AI models, which one could argue, physicists themselves innately are. This shift involves abandoning the pursuit of the elusive pink elephant, because the 'truth' of the matter is that the pink elephant has been dead all along and ought to have been buried a long time ago.

19 Conclusion

In the dynamic landscape of scientific research, often, the most unconventional theories propel us to break the boundaries of understanding and perceive the universe from a novel perspective. This thesis aimed to unearth the foundational principles of a little-explored 'neoclassical' theory presented by Tore Wessel-Berg in his book *Electromagnetic and Quantum Measurements: A Bitemporal Neoclassical Theory*, and scrutinize its intriguing ability to simulate and predict quantum phenomena.

The thesis is the result of an analytical journey, centered around a tripartite goal. This involves determining why Wessel-Berg's theory, referred to as Bitemporal Electromagnetism, can predict quantum phenomena, elucidating where it fits within the framework of established theories of modern physics, and developing a consistent and robust theoretical groundwork that leads to Wessel-Berg's equations used in his simulations.

The initial pursuit led us down an intellectual path towards redefining entropy as the empirically measurable information in a physical system for both discrete and continuous state spaces. For a consistent definition for continuous state spaces, the introduction of the pixel concept was necessary. The reconceptualization of entropy allowed us to identify an entropy problem in classical theories and identify quantum theories as a resolution to this problem. Thus, the identification of an entropy problem, which was made possible by the redefined entropy definition, served as a criteria for distinguishing classical theories from quantum theories. Upon employing this criterion, it was observed that Wessel-Berg's formulation indeed resolved the entropy problem. This conclusion subverted the initial question, guiding us towards a more nuanced perspective, suggesting that quantum mechanics and Bitemporal Electromagnetism both predict measurements accurately at smaller scales as they resolve the entropy problem.

The second stage of the investigation was enriched by a deep dive into microscopic systems and the exploration of Hamiltonian mechanics in phase space, where the microscopic systems were defined as deterministic, reversible, and conserving both energy and entropy during temporal evolution. A parallel was drawn between Wigner-Moyal formalism in phase space and quantum mechanics in Hilbert space, establishing that our proposed entropy definition solved the entropy problem in the symplectic manifold formalism in the same way Von Neumann entropy does for Hilbert space.

The thesis subsequently ventured into the intriguing realm of antiphotons and their role in negating the dire consequences of Hegerfeldt's theorem and explaining various physical phenomena. Our findings highlighted the negative repercussions of excluding negative energy solutions, revealing the pivotal role these solutions play in bridging the gap between abstract wave function models and actual measurements. Since Wessel-Berg's theory successfully predicts quantum phenomena, it can therefore be regarded as a first-quantized theory of electromagnetism. In the last part of the investigation, the key elements of the study were assembled, leading to the creation of a coherent and consistent microscopic theory of electromagnetism based on the discussions of the characteristics of microscopic systems in this thesis. It included advanced and retarded potential to maintain time symmetry necessary for entropy conservation. The exploration revealed that Wessel-Berg's enigmatic and little talked about reciprocity relation needed to describe the reciprocity between retarded and advanced fields and ensure energy conservation. This crucial aspect was overlooked in Wessel-Berg's original work, and is thus rectified in this thesis.

In essence, this thesis offers a deeper understanding of Wessel-Berg's theory, redefining it from a neoclassical framework to a more fitting characterization as a quantum theory since it solves the entropy problem. It elegantly weaves the intricate elements of the study, providing a robust foundation for Wessel-Berg's equations that underlie the simulations presented in his book. It demonstrates the potential of the theory to bridge the chasm between classical and quantum interpretations of the world, offering a first-quantized theory of electromagnetism with valuable insights into the enigma of quantum phenomena. The investigation culminates by fitting the theory within the broader fabric of modern physics, setting the stage for further studies and discussions on this unconventional yet fascinating perspective on electromagnetism. It is our hope that this investigation will inspire further examination of this undervalued theory, opening avenues for its application and refinement in the continually evolving realm of physics.
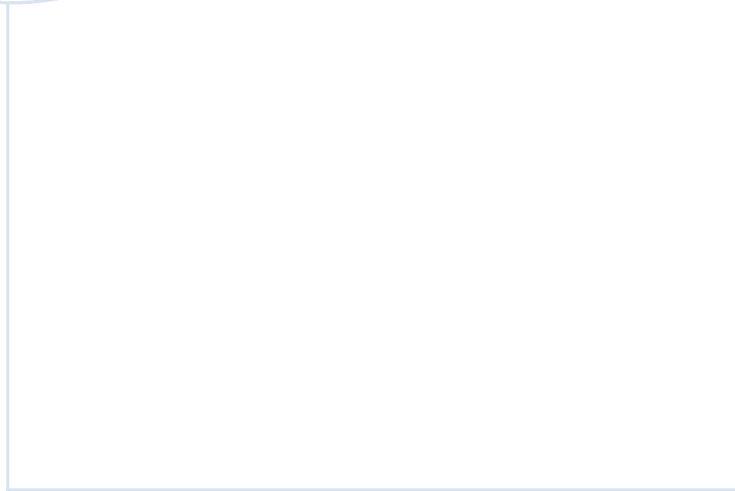
Bibliography

1. Abbott, T. A. & Griffiths, D. J. Acceleration without radiation. *American Journal of Physics* **53,** 1203 (1985).

2. Afanas'ev, G., Eliseev, S. & Stepanovskij, Y. On the photon densities, Hegerfeldt theorem and all that. *Submitted to Helvetica Physica Acta.* Report Number: JINR-E–2-96-278, Joint Institute for Nuclear Research (JINR) (1996).

3. Allcock, G. R. The time of arrival in quantum mechanics I. Formal considerations. *Ann. Phys. (N. Y)* **53,** 253–285 (1969).

4. Allcock, G. R. The time of arrival in quantum mechanics II. The individual measurement. *Ann. Phys. (N. Y)* **53,** 286–310 (1969).

5. Allcock, G. R. The time of arrival in quantum mechanics III. The measurement ensemble. *Ann. Phys. (N. Y)* **53,** 311–348 (1969).

6. Barat, N. & Kimball, J. Localization and causality for a free particle. *Physics Letters A* **308,** 110–115. ISSN: 0375-9601. https://www.sciencedirect.com/science/article/pii/S0375960102018066 (2003).

7. Bartlett, M. S. Negative probability. *Mathematical Proceedings of the Cambridge Philosophical Society* **41,** 71–73 (1945).

8. Beckner, W. Inequalities in Fourier Analysis. *Annals of Mathematics* **102,** 159–182 (1975).

9. Bialynicki-Birula, I. V Photon Wave Function. *Progress in Optics* **36** (ed Wolf, E.) 245–294. ISSN: 0079-6638. https://www.sciencedirect.com/science/article/pii/S0079663808703160 (1996).

10. Bondar, Cabrera, R., Zhdanov & Rabitz. Wigner Function's Negativity Demystified. *Physical Review A* **88,** 263. arXiv: 1202.3628 [quant-ph] (2013).

11. Bostelmann, H. & Cadamuro, D. Negative energy densities in integrable quantum field theories at one-particle level. *Phys. Rev. D* **93,** 065001 (2016).

12. Cabrera, R., Bondar & Rabitz. Relativistic Wigner function and consistent classical limit for spin 1/2 particles. arXiv: 1107.5139 [quant-ph] (2011).

13. Campos, A. G., Cabrera, R., Bondar, D. I. & Rabitz, H. A. Violation of Hudson's theorem in relativistic quantum mechanics. *Phys. Rev. A* **90,** 034102. https://link.aps.org/doi/10.1103/PhysRevA.90.034102 (3 Sept. 2014).

14. Carcassi, G. & Aidala, C. A. Hamiltonian Mechanics is Conservation of Information Entropy. *Studies in History and Philosophy of Science Part B: Studies in History and Philosophy of Modern Physics* **71,** 60–71. ISSN: 1355-2198. https://www.sciencedirect.com/science/article/pii/S1355219819300176 (2020).

15. Carinena, J. F., Garcia-Bondia, J. M. & Varilly, J. C. Relativistic quantum kinematics in the Moyal representation. *Journal of Physics A: Mathematical and General* **23,** 901. https://dx.doi.org/10.1088/0305-4470/23/6/015 (Mar. 1990).

16. Caves, C. Quantum-mechanical noise in an interferometer. *Physical Review D* **31,** 1897–1905 (1985).

17. Chen, Z., Shao, S. & Cai, W. A high order efficient numerical method for 4-D Wigner equation of quantum double-slit interferences. *Journal of Computational Physics* **396,** 54–71. ISSN: 0021-9991. https://www.sciencedirect.com/science/article/pii/S0021999119304553 (2019).

18. Conforti, M., Marini, A., Tran, T. X., Faccio, D. & Biancalana, F. Interaction between optical fields and their conjugates in nonlinear media. *Opt. Express* **21,** 31239 (2013).

19. Cook, R. J. Lorentz covariance of photon dynamics. *Phys. Rev. A* **26,** 2754–2760 (1982).

20. Cook, R. J. Photon dynamics. *Phys. Rev. A* **25,** 2164–2167 (1982).

21. Cover, T. M. & Thomas, J. A. *Elements of Information Theory* 2nd ed., 18–19. ISBN: 9780471241959. https://www.wiley.com/en-us/Elements+of+Information+Theory%5C%2C+2nd+Edition-p-9780471241959 (John Wiley Sons, 2006).

22. Cramer, J. G. The transactional interpretation of quantum mechanics. *Reviews of Modern Physics* **58,** 647 (1986).

23. Cramer, J. G. The Transactional Interpretation of Quantum Mechanics and Quantum Non-locality. *arXiv: Quantum Physics* (2015).

24. Cramer, J. G. & Mead, C. A. in *Symmetries in Quantum Mechanics* 5–48 (MDPI, 2022). https://resolver.caltech.edu/CaltechAUTHORS:20220114-163105179.

25. Davydov, A. P. & Zlydneva, T. P. On simulation of the photon wave function to explain the Young's experiment and prospects for its use in quantum cryptography. *Journal of Physics: Conference Series* **1661,** 012028. https://dx.doi.org/10.1088/1742-6596/1661/1/012028 (Nov. 2020).

26. Davydov, A. & Zlydneva, T. *The Modeling of the Young's Interference Experiment in terms of Single-photon wave function in the coordinate representation* in *Proceedings of the IV International research conference "Information technologies in Science, Management, Social sphere and Medicine" (ITSMSSM 2017)* (Atlantis Press, 2017/12), 257–265. ISBN: 978-94-6252-432-3. https://doi.org/10.2991/itsmssm-17.2017.54.

27. Deno, D. W. Transmission line fields. *IEEE Transactions on Power Apparatus and Systems* **95,** 1600–1611 (5 1976).

28. Dewdney, C., Holland, P., Kyprianidis, A. & Vigier, J. Relativistic Wigner function as the expectation value of the PT operator. *Physics Letters A* **114,** 440–444. ISSN: 0375-9601. https://www.sciencedirect.com/science/article/pii/0375960186906900 (1986).

29. Dickinson, R., Forshaw, J. & Millington, P. Probabilities and signalling in quantum field theory. *Phys. Rev. D* **93,** 065054 (2016).

30. Dirac, P. A. M. The quantum theory of the electron. *Proceedings of the Royal Society of London. Series A* **117,** 610–624. https://doi.org/10.1098/rspa.1928.0023 (1928).

31. Dutta, P. & Horn, P. M. Low-frequency fluctuations in solids: 1/f noise. *Reviews of Modern Physics* **53,** 497 (1981).

32. Eliezer, C. J. & Dirac, P. A. M. The Hydrogen Atom and the Classical Theory of Radiation.

33. Feynman, R. P. Space-Time Approach to Non-Relativistic Quantum Mechanics. *Reviews of Modern Physics* **20,** 367–387. https://link.aps.org/doi/10.1103/RevModPhys.20.367 (1948).

34. Feynman, R. P. & Wheeler, J. A. Interaction with the Absorber as the Mechanism of Radiation. *Reviews of Modern Physics* **17,** 157–181 (2-3 1945).

35. Field, J. H. Derivation of the Schrödinger equation from the Hamilton–Jacobi equation in Feynman's path integral formulation of quantum mechanics. *European Journal of Physics* **32,** 63. https://dx.doi.org/10.1088/0143-0807/32/1/007 (Nov. 2010).

36. Friedman, R. & Gurtler, P. The Stern-Gerlach Experiment Revisited. *The Physics Teacher* **50,** 170–172 (2012).

37. Gabriele Carcassi, C. A. & Barbour, J. Variability as a better characterization of Shannon entropy. *European Journal of Physics* **42,** 045102. https://doi.org/10.1088%5C%2F1361-6404%5C%2Fabe361 (May 2021).

38. Galili, I. & Goihbarg, E. Energy transfer in electrical circuits: A qualitative account. *American Journal of Physics* **73,** 141–144 (2 2005).

39. Goedecke, G. H. Classically Radiationless Motions and Possible Implications for Quantum Theory. *Physical Review* **135,** B281–B288 (1964).

40. Goldstein, H. *Classical Mechanics* 3rd ed., 368–375. ISBN: 0201657023. https://www.pearson.com/us/higher-education/program/Goldstein-Classical-Mechanics-3rd-Edition/PGM219550.html (Addison Wesley, 2001).

41. Goldstein, H. *Classical Mechanics* 3rd ed., 430–451. ISBN: 0201657023. https://www.pearson.com/us/higher-education/program/Goldstein-Classical-Mechanics-3rd-Edition/PGM219550.html (Addison Wesley, 2001).

42. Gozzi, E. & Mauro, D. On Koopman–Von Neumann Waves Ii. *International Journal of Modern Physics A* **19,** 1475. arXiv: `quant-ph/0306029 [quant-ph]` (2004).

43. Gozzi, E. & Pagani, C. Universal Local Symmetries and Nonsuperposition in Classical Mechanics. *Physical Review Letters* **105,** 150604. arXiv: 1006.3029 [`quant-ph`] (2010).

44. Griffiths, D. J. *Introduction to Electrodynamics* 4th ed., 394–406. ISBN: 9780321856562. https://www.pearson.com/us/higher-education/product/Griffiths-Introduction-to-Electrodynamics-4th-Edition/9780321856562.html (Pearson, 2013).

45. Haus, H. A. On the radiation from point charges. *American Journal of Physics* **54,** 1126–1129. https://aip.scitation.org/doi/10.1119/1.14729 (1986).

46. Hawton, M. Photon quantum mechanics in real Hilbert space. *arXiv* **2107,** 03262 (2021).

47. Hawton, M. & Debière, V. Photon position eigenvectors, Wigner's little group, and Berry's phase. *J. Math. Phys.* **60,** 052104 (2019).

48. Hawton, M. & Debierre, V. Maxwell meets Reeh–Schlieder: The quantum mechanics of neutral bosons. *Phys. Lett. A* **381,** 1926–1935 (2017).

49. Hawton, M. & Debierre, V. Photon position observable. arXiv: 1512.06067 [`quant-ph`] (2016).

50. Hegerfeldt, G. C. Remark on causality and particle localization. *Phys. Rev. D* **10,** 3320–3321. https://doi.org/10.1103/PhysRevD.10.3320 (1974).

51. Hegerfeldt, G. C. Causality problems for Fermi's two-atom system. *Phys. Rev. Lett.* **72,** 596–599 (1994).

52. Hegerfeldt, G. C. Instantaneous spreading and Einstein causality in quantum theory. *Ann. Phys.* **7,** 716–725 (7/8 1998).

53. Hegerfeldt, G. C. Violation of Causality in Relativistic Quantum Theory? *Phys. Rev. Lett.* **54,** 2395–2398. https://link.aps.org/doi/10.1103/PhysRevLett.54.2395 (22 June 1985).

54. Hegerfeldt, G. C. Difficulties with causality in particle localization. *Nuclear Physics B - Proceedings Supplements* **6,** 231–237. ISSN: 0920-5632. https://www.sciencedirect.com/science/article/pii/092056328990443X (1989).

55. Hodgson, D., Southall, J., Purdy, R. & Beige, A. Local photons. *Frontiers in Photonics* **3.** https://doi.org/10.3389%5C%2Ffphot.2022.978855 (Sept. 2022).

56. Hodgson, D. R. E. *A Theory of Local Photons with Applications in Quantum Field Theory* PhD thesis (The University of Leeds, School of Physics and Astronomy, Sept. 2022), 202. arXiv: 2303.04706 [`quant-ph`]. https://doi.org/10.48550/arXiv.2303.04706.

57. Holland, P., Kyprianidis, A. & Vigier, J. Trajectories and causal phase-space approach to relativistic quantum mechanics. *Found Phys* **17,** 531–548. https://doi.org/10.1007/BF01559700 (1987).

58. Hooge, F. N. 1/f noise. *IEEE Transactions on Electron Devices* **41,** 1926–1935 (1994).

59. Hudson, R. When is the Wigner quasi-probability density non-negative? *Reports on Mathematical Physics* **6,** 249–252 (1974).

60. Jr., I. I. H. A note on entropy. *American Journal of Mathematics* **79,** 152–156 (1957).

61. Kenfack, A. & Życzkowski, K. Negativity of the Wigner function as an indicator of non-classicality. *Journal of Optics B: Quantum and Semiclassical Optics* **6,** 396–404 (2004).

62. Kim, Y.-H., Yu, R., Kulik, S. P., Shih, Y. H. & Scully, M. O. A Delayed Choice Quantum Eraser. *Physical Review Letters* **84,** 1–5 (2000).

63. Koopman, B. Hamiltonian Systems and Transformations in Hilbert Space. *Proceedings of the National Academy of Sciences* **17,** 315–318 (1931).

64. Landau, L. D. & Lifshitz, E. M. *Course of Theoretical Physics, Volume 2: The Classical Theory of Fields* 4th ed. Relevant sections: pages 205-210, 166-168. ISBN: 978-0-08-057069-8 (Butterworth-Heinemann, 2013).

65. Leibfried, D., Pfau, T. & Monroe, C. Shadows and Mirrors: Reconstructing Quantum States of Atom Motion. *Physics Today* **51,** 22–28. eprint: https://doi.org/10.1063/1.882256. https://doi.org/10.1063/1.882256 (1998).

66. Lev, B. I., Semenov, A. A. & Usenko, C. V. *Relativistic Wigner Function, Charge Variable and Structure of Position Operator* 2001. arXiv: quant-ph/0112122 [`quant-ph`].

67. Mandel, L. Configuration-space photon number operators in quantum optics. *Phys. Rev.* **144,** 1071–1077 (1966).

68. Marsden, J. & Ratiu, T. *Introduction to Mechanics and Symmetry: A Basic Exposition of Classical Mechanical Systems* (Springer, 1999).

69. Mauro, D. On Koopman–Von Neumann Waves. *International Journal of Modern Physics A* **17,** 1301–1325. arXiv: `quant-ph/0105112` `[quant-ph]` (2002).

70. Mostafazadeh, A. & Zamani, F. Quantum mechanics of Klein–Gordon fields I: Hilbert Space, localized states, and chiral symmetry. *Annals of Physics* **321,** 2183–2209. `https://doi.org/10.1016%5C%2Fj.aop.2006.02.007` (Sept. 2006).

71. Müller, R. A semiquantitative treatment of surface charges in DC circuits. *American Journal of Physics* **80,** 782–788 (9 2012).

72. Newton, T. D. & Wigner, E. P. Localized states for elementary systems. *Reviews of Modern Physics* **21,** 400–406. `https://doi.org/10.1103/RevModPhys.21.400` (3 1949).

73. Nielsen, M. & Chuang, I. *Quantum Computation and Quantum Information* (Cambridge University Press, 2010).

74. Plancherel, M. Contribution à l'étude de la représentation d'une fonction arbitraire par des intégrales définies. *Rendiconti del Circolo Matematico di Palermo* **30,** 289–335 (1910).

75. Polonyi, J. The Abraham-Lorentz force and electrodynamics at the classical electron radius. *arXiv preprint arXiv:1701.04068.* `https://arxiv.org/abs/1701.04068` (2017).

76. Pryce, M. H. L. The mass-centre in the restricted theory of relativity and its connexion with the quantum theory of elementary particles. *Proceedings of the Royal Society of London. Series A. Mathematical and Physical Sciences* **195,** 62–81. `https://doi.org/10.1098/rspa.1948.0081` (1042 1948).

77. Riemann, B. Über die Fortpflanzung ebener Luftwellen von endlicher Schwingungsweite. *Abhandlungen der Königlichen Gesellschaft der Wissenschaften zu Göttingen* **8,** 43–65 (1861).

78. Sakurai, J. & Napolitano, J. *Modern Quantum Mechanics* (Pearson, 2010).

79. Schrödinger, E. An Undulatory Theory of the Mechanics of Atoms and Molecules. *Physical Review* **28,** 1049–1070 (1926).

80. Sefton, I. M. *Understanding electricity and circuits: What the text books don't tell you* in *Science Teachers' Workshop* (2002).

81. Shannon, C. E. A Mathematical Theory of Communication. *The Bell System Technical Journal* **27,** 379–423, 623–656. `https://onlinelibrary.wiley.com/doi/abs/10.1002/j.1538-7305.1948.tb01338.x` (3 July 1948).

82. Simon, R. Peres-Horodecki Separability Criterion for Continuous Variable Systems. *Physical Review Letters* **84,** 2726–2729 (2000).

83. Southall, J., Hodgson, D., Purdy, R. & Beige, A. Locally acting mirror Hamiltonians. *Journal of Modern Optics* **68,** 647–660. eprint: `https://doi.org/10.1080/09500340.2021.1936241`. `https://doi.org/10.1080/09500340.2021.1936241` (2021).

84. Stern, O. & Gerlach, W. Der experimentelle Nachweis der Richtungsquantelung im Magnetfeld. *Zeitschrift für Physik* **7,** 249–253 (1922).

85. Tamburini, F. & Vicino, D. Photon wave function: A covariant formulation and equivalence with QED. *Phys. Rev. A* **78,** 052116. `https://link.aps.org/doi/10.1103/PhysRevA.78.052116` (5 Nov. 2008).

86. Thomson, M. *Modern Particle Physics* 1st, 80–111. ISBN: 9781107289772 (Cambridge University Press, 2013).

87. Walls, D. & Milburn, G. Effect of Dissipation on Quantum Coherence. *Physical Review A* **27,** 3923–3933 (1983).

88. Wehrl, A. On the relation between classical and quantum-mechanical entropy. *Reports on Mathematical Physics* **16,** 353–358. `https://doi.org/10.1016/0034-4877(79)90070-3` (1979).

89. Weissman, M. B. 1/f noise and other slow, nonexponential kinetics in condensed matter. *Reviews of Modern Physics* **60,** 537 (1988).

90. Welch, W. J. Reciprocity theorems for electromagnetic fields whose time dependence is arbitrary. *IEEE Transactions on Antennas and Propagation* **8,** 68–73 (1960).

91. Wessel-Berg, T. *Electromagnetic and Quantum Measurements: A Bitemporal Neoclassical Theory* (Kluwer Academic Publishers, 2001).

92. Weyl, H. Quantenmechanik und Gruppentheorie. *Zeitschrift für Physik* **46,** 1–46 (1927).

93. Wheeler, J. A. & Feynman, R. P. Classical Electrodynamics in Terms of Direct Interparticle Action. *Reviews of Modern Physics* **21,** 425–433 (3 1949).

94. Wigner, E. On the Quantum Correction For Thermodynamic Equilibrium. *Physical Review* **40,** 749–759 (1932).

95. Zurek, W. H. & Paz, J. P. Sub-Planck Structure in Phase Space and Its Relevance for Quantum Decoherence. *Physical Review Letters* **86,** 3667–3670 (2001).